AD-A049 682    TRW INC CLEVELAND OHIO MATERIALS TECHNOLOGY    F/G 11/6
IMPROVED ULTRASONIC INSPECTION OF TITANIUM ALLOY FORGING BILLET--ETC(U)
JUL 77    I M MATAY    F33615-71-C-1712

UNCLASSIFIED    TRW-ER-7554    AFML-TR-77-111    NL

1 OF 4
AD
A049682

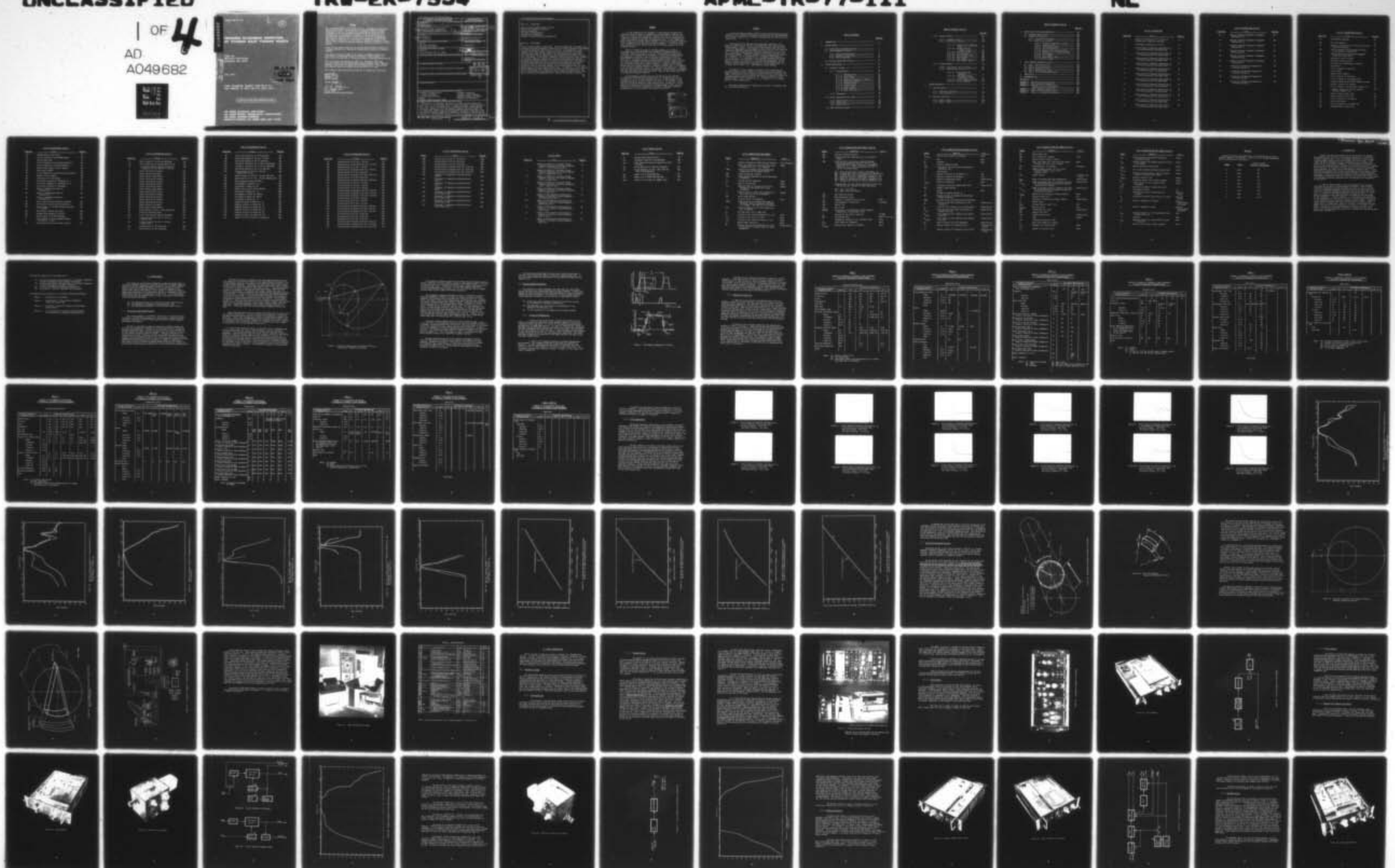

AFML-TR-77-111

R

2

# IMPROVED ULTRASONIC INSPECTION OF TITANIUM ALLOY FORGING BILLETS

TRW, Inc.
Materials Technology
Cleveland, OH. 44117





July 1977

FINAL TECHNICAL REPORT AFML-TR-77-111
FOR PERIOD 15 JULY 1971-30 JULY 1977

Approved for public release; distribution unlimited

AIR FORCE MATERIALS LABORATORY
AIR FORCE WRIGHT AERONAUTICAL LABORATORIES
AIR FORCE SYSTEMS COMMAND
WRIGHT-PATTERSON AIR FORCE BASE, OHIO 45433

## NOTICES

When Government drawings, specifications, or other data are used for any purpose other than in connection with a definitely related Government procurement operation, the United States Government thereby incurs no responsibility for any obligation whatsoever; and the fact that the Government may have formulated, furnished, or in any way supplied the said drawings, specifications, or other data, is not to be regarded by implication or otherwise as in any manner licensing the holder or any other person or corporation or conveying any rights or permission to manufacture, use, or sell any patented invention that may in any way be related thereof.

Copies of this report should not be returned unless return is required by security considerations, contractual obligations, or notice on a specific document.

This report has been reviewed by the Office of Information (OI) and is releasable to the National Technical Information Service (NTIS). At NTIS, it will be available to the general public, including foreign nations.

This final report was submitted by TRW, Inc., Cleveland, Ohio under Contract F33615-71-C-1712, Manufacturing Methods Project 225-1, "Improved Ultrasonic Inspection of Titanium Alloy Forging Billets". This program was conducted under the technical direction of Mr. K. L. Love.

This technical report has been reviewed and is approved for publication.

K. L. Love

KENNETH L. LOVE
Project Manager

FOR THE COMMANDER

H. A. Johnson

H. A. JOHNSON, CHIEF
Metals Branch
Manufacturing Technology Division

SECURITY CLASSIFICATION OF THIS PAGE (When Data Entered)

# 19 REPORT DOCUMENTATION PAGE

READ INSTRUCTIONS BEFORE COMPLETING FORM

1. REPORT NUMBER: 18 AFML-TR-77-111

2. GOVT ACCESSION NO.

3. RECIPIENT'S CATALOG NUMBER

4. TITLE (and Subtitle): 6 IMPROVED ULTRASONIC INSPECTION OF TITANIUM ALLOY FORGING BILLETS.

5. TYPE OF REPORT & PERIOD COVERED: 9 FINAL REP[redacted]T. 15 Jul 71-30 Jul 76
1971 July 15 - 1976 July 30

6. PERFORMING ORG. REPORT NUMBER: 14 TRW-ER-7554

7. AUTHOR(s): 10 I. M./Matay

8. CONTRACT OR GRANT NUMBER(s): 15 F33615-71-C-1712

9. PERFORMING ORGANIZATION NAME AND ADDRESS
TRW Inc.
Materials Technology
Cleveland, OH 44117

10. PROGRAM ELEMENT, PROJECT, TASK AREA & WORK UNIT NUMBERS
Project 225-1

11. CONTROLLING OFFICE NAME AND ADDRESS
AFML/LTM
Wright-Patterson AFB, OH 45433

12. REPORT DATE: 11 Jul[redacted]77

13. NUMBER OF PAGES: 257 12 284 p.

14. MONITORING AGENCY NAME & ADDRESS (if different from Controlling Office)

15. SECURITY CLASS. (of this report)
UNCLASSIFIED

15a. DECLASSIFICATION/DOWNGRADING SCHEDULE

16. DISTRIBUTION STATEMENT (of this Report)

Approved for public release; distribution unlimited.



17. DISTRIBUTION STATEMENT (of the abstract entered in Block 20, if different from Report)

18. SUPPLEMENTARY NOTES

19. KEY WORDS (Continue on reverse side if necessary and identify by block number)

Ultrasonic nondestructive evaluation (UNDE)
Titanium forging billets
Defects
Computer aided evaluation (CAE)
Automatic inspection
Automatic defect diagnosis
Automatic QC decision making
Hardware standardization

20. ABSTRACT (Continue on reverse side if necessary and identify by block number)

Titanium is an important raw material in both aircraft engines and structures. It is also being used in a larger-and-larger size forged billet form. The billets' increasing size, in addition to their coarser-grained structures, drastically limit the detection capabilities and reliability of finding small defects when using established ultrasonic techniques along with manually operated commercial instruments. Providing an improved billet inspection to insure greater reliability in the finished part at an improved

Block 19. (Continued)

Quality control accept/reject criteria
Statistical probability analysis
Pattern recognition
Ultrasonic instrumentation
Computerized ultrasonics
Automatic Distance-Amplitude Compensation

Block 20. (Continued)

overall process economy is desirable. Available commercial instruments were evaluated and proven incapable of meeting the critical inspection requirements. An original design for the ultrasonic circuitry, interfaced with a mini-computer, and a data display system which shows the billet in multiple cross-section slices was fabricated. All the detectable defects and/or only those which meet or exceed a selected quality control reject criteria, can be displayed. An Ultrasonic Diagnostic Inspection System, UDIS, capable of increased inspection sensitivity, resolution and speed with reduced equipment and operator variability was built and evaluated in this program. The performance characteristics of the system have been well defined by laboratory operations and the feasibility of its application to mill inspection of up to 16-inches diameter and 10-foot length billets has been demonstrated by limited in-plant field trials. In addition, a joint industry (billet maker/user) team evaluation of the UDIS has also been carried out for the establishment of an improved billet inspection specification. The report also covers recommendations for industry utilization of the UDIS.

## SUMMARY

At the inception of this program, it was generally accepted that titanium billets 16 inches in diameter and larger commonly used for production of large aircraft structural forgings could not be satisfactorily inspected ultrasonically because the coarse grain structure attenuated the signal and produced a high level of background noise. It was judged that better capability to detect smaller defects at the billet stage of production would be beneficial for both cost and safety aspects. It was also known that inspection results varied widely due to different operator skill and judgement factors.

After an extensive survey of candidate commercial ultrasonic instrumentation, those available but inadequate instruments had to be discarded. Original ultrasonic circuitry was designed, fabricated and interfaced with a commercial minicomputer. A unique data display method was developed to show the billet in multiple cross-section slices (a modified PPI or B-scan) for all the detected defects and/or only those which met or exceeded an operator selected quality control reject criteria. All inspection, defect data diagnosis and quality control accept/reject decision making functions are fully automatic. Inasmuch as the program established an Ultrasonic Diagnostic Inspection System, UDIS, it is capable of an increased inspection sensitivity, resolution and speed with a reduced equipment (and eliminated) operator variability. The ultrasonic instrumentation was fabricated utilizing a government (ERDA and NBS) established "NIM" instrumentation hardware standard.

The performance characteristics of the UDIS were well defined by laboratory operations and the feasibility of its application to mill inspection of up to 16-inches diameter and up to 10-foot length billets was demonstrated by limited in-plant field trials. In addition, a joint industry (billet producer/user) team evaluation was carried out. Billet sectioning, mechanical, metallurgical and metallographic tests were performed on billet sections inspected by the team. The report provides recommendations for the industry utilization of the UDIS.

## PREFACE

This Final Technical Report covers all work performed under Contract F33615-71-C-1712, entitled "Manufacturing Methods for an Improved Method of Ultrasonic Inspection of Ti Alloy," during the period 1971 July 15 to 1976 July 30.

This contract with the Materials Development Department, TRW Materials Technology of TRW Inc., Cleveland, Ohio was initiated under Project Number 225-1. The program is administered under the direction of the Manufacturing Technology Division of the Air Force Materials Laboratory, AFML/LTM, under the technical direction of Mr. K. L. Love. Mr. I. M. Matay of TRW Equipment's Material Technology Laboratory was the Program Manager. Technical support on data processing and controls was given by Mr. C. W. Fetheroff and on transducer development by Mr. T. Derkacs. The lead-technician in equipment assembly and system evaluation was Mr. J. Touhalisky. The material subcontractor was the RMI Co. of Niles, Ohio with Mr. M. Esler as Program Manager, and the computer software development subcontractor was the System Data, Inc., of Akron, Ohio with Mr. J. L. Sickafoose as Program Manager.

The Phase IV - Joint Industry Evaluation effort subcontractors were the General Electric Company, Aircraft Engine Group, Evendale, OH, United Technologies, Pratt & Whitney Aircraft Division, Middletown, CT, TIMET, a Division of Titanium Metals Corporation of America, Toronto, OH, and Wyman-Gordon Company, Worcester, MA. The subcontractor program managers were Mr. H. A. Truscott, Dr. J. E. Doherty, Mr. F. A. Brown and R. A. Eddy, respectively.

The report manuscript was released by the author in September 1976 for review and publication.

TABLE OF CONTENTS

TABLE OF CONTENTS (Cont'd)

TABLE OF CONTENTS (Cont'd)

## LIST OF ILLUSTRATIONS

## LIST OF ILLUSTRATIONS (Cont'd)

## LIST OF ILLUSTRATIONS (Cont'd)

## LIST OF ILLUSTRATIONS (Cont'd)

## LIST OF ILLUSTRATIONS (Cont'd)

## LIST OF ILLUSTRATIONS (Cont'd)

## LIST OF ILLUSTRATIONS (Cont'd)

## LIST OF ILLUSTRATIONS (Cont'd)

## LIST OF TABLES

## LIST OF TABLES (Cont'd)

## LIST OF ABBREVIATIONS AND SYMBOLS

| Symbol | Quantity | Unit |
|---|---|---|
| $\alpha$ | Acoustic attenuation coefficient of titanium | per centimeter |
| A | Short form symbol for titanium billet axial distance unit cell, $\Delta Ti_L$, location | meter |
| ADAC | A device for automatic distance-amplitude compensation of ultrasonic signals | - |
| ADC | Analog-to-digital converter | - |
| AEC | Atomic Energy Commission of the United States of America | - |
| $B_n$ | Minimum receiver bandwidth | hertz |
| b | Base of triangle CDE | meter |
| $\beta_{Ti}$ | Angle of focus in titanium billet (with reference to the normal axis of the transducer) | degree |
| $\beta_W$ | Angle of focus in water (with reference to the normal axis of the transducer) | degree |
| BCD | Binary coded decimal | - |
| C | Titanium billet circumference | meter |
| CAMAC | A specification for modular data handling equipment, based on standard interfaces to a highway. The name is not an acronym | - |
| CPU | Central processing unit, often referred to also as computer | - |
| CR | Carriage return (of a typewriter) | - |
| $\Delta C$ | Titanium billet surface dimension unit cell | meter |
| $\Delta Ti_L$ | Titanium billet axial unit cell | meter |
| $\Delta Ti_R$ | Titanium billet radial distance unit cell | meter |
| $\Delta_x$ | Defect depth resolution | meter |
| dB | Decibel (the unit for expressing the ratio of two values of acoustic power, or other phenomena) | dimensionless |

## LIST OF ABBREVIATIONS AND SYMBOLS (Cont'd)

| Symbol | Quantity | Unit |
|---|---|---|
| DAC | Digital-to-analog converter | - |
| DAC | Distance-amplitude compensation of an ultrasonic signal | - |
| DAC | While the DAC is an acronym, meaning Distance-Amplitude Compensation and as we can tell was established by the Sperry Division of Automation Industries, Inc., other expressions are also in use as illustrated below:<br><br>TCG - Time Corrected Gain, Branson Instruments, Inc.<br>DGC - Distance Gain Control, Krautkramer Ultrasonics,Inc.<br>DGS - Distance Gain Size, Krautkramer Ultrasonics, Inc.<br>SGC - Swept Gain Control, Krautkramer Ultrasonics, Inc.<br>MAC - Magnaflux Attenuation Correction, Magnaflux Corp.<br>DEC - Distance Echo Correction, Sonic Instruments, Inc.<br><br>Nethertheless, all the listed expressions arrived from the two earliest acronyms of radar technology:<br><br>GTC - Gain Time Control<br>STC - Sensitivity Time Control | - |
| DOS | Disk operating system | - |
| DPS | Data Processing system | - |
| $D_1$ | Diameter of inspection drive roller | meter |
| EMI | Electromagnetic interference | volt/meter |
| EOF | End of file | - |
| EOT | End of tape | - |
| EURATOM | Activities of the Commission of the European Communities in the nuclear field | - |
| e | The base of the natural logarithm | 2.71828 |
| FBH | Flat bottom hole | 64ths of an inch |
| f | Fundamental frequency of an ultrasonic wave | hertz |
| $f_{prf}$ | Pulse repetition frequency | hertz |
| $f_{prf_{max}}$ | Maximum pulse repetition frequency | hertz |

## LIST OF ABBREVIATIONS AND SYMBOLS (Cont'd)

| Symbol | Quantity | Unit |
|---|---|---|
| $f_{prf_{opt}}$ | Optimum pulse repetition frequency | hertz |
| g | Mass | gram |
| Hz | Frequency | hertz |
| ICT | Industry compatible tape | - |
| IEEE | Institute of the Electrical and Electronics Engineers, Inc. | - |
| I/O | Input/output | - |
| $I_o$ | Acoustic intensity at distance x = o | volt |
| $I_1$ | Acoustic intensity at distance x | volt |
| k | Acoustic transmission factor | dimensionless |
| $L_{trans}$ | Length of transducer | meter |
| M | Transducer receiving voltage sensitivity | dimensionless |
| MTO | Magnetic tape recorder | - |
| m | Length | meter |
| N | N-number of defect signals, $S_d$ | - |
| NBS | National Bureau of Standard of the United States of America | - |
| NEMA | National Electrical Manufacturers Association | - |
| $N_A$ | Titanium billet axial distance unit cell population | dimensionless |
| $N_C$ | Titanium billet angular unit cell population | dimensionless |
| $N_{P_{cal}}$ | Pulse population for ADAC calibration per angular unit cell | dimensionless |
| $N_{P_{insp}}$ | Pulse population for inspection per angular unit cell | dimensionless |
| $N_{P_{total}}$ | Total number of pulse population per angular unit cell | dimensionless |
| $N_R$ | Radial distance unit cell population | dimensionless |
| $n_{T_i}$ | Angular velocity of titanium billet | revolution per minute |
| $n_1$ | Angular velocity of inspection drive roller | revolution per minute |

LIST OF ABBREVIATIONS AND SYMBOLS (Cont'd)

| Symbol | Quantity | Unit |
|---|---|---|
| PLL | Phase locked loop | - |
| PRF | Pulse repetition frequency | hertz |
| QRC | Quality control reject criteria | - |
| R | Short form symbol for titanium billet radial distance unit cell, $\Delta Ti_R$, location | meter |
| RFI | Radiofrequency interference | volt/meter |
| RN | Number N defect signal, Sd, at R radial distance location, $\Delta Ti_R$, of the titanium billet | - |
| RPM | Angular motion | revolution per minute |
| $R_{DAC}$ | Range of distance-amplitude compensation | dimensionless |
| $R_{I_{1_{Ti_D}}}$ | Range of emergent acoustic intensity variation for pulse-reflection inspection through the titanium billet diameter | dimensionless |
| $R_{I_{1_{Ti_R}}}$ | Range of emergent acoustic intensity variation for pulse-reflection inspection through the titanium billet radius | dimensionless |
| $R_{focus}$ | Radius of the transducer surface curvature | meter |
| S | Receiver sensitivity | volt |
| S | Transducer transmitting voltage response | dimensionless |
| $S_d$ | Defect signal | - |
| $S_{min}$ | Minimum receiver sensitivity | volt |
| $S_{noise}$ | Receiver noise | volt |
| SCC | Significant cell count | dimensionless |
| SFE | Special front end | - |
| S/N | Signal-to-noise ratio | dimensionless |
| s | Time | second |
| TTL | Transistor-transistor logic | - |
| $T_i$ | Short form symbol for titanium | - |
| $T_{i_D}$ | Diameter of titanium billet | meter |
| $T_{i_L}$ | Length of titanium billet | meter |

| Symbol | Quantity | Unit |
|---|---|---|
| $T_{min}$ | Minimum elapsed time between successive ultrasonic pulses | second |
| $T_{opt}$ | Optimum elapsed time between successive ultrasonic pulses | second |
| $t_{P_{max}}$ | Maximum modulating pulse width | second |
| $t_{P_{rise}}$ | Rise time of maximum modulating pulse width | second |
| $t_{R_{min}}$ | Shortest pulse-reflection time, at maximum value of titanium billet radius | second |
| $t_{recov}$ | Receiver recovery time | second |
| $t_w$ | Ultrasonic travel time in water couplant | second |
| $t_{1_{rev}}$ | Time interval for unit titanium billet revolution | second |
| UDIS | Ultrasonic Diagnostic Inspection System | - |
| V | Electromotive force | volt |
| $V_L$ | Longitudinal acoustic wave velocity in titanium | meter per second |
| $V_{L_w}$ | Longitudinal acoustic wave velocity in water | meter per second |
| $Z_{Ti}$ | Acoustic impedance of titanium | gram per second-square centimeter |
| $Z_w$ | Acoustic impedance of water | gram per second-square centimeter |
| $X_{max}$ | Maximum distance for thru-transmission type of ADAC monitoring | meter |
| x | Distance | meter |
| $x_{max}$ | Maximum distance for pulse-reflection type of inspection | meter |
| $x_w$ | Acoustic path length in water couplant | meter |

## PREFIXES

Decimal multiples and submultiples of the engineering units are formed by means of the prefixes. A partial list of the NBS recommended units of prefixes are listed below:

| Symbol | Prefix | Factor by Which the Unit is Multiplied |
|---|---|---|
| G | giga | $10^9$ |
| M | mega | $10^6$ |
| k | kilo | $10^3$ |
| d | deci | $10^{-1}$ |
| c | centi | $10^{-2}$ |
| m | milli | $10^{-3}$ |
| µ | micro | $10^{-6}$ |
| n | nano | $10^{-9}$ |
| p | pico | $10^{-12}$ |

Preceding Page Blank - Not Filmed

# 1. INTRODUCTION

Titanium has been used extensively during the past two decades in both commercial and military aircraft engines because of its excellent strength-to-weight ratio. For the compressor sections of these engines, titanium blades, vanes and discs are forged from billet stock. In the larger engines on advanced aircraft, compressor discs are forged from billets of up to 16 inches in diameter. The performance requirements for newer aircraft demands greater utilization of titanium, not only in engines, but particularly in structural forgings and other structural components. These components are forged from large-diameter titanium billets. In the manufacturing sequence for titanium, large-diameter billets usually receive less work than small billets during forging and other thermal-mechanical processing. The larger billets have coarser-grained structures which limit the detection capabilities and the reliability of finding small defects when using standard ultrasonic techniques and instrumentation for determining billet quality.

In the finished component stage, many nondestructive inspection techniques may be used to determine defect conditions. Sophisticated inspection procedures have been developed for tests on discs; high sensitivity is achievable because of the care taken to provide high quality surface finishes and intermediate configurations specifically for inspection. For aircraft structural components, the same reliability is not possible, because of the prohibitive costs of machining and the shapes of most components. In both instances, it is desirable to provide better billet inspection prior to forging since this insures greater reliability in the finished part and results in overall process economy. Good cost control practice requires the location of defects in starting billets rather than in finished parts after all the costs of processing have been added. With this in mind, a program was initiated in July 1971, in an effort to establish an Ultrasonic Diagnostic Inspection System, UDIS, capable of increased inspection sensitivity and speed with reduced equipment and operator variability.

The specific objectives of the program were:

(1) to reduce the scatter and uncertainty in ultrasonic inspection results introduced by human operator variability,
(2) to reduce the scatter and uncertainty in ultrasonic inspection results introduced by equipment variability,
(3) to apply more sensitive inspection methods, and
(4) to establish inspection equipment and procedures.

To accomplish these objectives, a four-phase program was conducted:

Phase I - Optimization of Procedures

Phase II - Establishment of the Ultrasonic Diagnostic Inspection System, UDIS

Phase III - Preliminary Inspection Procedures and Equipment Specifications

Phase IV - Joint Evaluation of the UDIS and Establishment of Improved Billet Inspection Specifications

## 2. SYSTEM DESIGN

The concept of the Ultrasonic Diagnostic Inspection System, UDIS, is to apply an advanced diagnostic inspection method for increased inspection sensitivity and for reduced equipment variability, along with the use of today's modern data processing systems for real-time inspection data acquisition, analysis and storage. Such a system is intended to reduce scatter and uncertainty in the inspection results as introduced by both the human operator and the instrumentation variabilities. The system design effort of the UDIS was accomplished during the first phase of the program in the following three steps:

(1) the engineering design of a preliminary system specification,
(2) the evaluation of candidate system components, and
(3) the subsequent development of revised system specification.

### 2.1 Preliminary System Specification

The initial approach to the Phase I objectives of system design was to identify the detailed requirements of the ultrasonic inspection system. The effort resulted in the preliminary specification of system component performance requirements.

The UDIS is designed to operate by radiating ultrasonic energy and to detect the presence and character of the echo returned from reflecting defects (pulse-echo mode). The form of the ultrasonic signal radiated by the UDIS depends on certain physical properties of the titanium billet and on the desired information about the defect. Important titanium billet characteristics useful in determining the system specifications were the overall test piece dimensions, grain size, as well as the acoustic velocity, impedance and attenuation of their variation in commercial production billets. Other basic factors considered in designing the system included defect specifications such as desired detectable defect dimensions as referred to an arbitrarily determined unit volume cell in the cylindrically shaped billet.

The proper form of the radiated billet interrogating acoustic signal must depend on the information desired to be acquired about the defect. For accurate defect location, for example, the transmitted signal should occupy a wide spectral bandwidth. The shorter the pulse modulating width or pulse duration, the greater the spectral bandwidth will be. If the pulse duration is too long, it may also mask successive defect signals. When the pulse duration is expressed in distance of sound travel, rather than time, it should be short enough to distinguish the distance between successive defects to be resolved. In view of TRW's previous experience with defect detection in titanium billets (Ref. 1) a 3/64-inch value was selected as the design objective for the distance between defects to be resolved. The corresponding maximum allowable modulating pulse width, therefore, was calculated to be 376.5 ns. The pulse must contain sufficient energy to detect the smallest defects at the farthest distance. Hence, pulser output voltage level was important in establishing adequate sound energy to penetrate the billet under test. The design value for the pulse output voltage arrived at was 1kV.

Other important factors were the highest achievable receiver sensitivity and transducer parameters. For the ultrasonic test frequency, a compromise was made to satisfy the two opposing criteria of attenuation and defect size detection. Since higher frequencies are able to detect smaller defects, but are attenuated more, the optimum frequency was selected to be 5 MHz. Because of large grain billet structural effects, this frequency was later reduced to 2.25 MHz for the 16-inch diameter billets only.

In view of the inspection concept of the UDIS, which is dependent upon a time-related repetitive train of wave envelopes or pulses, the pulse-reflection times for both couplant and billet were very important design parameters. Considering the eight-inch radius largest billet for the program, along with a 6325 m/s fastest sound velocity property of titanium, the shortest pulse-reflection time for the system was calculated to be 64.25 μs. In addition, for the water acoustic couplant the minimum allowable distance was calculated to be 2.125-inches. The billet acoustic illumination patterns for the design limits of the 8 and 16-inch diameter billets, using flat-faced transducers are shown in Figure 1. This method is practiced by conventional inspection techniques.

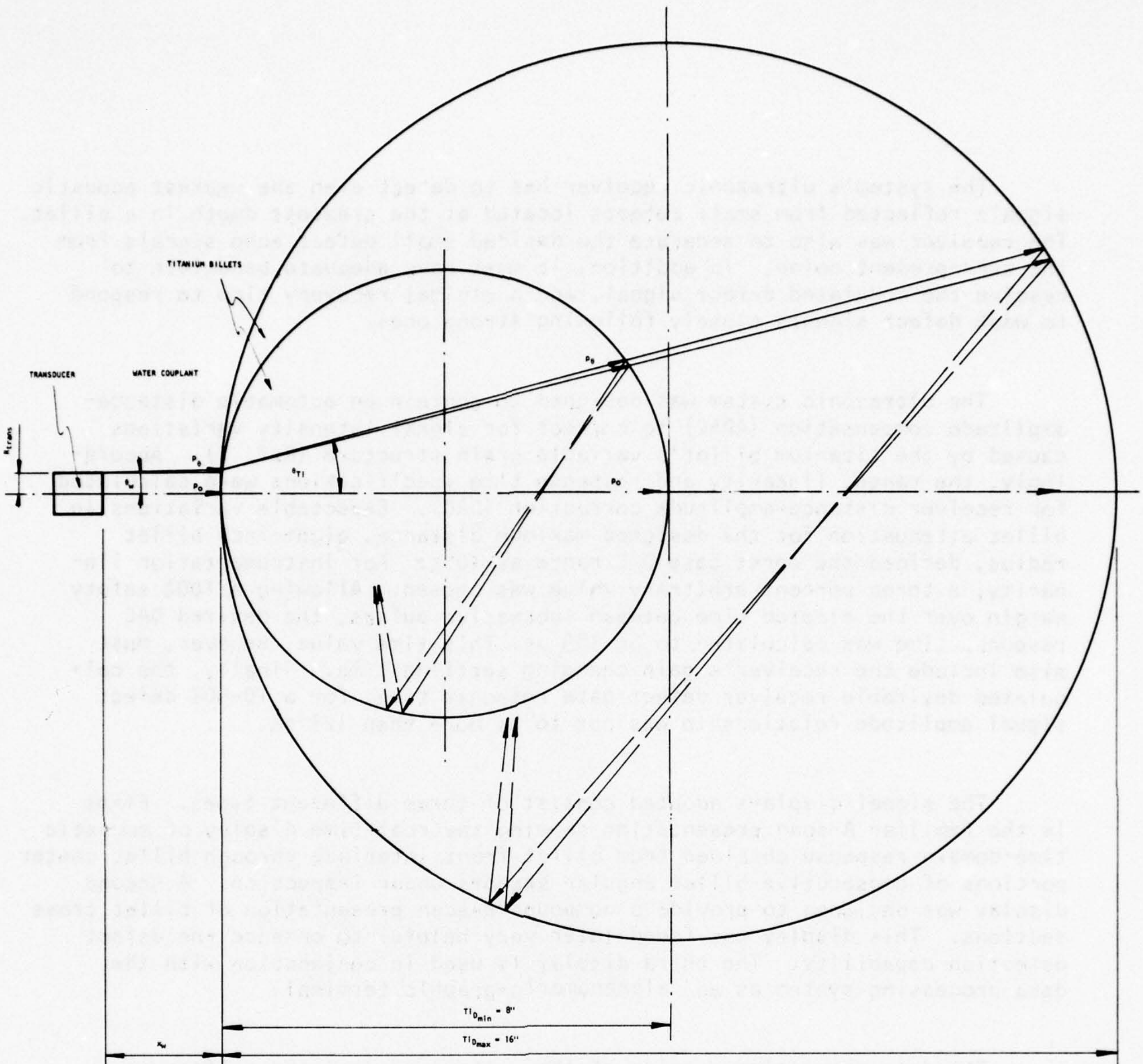


**Figure 1. Acoustic Illumination of Titanium Billets by Conventional Inspection Technique**

The system's ultrasonic receiver has to detect even the weakest acoustic signals reflected from small defects located at the greatest depth in a billet. The receiver was also to separate the desired small defect echo signals from the ever-present noise, In addition, it must have adequate bandwidth to resolve the modulated defect signal, and a minimal recovery time to respond to weak defect signals closely following strong ones.

The ultrasonic system was designed to contain an automatic distance-amplitude compensation (ADAC) to correct for signal intensity variations caused by the titanium billet's variable grain structure (Ref. 2). Accordingly, the range, linearity and response time specifications were calculated for receiver distance-amplitude correction (DAC). Expectable variations in billet attenuation for the designed maximum distance, eight-inch billet radius, defined the worst case DAC range as $10^4$X. For instrumentation linearity, a three percent arbitrary value was chosen. Allowing a 100% safety margin over the elapsed time between successive pulses, the desired DAC response time was calculated to be 385 μs. This time value, however, must also include the receiver's gain changing settling time. Finally, the calculated desirable receiver defect gate response time, for a 10-90% defect signal amplitude relationship was not to be more than 125 ns.

The signal displays adopted consist of three different types. First is the familiar A-scan presentation showing the real-time display of acoustic time-domain response obtained from billet front interface through billet center portions of consecutive billet angular sectors under inspection. A second display was designed to provide a compound B-scan presentation of billet cross sections. This display was found later very helpful to enhance the defect detection capability. The third display is used in conjunction with the data processing system as an alphanumeric-graphic terminal.

The data processing portion of the system was designed to feature real-time data acquisition and near-real-time or retrievable data interpretation, diagnosis and display. The ultrasonic test record is designed to be magnetic tape stored to permit a data review without having to physically reinspect a billet. These features were expected to improve inspection reliability and speed.

The Preliminary System Specifications were originally published in the First Interim Technical Report, IR-225-1(I), dated October 1971. It has later been updated and superceded by the Revised System Specification (Section 2.3).

## 2.2 System Component Evaluation

The selection of system components was based upon the requirements set by the preliminary system specifications just discussed. Initially an attempt was made to achieve the designed performance by using off-the-shelf commercial instrument modules. An evaluation of the available candidate system components, therefore, was carried out in three specific steps:

(1) an abstract design comparison obtained initially by a survey of the commercial instrument manufacturers,

(2) TRW laboratory test evaluations of the equipment of the commercial manufacturers, and

(3) a field evaluation of the commercially available systems.

### 2.2.1 Survey of Manufacturers

As part of the system design a survey was carried out in an effort to evaluate the usefulness of the candidate commercial ultrasonic inspection system components. An inquiry of the technical specifications was made by a six-page questionnaire. In order to normalize the information obtained from the different sources using their own in-house test procedures, the IEEE recommended test practices (Ref. 3) were followed. The highlights of this test practice is shown in Figure 2. Other test methods were accepted insofar as the particulars of the test method were identified. The survey was then followed up by discussions of the specifications with each of the instrument manufacturers.

A total of five leading ultrasonic instrument manufacturers were surveyed. Four companies complied by providing the requested information. In order to expedite the procurement of the data, the home offices of three of these companies were also visited by the writer. The instruments evaluated and reported in Tables I through X of this report are listed in Appendix F.

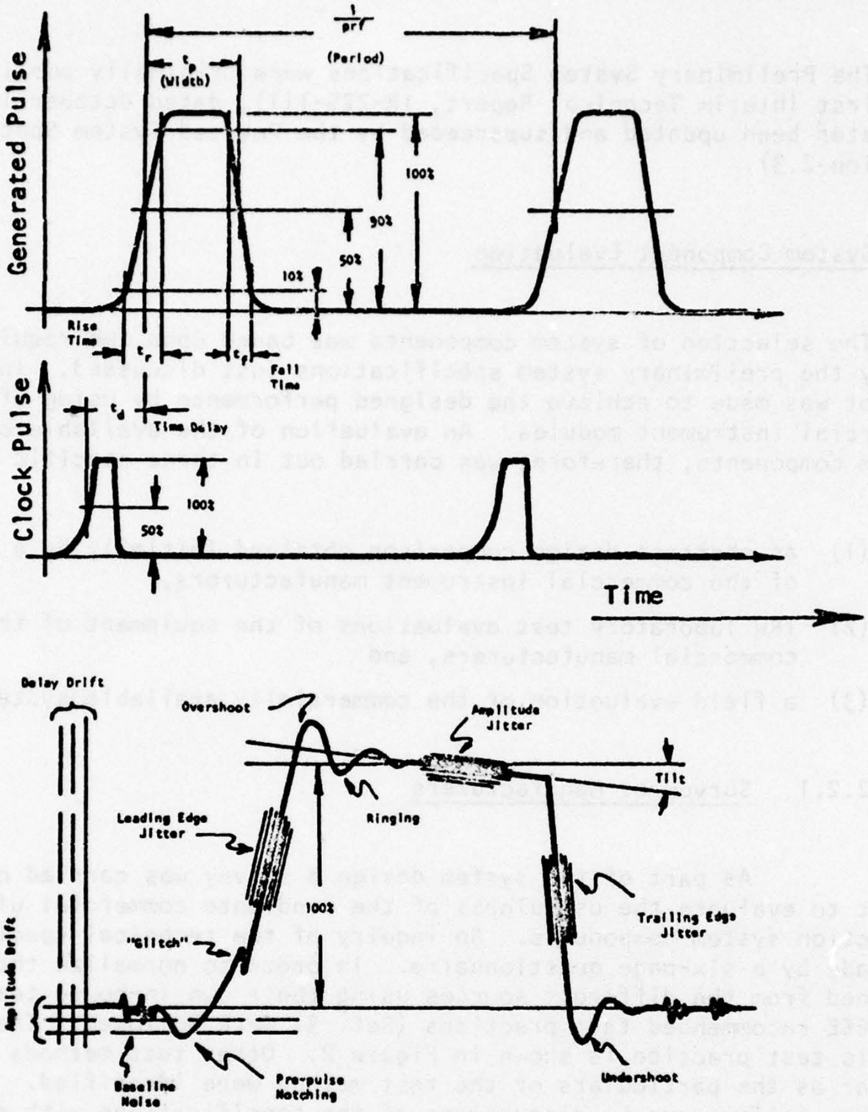


**Figure 2. Time Domain Parameters of a Pulse.**

A display of the information received is compiled in Tables I through V. Since the objective of the survey was to obtain instrument specifications in order to qualify them as candidate components to be used for the UDIS, the furnished information is presented here purely for technical specification comparison purposes. Unless otherwise specified, the data are normalized for easy comparison using the IEEE recommended test practices and the metric units of measurements. Blank spaces in the tables indicate information not furnished by the manufacturers.

### 2.2.2 Laboratory Evaluations

In addition to the survey of the manufacturers, TRW performed an extensive in-house laboratory evaluation on numerous available candidate system components. The laboratory test evaluations included those instrument characteristics which were important for the system performance of the UDIS. Some of these characteristics were already furnished to us by the manufacturers, others were not. Nevertheless, the laboratory evaluations were carried out, first, to confirm the information already on hand, and second, to establish variations in the production line produced commercial ultrasonic instruments from the specifications published. Most of these instruments evaluated were obtained from the manufacturers for a very short period of time on a loan basis specifically for the evaluation purpose.

A display of the instrument characteristics measured are compiled in Tables VI through X. Observing the same objectives described in the previous section of survey of manufacturers, the characteristics measured are presented in this report for comparison purposes only. Unless otherwise specified, the data are normalized for easy comparison using the IEEE recommended test practices (Ref. 3, and Figure 2) and the metric units of measurements. Most of the listed characteristics were measured with external laboratory test instrumentation, such as signal generator and oscilloscope, while maintaining proper impedance terminations. Blank spaces in the tables indicate characteristics which could not be measured due to limitations of available circuit diagrams and the loan time for evaluations.

TABLE I

SUMMARY OF COMMERCIAL ULTRASONIC SYSTEM COMPONENT EVALUATION FURNISHED BY MANUFACTURERS

Indicator/Display Units

| Instrument Evaluation Characteristics | Unit | Instrument Manufacturer A | B | C | D |
|---|---|---|---|---|---|
| Beam Position | | yes | yes | yes | yes (1) |
| Intensity | | yes | yes | yes | yes (1) |
| Focus | | yes | yes | yes | yes |
| Astigmatism | | yes | yes | yes | yes (1) |
| CRT Type | | NA | (2) | | |
| CRT Size | cm | 8x10 | 13.34 | 12.70 | |
| CRT Phosphor Type | | NA | P-31 | | |
| Display, Horizontal Scale | | cm | cm | inch | cm |
| Range | cm | 10 | 10 | 10.16 (3) | 10 |
| Increments | cm | 1 | 0.1 | 0.254 (3) | 0.1 |
| Accuracy | % FS | NA | 5 | | |
| Linearity | % FS | NA | 2 | | |
| Stability | % FS | NA | 10 | | |
| Display, Vertical Scale | | cm | inch | inch | inch |
| Range | cm | 8 | 6.35 (3) | 6.99 (3) | 6.35 (3) |
| Increments | cm | 0.8 | 0.635 (3) | 0.254 (3) | 1.27 (3) |
| Accuracy | % FS | | 2 | | |
| Linearity | % FS | | 3 | | |
| Stability | % FS | | 5 | | |
| Vertical Bandwidth | MHz | | 25.0 | | 25.0 |
| Horizontal Bandwidth | MHz | | 0.5 | | 0.5 |
| Other | | | | | |

Notes: (1) Internal control only
(2) Post accelerator
(3) Instrument display scale graduations are in inches, data shown are in centimeters

TABLE II

SUMMARY OF COMMERCIAL ULTRASONIC SYSTEM COMPONENT EVALUATION FURNISHED BY MANUFACTURERS

Sweep/Timer Units

| Instrument Evaluation Characteristics | Unit | Instrument Manufacturer A | B | C | D |
|---|---|---|---|---|---|
| Pulse Repetition Freq. | | | | | |
| Range | Hz | 100-2000 | 100-2000 | 100-5000 | 63-1000 |
| Accuracy | % FS | NA | | | |
| Linearity | % FS | NA | | | |
| Stability | % FS | NA | 5 | | |
| Other | | | | | |
| Sweep | | | | | |
| Range | µs/cm | | | 0.172-82.8 | |
| Accuracy | % FS | uncal | 5 | | |
| Linearity | % FS | 1.0 | 2 | | |
| Stability | % FS | NA | 10 | | |
| Other | | | | | |
| Delayed Sweep | | | | | |
| Range | µs | 0-1250 | 10-500 | 0-82 | |
| Accuracy | % FS | uncal. | 10 | | |
| Linearity | % FS | uncal. | | | |
| Stability | % FS | 1.0 | | | |
| Other | | | | | |
| Interface Sync. | | No | Yes | | |
| Marker Generator | | | | | |
| Type | | | | | |
| Range | µs | 0.4-64 | | 0-0.295 | |
| Accuracy | % FS | uncal. | | | |
| Linearity | % FS | uncal. | | | |
| Stability | % FS | 0.1 | | | |
| Other | | | | | |

TABLE III

SUMMARY OF COMMERCIAL ULTRASONIC SYSTEM COMPONENT EVALUATION FURNISHED BY MANUFACTURERS

Pulser Units

| Instrument Evaluation Characteristics | Unit | Instrument Manufacturer A | B | C |
|---|---|---|---|---|
| Type (tuned/dampened-undampened, cap. discharged, etc.) | | (1) | (2) | (3) |
| Frequency | MHz | | 2.25, 5.0 10.0 | 2.25, 5.0 10.0 |
| Accuracy | % FS | | NA | |
| Stability | % FS | | 2 | |
| Pulse Amplitude | | | | |
| Range | V | 300 | 400-600 | 2000 (4) |
| Accuracy | % FS | NA | NA | |
| Linearity | % FS | NA | NA | |
| Stability | % FS | NA | NA | |
| Pulse Rise Time (at 10-90%) Fixed or function of other parameters? | μs | 0.015 | 10-15 | 0.050 |
| Pulse Width (at 50-50%) Fixed or function of other parameters? | μs | NA | NA | |
| Pulse Fall Time (at 90-10%) Fixed or function of other parameters? | μs | NA | NA | |
| Pulse Overshoot (max.) Fixed or function of other parameters? | V | NA | $\leq$60 | |
| Pulse Undershoot (max.) Fixed or function of other parameters? | V | (5) | <60 | |
| Pulse Ringing (max.) Fixed or function of other parameters? | Hz | (5) | NA | |
| Pulse Jitter, Leading Edge Fixed or function of other parameters? | μs | | NA | |
| Pulse Jitter, Trailing Edge Fixed or function of other parameters? | μs | | NA | |
| Pulse Amplitude Jitter Fixed or function of other parameters? | V | | NA | |
| Output Impedance, Z or RC | Ω pF | | 1000, 2000 | |
| Synch. Frequency | Hz | | (6) | |

Notes: (1) Capacitor discharge (2) Tuned (3) Wideband (4) Open circuit (5) None with open circuit, depends on load (6) One-half of sweep repetition rate

TABLE IV

SUMMARY OF COMMERCIAL ULTRASONIC SYSTEM COMPONENT EVALUATION FURNISHED BY MANUFACTURERS

Receiver Units

| Instrument Evaluation Characteristics | Unit | Instrument Manufacturer A | B | C | D |
|---|---|---|---|---|---|
| Type (tuned, wideband, heterodyne) | | (1) | (2) | (2) | (1) |
| Input RC | Ω pF | 629, 800 | | | |
| Frequency, Center | MHz | 14 | 2.25, 5.0 10.0 | 2.25, 5.0 10.0 | |
| Accuracy | % FS | 3 | 0.5 MHz | | |
| Stability | % FS | | 10 | | |
| Bandwidth (-3dB below & above $f_n$) | MHz | 2-25 | 0.5 | (3) | |
| Sensitivity | μV | NA | NA | | |
| Range | μV | NA | NA | | |
| Accuracy | % FS | NA | NA | | |
| Linearity | % FS | 3 | NA | | |
| Noise (measured tangentially at full bandwidth while input terminated with a source resistance equal to the input 2) | μV | | NA | | |
| Recovery Time | μs | | | | |
| Pulser/Receiver Crosstalk | dB | -60 | -80 | -60 | |
| Other | | | | | |

Notes: (1) Wideband
(2) Tuned
(3) 1.0 MHz for 2.25 and 5.0 MHz center frequency bands; 2.0 MHz for 10.0 MHz center frequency band.

## TABLE V

## SUMMARY OF COMMERCIAL ULTRASONIC SYSTEM COMPONENT EVALUATION FURNISHED BY MANUFACTURERS

Gate Units

| Instrument Evaluation Characteristics | Unit | Instrument Manufacturer A | B | C | D |
|---|---|---|---|---|---|
| Gate Range, Start Time | μs | | (1) | 1.0-3000.0 | |
| Accuracy | % FS | NA | NA | | |
| Linearity | % FS | NA | NA | | |
| Stability | % FS | >0.1 | 3 | | |
| Resolution | μs | 0.1 | NA | | |
| Gate Range, Stop Time | μs | 0.05-1000.0 | 0.5-3000.0 | | |
| Accuracy | % FS | NA | NA | | |
| Linearity | % FS | NA | NA | | |
| Stability | % FS | 0.1 | 3 | | |
| Resolution | μs | 0.1 | NA | | |
| Delayed Gate, Range | μs | | 0-400 | | |
| Accuracy | % FS | | NA | | |
| Linearity | % FS | | NA | | |
| Stability | % FS | >0.1 | NA | | |
| Sensitivity | μV | (2) | (3) | | |
| Range | μV | NA | | | |
| Accuracy | % FS | 5 | NA | | |
| Linearity | % FS | 5 | NA | | |
| Stability | % FS | 2 | NA | | |
| Response Time | ns | 100 | NA | | |
| Accuracy | % FS | | NA | | |
| Stability | % FS | | NA | | |
| Output for Display | V | 0-10 | NA | | |

(continued)

6130 C

TABLE V (CONT'D)

SUMMARY OF COMMERCIAL ULTRASONIC SYSTEM COMPONENT
EVALUATION FURNISHED BY MANUFACTURERS

Gate Units

| Instrument Evaluation Characteristics | Unit | Instrument Manufacturer A | B | C | D |
|---|---|---|---|---|---|
| Analog Output for External Use | | | NA | | |
| Amplitude | V | 0≥10 | 0-12.0 | 0-2.5 | |
| Accuracy | % FS | 5 | 5 | | |
| Stability | % FS | 2 | 3 | | |
| Rise Time | ηs | 100 | NA | | |
| Duration | ηs | (4) | (4) | | |
| Current | mA | 20 | (5) | | |
| Accuracy | % FS | NA | NA | | |
| Stability | % FS | NA | NA | | |
| Rise Time | ηs | NA | NA | | |
| Duration | ηs | NA | NA | | |
| Digital Output for External Use | | | | | |
| Code | | NA | | | |
| Amplitude | V | | 0-10 | | |

Notes:
(1) Variable from before to 1000 μs after initial pulse
(2) One-half of vertical display scale division
(3) 6 volts video in triggered on 0.2V
(4) One of pulse repetition rate
(5) 1.0 kΩ output impedance

TABLE VI

SUMMARY OF TRW LABORATORY EVALUATIONS
OF COMMERCIAL ULTRASONIC SYSTEM COMPONENTS

Indicator/Display Units

| Instrument Evaluation Characteristics | Unit | Instrument Manufacturer $A_1$ | $A_2$ | D | $B_1$ | $B_2$ | C |
|---|---|---|---|---|---|---|---|
| Beam Position | | yes | yes | yes (1) | yes | yes | yes |
| Intensity | | yes | yes | yes (1) | yes | yes | yes |
| Focus | | yes | yes | yes (1) | yes | yes | yes |
| Astigmatism | | yes | yes | yes (1) | yes | yes | yes |
| CRT Type | | (2) | (2) | | | | |
| CRT Size | cm | 8x10 | 8x10 | 12.70 | | 13.345 | 12.70 |
| CRT Phosphor Type | | P-31 | P-31 | | P-31 | | |
| Display, Horizontal Scale | | cm | cm | cm | cm | inch | inch |
| Range | cm | 10 | 10 | 10 | 10 | 7.62 (3) | 8.890 |
| Increments | cm | 0.2 | 0.2 | 0.2 | 0.2 | 0.64 (3) | 0.254 |
| Accuracy | % FS | | | | | | |
| Linearity | % FS | | | | | | |
| Stability | % FS | | | | | | |
| Display, Vertical Scale | | cm | cm | inch | inch | inch | inch |
| Range | cm | 8 | 8 | 5.08 (3) | 6.35 (3) | 7.62 (3) | 10.16 |
| Increments | cm | 0.2 | 0.2 | 1.27 (3) | 0.64 (3) | 2.54 (3) | 0.254 |
| Accuracy | % FS | | | | | | |
| Linearity | % FS | | | | | | |
| Stability | % FS | | | | | | |
| Vertical Bandwidth | MHz | 10 | 10 | | | | |
| Horizontal Bandwidth | MHz | 30 | 30 | | | | |
| Other | | | | | | | |

Notes: (1) Internal control only
(2) Post accelerator
(3) Instrument display scale graduations are in inches, data shown are in centimeters

TABLE VII

SUMMARY OF TRW LABORATORY EVALUATIONS
OF COMMERCIAL ULTRASONIC SYSTEM COMPONENTS

Sweep/Timer Units

| Instrument Evaluation Characteristics | Unit | Instrument Manufacturer $A_1$ | $A_2$ | D | $B_1$ | $B_2$ | C |
|---|---|---|---|---|---|---|---|
| Pulse Repetition Freq. | | | | | | | |
| Range | Hz | 78.1-2000 | 73.5-2272 | 50-3200 | 178.5-9756.0 | 444.0-8510.6 | 181-9090 |
| Accuracy | % FS | | | | | | |
| Linearity | % FS | | | | | | |
| Stability | | | | | | | |
| Other | | | | | | | |
| Sweep | | | | | | | |
| Range | μs | 7-4000 | 6-2800 | | 50-310 | 1.6-15,600 | 20-2950 |
| Accuracy | % FS | | | | | | |
| Linearity | % FS | | | | | | |
| Stability | % FS | | | | | | |
| Other | | | | | | | |
| Delayed Sweep | | | | | | | |
| Range | μs | 0-1650 | 0-1575 | | 0-1654 | 0-2279 | 0-475 |
| Accuracy | % FS | | | | | | |
| Linearity | % FS | | | | | | |
| Stability | % FS | | | | | | |
| Other | | | | | | | |
| Interface Sync. | | no | no | no | yes | yes | yes |
| Marker Generator | | | | | | | |
| Type | | | | | | | |
| Range | μs | | | | | | |
| Accuracy | % FS | | | | | | |
| Linearity | % FS | | | | | | |
| Stability | % FS | | | | | | |
| Other | | | | | | | |

TABLE VIII

SUMMARY OF TRW LABORATORY EVALUATIONS
OF COMMERCIAL ULTRASONIC SYSTEM COMPONENTS

Pulser Units

| Instrument Evaluation Characteristics | Unit | Instrument Manufacturer $A_1$ | $A_2$ | D | $B_1$ | $B_2$ | C |
|---|---|---|---|---|---|---|---|
| Type (tuned/dampened-undampened, cap. discharged, etc.) | | (1) | (1) | (2) | (2) | (2) | (1) |
| Frequency | MHz | | | 1.0, 2.0, 4.0, 8.0 | 1.0, 2.25, 5.0, 10.0 | 1.0, 2.25, 10.0 | |
| Accuracy | % FS | | | | | | |
| Stability | % FS | | | | | | |
| Pulse Amplitude | | | | | | | |
| Range | V | 540-570 | 230-260 | 150-170 | 1200 | 1250 | 200-1060 |
| Accuracy | % FS | | | | | | |
| Linearity | % FS | | | | | | |
| Stability | % FS | | | | | | |
| Pulse Rise Time (at 10-90%) Fixed or function of other parameters? | μs | 0.01 | 0.05 | 0.05 | 0.025 | 0.015 | 0.015 |
| Pulse Width (at 50-50%) Fixed or function of other parameters? | μs | 0.10 | 0.22 | 0.28 | 0.022 | 0.045 | 0.210 |
| Pulse Fall Time Fixed or function of other parameters? | μs | 0.32 | 0.56 | 1.0 | 0.42 | 0.015 | 0.32 |
| Pulse Overshoot (max.) Fixed or function of other parameters? | V | none | none | none | none | none | none |
| Pulse Undershoot (max.) Fixed or function of other parameters? | V | none | none | none | none | none | none |
| Pulse Ringing (max.) Fixed or function of other parameters? | Hz | none | none | some | none | none | none |
| Pulse Jitter, Leading Edge Fixed or function of other parameters? | μs | none | none | none | none | none | none |
| Pulse Jitter, Trailing Edge Fixed or function of other parameters? | μs | some | none | none | none | none | none |
| Pulse Amplitude Jitter Fixed or function of other parameters? | V | none | none | none | none | none | none |
| Output Impedance, Z or RC | ΩpF | | | | | | |
| Synch. Frequency | Hz | | | | | | |

Notes: (1) Capacitor discharge
(2) Tuned

TABLE IX

SUMMARY OF TRW LABORATORY EVALUATIONS
OF COMMERCIAL ULTRASONIC SYSTEM COMPONENTS

Receiver Units

| Instrument Evaluation Characteristics | Unit | Instrument Manufacturer $A_1$ | $A_2$ | D | $B_1$ | $B_2$ | C |
|---|---|---|---|---|---|---|---|
| Type (tuned, wideband, heterodyne) | | (1) | (1) | (2) | (2) | (2) | (2) |
| Input RC | ΩpF | 1M | 1M | | | | 47K |
| Frequency, Center | MHz | 3.0 | 2.9 | 2.5 | 3.95 | 4.5 | 5.0 |
| Accuracy | % FS | | | | | | |
| Stability | % FS | | | | | | |
| Bandwidth (-3dB below & above $f_n$) | MHz | 1.4 | 1.85 | 2.15 | 0.7 | 1.0 | 1.5 |
| Sensitivity | | | | | | | |
| Range | μV | 24.24-1777.0 | 33.73-2323.0 | (3) | 50-1600 | ~40.0 | 90-1600 |
| Accuracy | % FS | | | | | | |
| Linearity | % FS | | | | | | |
| Noise (measured tangentially at full bandwidth while input terminated with a source resistance equal to the input R) | μV | ≤16 | ≤18 | ≤1000 | ≤24,900 | | ≤3400 |
| Recovery Time | μs | | | | | | |
| Pulser/Receiver Crosstalk | dB | -30 | | | +10 | | -27 |
| Other | | | | | | | |

Notes: (1) Wideband
(2) Tuned
(3) 78.0μV, 48.2μV and 103.0μV at 5.0, 3.5 and 2.25 MHz frequencies, respectively.

TABLE X

SUMMARY OF TRW LABORATORY EVALUATIONS
OF COMMERCIAL ULTRASONIC SYSTEM COMPONENTS

Gate Units

| Instrument Evaluation Characteristics | Unit | $A_1$ | $A_2$ | D | $B_1$ | $B_2$ | C |
|---|---|---|---|---|---|---|---|
| Gate Range, Start Time | μs | | | | 0.28-2900 | 0.65-3000 | (1) |
| Accuracy | % FS | | | | | | |
| Linearity | % FS | | | | | | |
| Stability | % FS | | | | | | |
| Resolution | μs | | | | | | |
| Gate Range, Stop Time | μs | | | | 0.37-1550 | 0.775-6500 | 0.35-2850 |
| Accuracy | % FS | | | | | | |
| Linearity | % FS | | | | | | |
| Stability | % FS | | | | | | |
| Resolution | μs | | | | | | |
| Delayed Gate, Range | μs | | | | 0-1654.0 | | |
| Accuracy | % FS | | | | | | |
| Linearity | % FS | | | | | | |
| Stability | % FS | | | | | | |
| Sensitivity | μV | | | | | | |
| Range | μV | | | | | | |
| Accuracy | % FS | | | | | | |
| Linearity | % FS | | | | | | |
| Stability | % FS | | | | | | |
| Response Time | ns | | | | | | |
| Accuracy | % FS | | | | | | |
| Stability | % FS | | | | | | |
| Output for Display | V | | | | | | |

(continued)

TABLE X (CONT'D)

SUMMARY OF TRW LABORATORY EVALUATIONS
OF COMMERCIAL ULTRASONIC SYSTEM COMPONENTS

Gate Units

| Instrument Evaluation Characteristics | Unit | Instrument Manufacturer $A_1$ | $A_2$ | D | $B_1$ | $B_2$ | C |
|---|---|---|---|---|---|---|---|
| Analog Output for External Use | | | | | | | |
| Amplitude | V | | | | | | |
| Accuracy | % FS | | | | | | |
| Stability | % FS | | | | | | |
| Rise Time | ns | | | | | | |
| Duration | ns | | | | | | |
| Current | mA | | | | | | |
| Accuracy | % FS | | | | | | |
| Stability | % FS | | | | | | |
| Rise Time | ns | | | | | | |
| Duration | ns | | | | | | |
| Digital Output for External Use | | | | | | | |
| Code | | | | | | | |
| Amplitude | | | | | | | |

In addition to the tables, further information is given by Figures 3 through 20. The electric output of the pulser units are shown by oscilloscope photographs displayed in Figures 3 through 14. Also, the frequency response of the receiver units around the center frequency of interest are plotted in Figures 15 through 20.

### 2.2.3 Field Evaluations

Beside the laboratory evaluations of the candidate instrument components, four commercial ultrasonic instrumentation systems were obtained on a loan basis and were evaluated in the subcontractor RMI Company's production floor mill environment using three eight-inch diameter and one 16-inch diameter titanium billets. The field evaluation was aimed to cover both instrumentation and material effects or variabilities. Accordingly, each of the four titanium billets were inspected repeatedly, using the four different commercial instrument systems. Detailed account of the results, because they are highly material related, is given in Section 4.3.1 - Phase I Effort of Materials Evaluations.

The four commercial ultrasonic instrument systems used in the field evaluation effort were also investigated to establish their area-amplitude characteristics or vertical cathode ray tube display linearity. The established method of ASTM Recommended Practice, Designation E-127 has been used for this purpose. The method relies on the pulses reflected back by known size spherical reflectors. By maintaining a uniform water couplant distance between the transducer and the reflector top surface points, and setting the instrument sensitivity to obtain an indication whose amplitude is 50% of the maximum amplitude indication that the instrument can display for the 0.5-inch diameter spherical reflector the test is performed by plotting the back reflection amplitudes obtained from the rest of the spherical reflectors. Graphs of the ultrasonic instrument responses versus the diameter of the spherical reflectors as area-amplitude responses are shown in Figures 21 through 24 for the instrumentation system "A3", "B1", "C" and "D2" respectively.

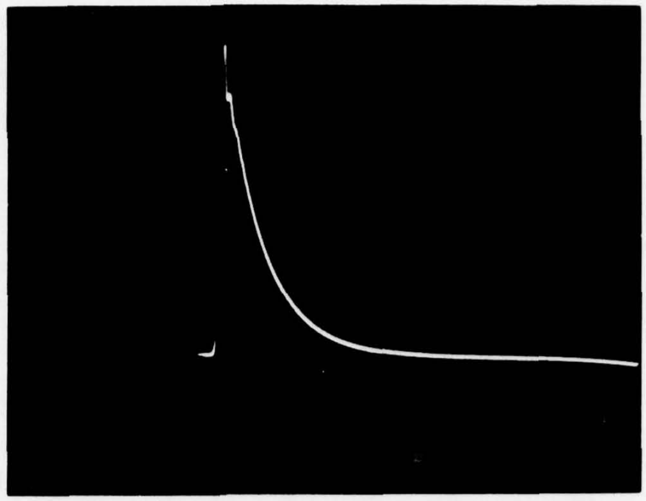

Figure 3. Pulser Output of Component Manufacturer $A_1$ in Pulse-Reflection Instrument Mode. (Vertical Display: 100.0 V/cm Horizontal Display: 0.2 μs/cm)

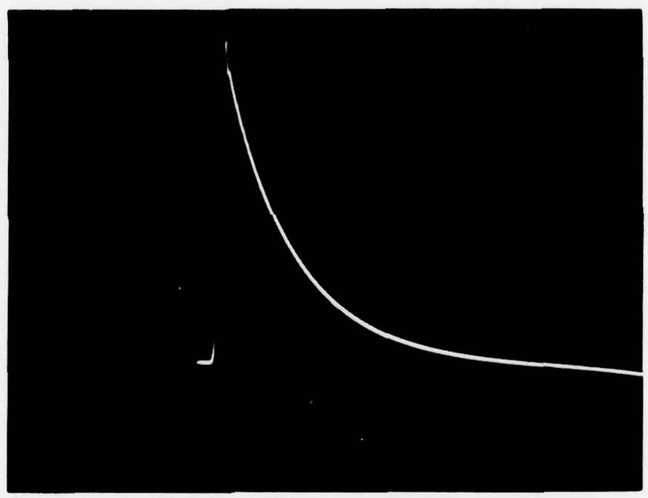

Figure 4. Pulser Output of Component Manufacturer $A_1$ in Thru-Transmission Instrument Mode. (Vertical Display: 100.0 V/cm Horizontal Display: 0.2 μs/cm)

2160 C

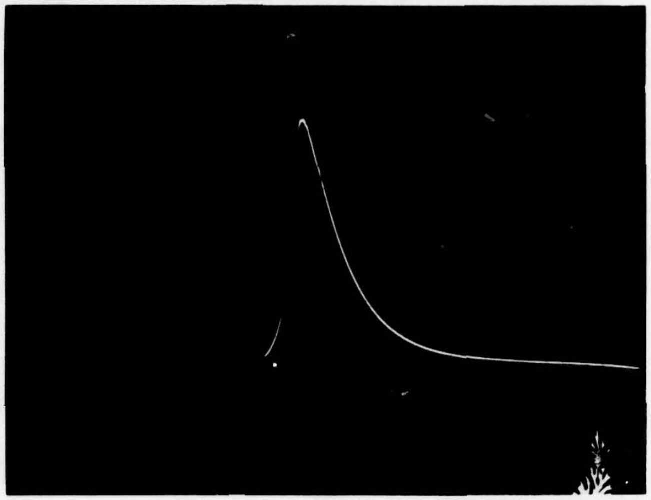

Figure 5. Pulser Output of Component Manufacturer $A_2$ in Pulse-Reflection Instrument Mode. (Vertical Display: 50.0 V/cm Horizontal Display: 0.2 μs/cm)

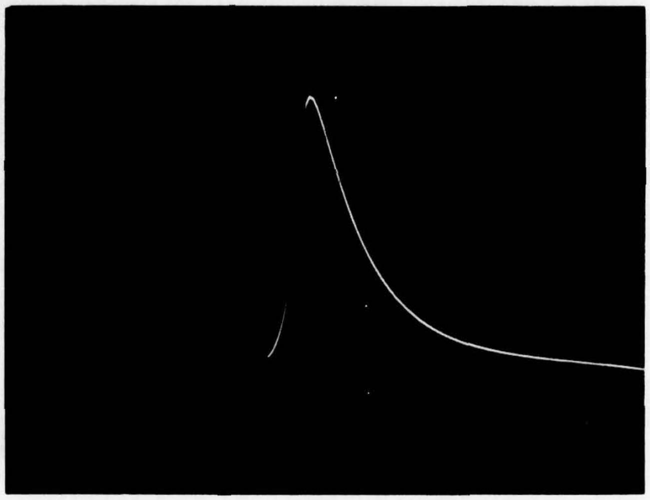

Figure 6. Pulser Output of Component Manufacturer $A_2$ in Thru-Transmission Instrument Mode. (Vertical Display: 50.0 V/cm Horizontal Display: 0.2 μs/cm)

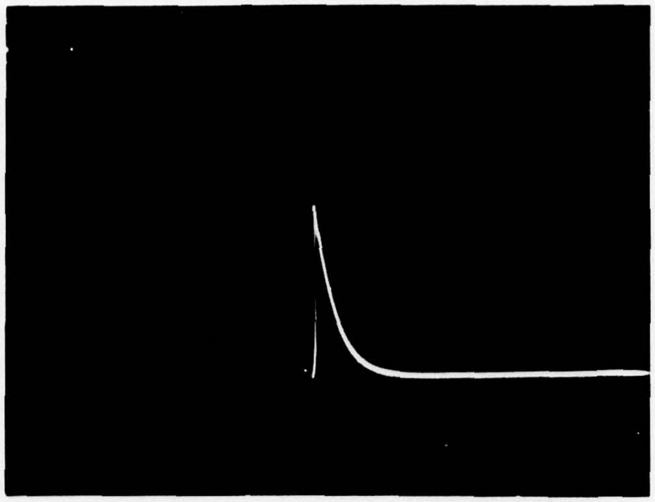

Figure 7. Pulser Output of Component Manufacturer D in Pulse-Reflection Instrument Mode. (Vertical Display: 50.0 V/cm Horizontal Display: 1.0 μs/cm)

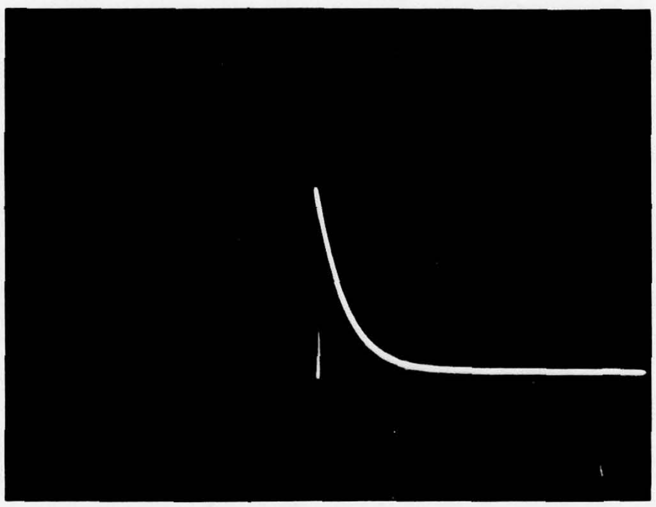

Figure 8. Pulser Output of Component Manufacturer D in Thru-Transmission Instrument Mode. (Vertical Display: 50.0 V/cm Horizontal Display: 1.0 μs/cm)

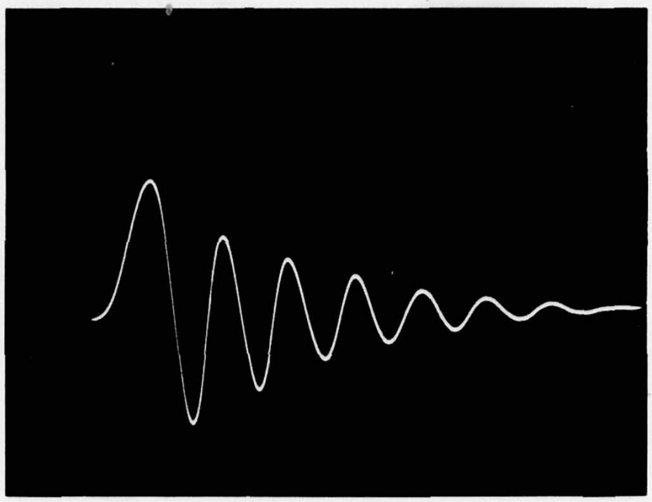

Figure 9. Pulser Output of Component Manufacturer $B_1$ in Pulse-Reflection Instrument Mode. (Vertical Display: 500.0 V/cm Horizontal Display: 0.1 μs/cm)

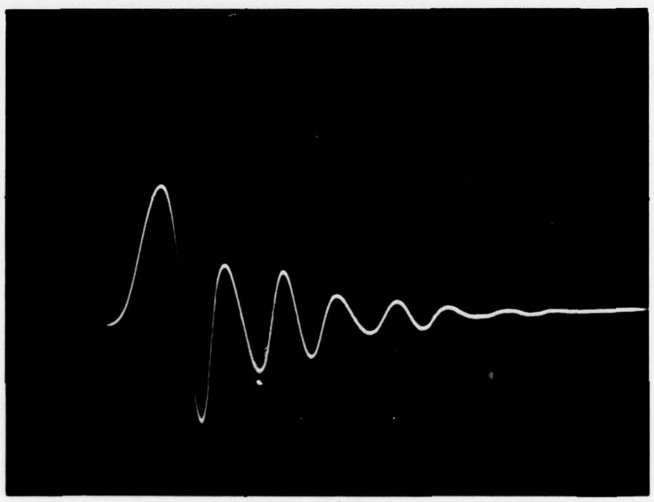

Figure 10. Pulser Output of Component Manufacturer $B_1$ in Thru-Transmission Instrument Mode. (Vertical Display: 500.0 V/cm Horizontal Display: 0.1 μs/cm)

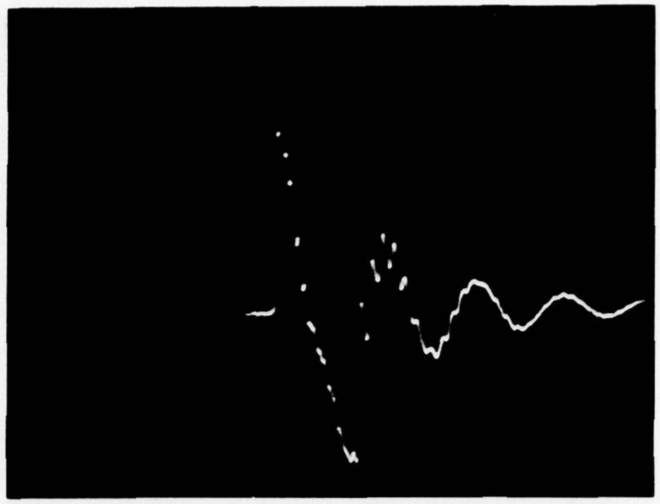

Figure 11. Pulser Output of Component Manufacturer $B_2$ in Pulse-Reflection Instrument Mode. (Vertical Display: 100.0 V/cm Horizontal Display: 0.1 μs/cm)

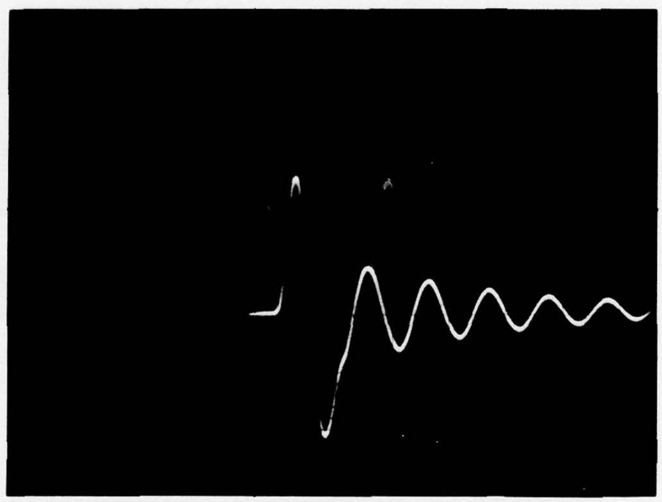

Figure 12. Pulser Output of Component Manufacturer $B_2$ in Thru-Transmission Instrument Mode. (Vertical Display: 500.0 V/cm Horizontal Display: 0.1 μs/cm)

2164 c

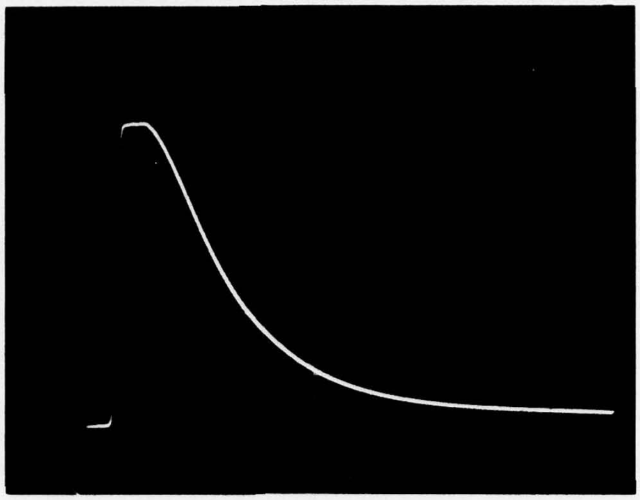

Figure 13. Pulser Output of Component Manufacturer C in Pulse-Reflection Instrument Mode. (Vertical Display: 200.0 V/cm Horizontal Display: 0.1 μs/cm)

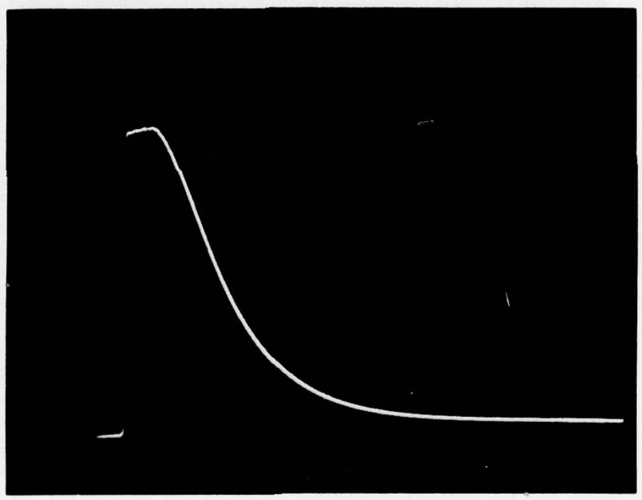

Figure 14. Pulser Output of Component Manufacturer C in Thru-Transmission Instrument Mode. (Vertical Display: 200.0 V/cm Horizontal Display: 0.1 μs/cm)

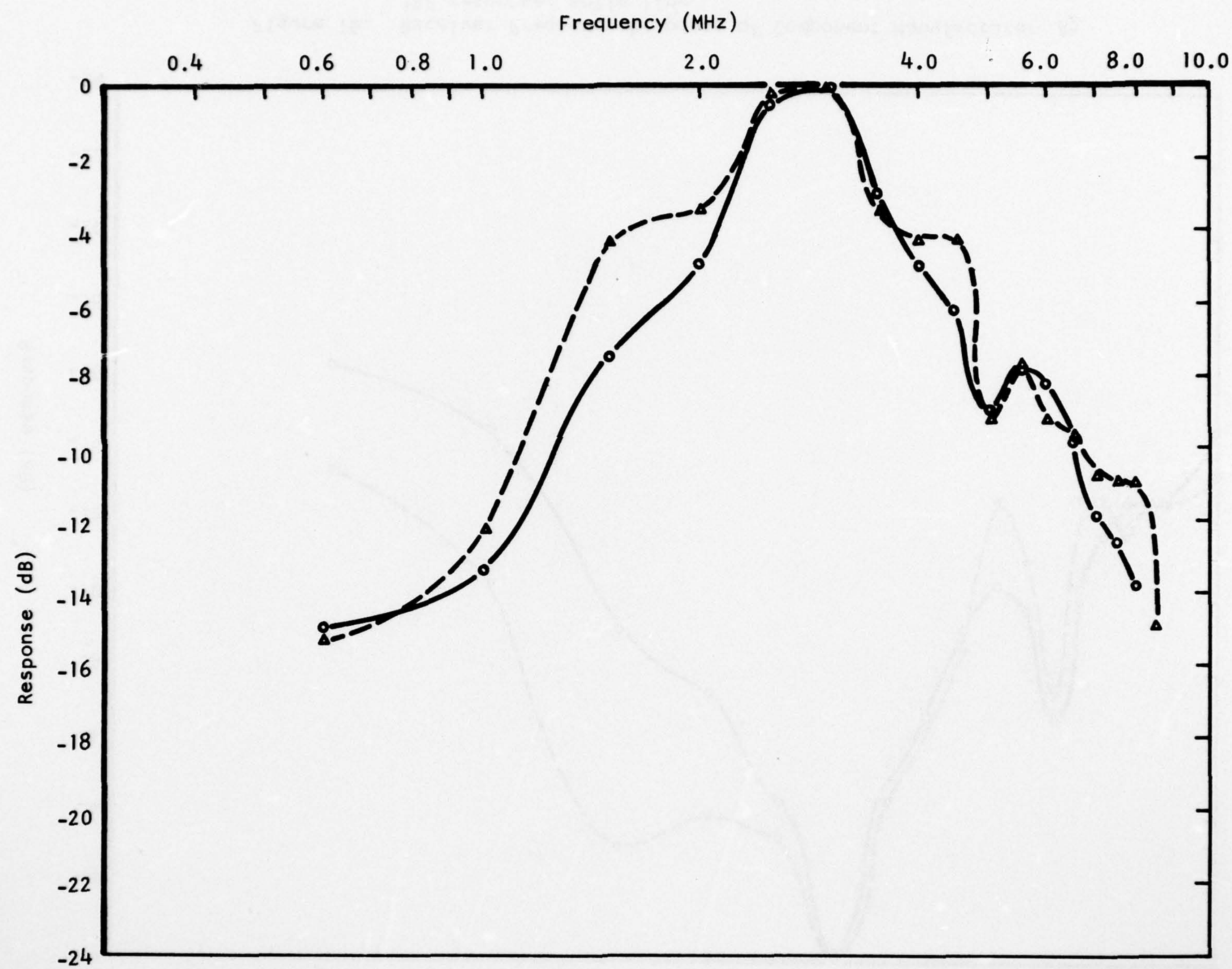


Figure 15. Receiver Frequency Response of Component Manufacturer $A_1$
(RF response: solid line
Video response: dashed line)

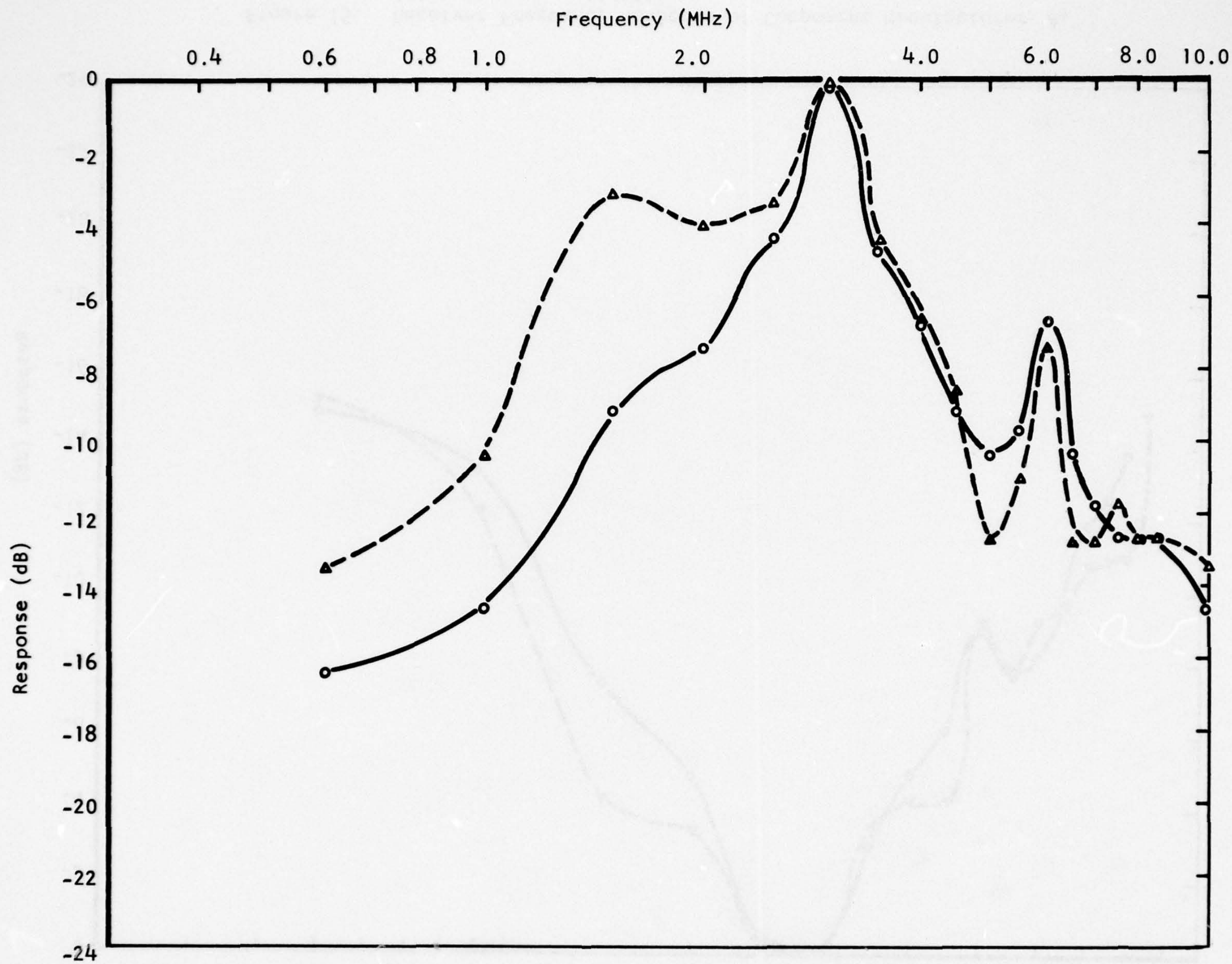


Figure 16. Receiver Frequency Response of Component Manufacturer $A_2$
(RF response: solid line
Video response: dashed line)

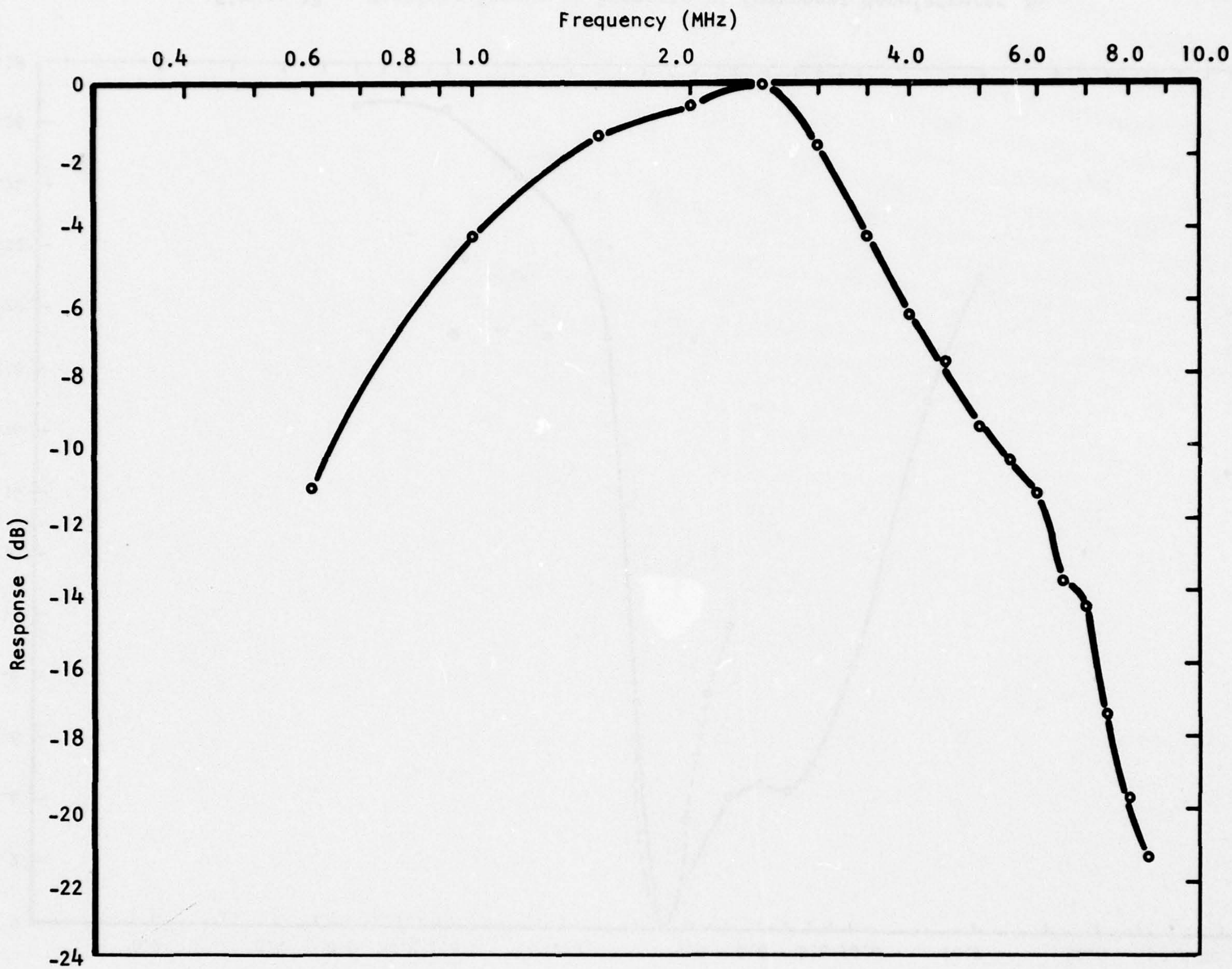


Figure 17. Receiver Frequency Response of Component Manufacturer D (RF response)

3698 c

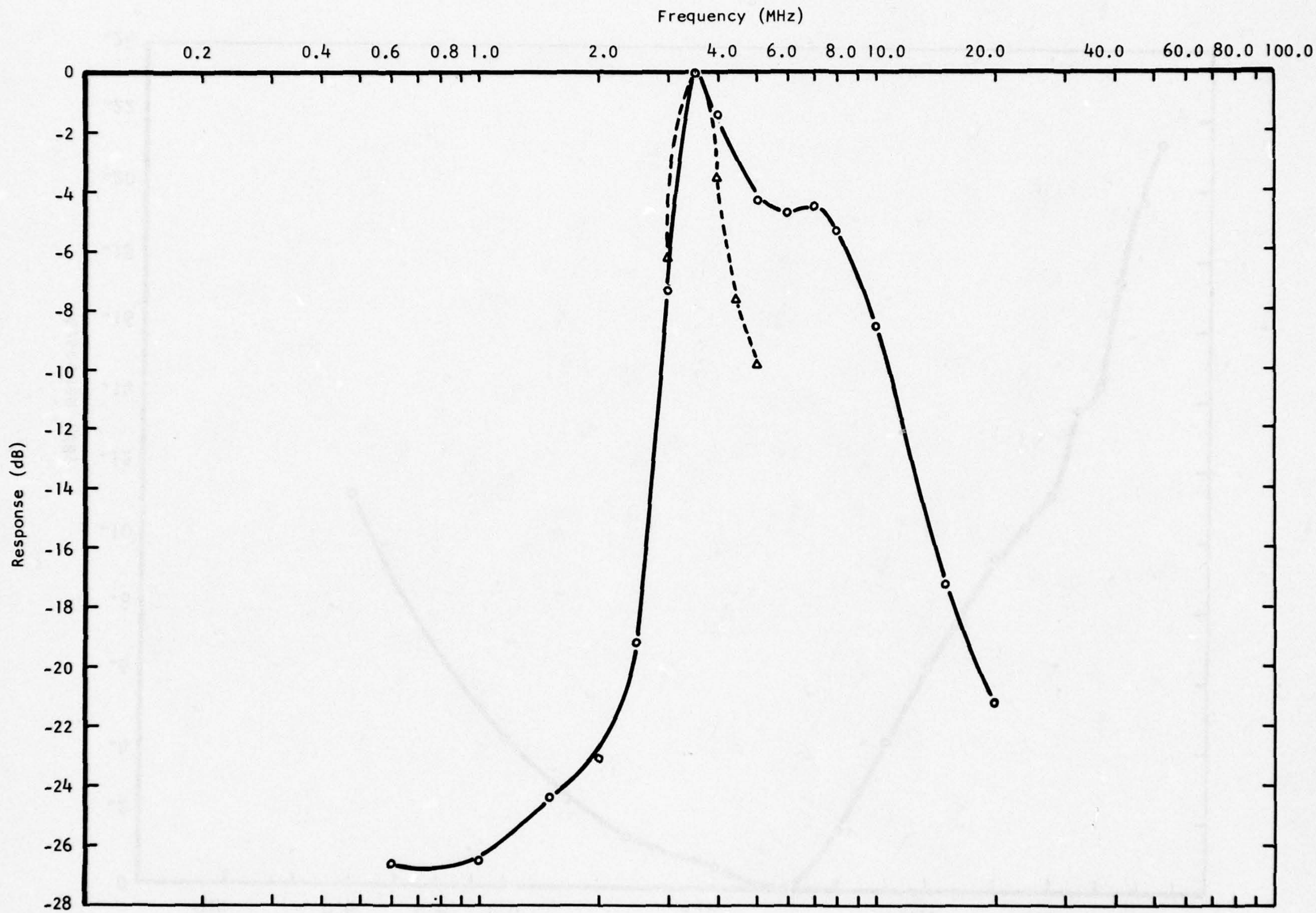


Figure 18. Receiver Frequency Response of Component Manufacturer $B_1$.
(RF response: solid line
Video response: dashed line)

3723 C

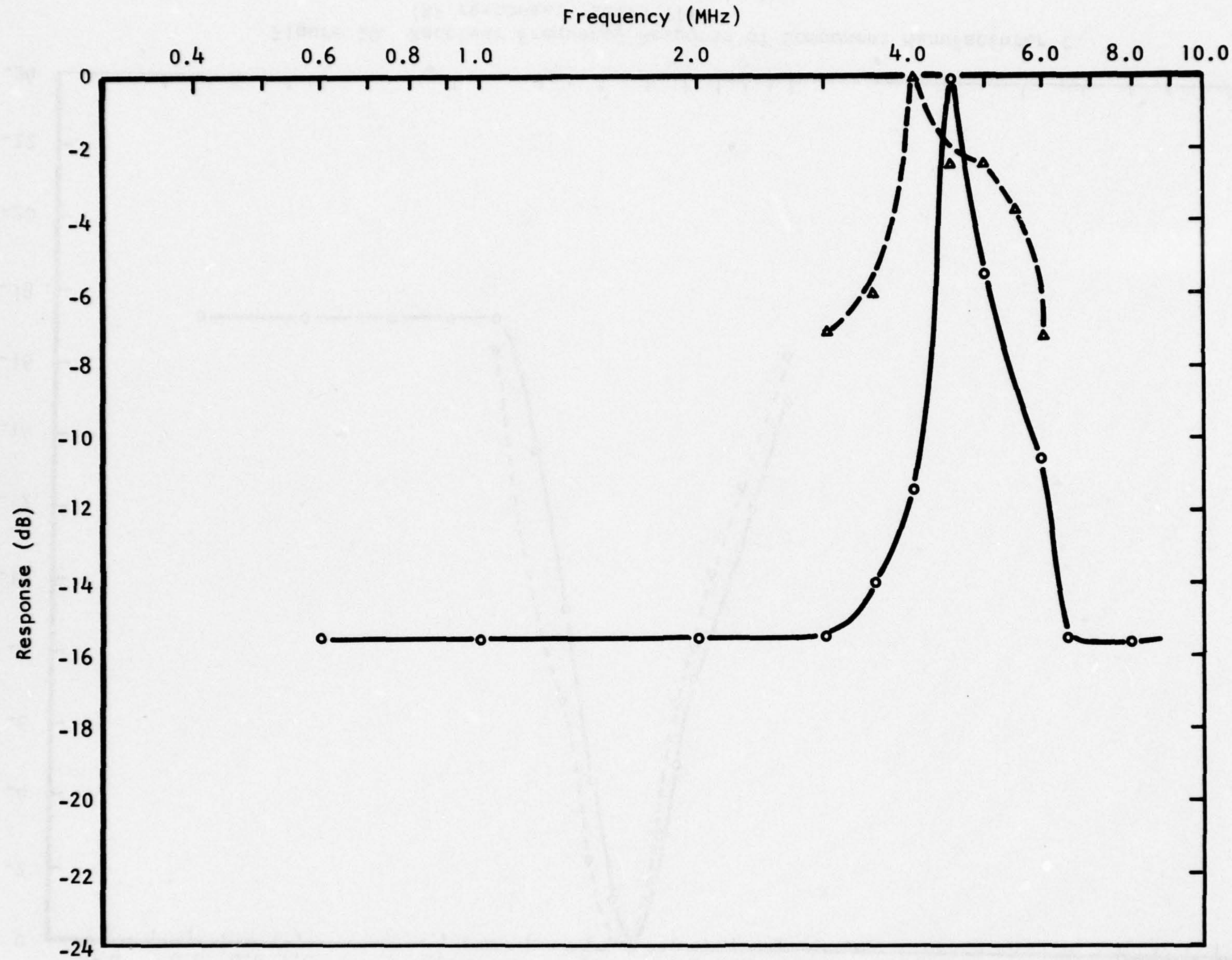


Figure 19. Receiver Frequency Response of Component Manufacturer $B_2$
(RF response: solid line
Video response: dashed line)

3699 C

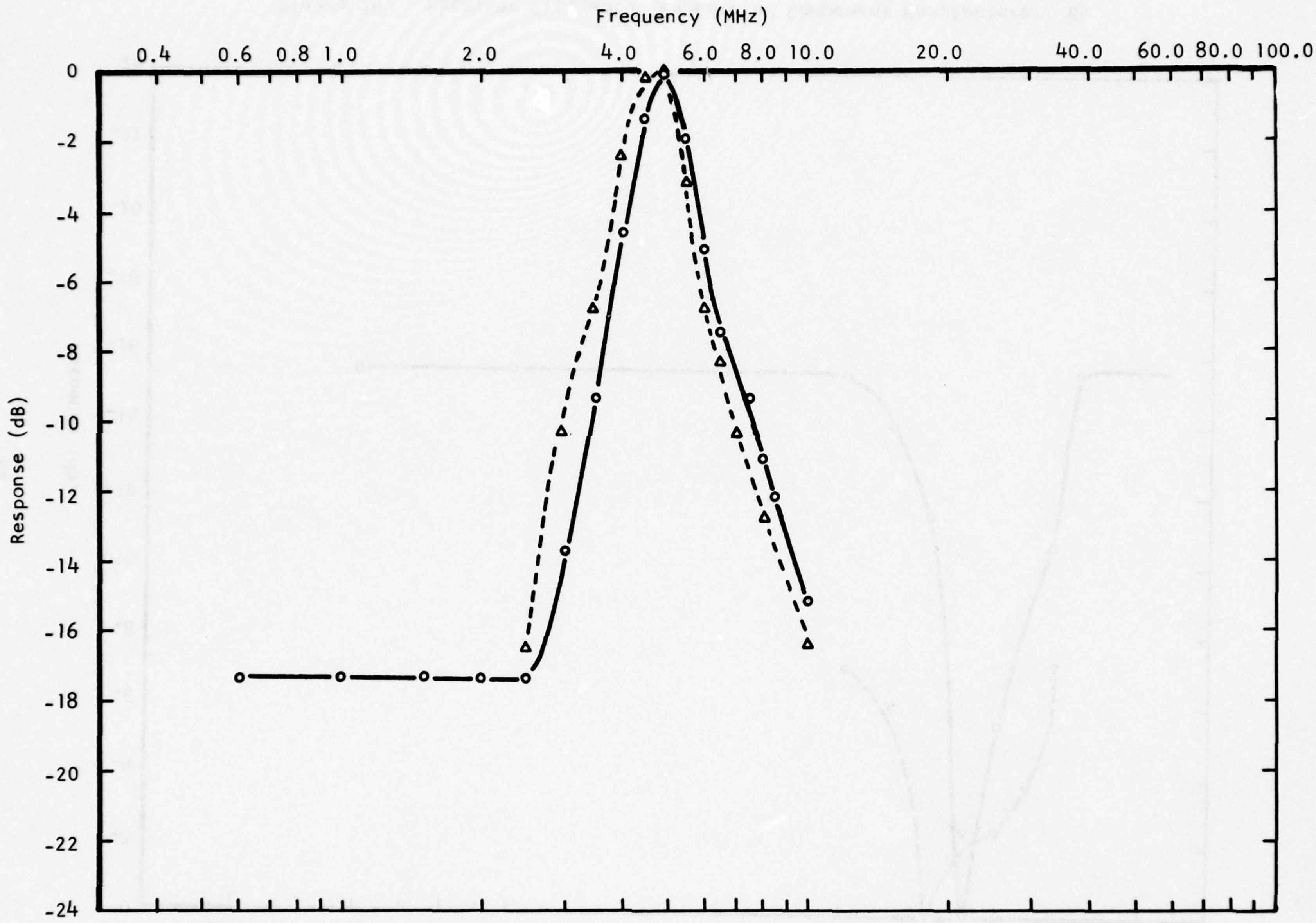


Figure 20. Receiver Frequency Response of Component Manufacturer C.
(RF response: solid line
Video response: dashed line)

3774 c

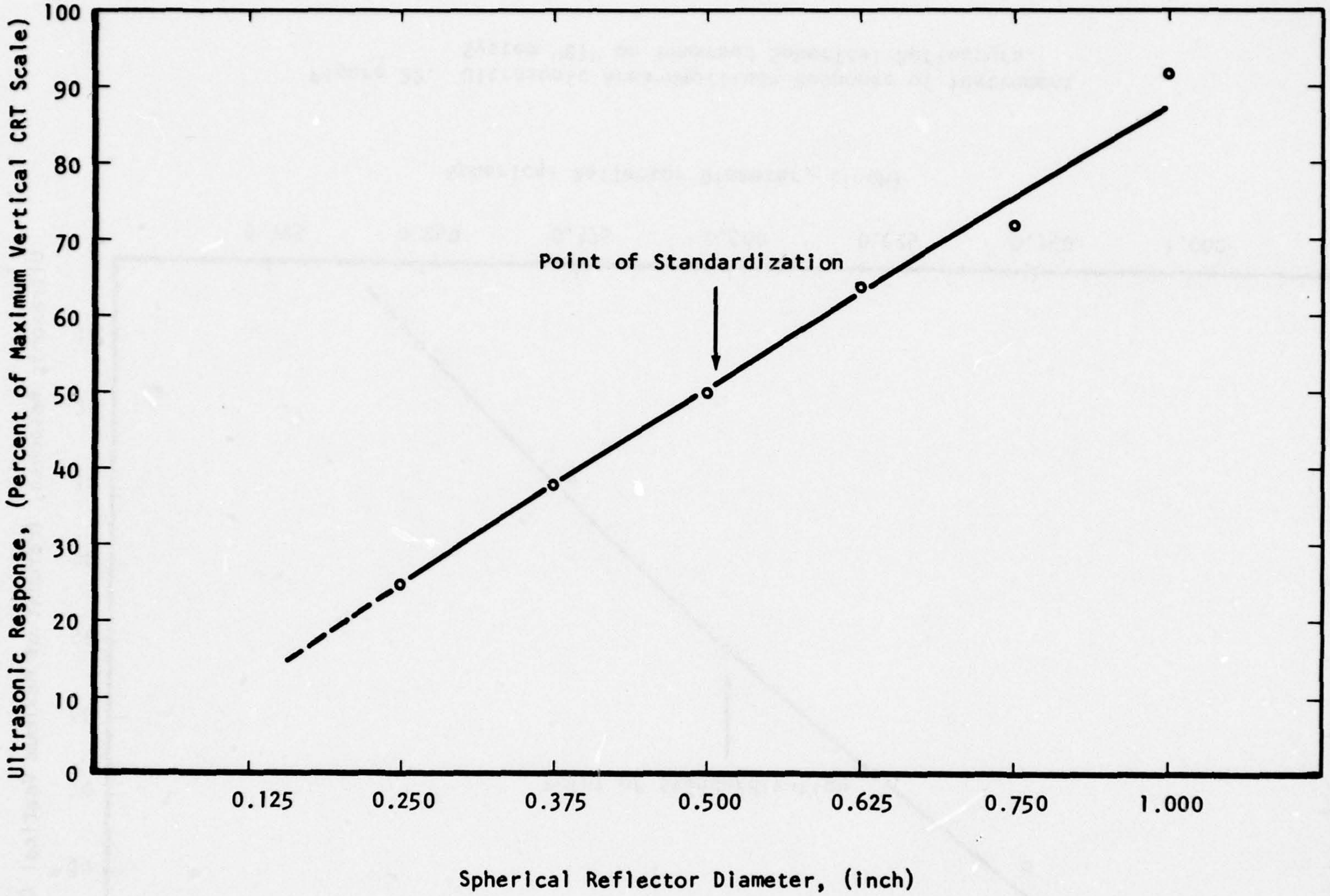


Figure 21. Ultrasonic Area-Amplitude Response of Instrument System "A3" on Immersed Spherical Reflectors.

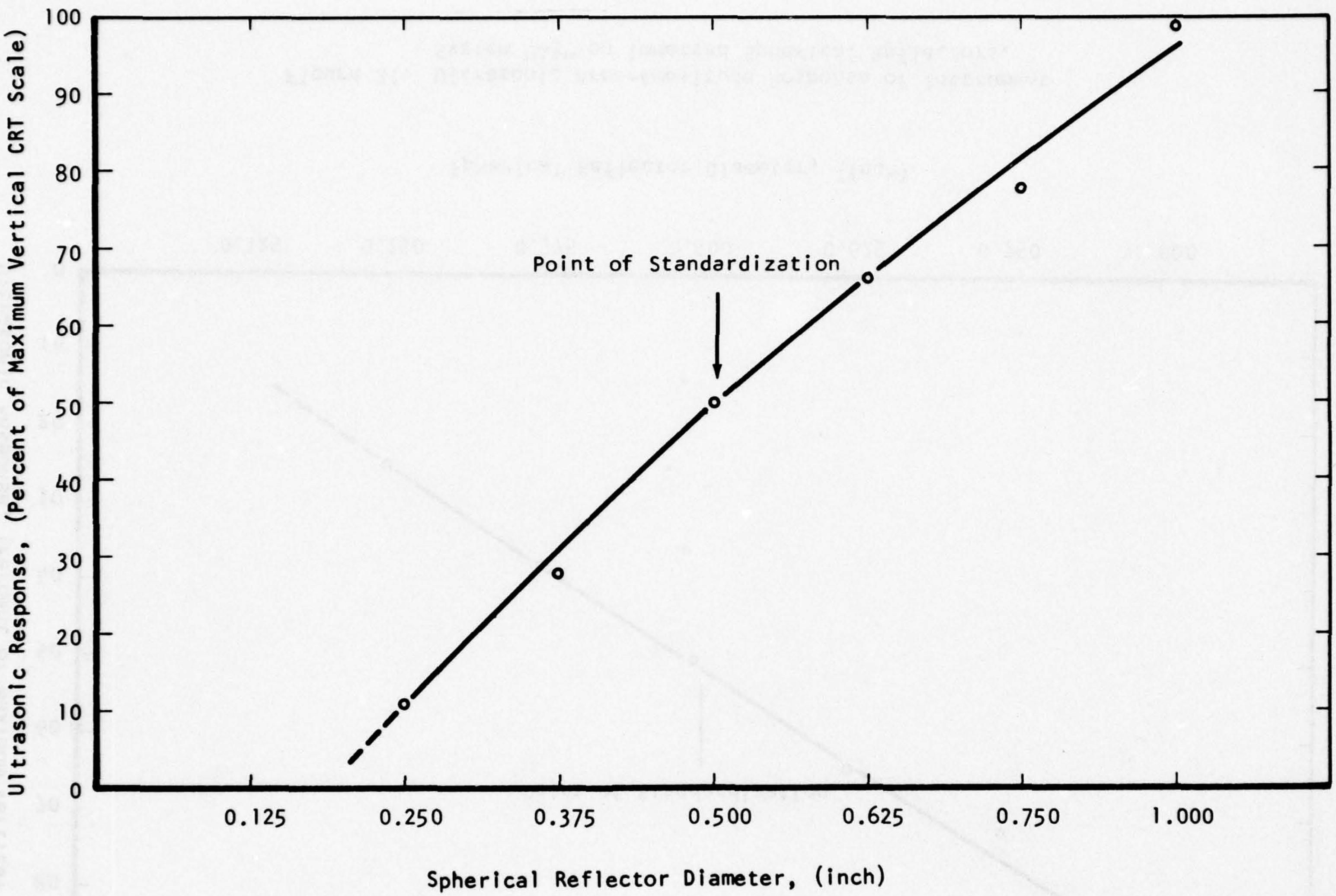


Figure 22. Ultrasonic Area-Amplitude Response of Instrument System "B1" on Immersed Spherical Reflectors.

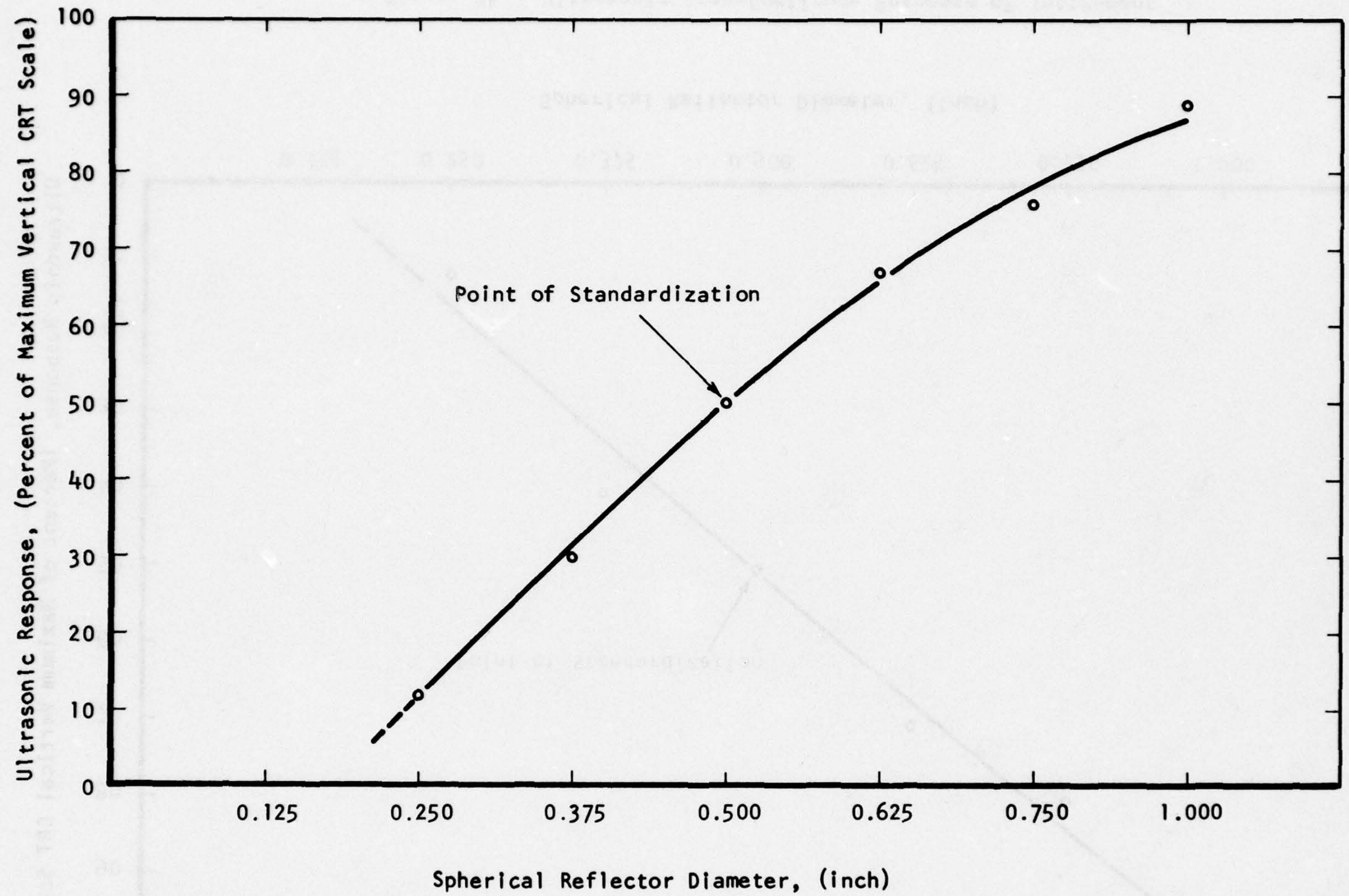


Figure 23. Ultrasonic Area-Amplitude Response of Instrument System "C" on Immersed Spherical Reflectors.

3776 C

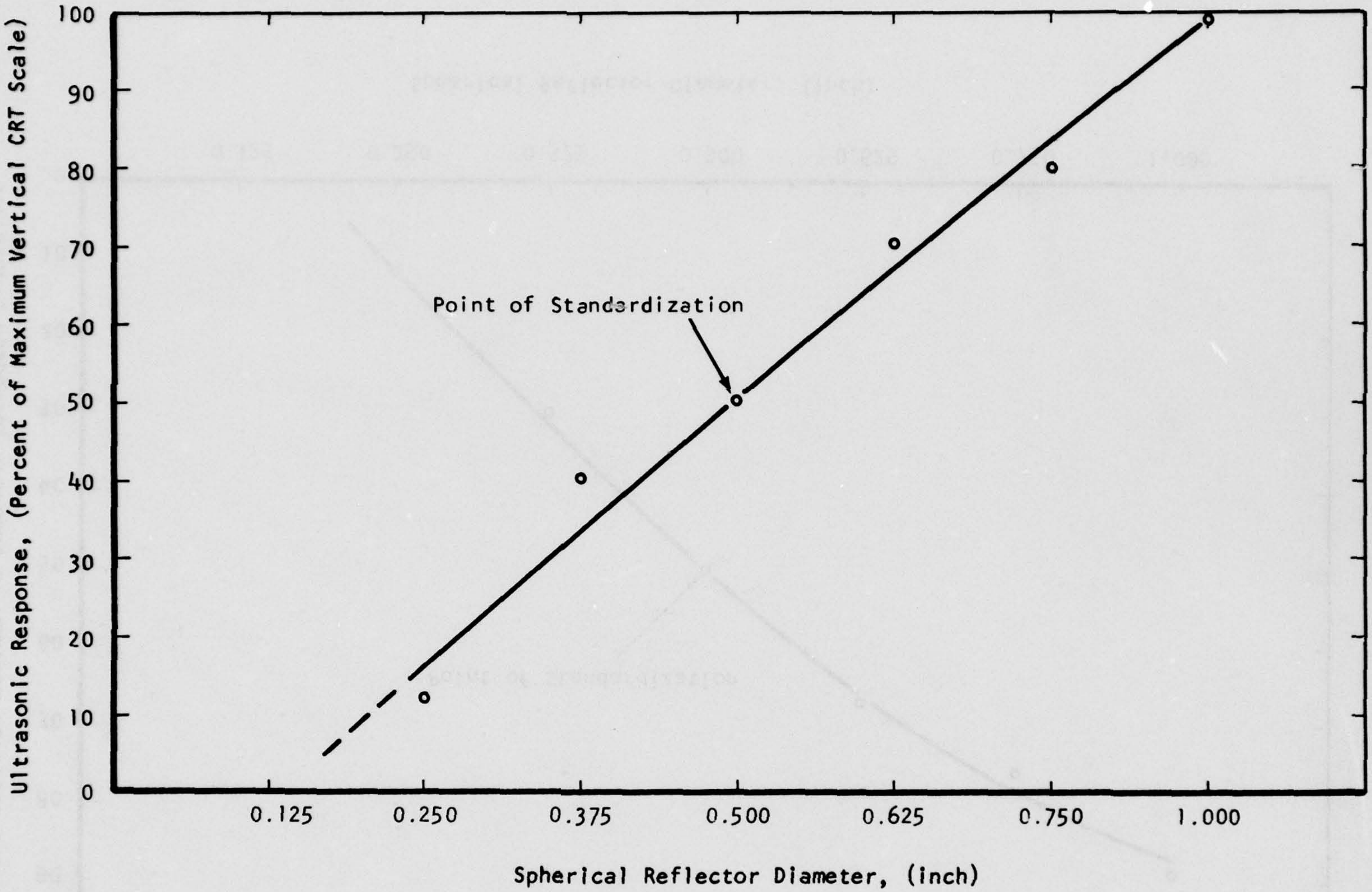


Figure 24. Ultrasonic Area-Amplitude Response of Instrument System "D2" on Immersed Spherical Reflectors.

3777 c

A comment may also be made here on the field evaluation of the instrument systems. Hostile mill environmental conditions of extreme cold have been observed to markedly affect some of the instruments. Instrumentation sensitivity drift of -4 dB (an approximate 40% drop) has been noted to be associated with a 10°F environmental temperature drop. This sensitivity versus temperature variation is noted because the field inspection was carried out on the production floor of a sheltered but unheated plant area where the temperature varied between 29°F and -4°F during the six days of evaluations during February 1972.

## 2.3 Revised System Specifications

Experience gained in activities discussed in Section 2.2 - System Component Evaluation suggested revision of the Preliminary System Specification. Several design changes were made to the UDIS to provide an improved system performance. Discussion of the specification, however, requires a brief review of the inspection method.

The ultrasonic method selected for the inspection of the large dimension titanium billets is a novel combination of pulse-reflection defect detection and thru-transmission automatic distance-amplitude compensation. The operation of the method may be best described considering the basic objective of the program: inspecting round billets. Considering the titanium billet as a simple cylindrical shaped object the existance of the billet/defect geometric relationship suggested the use of the concept of a three-dimensional polar-rectangular coordinate system. Billet inspection using this concept is shown in Figure 25. The billet is inspected by a longitudinal wave injected to travel in billet radial coordinate, R, from the outside diameter toward the center. Defect caused reflections received and processed by the same interrogating transducer. Repeated radial direction inspections accomplished for successive billet angular coordinates, Θ, result in the inspection of a billet cross-section slice (shaded section of Figure 25). The entire billet is then inspected by repeated billet cross-section slice inspections accomplished for successive billet axial coordinates, A. The billet inspection is therefore accomplished using the polar coordinates R and Θ for repeated billet cross-section slices of successive billet axial length increments along the billet rectangular coordinate A. With the assignment of unit dimensions to the coordinate system, a specification of unit cell geometry was established, as shown in Figure 26. This unit cell geometry is called a "sector-of-rectangular torus."

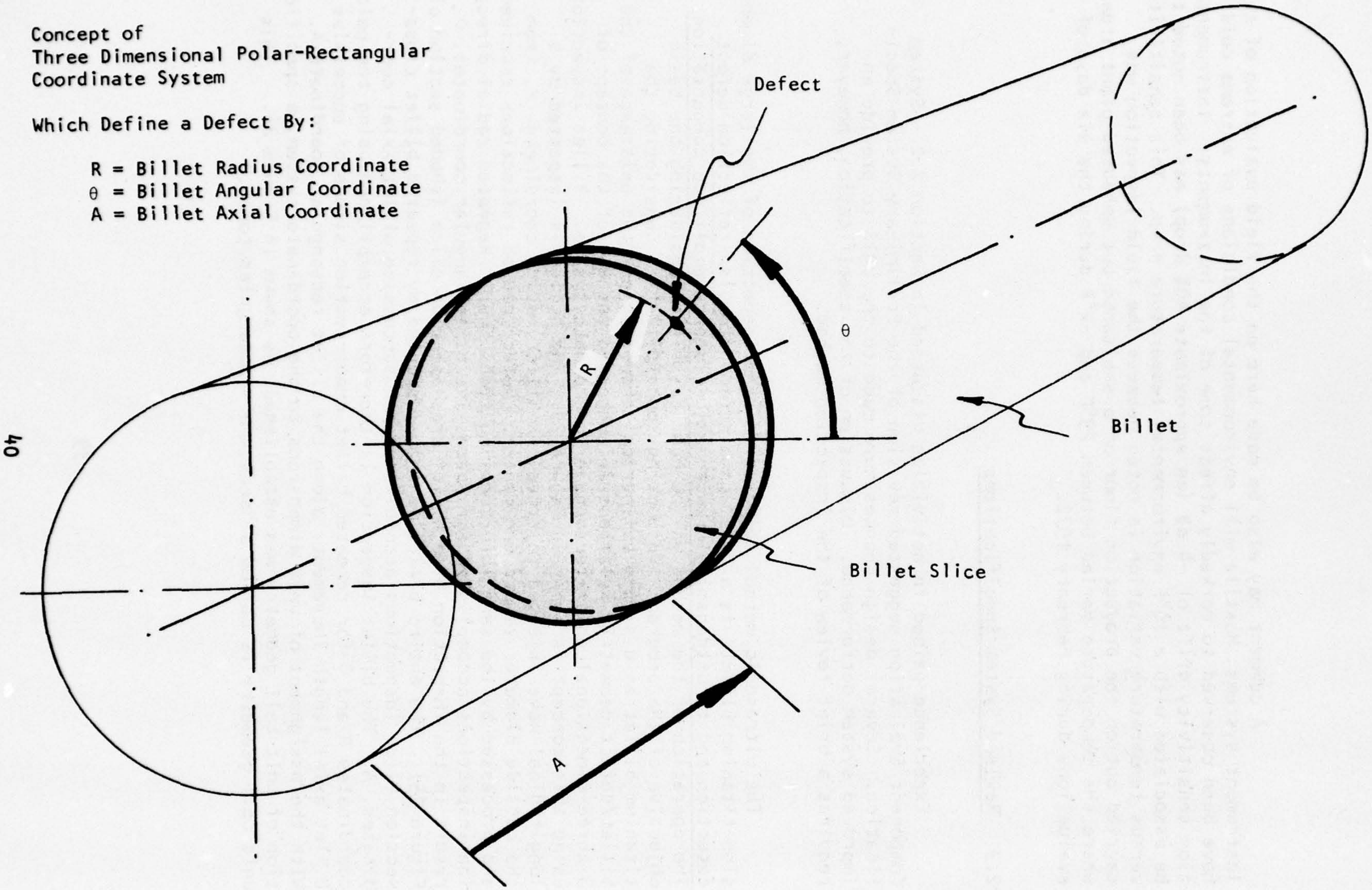


Figure 25. Defect/Billet Geometry Concept of the UDIS.

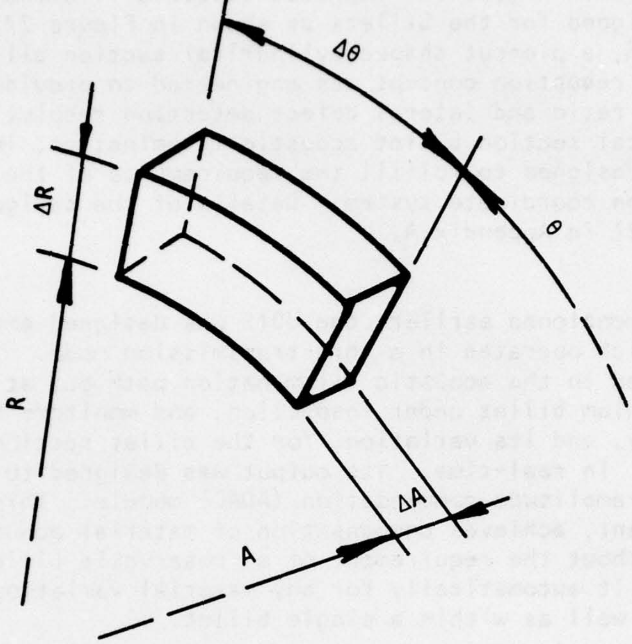


Figure 26. Unit Cell Geometry
(Sector-of-Rectangular Torus).

The conventional flat-face transducer to transmit and receive ultrasonic energy in the cases of the eight and 16-inch diameter billets considered in this program would provide illumination and detection patterns as modeled in Figure 1. Improved acoustic illumination patterns were therefore designed for the billets as shown in Figure 27. With reference to Figure 28, a pie-cut shaped cylindrical section billet acoustic illumination and reception concept was engineered to provide both an improved signal-to-noise ratio and lateral defect detection resolution. This pie-cut shaped cylindrical section billet acoustic illumination, incidentally, was specifically designed to fulfill the requirements of the polar-rectangular billet inspection coordinate system. Details of the design are illustrated in Figure 121 in Appendix A.

As mentioned earlier, the UDIS was designed employing a second transducer which operates in a thru-transmission mode. This second transducer is mounted in the acoustic illumination path but at the opposite side of the titanium billet under inspection, and monitors the acoustic energy intensity, and its variation, for the billet section under scan. It operates in real-time. Its output was designed to drive an automatic distance-amplitude compensation (ADAC) module. This unique TRW patented development, achieves compensation of material acoustic attenuation variations without the requirement of an observable billet rear-interface echo and does it automatically for any material variation between various billet heats as well as within a single billet.

Another major change in the system design was to use only digital encoder devices to monitor real-time billet angular and axial position locations for the inspection. These encoders are mechanically coupled to the billet and the transducer support bridge. Details of it are described in Section 3.2 - Billet Scan Monitoring System. Figure 29 shows the revised block diagram of the UDIS. Going straight digital, from the billet scan mechanism to the minicomputer, enables error-free transmission of the data and the elimination of the previously designed synchro analog-to-digital converters.

Two important diagnostic features of the UDIS must be mentioned here: a defect data diagnosis for accept/reject decision based on a programmable criteria of three-dimensional unit cell cluster size; and a statistical probability analysis performed on each defect based on a programmable criteria of cross-correlation of the angular compound scan provided data. These and other features are discussed in detail in the following sections.

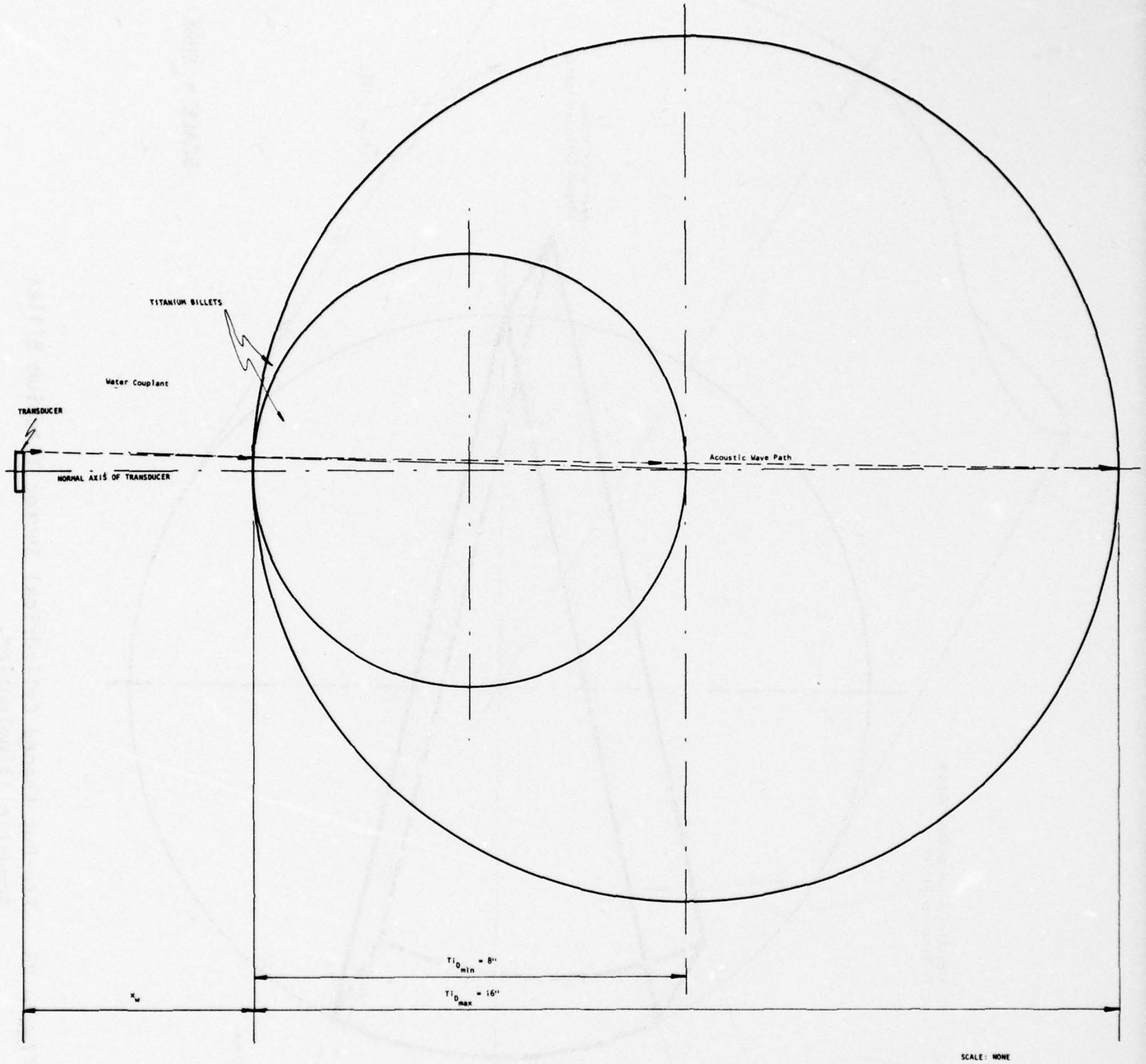


Figure 27. Acoustic Illumination of Titanium Billets by Improved Inspection Technique

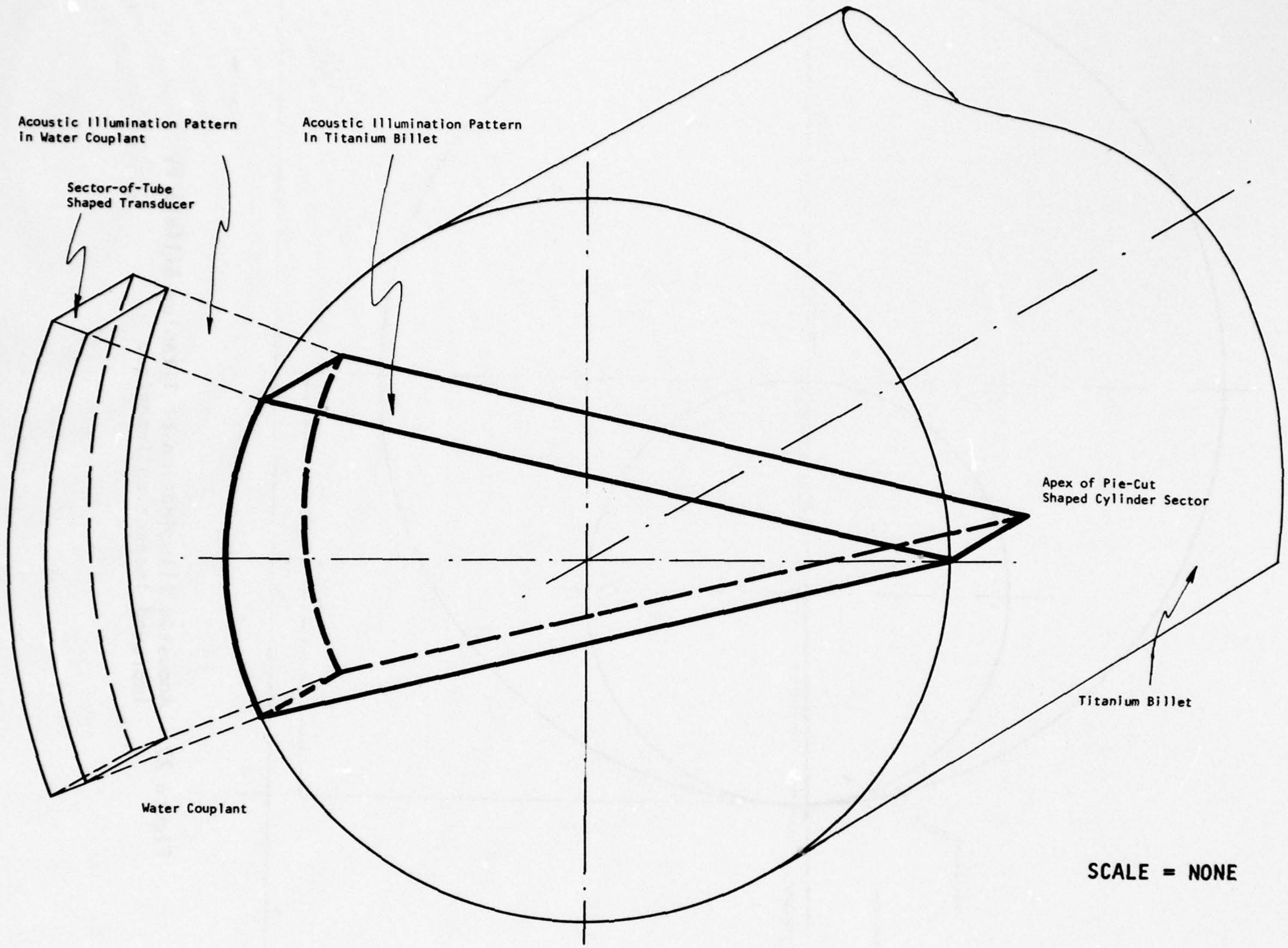


Figure 28. Pie-Cut Shaped Cylindrical Sector Titanium Billet Acoustic Illumination.



3702 C

J 8819

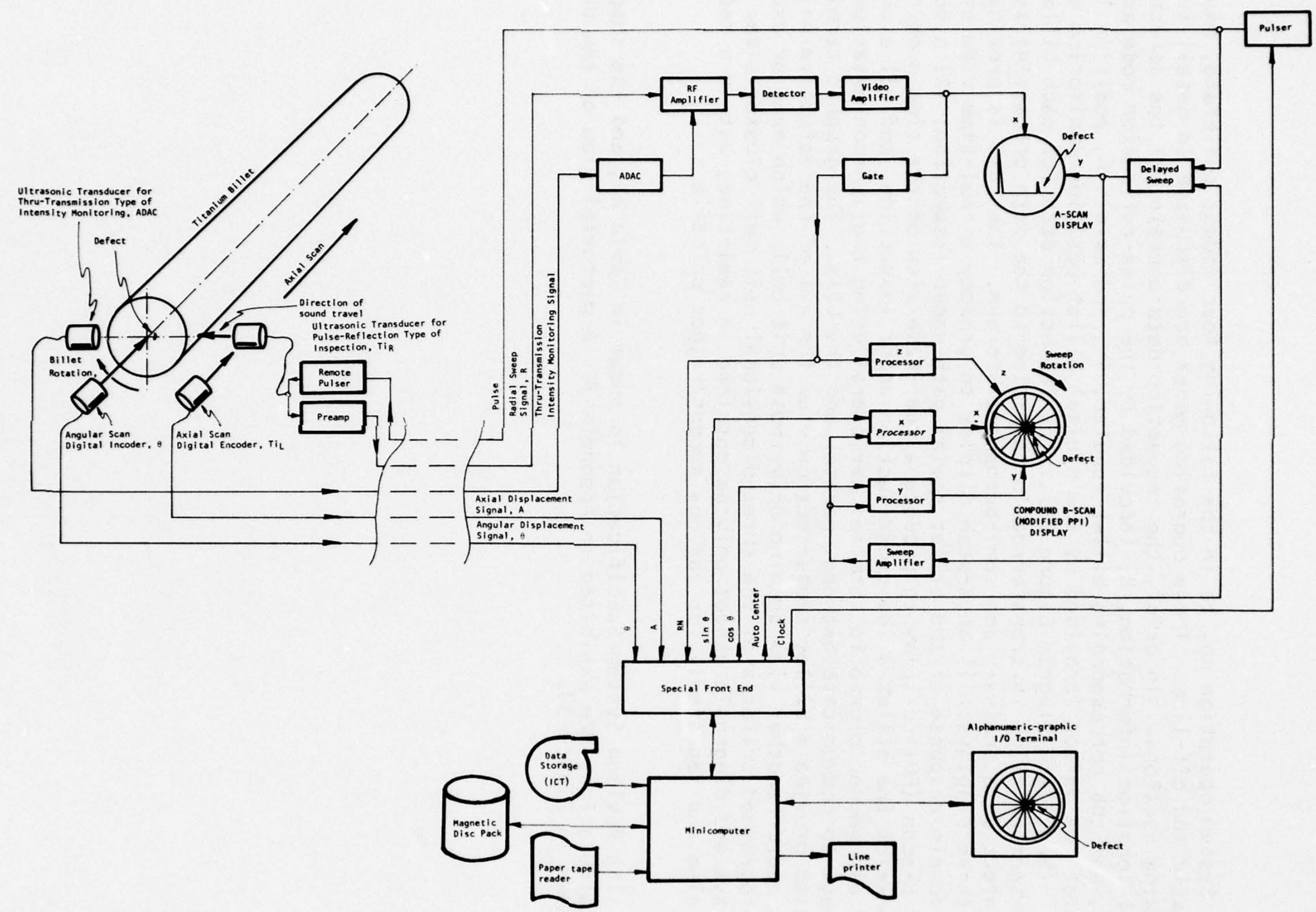


Figure 29. Ultrasonic Diagnostic Inspection System, UDIS.

System operation may be in the following four modes; calibrate, manual, automatic and off-line. These operating modes are discussed in detail in the following sections. In brief, the inspection data contain (1) the defect radial location information, R, (provided by the pulse-reflection mode acquired echo), and the corresponding billet angular, $\Theta$, and axial, A, position locations of the defect (provided by the digital billet position monitoring encoders). (See Block Diagram Figure 29). The inspection data for each billet cross-section slice is transferred in real-time to the data processing system for defect data analysis and semi-permanent storage. The UDIS is provided with three displays: (1) an A-scan display to produce a real-time view of the time-domain response of the billet radial path under inspection; (2) a compound B-scan (PPI) display to produce a real-time view of the time domain response of the billet slice cross-section under inspection, and (3) a computer alphanumeric-graphic terminal peripheral using english-conversational language to communicate between operator and the UDIS. The graphic terminal can also provide a billet cross-section view for all of the defective unit cells and/or another view showing only those unit cells which meet or exceed the programmed criteria of the three-dimensional unit cell cluster size. These displays and diagnosis cannot only be obtained in real-time, but in a retrieved mode also and repeatedly for various accept/reject criteria.

The Revised System Specification is shown in Table XI, and its supporting calculations are exhibited in Appendix A. A pictorial view of the UDIS is shown in Figure 30.

Figure 30.  UDIS Installation at TRW.

TABLE XI SYSTEM SPECIFICATION

| No. | Characteristics | | Symbol | Quantity & Unit | Design Reference(1) |
|---|---|---|---|---|---|
| 1 | Titanium Billet | diameter range | $Ti_D$ | 8-16 inch | 1 |
| 2 | | length range | $Ti_L$ | 1-120 inch | 1 |
| 3 | | radial distance unit cell | $\Delta Ti_R$ | 0.2 inch | 9 |
| 4 | | radial distance unit cell population | $N_R$ | 20 for 8" billet<br>40 for 16" billet | 10 |
| 5 | | axial distance unit cell | $\Delta Ti_L$ | 0.5 inch | 41 |
| 6 | | surface dimension unit cell | $\Delta C$ | 0.5 inch | 38 |
| 7 | | angular displacement unit cell | $\Delta\theta$ | 7.2° for 8" billet<br>3.6° for 16" billet | 40 |
| 8 | | angular displacement unit cell population | $N_C$ | 50 for 8" billet<br>100 for 16" billet | 39 |
| 9 | | acoustic illumination's angle of focus | $\beta_{Ti}$ | 1.79° for 8" billet<br>0.895° for 16" billet | 29 |
| 10 | | inspection angular velocity | $n_{Ti}$ | 86.7 RPM for 8" billet<br>43.5 RPM for 16" billet | 46 |
| 11 | System | maximum radial distance for inspection | $x_{max}$ | 4" for 8" billet<br>8" for 16" billet | 3 |
| 12 | | resolving capability between defects | $\Delta x$ | 3/64 inch | 5 |
| 13 | | total pulse population per angular displacement unit cell | $N_{P_{total}}$ | 18 pulses/$\Delta\theta$ | 43 |
| 14 | | water couplant distance | $x_w$ | 4-1/4 inch | 26 |
| 15 | Transducer | half-angle of surface curvature | $\beta_W$ | 3.149° for 8" billet<br>1.574° for 16" billet | 32 |
| 16 | | radius of surface curvatrue | $R_{focus}$ | 22.342 cm for 8" billet<br>33.909 cm for 16" billet | 33 |
| 17 | | length | $L_{trans}$ | 1.27 cm | 34 |
| 18 | Pulser | max. modulating pulse width | $t_{p_{max}}$ | 376.46 ns | 6 |
| 19 | | acoustic test frequency | $f$ | 5.0 MHz | 12 |
| 20 | | pulse repetition frequency | $f_{prf_{opt}}$ | 1.3 kHz | 43 |
| 21 | Receiver | center frequency | $f$ | 5.0 MHz | 12 |
| 22 | | bandwidth | $B_n$ | 2.66 MHz | 20 |
| 23 | | sensitivity | $S_{min}$ | 2.47 mV | 19 |
| 24 | | noise | $S_{noise}$ | 247.0 μV | 36 |
| 25 | | recovery time | $t_{recov}$ | 1.6 μs | 37 |
| 26 | | pulse population for billet inspection per angular displacement unit cell | $N_{P_{insp}}$ | 15 pulses/$\Delta\theta$ | 43 |
| 27 | ADAC | maximum axial distance for ADAC by through transmission | $X_{max}$ | 8" for 8" billet<br>16" for 16" billet | 3 |
| 28 | | range | $R_{DAC}$ | $3.05\text{-}7.7 \times 10^4$ | 21 |
| 29 | | linearity | - | 5% | 22 |
| 30 | | response time | $t_{ADAC}$ | 385.0 μs | 23 |
| 31 | | pulse population for ADAC per angular displacement unit cell | $N_{P_{cal}}$ | 3 pulses/$\Delta\theta$ | 43 |
| 32 | Gate | minimum time interval between successive defect signals | $t_d$ | 1.6 μs | 11 |
| 33 | | response time | $t_g$ | 125.0 ns | 24 |

NOTES: (1) Design reference numbers relate to appropriate Appendix II calculation step.

# 3. SYSTEM CONSTRUCTION

While the UDIS is relatively simple in concept, its implementation was not. In order to accomplish the automatic ultrasonic inspection of large diameter titanium billets with defect diagnosis capabilities, it was necessary to pool together the best instrumentation available from such various technologies as ultrasonics and data processing. The system construction effort of the program is discussed in the three following sections separately for the ultrasonic, billet scan monitoring and data processing areas.

## 3.1 Ultrasonic System

The requirements posed by the Revised System Specification (Section 2.3) for the inspection of large diameter titanium billets demanded the highest quality instrumentation for which specification no commercial ultrasonic instrumentation was available or is available today. Alternate choices to accomplish the UDIS were to modify the best ultrasonic system components selected from the various instrument houses, or to design and construct the UDIS as an in-house effort. In order to successfully meet the program objectives, the in-house effort was selected. Construction of the ultrasonic system part of the UDIS covered two major technical areas, namely, the instrumentation and the transducer efforts. These are discussed in the following two sections.

### 3.1.1 Instrumentation

The ultrasonic instrumentation system construction was oriented to achieve an optimized system which would provide higher sensitivity at the lowest possible level of scatter and uncertainty than commercial instrumentation, and also be able to interface with data processing equipment. This effort called for standardization.

#### 3.1.1.1 Standardization

Throughout all its history the electronics industry has had a worldwide accepted modular packaging system of the 19-inch "relay rack" panel, using an integral multiple of 1-3/4 inch vertical dimension. Beside the telephone relays, the system has an obvious drawback for other kinds of equipment; this became especially apparent when transistors came along, followed by integrated circuits. In recent years, manufacturers have independently devised a number of other packaging systems. While everyone else was contributing to the proliferation of boxes and odd sizes and shapes (Ref. 4), the nuclear laboratories in this country and abroad were solving this problem.

Accordingly, rather than follow any one ultrasonic manufacturer's module design, or to develop another of our own, TRW's approach was the adoption of the successful standardization program of nuclear instruments. This standard, known as the Nuclear Instrument Module, NIM, was first established over a decade ago by the U. S. Atomic Energy Commission, later adopted by the U. S. National Bureau of Standards, and recently by the European Standards Organization for Nuclear Energy, a EURATOM organization for twelve countries. This instrumentation packaging standardization proved to help both instrumentation users as well as manufacturers. The most important advantage for the user is system compatibility;the user can put together a system composed of units produced by many different manufacturers without the need for special interfacing devices. Solving the problems posed by the need to integrate two or more instruments with different logic, power supply and connector requirements represents a complete waste of time to the user. For him, instrumentation standardization is the solution to his compatibility problems. The standard also makes it practical to establish an ultrasonic instrument "bank" from which various individuals may select equipment to build their own specialized system. However, the ultrasonic instrument manufacturers can gain an advantage as well; standardization can actually save them expenses in the long run. As it turned out in the nuclear instrumentation field, it enabled the instrument manufacturing engineers to go about the business of designing new functions without the necessity of worrying about packaging, mechanical considerations and power supply design; since these are all basic to the system.

The NIM system specification referred to here is designated as TID-20893 (Rev. 3), dated December 1969, (Ref. 5). Briefly, it specifies two types of instrument modules of different heights; the 8.75-inches height which was selected for the UDIS. In the case of the UDIS, each module contains a single ultrasonic instrument function, such as the pulser, receiver, gate, etc., and all units are plugged into a NIM-bin. The bin provides spaces and connectors for twelve instrument modules of unit size. Instrument modules could also be integral multiples of the standard single bin space, so that double, triple or quad-width packages may be used without bin modifications or adjustments. The NIM-bin, in turn, is mounted into an EIA standard 19-inch relay rack equipped with a NEMA water drip-proof enclosure.

Typical NIM system modules and a bin, as used in the nuclear instrumentation field, is shown in Figure 31, reprinted from the NIM standard TID-20893, with the permission of the AEC Committee on Nuclear Instrument Modules. This figure illustrates the standardized system in operation in respect to its compatibility among modules of different manufacturers. One supplier's amplifier, for example, is interchangeable physically and electrically with another's with the exception of module width, which is usually determined by the amount of flexibility built into a particular instrument. What this means is that the user can now pick the best instrument for his needs from among several suppliers offering it, with the knowledge in advance that it will be completely compatible with the rest of his system.

It is also believed that data processing systems (computers) are going to play a large part in advancing the cause of instrumentation standardization. More and more, ultrasonic instrumentation users are engaged in sophisticated projects which are demanding the ability to set up, run, and process an experiment or inspection without the necessity of making manual adjustments, repeated calibrations and calculations. These users would like to be able to make decisions about which experiment or inspection to run, take a program from the shelf, plug it into the computer, and wait for the results; thus becoming free to pursue the more creative tasks associated with their disciplines. An important step in this direction has been taken with the recent introduction of the Computer Activated Measurement and Control, CAMAC, (Ref. 6, 7, 8, 9) developed by the EURATOM organization mentioned earlier. This system is concerned primarily with the transfer of information in the form of digital signals; provides a digital interface among controlled instruments and a computer or digital controller.

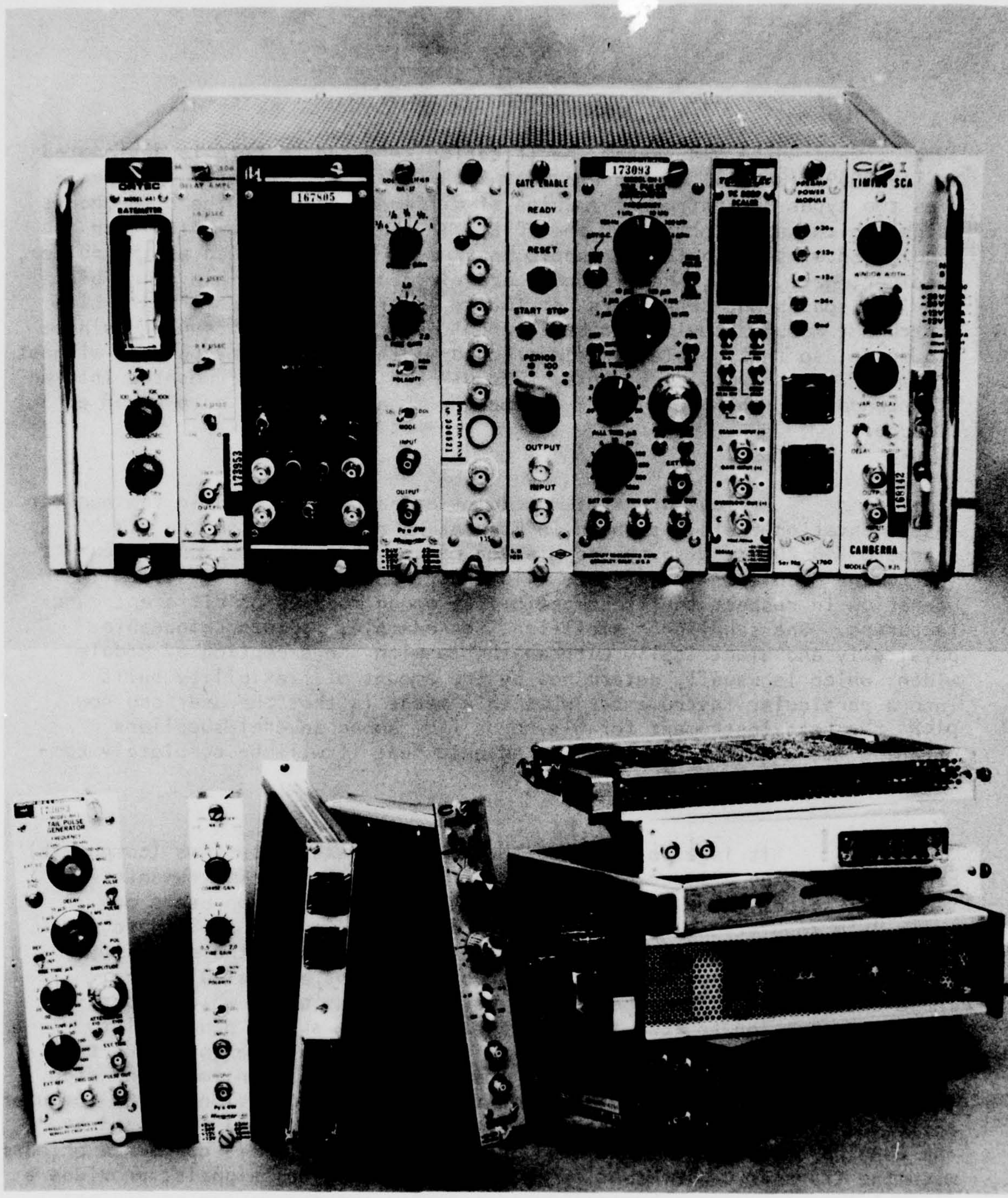


(Photo courtesy of the USNBS, Washington, DC)

Figure 31. NIM System Modules and Bin.

(Modules of any standard width can be inserted into the bin without any changes in the bin.)

The CAMAC is primarily intended for module-to-module communication in parallel over a common bus, as opposed to the NIM system, in which many instruments may communicate simultaneously. Any module, upon command, can communicate with another module, with the computer or with the instrument it is controlling. Nevertheless, the CAMAC and NIM are fully interfaceable.

Since the diagnostic ultrasonic inspection concept of the UDIS (where ultrasonics and data processing systems are directly interfaced), is quite similar to the CAMAC system, it is believed that the application of the successful NIM system offers a great advantage to the ultrasonic NDI of titanium alloy forging billets.

Figure 32 shows the ultrasonic instrumentation of the UDIS, utilizing the NIM system modules and bin. The NIM-bin is installed in a standard 19-inch water drip-proof relay rack cabinet.

3.1.1.2 Clock Module

With reference to Figure 29, UDIS Block Diagram, the clock, or timing generator allows the operator to vary the ultrasonic pulse repetition frequency in the manual mode of billet inspection operation of the UDIS. In the automatic mode of billet inspection operation of the UDIS, the clock unit is driven by the data processing computer. The clock unit is designed so that it is housed in a single-width NIM-module and was built using standard TTL integrated circuit components. The clock provides a pulse repetition frequency of 100 through 5000 Hz with a continuous adjustment in the manual system operation mode, and a 500 to 1500 Hz with a 50 Hz incremental adjustment in the automatic system operation mode.

The clock unit is shown in Figure 33 with the side shield-cover removed, and its circuit diagram is shown in Figure 34.

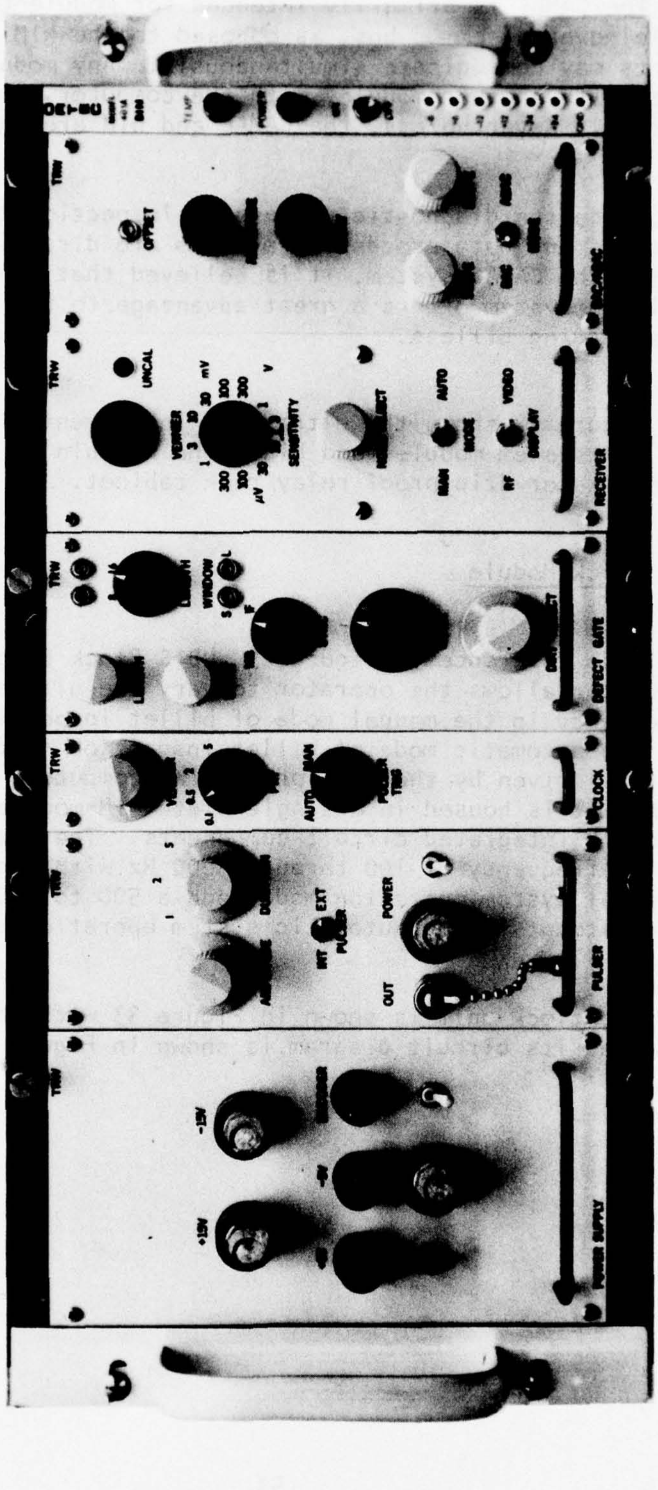


Figure 32. Ultrasonic Hardware of the UDIS.

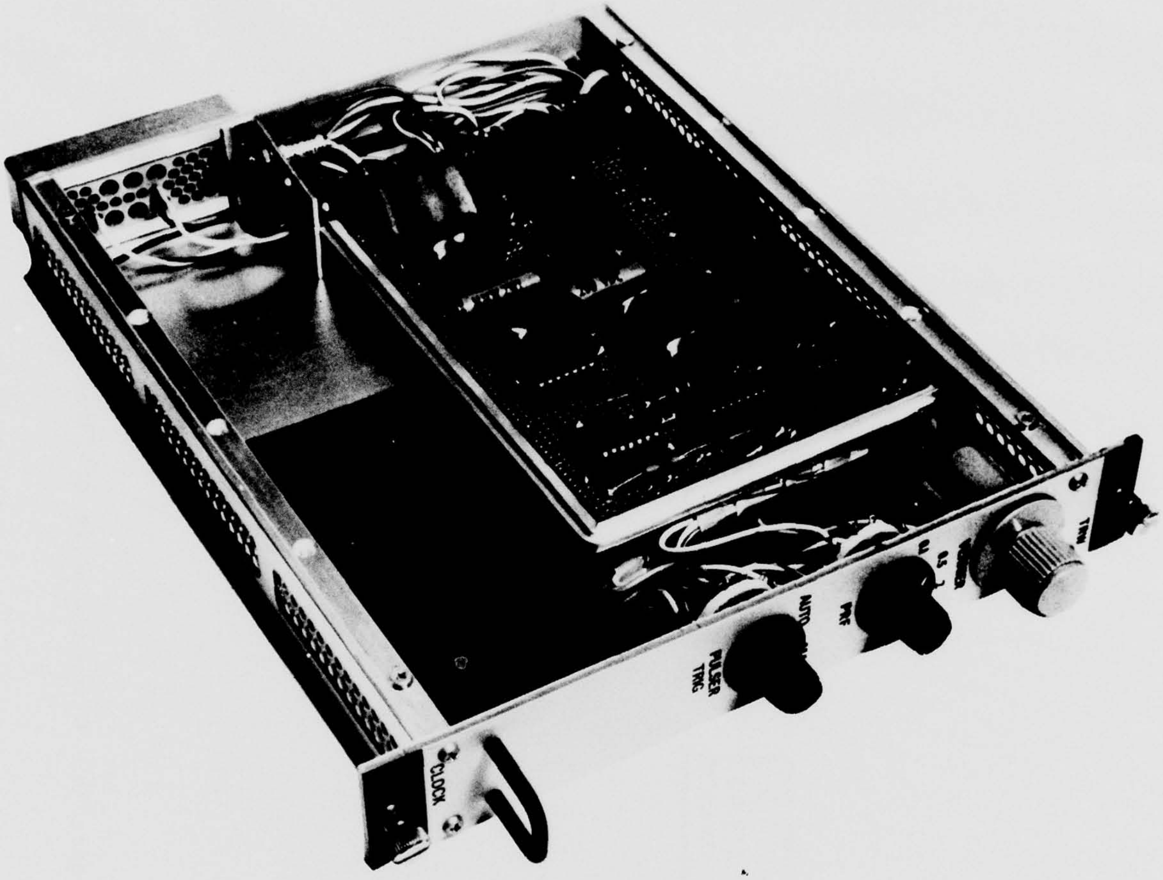


Figure 33. Clock Module

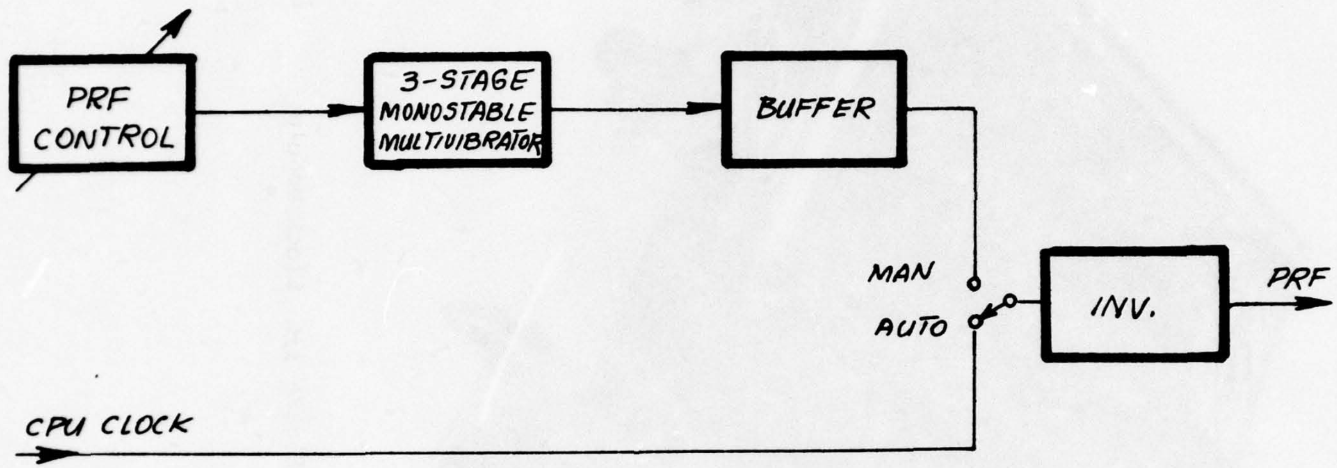


Figure 34. Circuit Diagram of Clock Module

### 3.1.1.3 Pulser Module

The pulser unit allows the operator to preset the ultrasonic pulse amplitude and pulse duration to an advantageous level for a given type of billet inspection. The pulser unit, therefore, is designed to provide adjustable pulse heights and widths to drive low impedance, polycrystalline piezoelectric element transducers. Unlike commercial pulsers, this unit is capable of delivering high-voltage pulses of short duration and very fast rise times without decaying oscillations (ringing). Acoustic energy penetration of attenuative and/or large material cross sections, therefore, are ensured along with excellent defect detection resolution. The unit is housed in a double-width NIM-module and has been built with solid-state components only.

While the trailer-mounted field inspection equipment design is a required feature of the UDIS for portable computerized field inspection purposes, it also created a disadvantage in view of an increase in length of transducer cables. Longer transducer cables place an increased capacitive load on the transducers, an undesired effect, which was eliminated by a unique design of the UDIS. By placing another pulser near the transducer, the transducer cable was kept short. Accordingly, the pulser is designed to also be operated from the trailer-mounted UDIS, thus, this additional pulser is called the Remote Pulser.

Figure 35 shows the pulser with the side cover shield removed. Figure 36 shows the remote pulser with its cover removed. Circuit diagrams of the pulser and the remote pulser are shown in Figures 37 and 38, respectively.

### 3.1.1.4 Receiver and Preamplifier Modules

Similar to the Remote Pulser, the long transducer cable connecting to the trailer-mounted ultrasonic receiver is also eliminated by a Receiver Preamplifier which is designed to be placed near the transducer. The Receiver Preamplifier features an improved frequency bandwidth over commercial ultrasonic equipment. Figure 39 illustrates the frequency

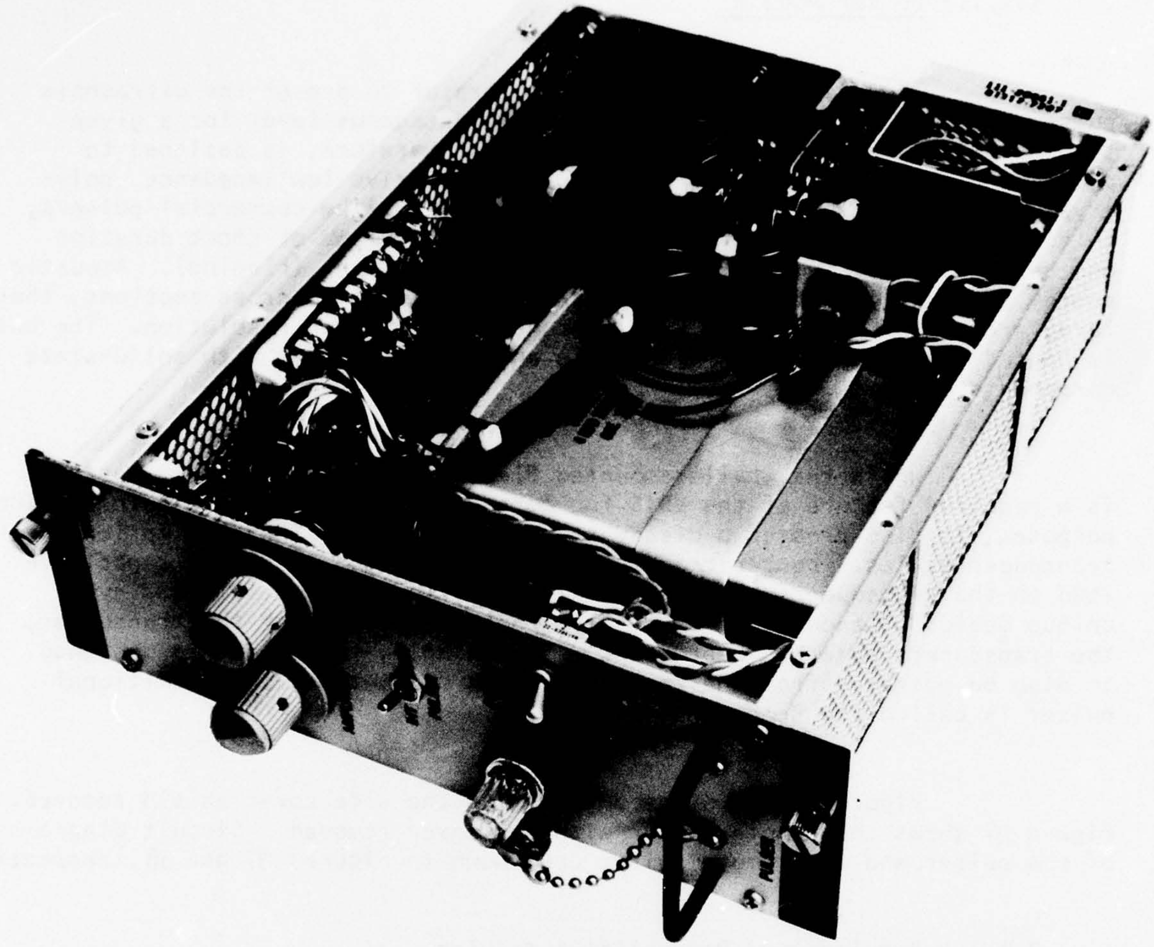

Figure 35. Pulser Module

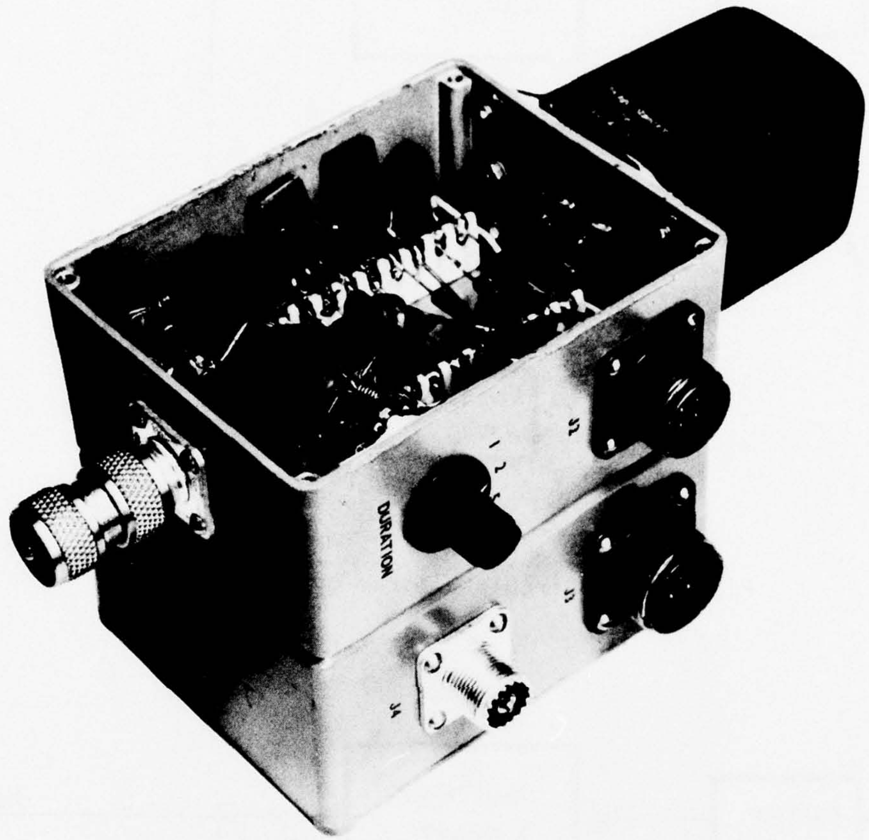


Figure 36. Remote Pulser Assembly

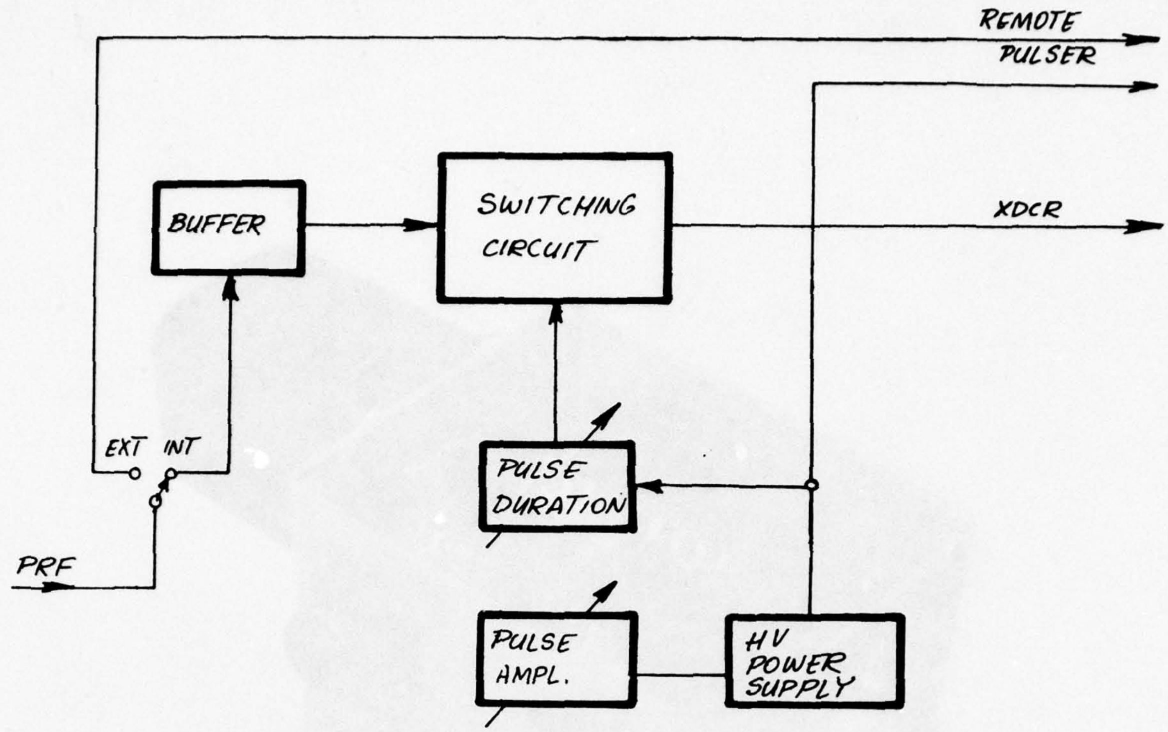


Figure 37. Circuit Diagram of the Pulser.

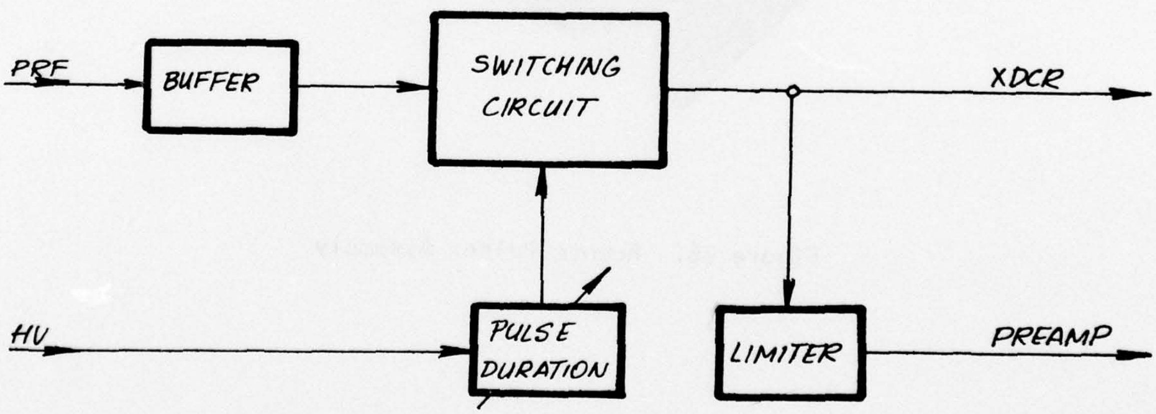


Figure 38. Circuit Diagram of Remote Pulser.

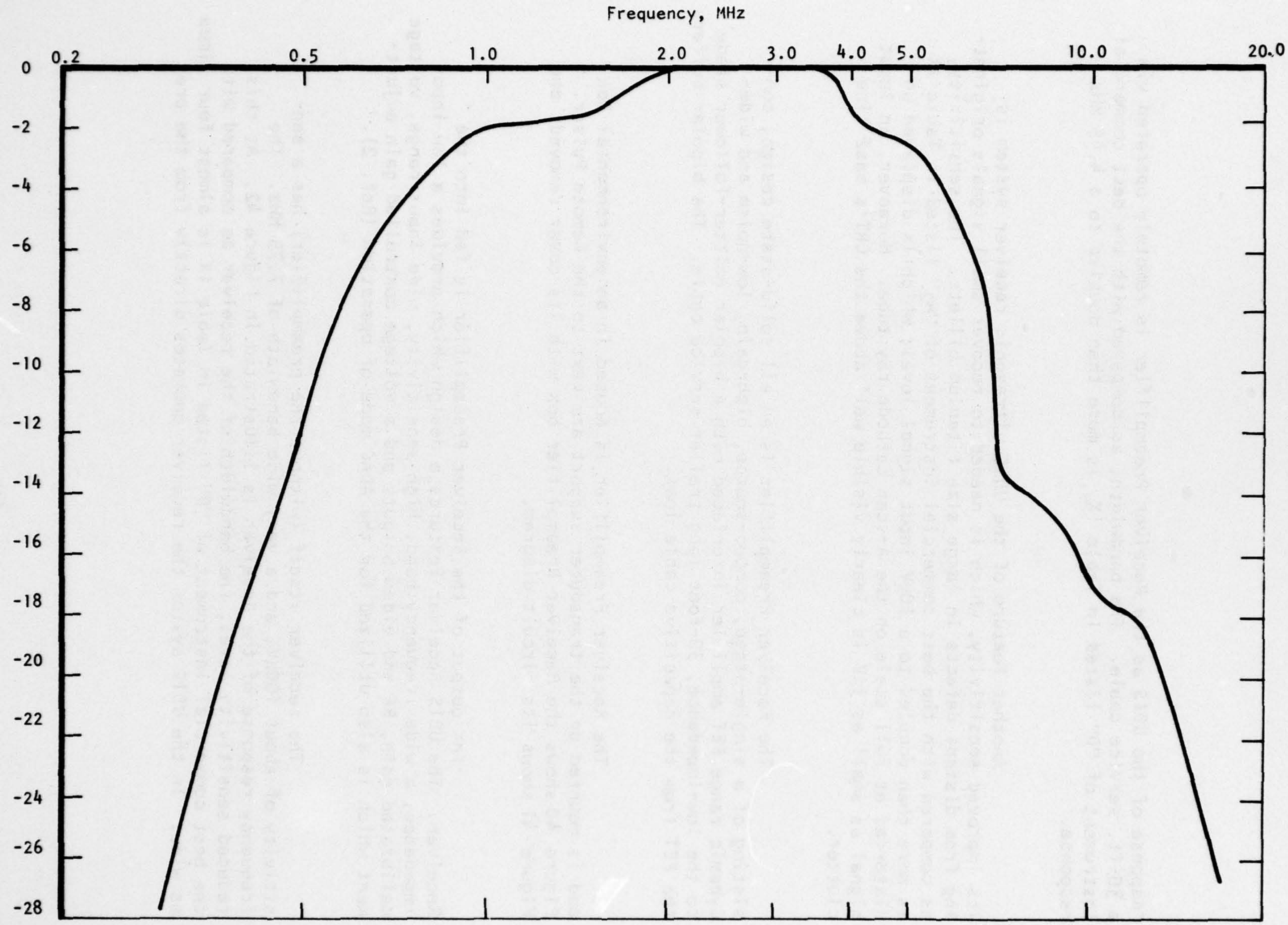


Figure 39. Frequency Response of the UDIS Receiver System

response of the UDIS as the Receiver Preamplifier is remotely operated via a 30-ft. service cable. The bandwidth, as compared with the best commercial instrument of "D" listed in Table IX, is more than doubled to a 4.45 MHz response.

Another feature of the UDIS ultrasonic receiver system is its improved sensitivity, which is needed to recover small signals originating from distant defects in large size titanium billets. The sensitivity, as compared with the best commercial instrument of "$A_2$" listed in Table IX is more than doubled to a 10µV input signal level; which is displayed undistorted at full scale on the A-scan cathode ray tube. Moreover, an input signal as small as 3µV is clearly visible well above the CRT's base line clutter.

The Receiver Preamplifier is an all solid-state design, consisting of a single-stage, common-source, high-gain, low-noise and wide-dynamic range FET amplifier interfaced with a bipolar emitter-follower stage to the low-impedance, 30-foot long trailer service cable. The bipolar buffers the FET from the capacitive cable load.

The Receiver Preamplifier is housed in an environmental box and is mounted on the transducer support arm next to the Remote Pulser. Figure 40 shows the Receiver Preamplifier box with its cover removed, and Figure 41 shows its circuit diagram.

The output of the Receiver Preamplifier is fed into the Receiver. The UDIS Receiver features a design which provides a low input impedance, a wide frequency band, high sensitivity, wide input range, voltage calibrated gain, RF and video outputs and a voltage controlled gain adjustment which is also utilized for the ADAC mode of operation (Ref. 2).

The receiver itself (without the preamplifier) has a sensitivity of about 100µV, and a very wide bandwidth of 7.75 MHz. The frequency response of the Receiver is illustrated in Figure 42. At this reduced sensitivity level, the bandwidth of the receiver as compared with the best commercial instrument of "D" listed in Table IX is almost four times as wide. In the UDIS system the receiver operates directly from the pre-

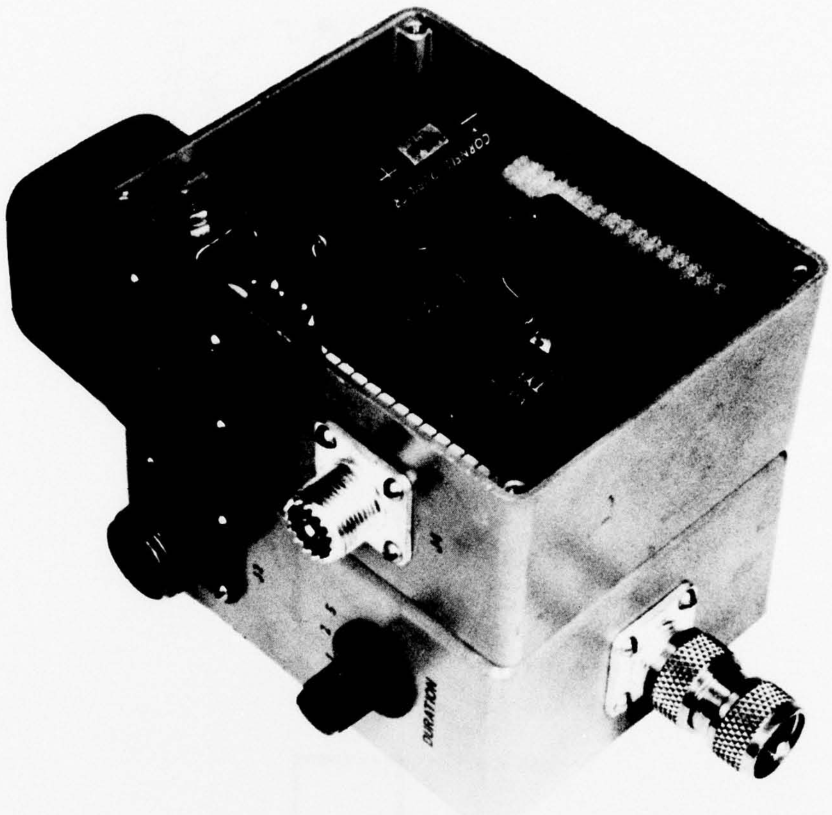


Figure 40. Receiver Preamplifier Assembly

6195 C

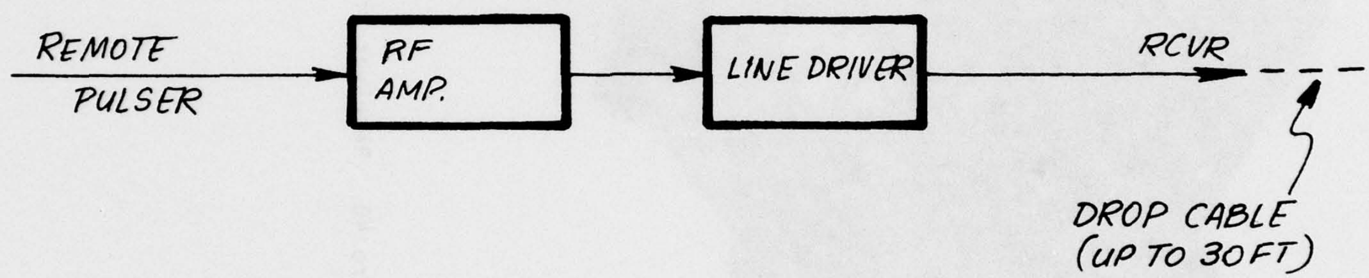


Figure 41. Circuit Diagram of the Receiver Preamplifier

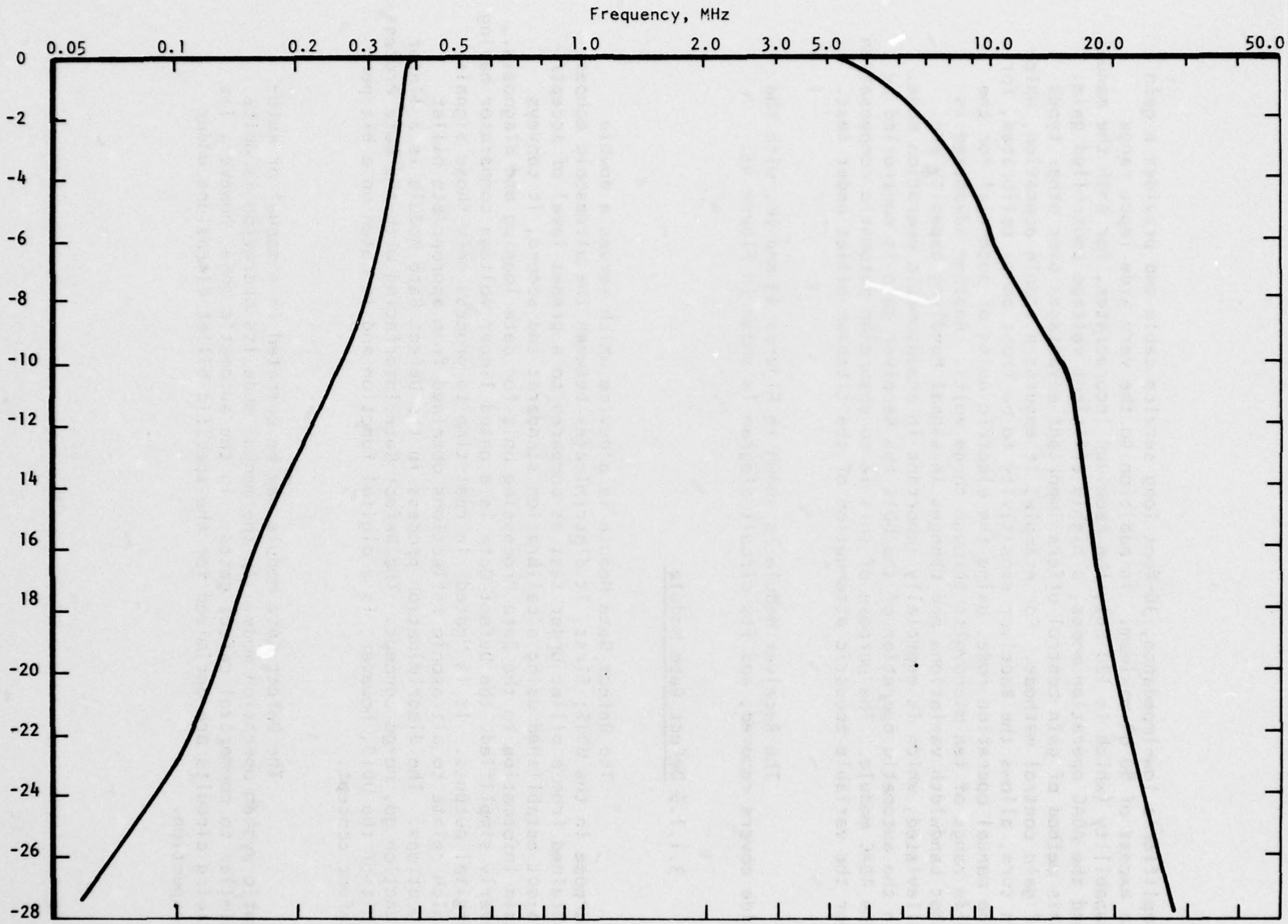


Figure 42. Frequency Response of the UDIS Receiver (without Preamplifier).

amplifier's low-impedance, 30-foot long service cable and provides a gain in excess of 80 dB maximum. In addition to the very wide input range capability (which is 120 dB), the Receiver incorporates, for both the manual and the ADAC operation modes, a highly efficient voltage controlled gain. This method of gain control offers important advantages over other types of gain control methods. For example, it ensures a stable operation, which in turn, allows the Receiver sensitivity to be front panel calibrated, for the manual operation mode, using the electric units of potential for the wide range of ten microvolts through three volts. Another advantage is that bandwidth variations and changes in signal handling capacity are alleviated, which is especially important in an automatic operation mode. In the automatic operation of the UDIS the Receiver gain is controlled by the ADAC module. The purpose of this is to ensure an automatic compensation for the variable acoustic attenuation of the titanium billet under test.

The Receiver Module is shown in Figures 43 and 44, with the side covers removed, and its circuit diagram is shown in Figure 45.

#### 3.1.1.5 Defect Gate Module

The Defect Gate Module is a device which serves a double purpose in the UDIS; first, it discriminates between the ultrasonic echoes obtained from a billet under test as compared to a preset level of accept/reject established using a calibration standard; and second, it conveys said information to the Data Processing Unit for data logging and diagnosis. Overly simplified, the Defect Gate is a gated linear voltage comparator having digital outputs. It is "gated" in real-time to process only those signals which relate to ultrasonic reflections obtained from appropriate billet locations. The discrimination process in the Defect Gate Module is a linear function go, no-go concept. The Defect Gate interfacing with the Data Processing Unit of the UDIS, however, is a digital function and is based on a bit-per-defect concept.

The Defect Gate Module may be operated in a manual or automatic system operation mode. In the manual mode its operation is quite similar to commercial defect gates. In the automatic mode, however, its timing circuits are optimized for the specific billet dimensions under inspection.

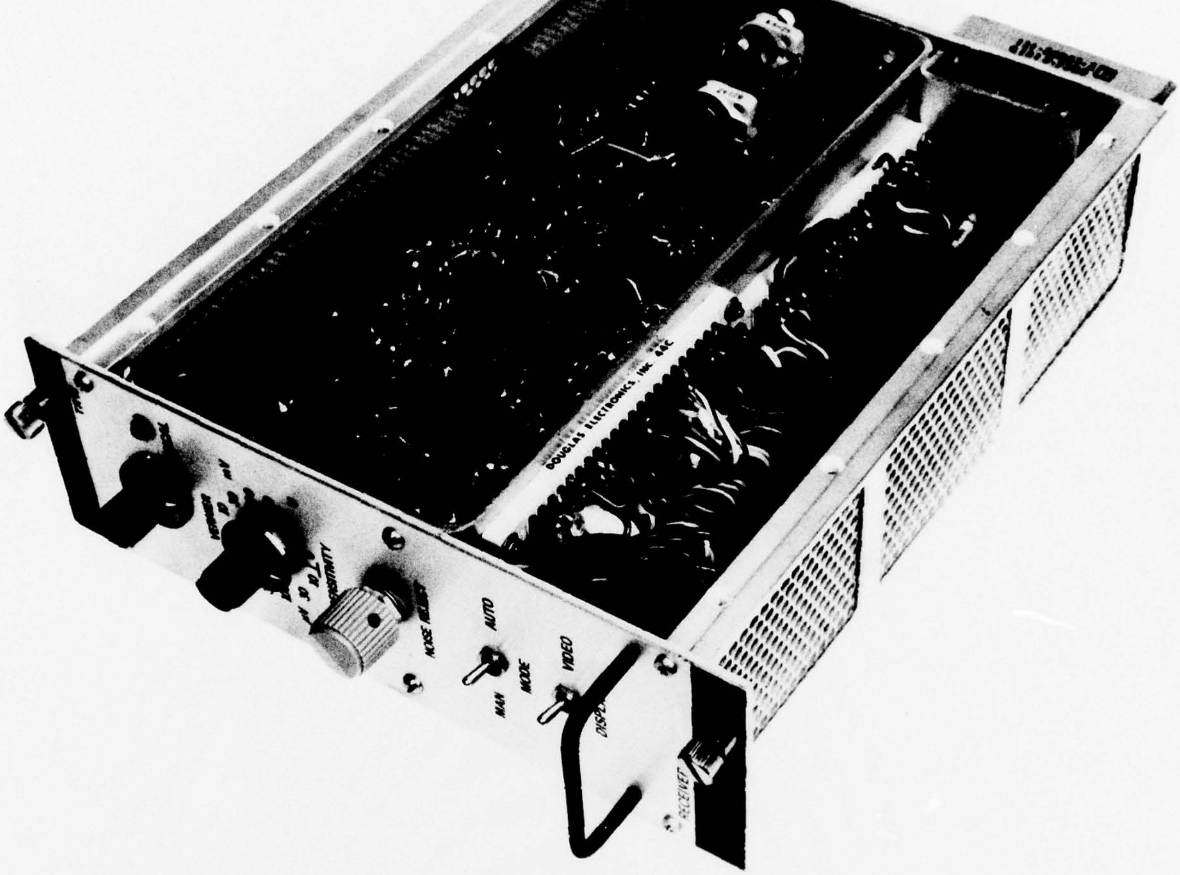


Figure 43.  Receiver Module (Right Side)

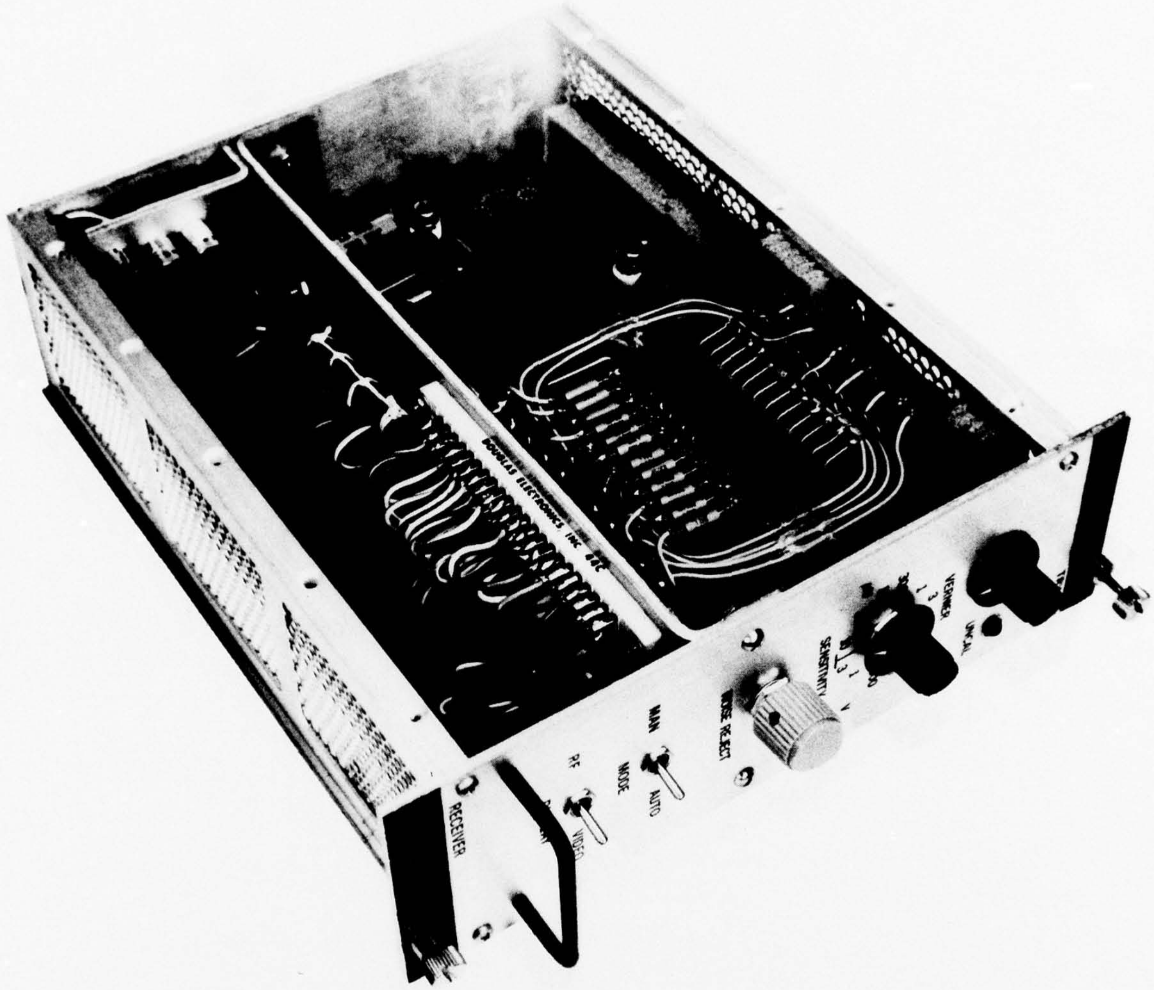


Figure 44. Receiver Module (Left Side)

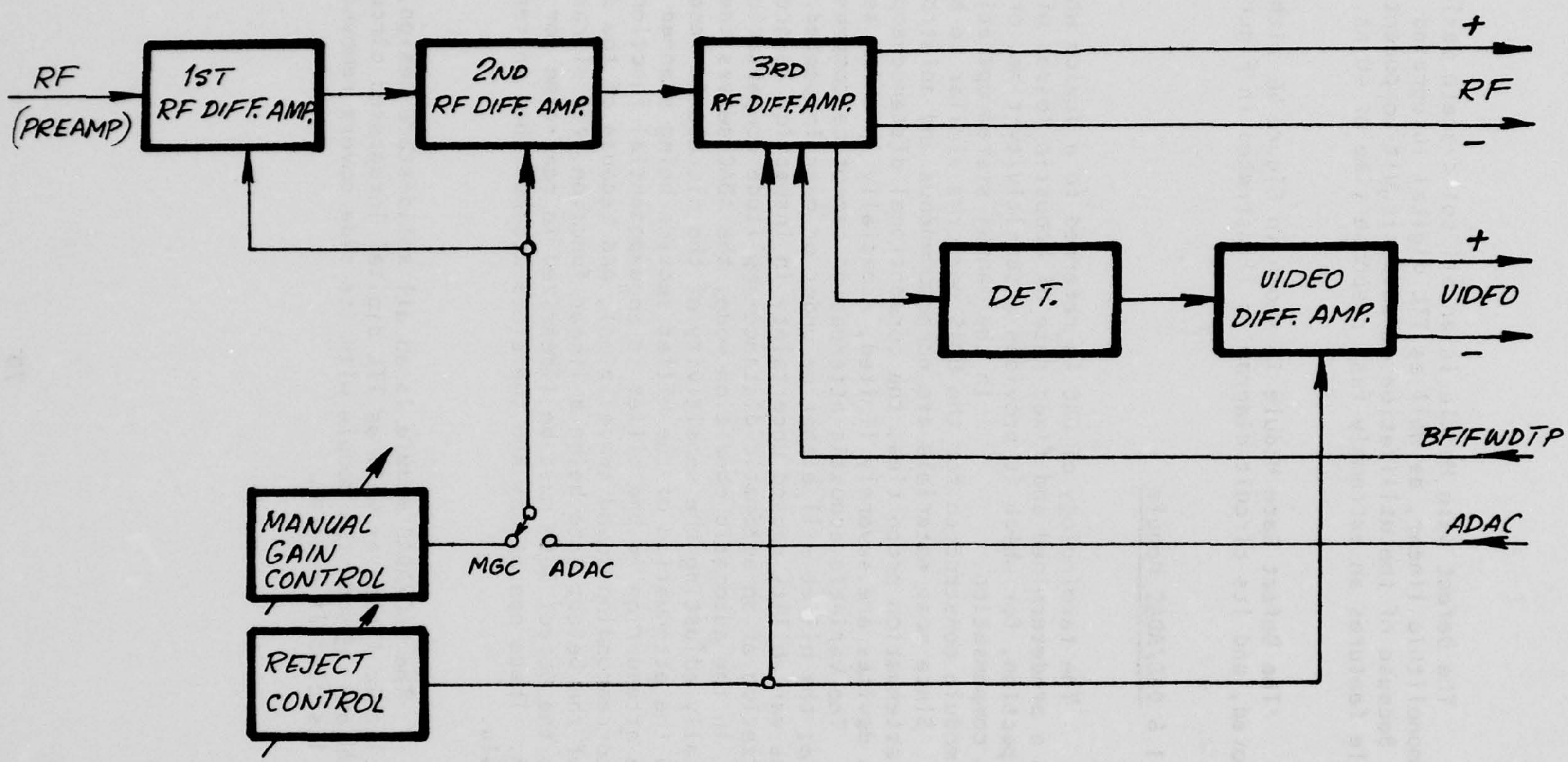


Figure 45. Circuit Diagram of the Receiver

The Defect Gate Module is an all solid-state design, utilizing both monolithic linear, as well as TTL digital integrated circuit components. Because of the utilization of said circuit components, the Defect Gate Module features an extremely fast response time of 40 ns.

The Defect Gate Module is shown in Figure 46 with its side cover removed, and its circuit diagram is illustrated in Figure 47.

3.1.1.6 DAC/ADAC Module

The terminology of DAC is referred to a device which may be preset to a predetermined and fixed rate of acoustic losses of an object under inspection, for which it provides a sensitivity-time, or, distance-amplitude compensation. In the manual system operation mode the DAC/ADAC module constructed for the UDIS performs similar to any commercial DAC unit. Since most materials are nonhomogeneous and anistropic for their acoustic attenuation properties, the conventional distance-amplitude compensation devices are severely limited, especially in thick sections of titanium. The variable acoustic attenuation cannot be compensated for by a fixed rate; the billet will either be under or over inspected. This material properties variability caused uncertainty in inspection is greatly reduced by the utilization of an automatic distance-amplitude compensation, ADAC, device (Ref.2). In the automatic operation mode, the ADAC serves the purpose of automatically adjusting the sensitivity of the ultrasonic receiver in accordance with the attenuation of the billet section being scanned in real time. Since the attenuation in the billet is an exponential function of distance (or the corresponding sound travel time), and because of the discriminating process of the Defect Gate being a linear function, the ultrasonic receiver output to the Defect Gate must be linearized in real-time for accurate defect detection. These operations are therefore accomplished in real-time by the ADAC module.

The DAC/ADAC module is an all solid-state design, utilizing both monolithic linear as well as TTL digital integrated circuit components. Figures 48 and 49 show the module with its side covers removed, and Figure 50 shows its circuit diagram.

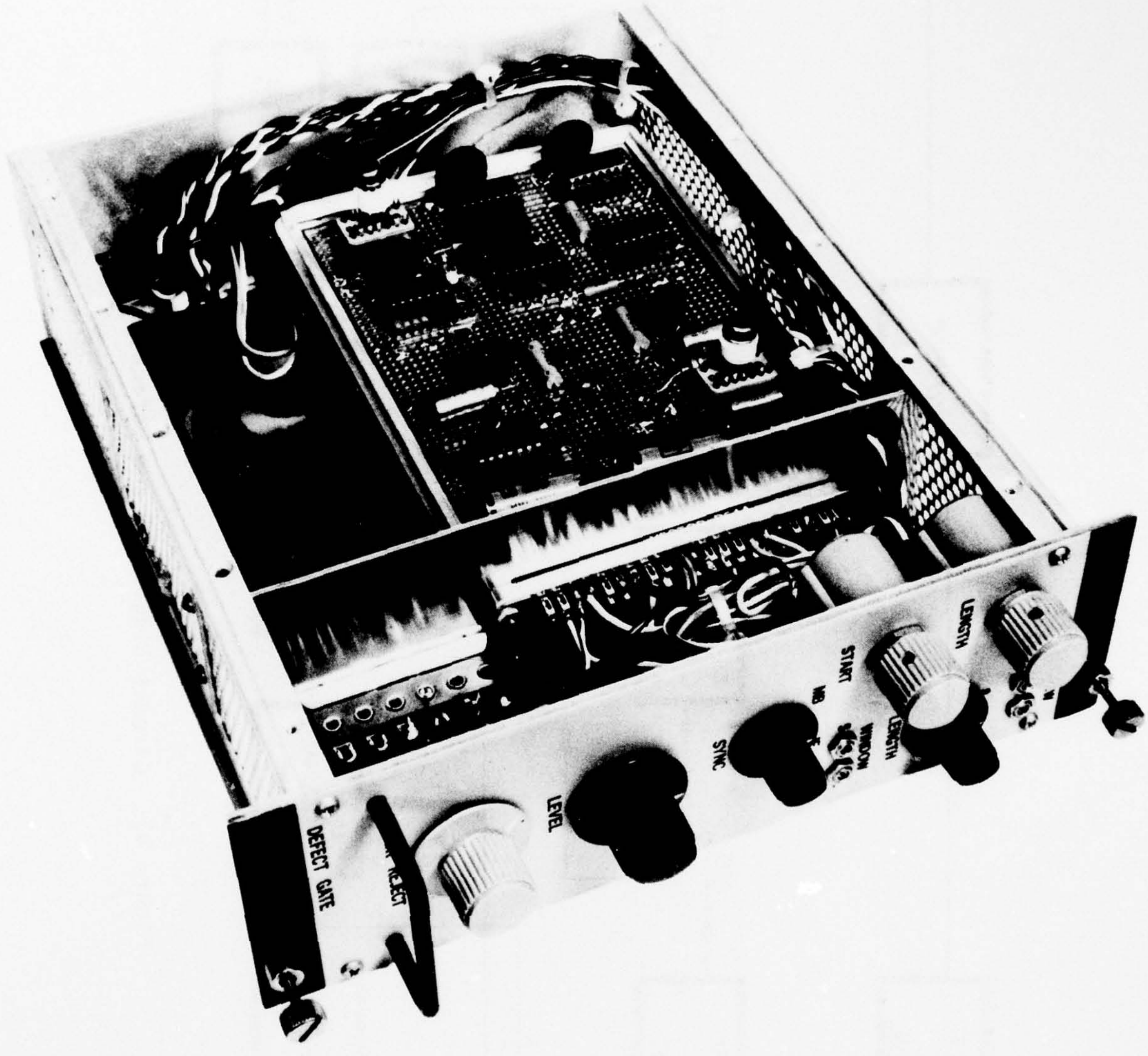


Figure 46. Defect Gate Module

AD-A049 682 TRW INC CLEVELAND OHIO MATERIALS TECHNOLOGY F/G 11/6
IMPROVED ULTRASONIC INSPECTION OF TITANIUM ALLOY FORGING BILLET--ETC(U)
JUL 77 I M MATAY F33615-71-C-1712
UNCLASSIFIED TRW-ER-7554 AFML-TR-77-111 NL

2 OF 4
AD
A049682

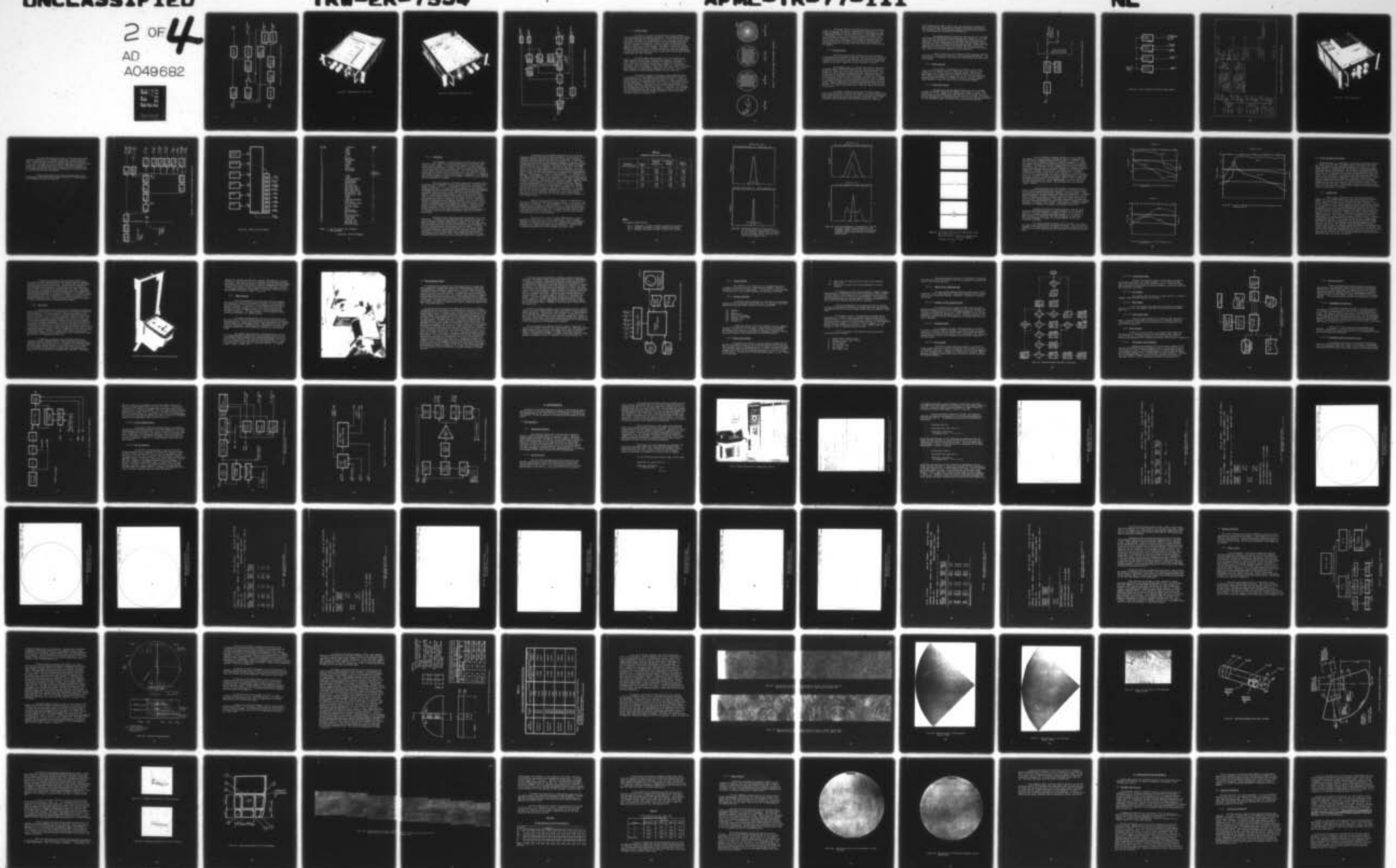

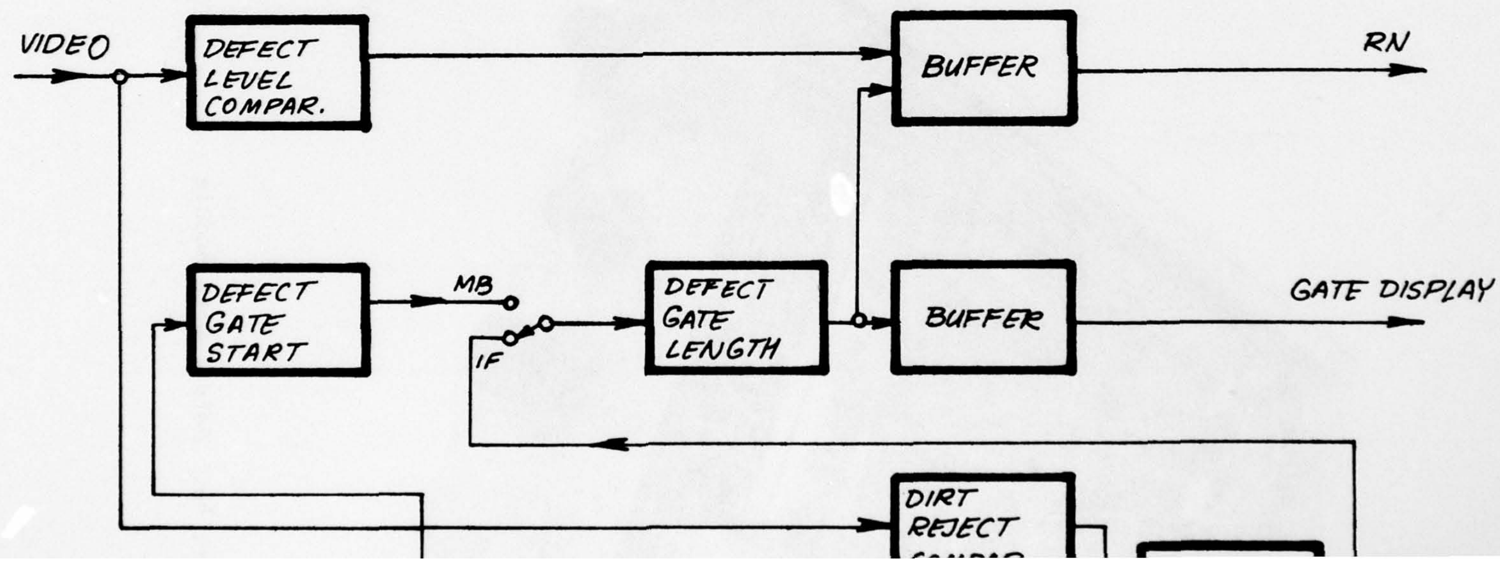
VIDEO
DEFECT LEVEL COMPAR.
BUFFER
RN
DEFECT GATE START
MB
IF
DEFECT GATE LENGTH
BUFFER
GATE DISPLAY
DIRT REJECT

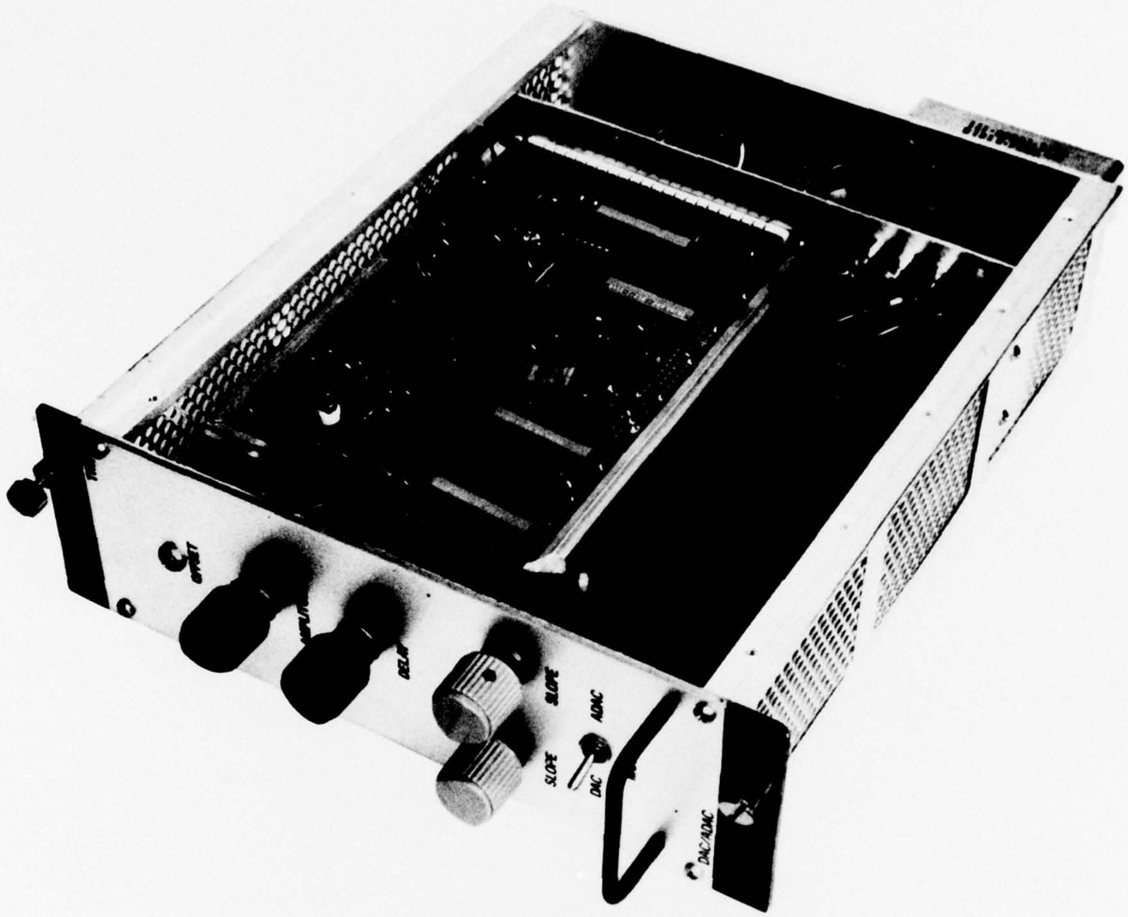


Figure 48. DAC/ADAC Module (Right Side)

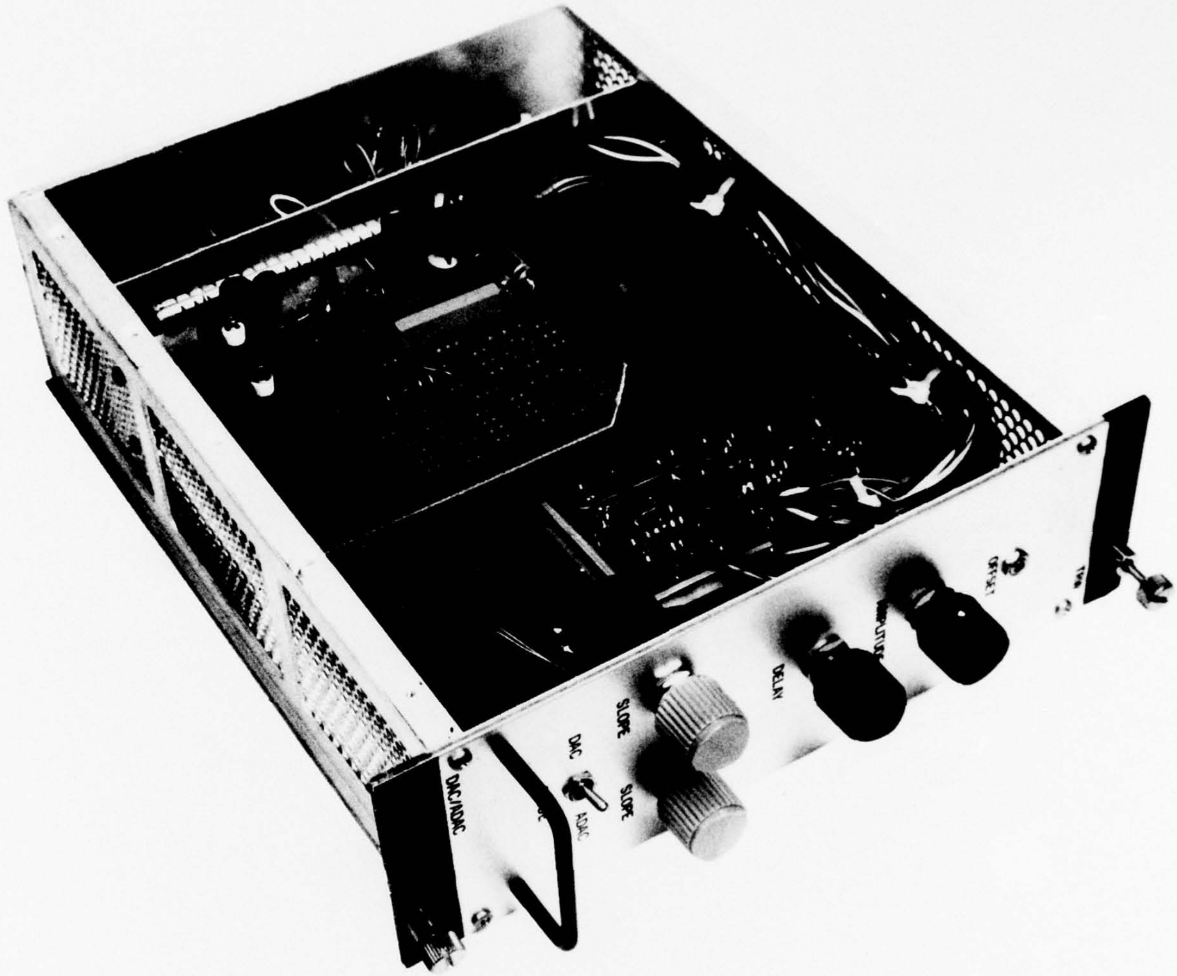


Figure 49. DAC/ADAC Module (Left Side)

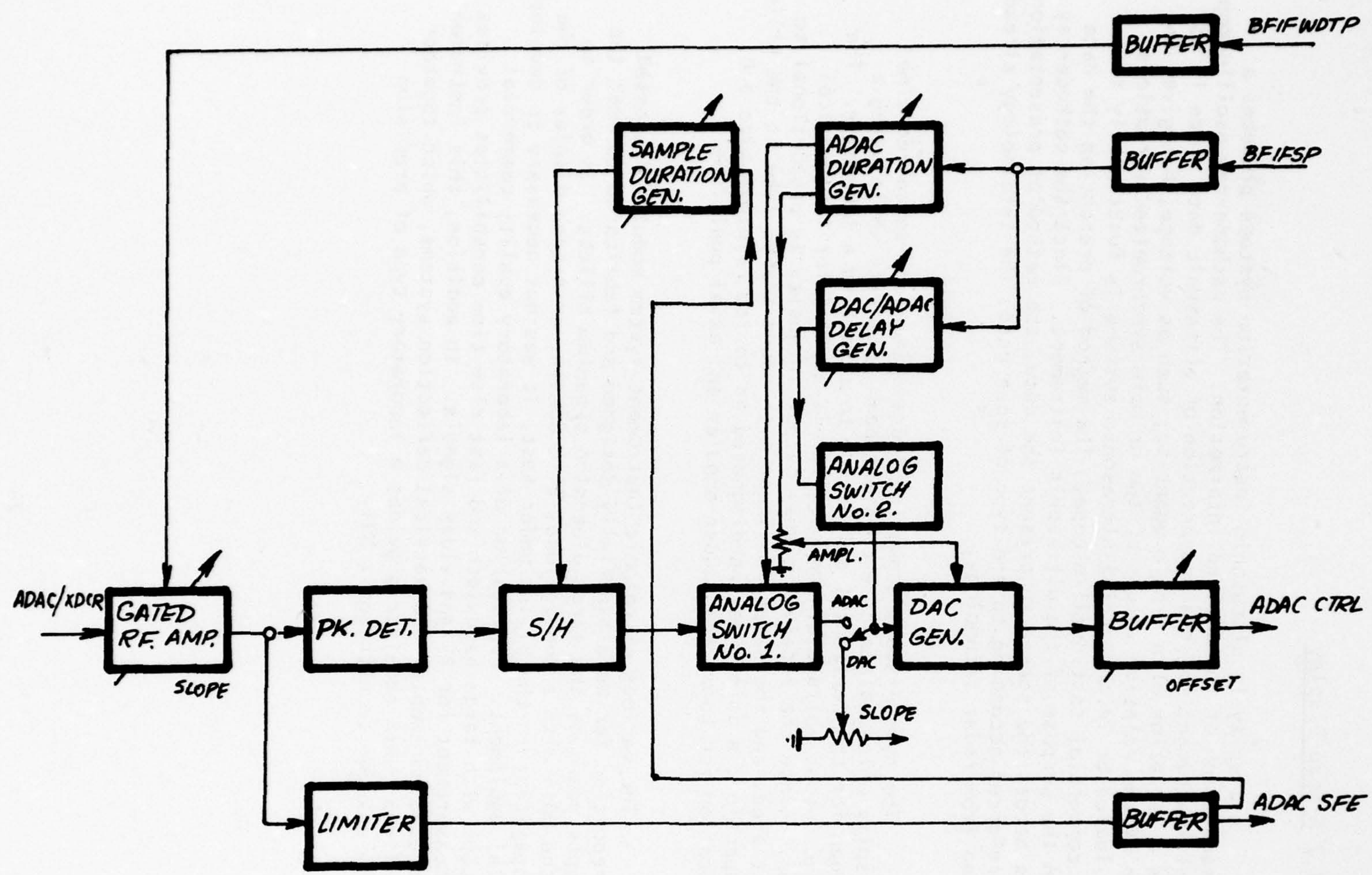


Figure 50. Circuit Diagram of DAC/ADAC Module

### 3.1.1.7 A-Scan Display

A display in ultrasonic instrumentation systems produces a visual presentation of the desired information. The cathode-ray oscilloscope is an ideal instrument for the presentation of ultrasonic data since it not only shows a variation of a single quantity, such as voltage, but gives an indication of the relative values of two or more synchronized variations. The usual indicator in commercial ultrasonic systems is functionally the same as a commercial test oscilloscope. The method of presenting the data depends on the purpose of the ultrasonic instrument. Since the cathode-ray spot scans across the screen to present the data, the method of presentation is often referred according to the type of scan used, the terminology already established from radar technology.

The type A-scan, shown in Figure 51A, is a so-called time domain display which maintains a constant beam intensity while using a linear sweep for the horizontal deflection to establish a time base. The RF or video output voltage of the receiver is applied for the vertical deflection. Since the receiver signal output intensity is proportional to the defect area, and the sweep is linear with sound travel time in the billet under inspection, a defect may be diagnosed as to its relative size and radial location for known transducer angular and axial positions.

The various ultrasonic instrument system modules discussed in this report so far were especially designed and fabricated to meet the requirements posed by the large dimension titanium billets. In order to provide the UDIS with a conventional time domain, or A-scan display of the sound propagating in the billet under test, it was not necessary to develop any special equipment. Application of a laboratory quality commercial oscilloscope with large bandwidth and fast rise time capabilities provides precise measurement for RF and video signals. In addition, this instrument has calibrated horizontal and vertical deflection systems, which together with the linear UDIS receiver provides a laboratory type of precision previously unknown to ultrasonic NDI.

3 8119

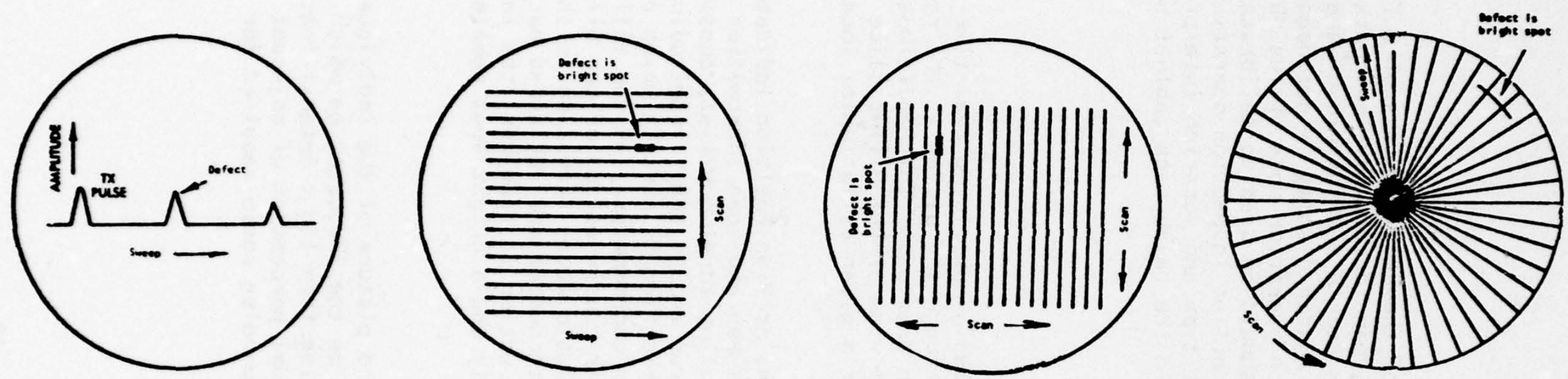


A
Type A-Scan

B
Type B-Scan

C
Type C-Scan

D
Type PPI-Scan

Figure 51. Various Scan Types of Ultrasonic Indicators

The A-scan display of the UDIS consists of a Type 556 main frame with two Type 1A1 plug-ins, manufactured by Tektronix, Inc. The display accommodates the Receiver module's RF or video waveform outputs. It should be pointed out the the A-scan display is not needed, as such, in the automatic billet inspection operation mode of the UDIS to be observed by anyone, however, it should be used to calibrate the system. It is further used in the manual billet inspection operation mode, to analyze an echo signal for defect type and location interpretations. The A-scan display is installed in the relay rack cabinet below the NIM-bin assembly.

3.1.1.8 B-Scan Display

Beside the A-scan display providing real-time information on the acoustic waves sweeping through the billet in the radial direction, a compound B-scan display is also provided. This additional display provides a real-time cross-sectional view of the billet slice circular scan composed by the radial sweeps for a given billet axial location.

This compound B-scan, or Plan Position Indicator (PPI-scan), is another method of presenting sweep and scan information as shown in Figure 51D. Since the titanium alloy forging billets considered in this program are rounds, and are rotated around their longitudinal axis, the PPI scan can be visualized as a modified B-scan, in which rectangular coordinates are replaced by polar coordinates. As the billet is rotated, so is the sweep so that a circular cross-section of the billet is probed by the sweeps (analog to the acoustic waves traveling in the billet from its outside front interface to its center and reflected back by discontinuities). When a defect back reflection is received, the intensity of the CRT spot is increased considerably and a bright spot remains at the point on the screen.

To provide a compound picture of the individual sweeps, a split-screen storage CRT is used as the indicator on which ultrasonic video signal integration occurs resulting from light intensification produced by the phosphor persistence and visual perception of adjacent spots. This integration reduces the signal-to-noise ratio required for detection.

After accomplishing a 360° circular scan, the display may be erased and a new circular scan may be started for the next billet axial scan location. For the manual billet inspection mode operation of the UDIS system the circular scan display may be stored for a limited time.

The compound B-scan display of the UDIS consists of a Type 564B main frame with two Type 3A9 plug-ins, manufactured by Tektronix, Inc. The display utilizes the outputs of the billet angular position monitoring encoder after the data processing system processes them continuously, and in real-time, for their corresponding sine and cosine values. Defect reflected acoustic echo signals available from the Defect Gate Module are further amplified by the Z-Processor Amplifier and then fed into the B-scan display oscilloscope to provide the necessary intensity modulation.

Figure 52 shows the circuit diagram of the Z-processor amplifier and Figure 29 illustrates the operation of the compound B-scan display. The B-scan display is installed in the relay rack cabinet below the A-scan display oscilloscope.

#### 3.1.1.9 Power Supplies

The ultrasonic instrumentation of the UDIS is built using linear and TTL integrated circuits. Accordingly, power supplies of ±5, ±12 and ±15 volts service the various function modules. The ±12 volt power supply is an integral part of the NIM-bin, the others are TRW built into a quad-size NIM-module and plugged into the bin. Circuit diagrams of the power supplies are shown in Figures 53 and 54 and the power supply module assembly is shown in Figure 55 with its side panel removed.

#### 3.1.1.10 Power Distribution

The power distribution systems of the entire UDIS is designed to accept the popular industrial 440V 60Hz AC power source as input. This voltage level is then stepped down, regulated and filtered to provide a constant voltage and noise disturbance-free power source to the UDIS. The system may also be operated from 220V 60Hz AC power line without a step-down transformer, or from 110V 60Hz AC power line without the internal voltage regulator.

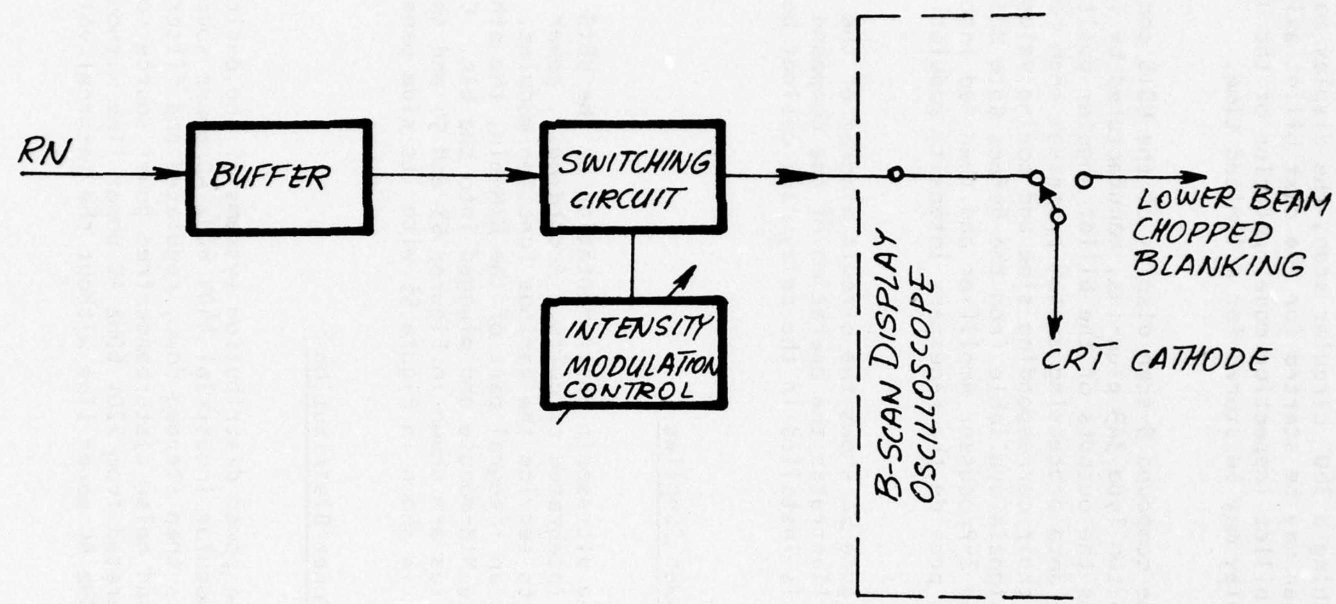


Figure 52. Circuit Diagram of the Z-Process Amplifier

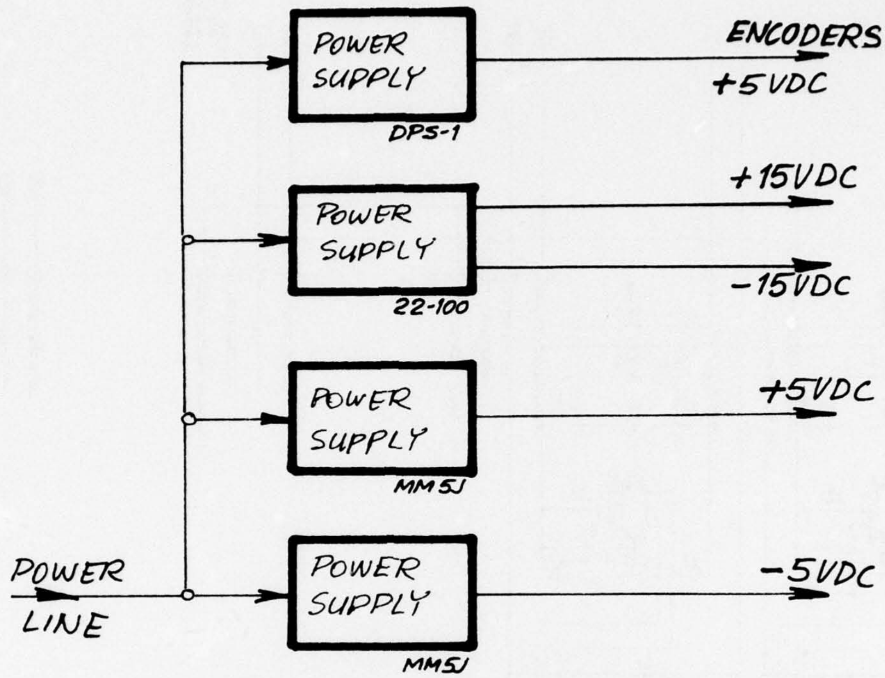


Figure 53. Circuit Diagram of the Power Supply Module

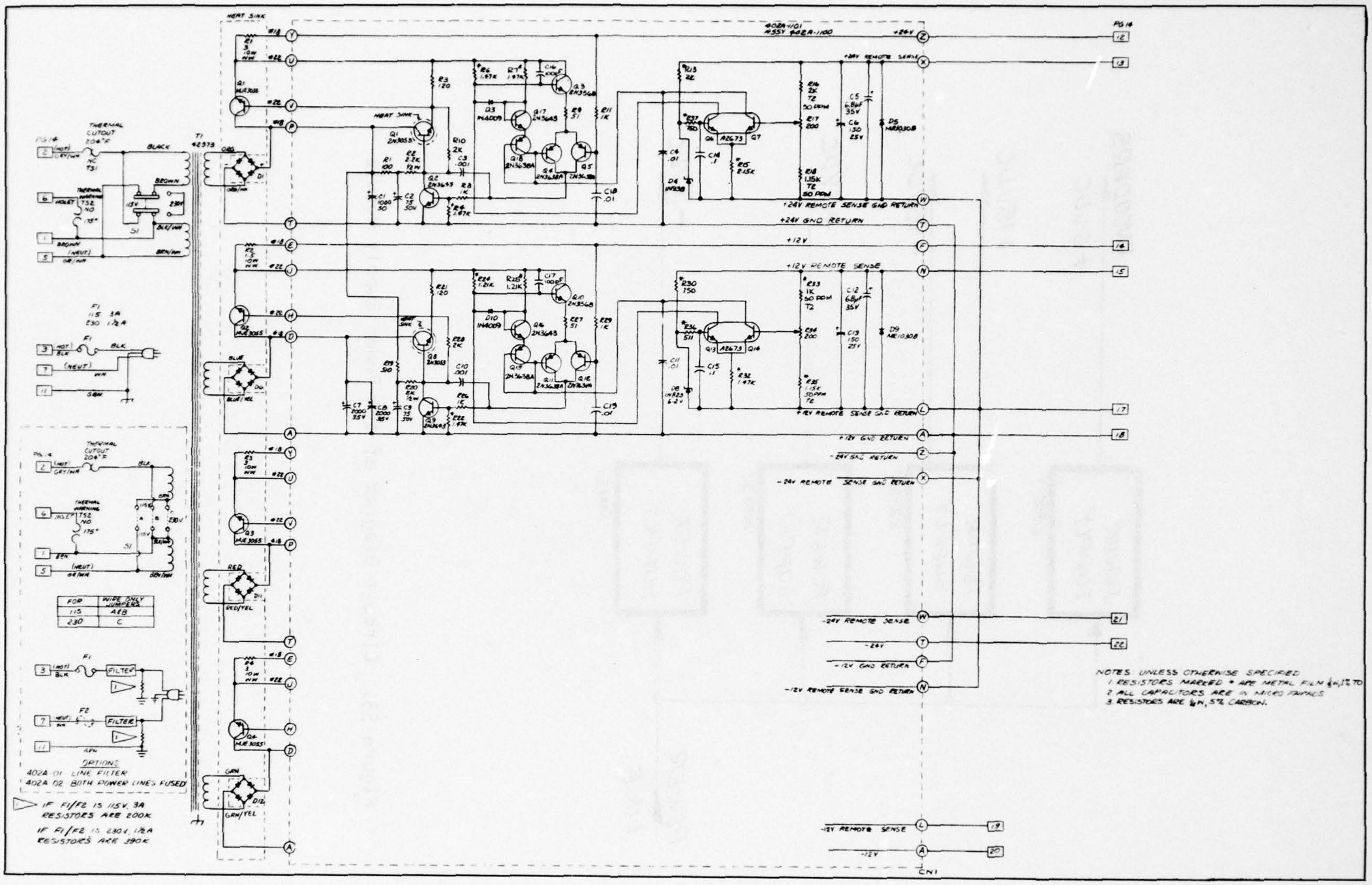


Figure 54. Circuit Diagram of the NIM-Bin Power Supply

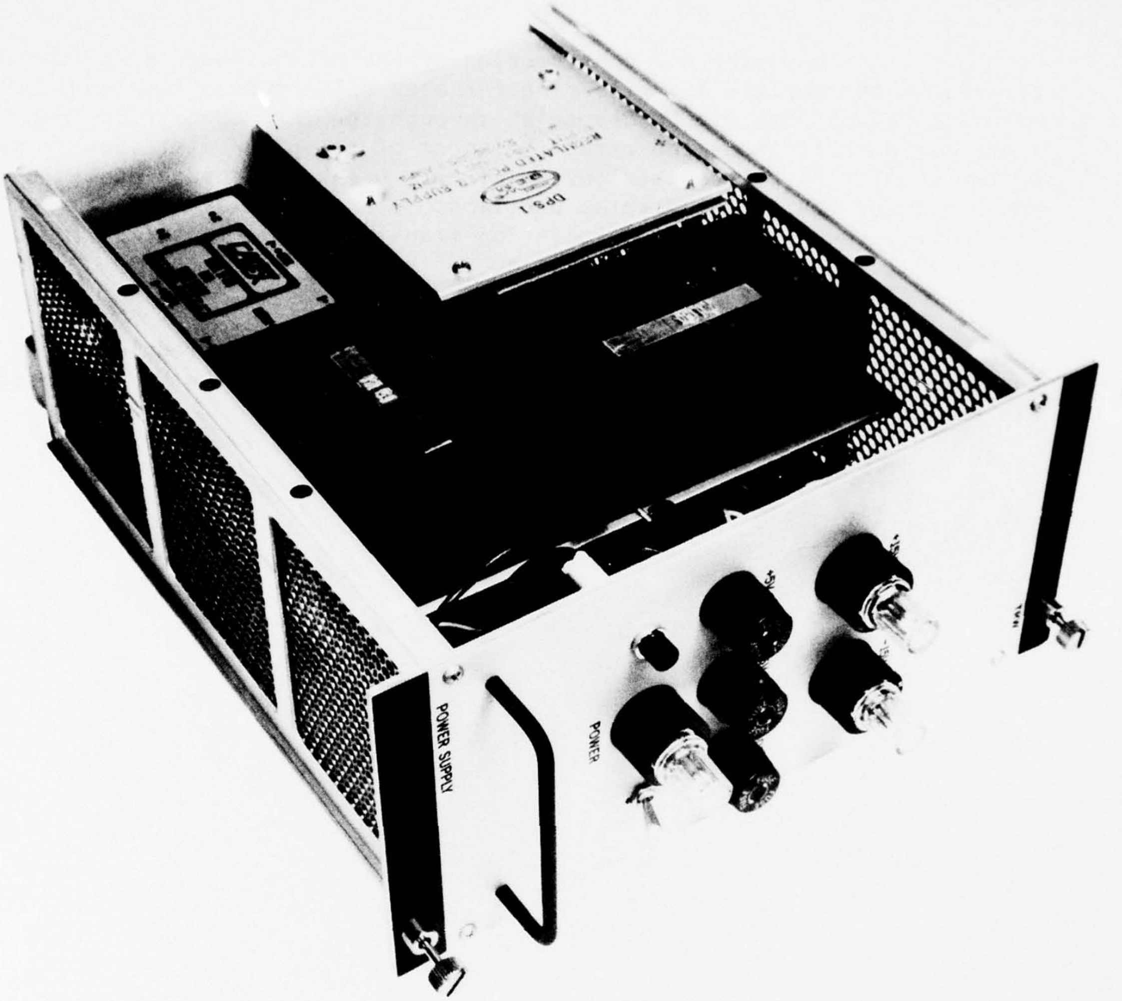


Figure 55. Power Supply Module

The design and construction effort of the power distribution covered an appropriate EMI filtering for each major system component in order to reduce possible "cross-talk" through the interconnecting power lines. Figure 56 shows the circuit diagram of the power distribution system of the UDIS. The power distribution circuit breaker and fuse panel is mounted under the B-scan display oscilloscope in the relay rack cabinet. The voltage regulator and the isolation transformer are installed inside at the bottom of the relay rack cabinet.

As part of the power distribution the system module interconnections of the NIM-modules are shown in Figure 57. The NIM-connector pin assignments are shown in Figure 58.

6189 C

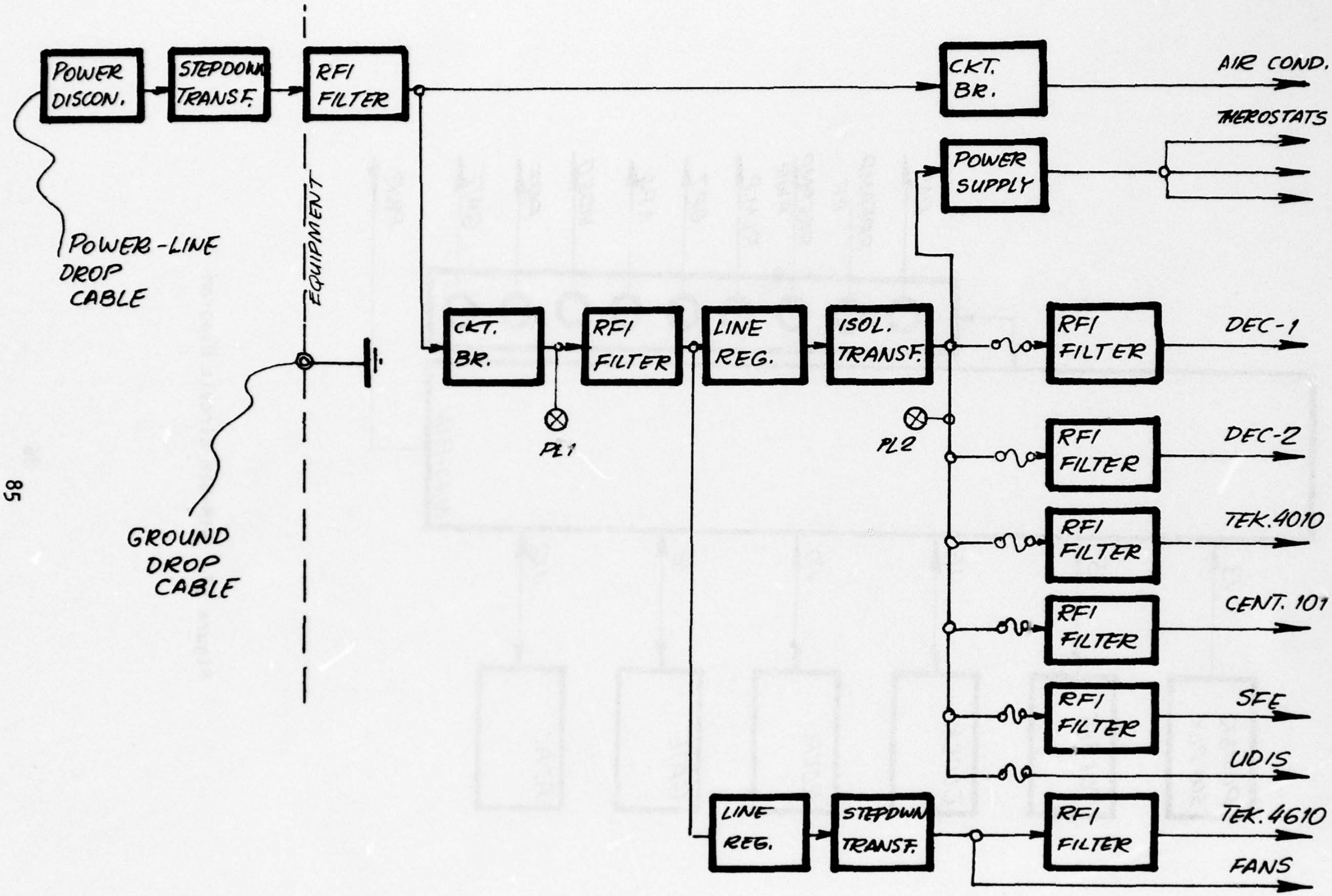


Figure 56. Circuit Diagram of the UDIS Power Distribution

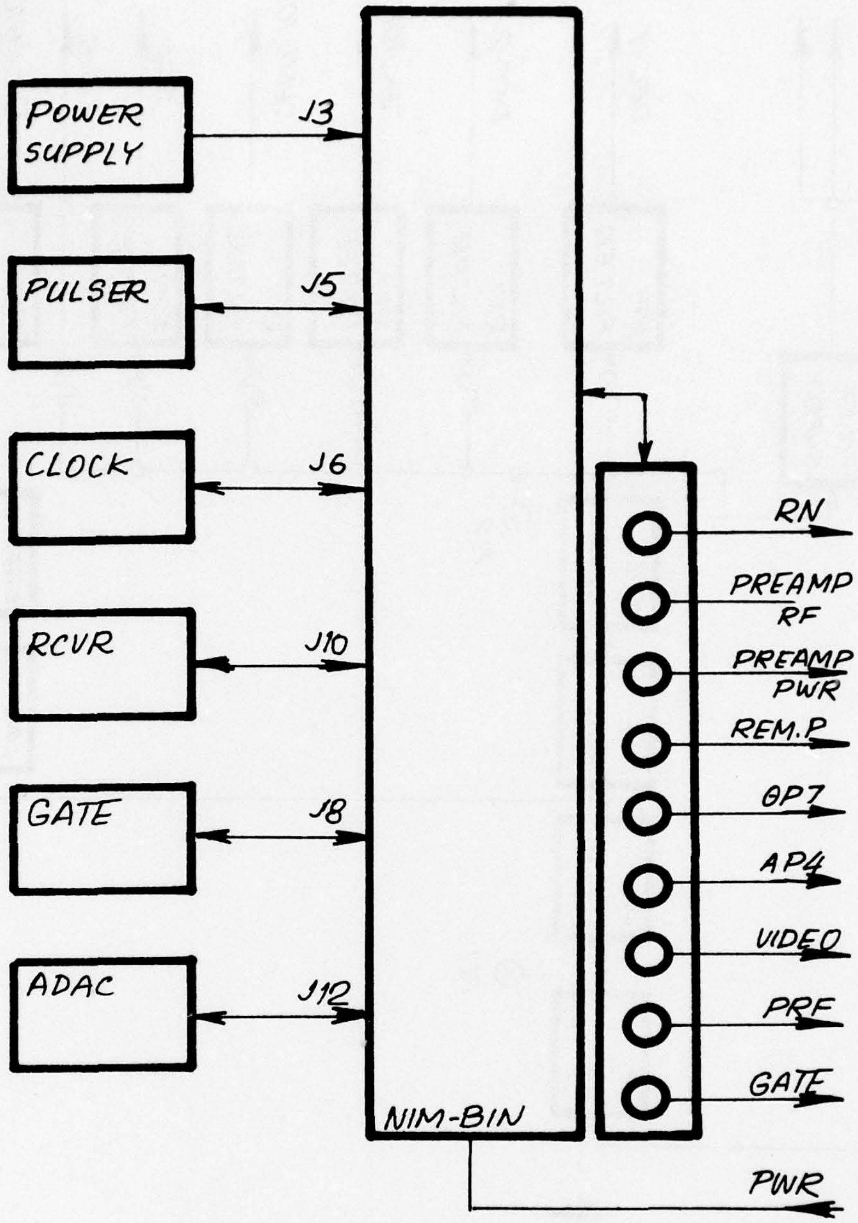


Figure 57. NIM-Bin Circuit Diagram

| Pin No. | Use | Notes |
|---|---|---|
| 1 | +5VDC | *✓ |
| 2 | -5VDC | *✓ |
| 3 | +15VDC | - |
| 4 | -15VDC | ✓ |
| 5 | RN | - |
| 6 | ADAC/SFE | - |
| 7 | ADAC/XDUCER | - |
| 8 | +200VDC | - |
| 9 | +1.2KVDC | - |
| 10 | +6VDC | *✓ |
| 11 | -6VDC | *✓ |
| 12 | BFIFSP(HOT) | - |
| 13 | BFIFSP(NEUT) | - |
| 14 | | (spare) |
| 15 | | ✓(reserved) |
| 16 | +12VDC | *✓ |
| 17 | -12VDC | *✓ |
| 18 | +5VDC-HOT(ENCODER) | - |
| 19 | BFIFWDTP(HOT) | - |
| 20 | BFIFWDTP(NEUT) | - |
| 21 | GATE DRIVE | - |
| 22 | ADAC RCVR GATE | ✓ |
| 23 | ADAC SLOPE CTRL-1 | ✓ |
| 24 | ADAC SLOPE CTRL-2 | ✓ |
| 25 | ADAC SLOPE CTRL-3 | ✓ |
| 26 | PULSER DRIVE - HIGH | - |
| 27 | PULSER DRIVE - LOW | - |
| 28 | +24VDC | *✓ |
| 29 | -24VDC | *✓ |
| 30 | +5VDC-NEUT(ENCODER) | - |
| 31 | CARRY NO. 2 | ✓ |
| 32 | TRIG.(REMOTE PULSER) | - |
| 33 | 115 VAC - HOT | *✓ |
| 34 | PWR. GND. RETURN | *✓ |
| 35 | RESET | ✓ |
| 36 | GATE(DISPLAY) | ✓ |
| 37 | ADAC-CONTROL/DC | - |
| 38 | PRF | - |
| 39 | RCVR-OUT(VIDEO/RF) | - |
| 40 | RCVR-RFINPUT | - |
| 41 | 115VAC-NEUT | *✓ |
| 42 | HIGH QUAL. GND. | *✓ |
| G | GND GUIDE PIN | ✓ |
| | GND GUIDE SOCKET | |

NOTES: * - Must be bussed to all connectors
✓ - AEC assignment

Figure 58. NIM Pin Assignment

### 3.1.2 Transducers

The transducer is a device by means of which energy can flow from one or more transmission system or media to one or more other transmission system or media. In the ultrasonic inspection of the titanium billets the instrumentation discussed in Section 3.1.1 performs the generation and detection of electric waveforms which are analog to the interrogating and defect reflected acoustic energies. It is very important in this process that the fidelity of the energy conversion from electric to acoustic, and to electric again, be carefully maintained. Furthermore, it is important that the billet acoustic illumination be properly oriented to permit accurate position location of the defect.

The billet acoustic illumination patterns for the design limits of the 8 and 16-inch diameter billets, using conventional flat-faced transducers are shown in Figure 1. This method is practiced by conventional inspection techniques. In view of the novel combination of pulse-reflection defect detection and thru-transmission automatic distance-amplitude compensation method used by the UDIS for the three dimensional combined polar-rectangular coordinate system (Section 2.3 and Figure 25), an improved acoustic illumination and defect detection pattern was designed. Resultingly, a pie-cut shaped cylindrical section billet acoustic illumination was established as shown in Figure 28. The change in billet illumination reduced the widespread acoustic beam and confined it to a discrete billet section in accordance with the designed billet coordinate system. The significant differences between the conventional (Figure 1) and the pie-cut shaped cylindrical section (Figure 28) billet acoustic illuminations may be seen as modeled in Figure 27 and Figure121 (of Section Appendix I). The new billet illumination concept provides two significant advantages of an increased signal-to-noise ratio and improved resolution for billet angular scan.

Transducer design, therefore, played an important role in the UDIS design. To procure the required transducer, specifications were provided to numerous transducer manufacturers. Special effort was made in negotiating specifications to obtain the transducers with the highest available transmitting and receiving sensitivities and with optimum damping. As a result, three transducers were purchased from two vendors. For the 8 and 16-inch diameter billets the desired special pie-cut shaped acoustic illuminations have been accomplished by PZT-5 type piezoelectric element transducers of 5 and 2.25 MHz frequencies, respectively, and focused in their appropriate cylindrical shape. A TRW in-house evaluation of these transducers was also carried out with transducers identified in Table XII.

The purpose of the transducer evaluation was to utilize the transducer type which provides the best performance. The end result of the transducer evaluation was aimed at obtaining electroacoustic parameters which would relate an electric variable to an acoustic one, or the inverse. Typically the most often used electroacoustic parameter is the sensitivity (voltage/pressure) or the response (pressure/voltage) computed from measured electric data and various constants. Accordingly, the free-field voltage sensitivity of the three transducers purchased were measured. This parameter is useful for sound reception as the ratio of the output open circuit voltage to the free-field sound pressure in an undisturbed plane progressive wave. In addition, the transmitting voltage response of the transducers was measured. This parameter is useful for sound emission; it is the ratio of the sound pressure apparent at a unit distance in a specified direction from the effective acoustic center of the transducer to the signal voltage applied across the transducer. Measurements were carried out using a secondary method in which a known transducer was used as a reference standard. Both the receiving voltage sensitivity, M, and the transmitting voltage response, S, are dimensionless numbers and are expressed as a function of frequency. The data are compiled in Table XII, and identify transducer No. 1 as the best transmitter for any frequency measured; transducer No. 3 as the best receiver for 2.25 MHz frequency; transducer No. 2 as the best receiver for both 1.0 and 5.0 MHz frequencies; and the best overall (pulse-receive) transducers are No. 1, No. 3 and No. 2 for the corresponding frequencies of 1.0, 2.25 and 5.0 MHz.

When the relative sensitivity, or response, is measured as a function of direction, the directional response pattern, or more simply, the beam pattern is obtained. For the transducers No. 2 and 3 the acoustic beam pattern profiles are shown in Figures 59 and 60. It should be noted that in each figure the beam profiles relate to an acoustic wave path distance of 4.25-inches (A) and 13.35 inches (B). The shorter distance relates to the transducer-billet front interface water distance, and the longer distance is at the focal lines of the transducers.

The time domain responses of the transducers No. 1, 2 and 3 are shown in Figures 61A, 61B and 61C, respectively. These transducer response curves were obtained by pulsing the transducer and by subsequently recording its reflected signal from a 1-inch diameter steel sphere target suspended at an 13.35-inch distance from the transducer. The variations in damping characteristics of the transducers are readily seen.

## TABLE XII

## TRANSDUCER SENSITIVITY AND RESPONSE

| Transducer Identification[(1)] | Frequency MHz | Receiving Voltage Sensitivity M | Transmitting Voltage Response S | Overall Response O |
|---|---|---|---|---|
| 1 | 1.0 | 0.54 | 4.17 | 2.25 |
| | 2.25 | 0.82 | 4.64 | 3.80 |
| | 5.0 | 0.58 | 3.28 | 1.89 |
| 2 | 1.0 | 1.47 | 1.20 | 1.68 |
| | 2.25 | 1.48 | 1.43 | 2.12 |
| | 5.0 | 1.54 | 1.38 | 2.13 |
| 3 | 1.0 | 1.04 | 1.40 | 1.46 |
| | 2.25 | 2.61 | 2.23 | 5.82 |
| | 5.0 | 1.25 | 1.56 | 1.95 |

Notes:

(1) Transducer identification:

No. 1: Panametrics, S/N 772, 2.25 MHz, 0.5x0.75-inch, focused
No. 2: Aerotech, S/N 13600, 5.0 MHz, 0.75x2.5-inch, focused
No. 3: Aerotech, S/N 13601, 2.25 MHz, 0.75x2.5-inch, focused

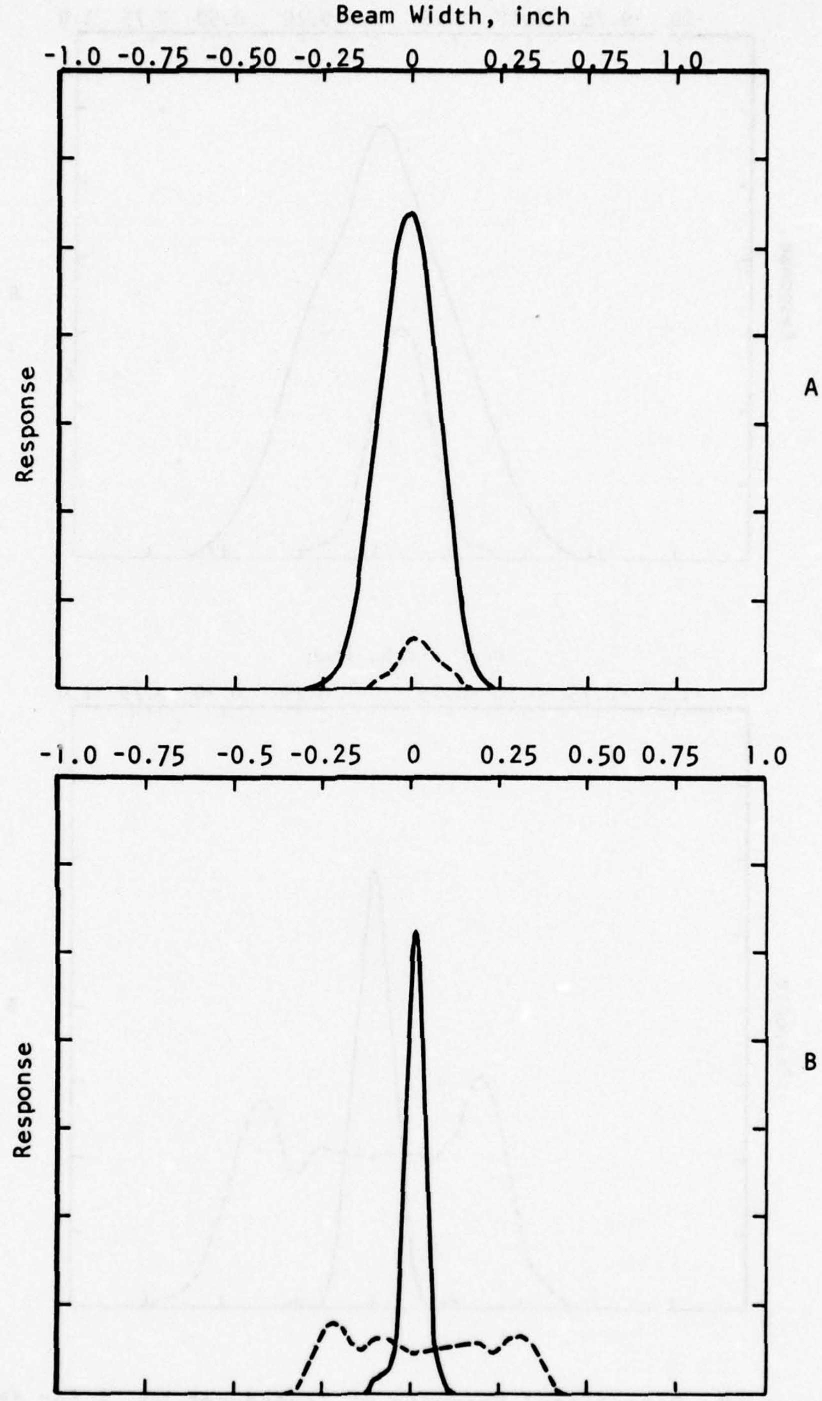


Figure 59. Directional Response of Transducer No. 2 for the Transducer "Width" Direction (A)and for the Transducer "Length" Direction (B), at 9.25-inch Distances (solid lines) and 4.25-inch Distance (dashed lines).

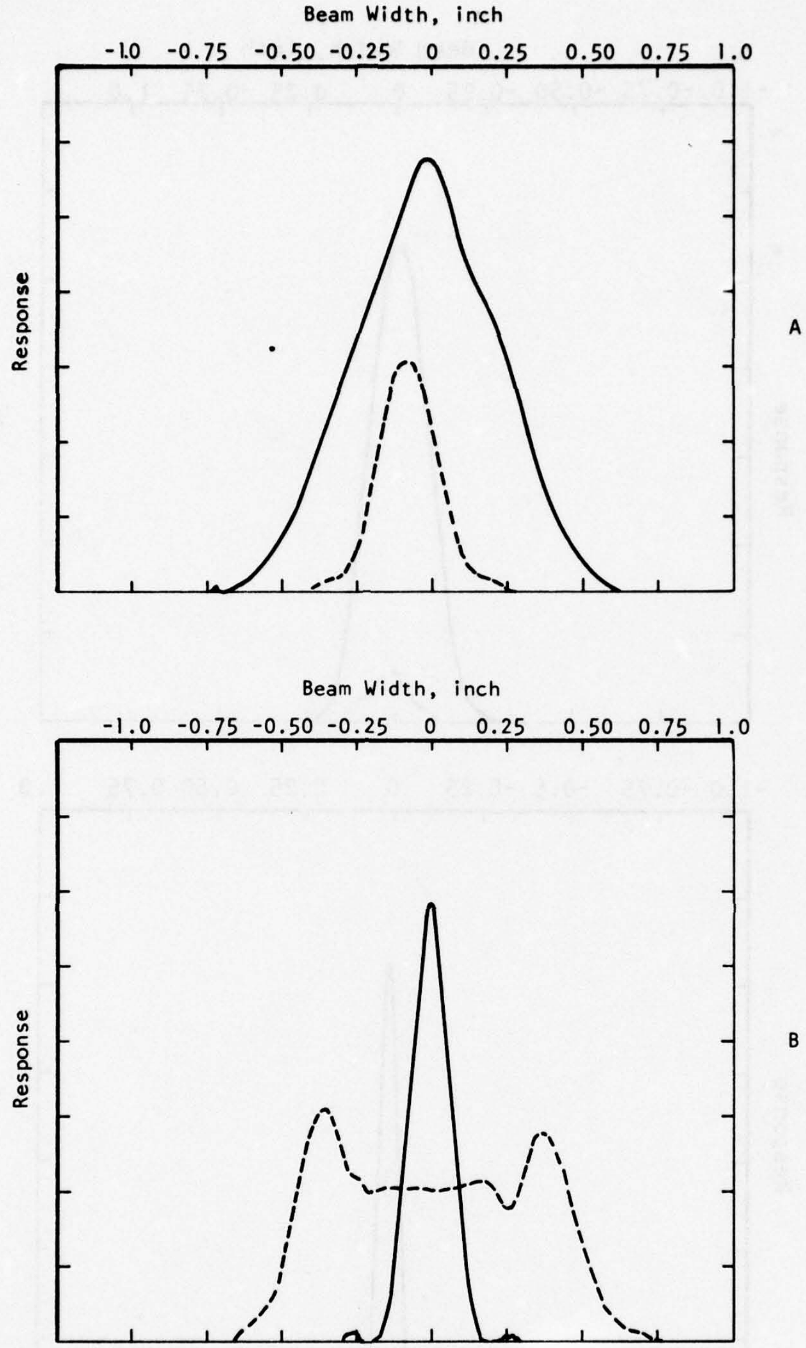


Figure 60. Directional Response of Transducer No. 3 for the Transducer "Width" Direction (A) and for the Transducer "Length" Direction (B), at 13.35-inch Distances (solid lines) and 4.25-inch Distance (dashed lines).

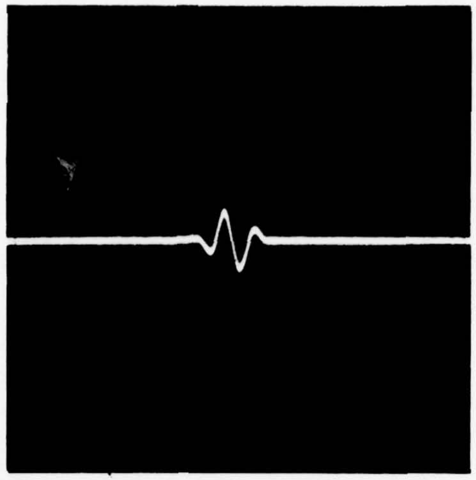

A

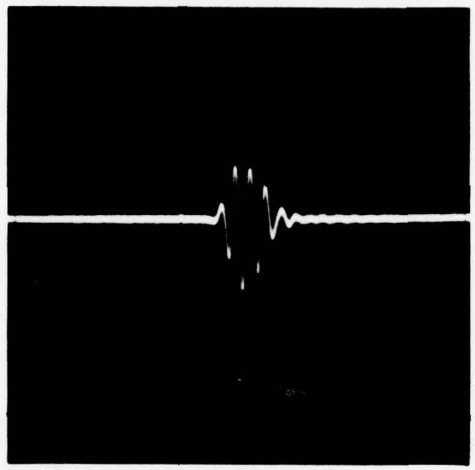

B

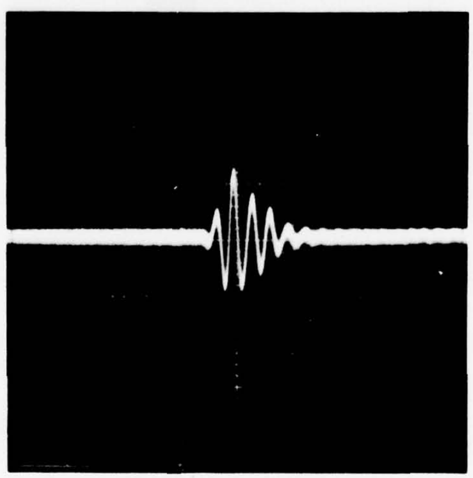

C

**Figure 61.** Time Domain Response of Transducers No. 1 (A), No. 2 (B) and No. 3 (C).
(Vertical Display: 1mV/cm for Figures A & B
2mV/cm for Figure C
Horizontal Display: 1μs/cm)

Finally, transducer impedance characteristics were measured. The impedance of an electroacoustic transducer usually is understood to mean the electric impedance as measured at its electric terminals. Along with sensitivity or response patterns, the electric impedance is a common and standard parameter in the calibration and evaluation of electroacoustic transducers. The transducer electric impedance may be used for the following three purposes; for one, it provides information for impedance matching between the transducer and the electronic transmitting and receiving instrumentation; second, it may be used in the computation of transducer efficiency and driving voltage from current responses, or vice versa, and third, it is an analytical tool for studying the performance of a transducer. Figures 62, 63 and 64 illustrate the electric impedances (solid lines) and the phases (dashed lines) for the transducers, No. 1, 2 and 3 respectively. For reference purpose only, the zero degree phase, as well as the 10 and 100-ohms impedances are also drawn. The data shown cover the frequency range of interest.

In addition and prior to the transducer procurements, acoustic billet illumination experiments were also carried out using flat PZT-5 and PZT-7 thickness expander piezoelectric elements. Characterization of these transducer elements included frequency and time domain measurements. Frequency domain measurements included two terminal transfer characteristics (such as electric impedance, and phase), acoustic free-field voltage sensitivities and directional response patterns. Time domain measurements included pulse-reflection responses obtained from sphere steel targets suspended at distances equivalent to transducer focal lengths. These experiments yielded valuable information on transducer procurements and subsequent evaluations.

Beside the cylindrically focused transducer used for pulse-reflection mode defect detection, a second transducer is also applied in the billet illumination plane at the opposite side of the billet and is used for the automatic distance-amplitude compensation. The second, or ADAC transducer is a commercial flat-faced, unfocused one which has a PZT-5 type piezoelectric element of the same frequency as the pulse-reflection transducer.

The electro-acoustic transducer is a key element in an ultrasonic NDE system, strongly affecting system performance. Application of the transducer in the UDIS, however, was based on a tradeoff between the required specifications and the best characteristics obtained from the procured transducers.

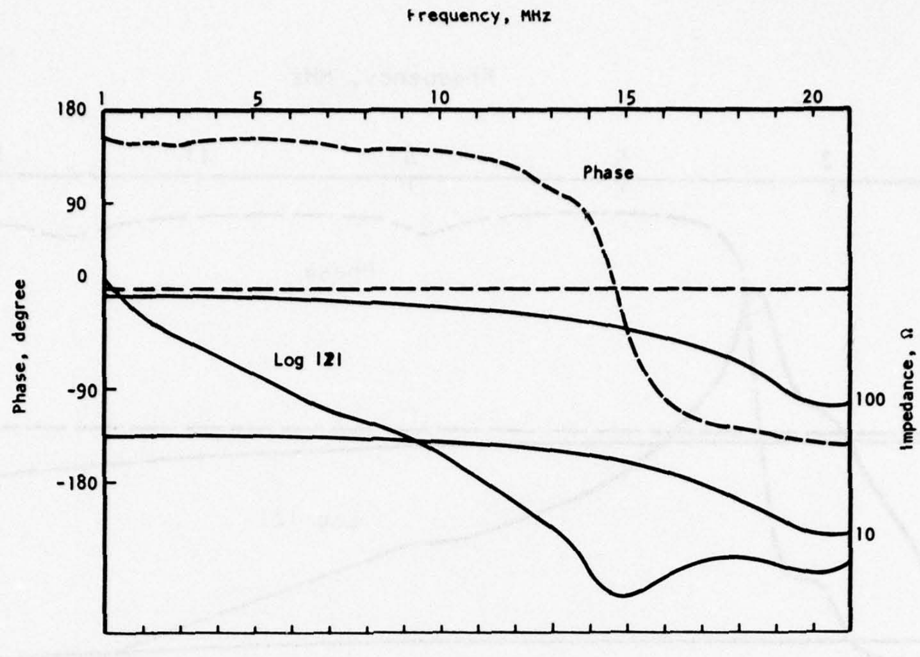


Figure 62. Electric Impedance (solid line) and Phase (dashed line) of Transducer No. 1.

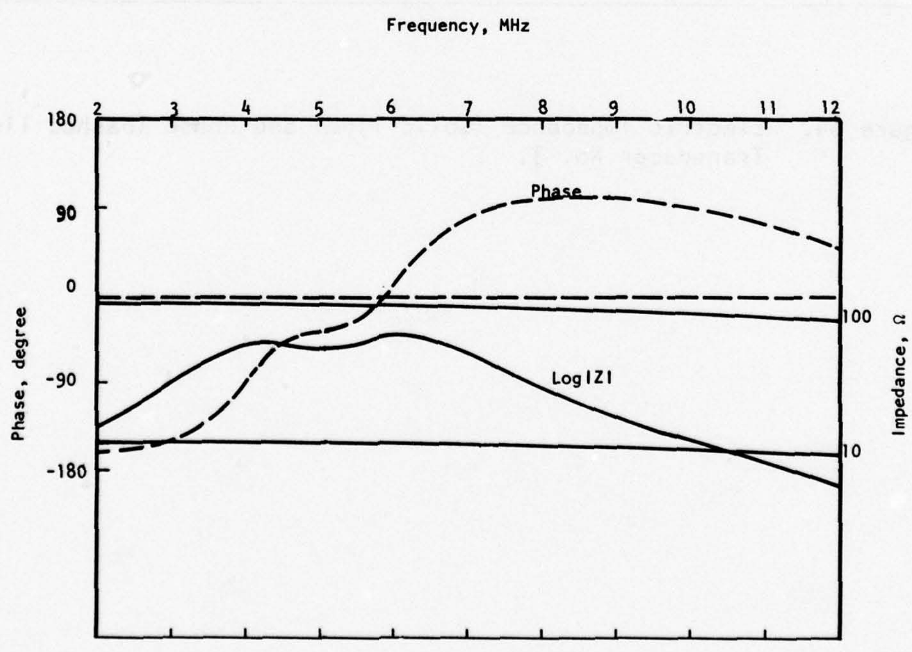


Figure 63. Electric Impedance (solid line) and Phase (dashed line) of Transducer No. 2.

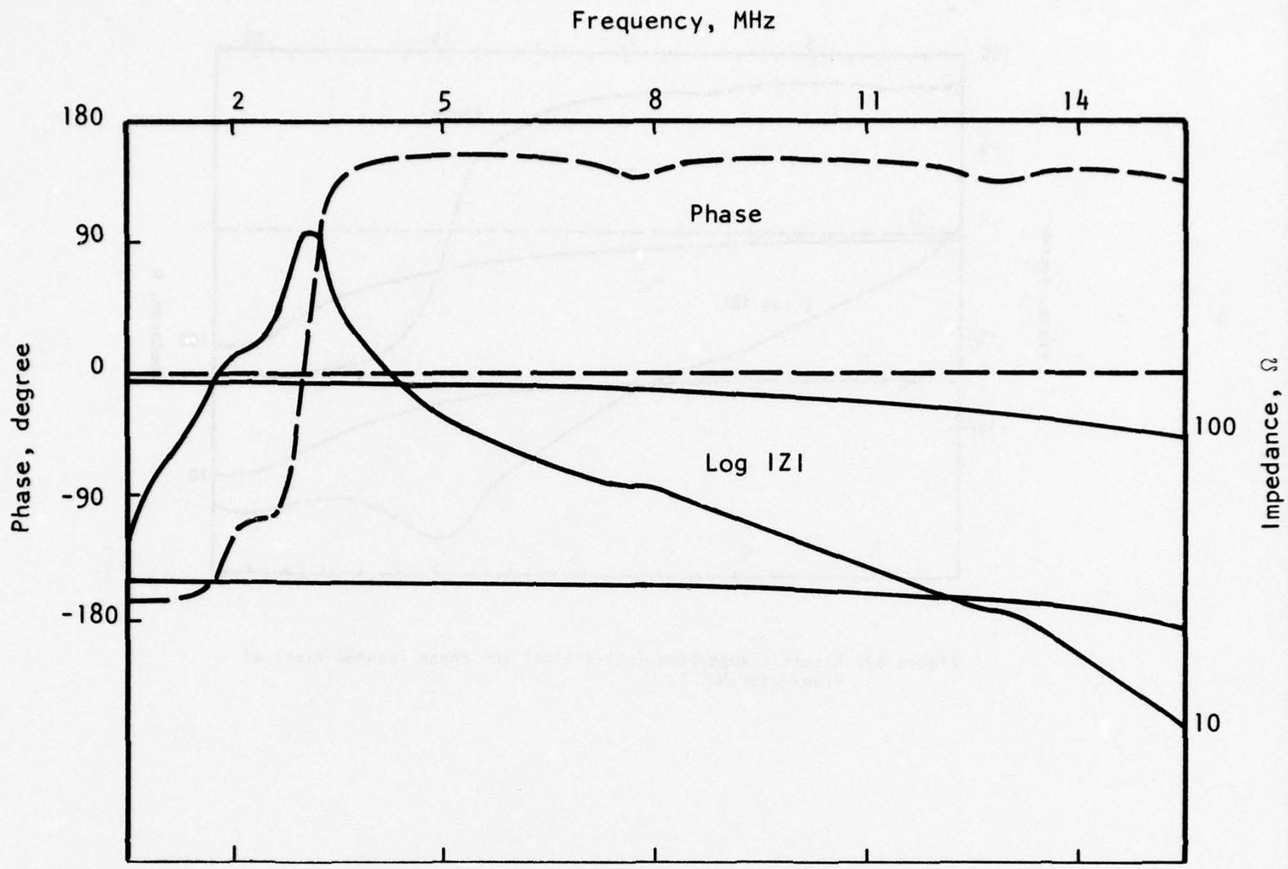


Figure 64. Electric Impedance (solid line) and Phase (dashed line) of Transducer No. 3.

## 3.2 Billet Scan Monitoring System

Defect detection is accomplished by the UDIS for both defect size and its location in the billet. The defect size is determined by the ultrasonic instrumentation and transducers (Sections 3.1.1 and 3.1.2). The defect location, in accordance with the combined billet polar-rectangular coordinate system, is determined by the ultrasonic instrumentation and by the billet scan monitoring system. Defect location measured by the billet radial axis, R, is obtained from the timing information of the defect echo itself. This information is calculated by the data processing system in real-time from the acoustic sweep data of the billet (Section 3.3). Defect locations measured by the two additional coordinates of billet angular position, θ, and axial position A, are established by two digital shaft encoder devices, which are attached to the billet handling immersion tank facility as described below. These encoders monitor the ultrasonic transducer and billet rotational positions and are sampled by the data processing system for each defect in real-time.

### 3.2.1 Angular Scan

Defect location measured by the billet polar coordinate's angular axis, θ, is established by the billet angular position monitoring device. This device has a digital shaft encoder, which monitors the billet rotation in respect to the stationery ultrasonic transducer. Prior to billet inspection, an arbitrary angular billet position must be selected as a reference. In view of the program requirements, where the UDIS was to be operated in the billet producer subcontractor's facility using their existing ultrasonic water tank, accurate billet angular position monitoring was very difficult to establish. Because the billet is being rotated by supporting rollers, there can be a significant slippage accumulate during billet inspection. This would result in an inaccurate billet rotation measurement if the encoder would be attached to the drive shaft. Therefore, billet angular position monitoring was carried out with a slippage-free attachment to the billet. Accordingly, the entire digital shaft encoder and its drive mechanism was designed for an underwater operation, direct coupled to the billet. The mechanical coupling was accomplished via a flexible coupling (clutch) connected between the encoder drive mechanism and a small shaft cemented to the approximate center of the billet end face. The flexible shaft coupling was designed to allow liberal axial and radial (centerless) sway for the billet attached shaft while maintaining precise billet angular position monitoring. This approach ensured the required accuracy for the helical scan of a ten foot long billet.

A commercial non-contact type, continuous rotation, bi-directional, digital, absolute position indicating encoder was selected to monitor the billet angular position. The encoder provides one-hundred discrete location codes in cyclic binary decimal code per revolution. This information was designed to be transmitted to the data processing system in the 5-volt positive TTL compatible BCD logic form. The encoder was installed in a sealed cast aluminum housing along with an appropriate TRW in-house designed gear drive and clutch mechanism. The Angular Billet Position Monitoring Device, as assembled, provides a total counting capacity of one-hundred counts of 0 through 99 and is capable of operating up to 80 RPM of rotational speed. The Billet Angular position monitoring device is shown in Figure 65, with its waterproof cover removed.

### 3.2.2 Axial Scan

Defect location measured by the billet rectangular coordinate's billet length or axial axis, A, is established by the Axial Billet Position Monitoring Device. This device employs a digital shaft encoder, which monitors the position of the ultrasonic transducer along the longitudinal axis of the billet. Prior to billet inspection, an arbitrary axial billet position must be selected as zero reference (most likely one billet end). In view of the program requirements, whereas the UDIS was to be operated in the billet producer subcontractor's facility using their existing ultrasonic water tank, accurate billet axial position monitoring was difficult to establish. Because the mill produced billets are neither a perfect circle in cross section nor are they straight in lengths the billets tend to "walk" along their supporting rollers. This axial wobbling of the billet can cause a significant error. Therefore, a special effort had to be maintained during billet inspection at the subcontractor's plant to mechanically retain the billet at its referenced axial position.

A commercial non-contact type, continuous rotation, bi-directional digital, absolute position indicating encoder was selected to monitor the billet angular position. The encoder-drive mechanism system provides a total counting capacity of one-thousand counts (0 through 999) for the designed thousand discrete location codes using the grey code. This information was designed to be transmitted to the data processing system in the 5-volt positive TTL compatible BCD logic form. The encoder

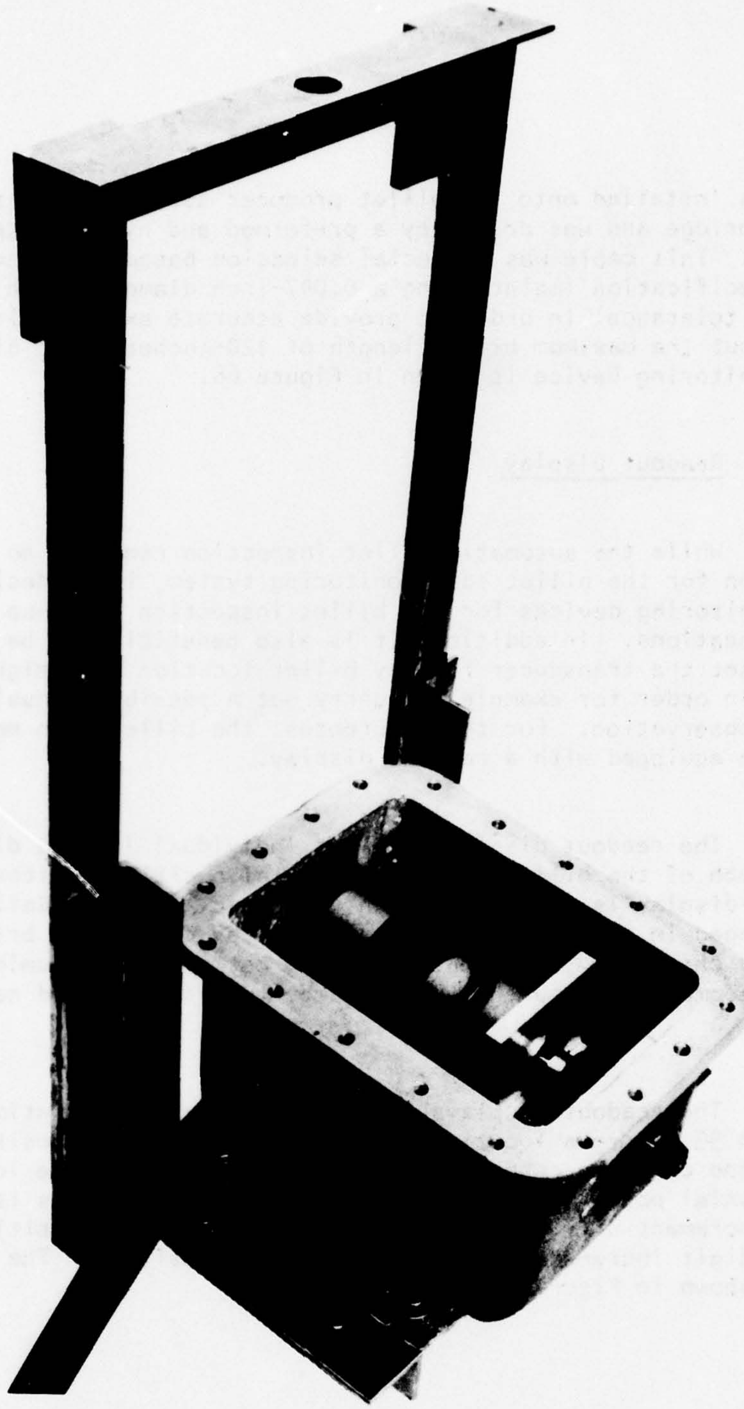

Figure 65. Billet Angular Position Monitoring Device

assembly was installed onto the billet producer subcontractor's ultrasonic transducer bridge and was driven by a preformed and nylon coated stainless steel cable. This cable was a special selection based upon the MIL-C-5424A-1 HCC 100X specification (maintaining a 0.047-inch diameter with +0.003 and -0.000-inch tolerance) in order to provide accurate axial position monitoring throughout the maximum billet length of 120-inches. The Billet Axial Position Monitoring Device is shown in Figure 66.

### 3.2.3 Readout Display

While the automatic billet inspection requires no operator participation for the billet scan monitoring system, it is desirable to zero the monitoring devices for the billet inspection start-up angular and axial locations. In addition, it is also beneficial to be able to manually reset the transducer for any billet location that might be desirable, in order for example, to carry out a possible manual mode ultrasonic observation. For these purposes, the billet scan monitoring devices were equipped with a readout display.

The readout display contains individual in-line digital displays for both of the billet angular and axial position monitoring devices. The readout-display is made up of high efficiency discrete Gallium Phosphide diodes arranged in a seven segment format. They generate a bright, highly eligible red character. The contrast ratio between the illuminated and background segments was further enhanced by the use of a red non-glare window.

The readout displays provide a one-hundred counting capacity of 0 through 99 discrete locations for the billet angular position, and a one-thousand counting capability of 0 through 999 discrete location for the billet axial position. The resolution of these displays is a single unit cell increment of 3.6°/digit for the billet angular position, and a 0.125-inch/digit increment for the billet axial position. The readout display is shown in Figure 30.

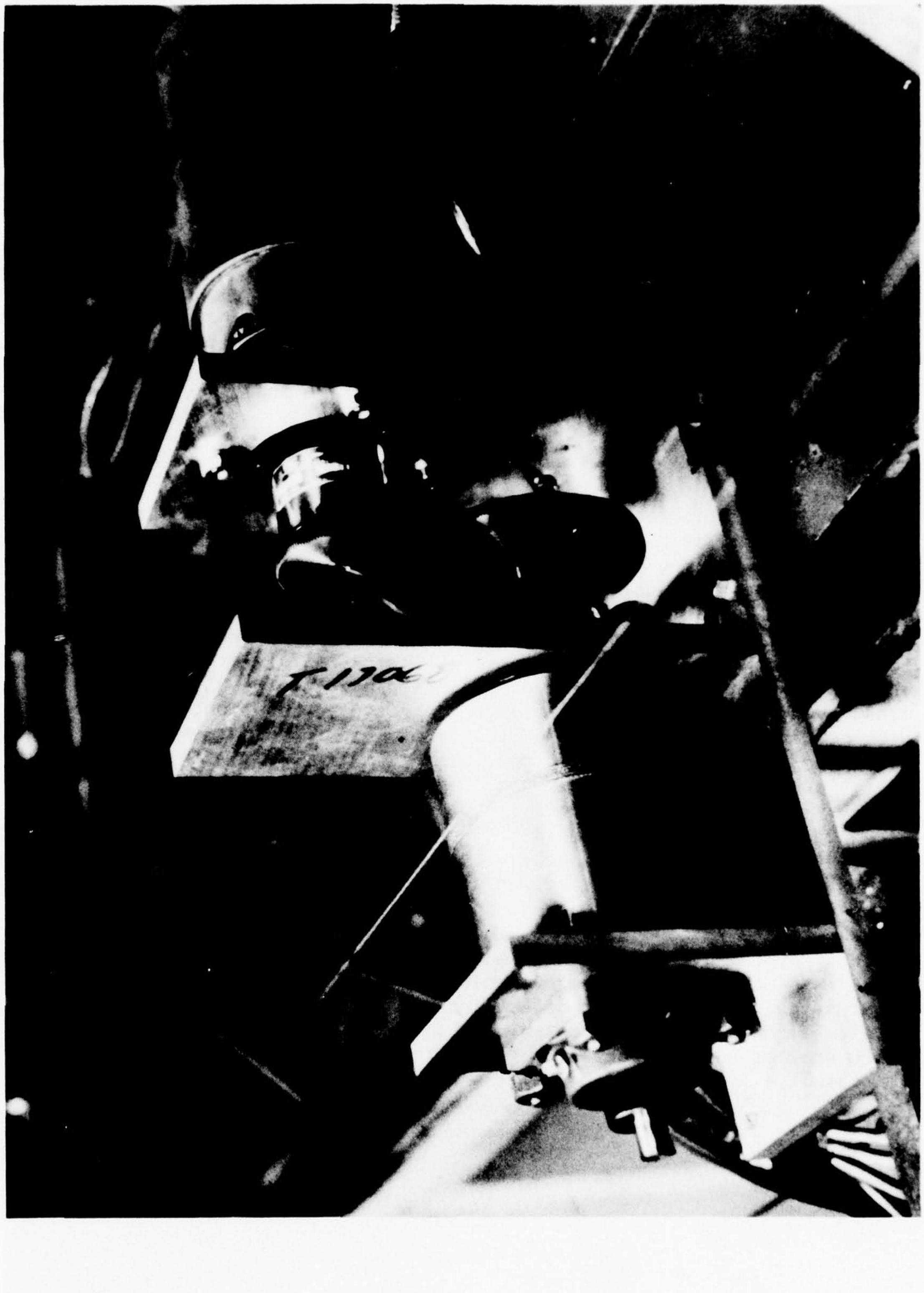

Figure 66. Billet Axial Position Monitoring Device

## 3.3 Data Processing System

To eliminate the variability of a human operator and to improve diagnostic capabilities beyond human capacity, a data processing system, DPS, was developed and incorporated into the UDIS. The DPS accepts the digital information of each ultrasonic sweep of a billet radius. This digital data under the control of an input terminal, is summed over repetitive sweeps to enhance the signal-to-noise ratio. As a result, output reports are produced showing defect locations and extensions at selected quality control reject criteria in 0.125 to 0.5-inch thick billet axial cross-sections for the entire billet length. On completion of the cross-section analysis, the new data for each billet cross-section is dumped onto an industry compatible magnetic tape, ICT, for possible later use.

For any particular setting of the Defect Gate of the UDIS ultrasonic instrumentation, an output gate signal indicates the presence of a reflection exceeding the setting of the gate. Since a marginally sized defect will not always create a reflection strong enough to trip the gate (due to the billet rotation caused variable aspect view of the interrograting transducer over the defect), the output gate signal can vary randomly between "ON" and "OFF" for small defects. The ON/OFF ratio will vary rapidly at defect sizes near the gate setting, with the larger defects producing the higher ratios. A measurement of this ratio related to a particular location within the billet provides a measurement of the certainty of defect indication at that location. The necessary coordinates for localizing a small volume within a titanium billet are given by the rotation ($\theta$) and axial translation (A) of the billet, and by the elapsed time between the pulse and the reflection, which is related to the radial position (R). The ratio is evaluated simply by pulsing the given location a fixed number of times and counting the number of output gate signals. For a cross section through a billet at axial translation A, these counts are stored in the computer's core in cells (core locations) related to the $R\theta$ coordinates of the billet. Through the variation in R produced by the ultrasonic sweep and the $\theta$ scan produced by billet rotation, a matrix of cells in the computer core are filled with counts showing the point-by-point certainty of defect indications in a particular cross section. By establishing a level of certainty, i.e., N "ON's" out of M pulses, the cells are tested for count significance and outputs prepared to indicate the result.

Two output devices are provided by the UDIS; a graphic display and a printer. The graphic display is a highly powerful form of presentation. In the UDIS it provides a conversation capability between man and machine. Its alphanumeric-graphic output provides questions for the operator to initiate and set inspection criteria and, after the inspection, it displays the results. The inspection results are provided by a display of billet cross sections with an identification of defective unit cells. The defective unit cells are displayed by a graphic symbol of "sector-of-annulus-with-point." This symbol represents a defective "Sector-of-rectangular torus" unit cell volume of the billet. Typical graphical displays are seen in Figures 75 and 76. The second output of the UDIS is a high-speed line-printer. This device prepares permanent documentation concerning the billet inspection. The UDIS application software provides for a choice of two types of printouts; a complete billet defect coordination report, and a billet reject report. Examples of these are seen in Figures 77 and 78, respectively.

As part of the defect diagnosis, one or more quality control rejection (QRC) criteria may be applied which relate to the nature, size and shape of significant defects. The necessary scan information is an inherent feature of the computer core images of the billet sections. By analysis of the one-, two-, and three-dimensional interconnections between cells containing significant defect counts, the computer evaluates the data with respect to a given QRC criteria and reports the location parameters of critical defects, as well as specifying billet acceptance or rejection.

The block diagram of the DPS of the UDIS is shown in Figure 67. It consists of a special front end, SFE; a minicomputer; an input/output alphanumeric-graphic, I/O, terminal; a high-speed line printer; a paper-tape reader; and program/data storages of a magnetic disk pack and a tape recorder. Description of the DPS is divided into two major areas of system software and hardware, which are discussed in the following sections.

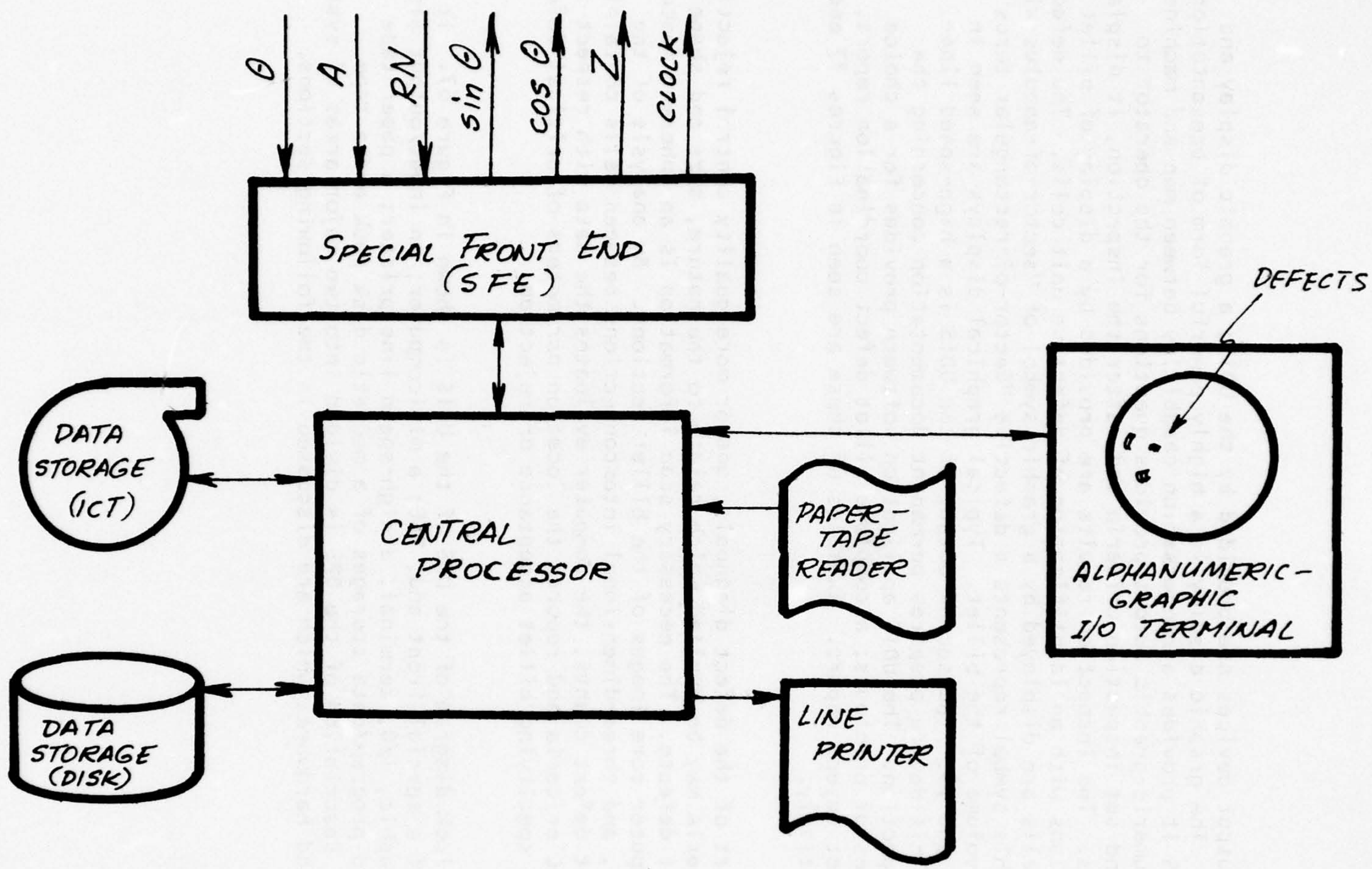


Figure 67. Block Diagram of the Data Processing System of the UDIS

3.3.1 System Software

The software is the collection of all programs required for a computer to perform as desired. Proper software support is the key to successful application of a minicomputer. For the DPS of the UDIS two types of softwares are in use; standard softwares and application softwares.

3.3.1.1 Standard Softwares

The standard software packages are supplied by the minicomputer manufacturer Digital Equipment Corporation, DEC. The package is DEC's Disk Operating System, DOS, which includes the following softwares:

(1) Assembler
(2) Editor
(3) Debug Routine
(4) File Utility Package
(5) Relocate Linking Loader
(6) Librarian, and
(7) Diagnostics

In addition, "Basic" and "Fortran" compilers are also supplied. In view of the objectives of this report, no description of the standard softwares is given here, but a reference is made to DEC publication No. DEC-11-MWDC-D "Disk Operating System Monitor Programmer's Handbook" and the associated documents listed therein describe the DOS operations.

3.3.1.2 Application Software

The application software is the collection of programs for the DEC PDP-11/20 computer system in use, to perform the UDIS billet inspection. These softwares are disc resident and can be initiated by the operator entering a RUN EXEC command while the DOS monitor is active. Similarly, a MOnitor command, while the billet test routine's executive is active will initiate the DOS monitor. The application softwares developed consist of two different sets of programs:

(1) those which are used during the on-line billet inspecting period, and
(2) those which are used for test and maintenance of the SFE hardware.

All programs are written using the MACRO-11 assembly language. The programming is accomplished using modular techniques so that the many different modes of system operation can be implemented by setting up the required configurations of program sub-routine modules. This approach to system programming requires the least amount of program storage and facilitates future system software modifications or additions.

Since the implementation of the software system for the DPS involves the simultaneous interaction of several functional program modules, the executive control and monitor program (SFEXEC) was very carefully formulated

The different modes of system operation are established by the executive in response to operator commands entered through the I/O keyboard terminal. All of these commands are inserted in a conversational format that does not require a skilled computer operator for system operation. The conversational capability of the DPS is shown in Appendix II. The operator-inserted messages are denoted by italics; computer-generated messages are shown in capitalized bold-face type.

The DPS of the UDIS is provided with the following seven system application softwares:

1. Manual Billet Inspection Mode
2. Automatic Billet Inspection Mode
3. Calibration Mode
4. Off-line Mode
5. Initialization Mode
6. Zero Command
7. Power Restart Mode

The system concept of the UDIS is illustrated in Figure 68, Flow Chart and a brief description of the various application softwares are given in the following sections.

#### 3.3.1.2.1 Manual Billet Inspection Mode

This application software provides a manual mode of billet inspection. While system operation is performed automatically for discrete billet slices, nevertheless operator interaction is required to continue the process.

#### 3.3.1.2.2 Automatic Billet Inspection Mode

The "Automatic Billet Inspection Mode" system application software provides a fully automatic inspection of billets by the UDIS. The test may be stopped manually, or will be stopped automatically by the DPS if certain test conditions are not met. Billet inspection may be restarted provided all required test parameters are met. The billet inspection, including the printouts of data, are automatically terminated when the billet scan is complete.

#### 3.3.1.2.3 Calibration Mode

It is important to check system performance of the UDIS, for which a calibration mode was designed. This mode provides an automatic inspection of a known billet and the UDIS compares the inspection results with those of the known billet already on file. Accordingly, the "CAlibrate" command instructs the DPS that a calibration mode of billet inspection is to be performed.

#### 3.3.1.2.4 Off-Line Mode

The "Off-Line Mode" application software of the UDIS provides a system operation to review an inspection result already on file, or to rediagnose said record. Because this operation is entirely DPS dependent, no billet reinspection by ultrasonics in a water tank is required. Merely replaying the magnetic tape provides data retrieval for the CPU to perform the requested diagnosis.

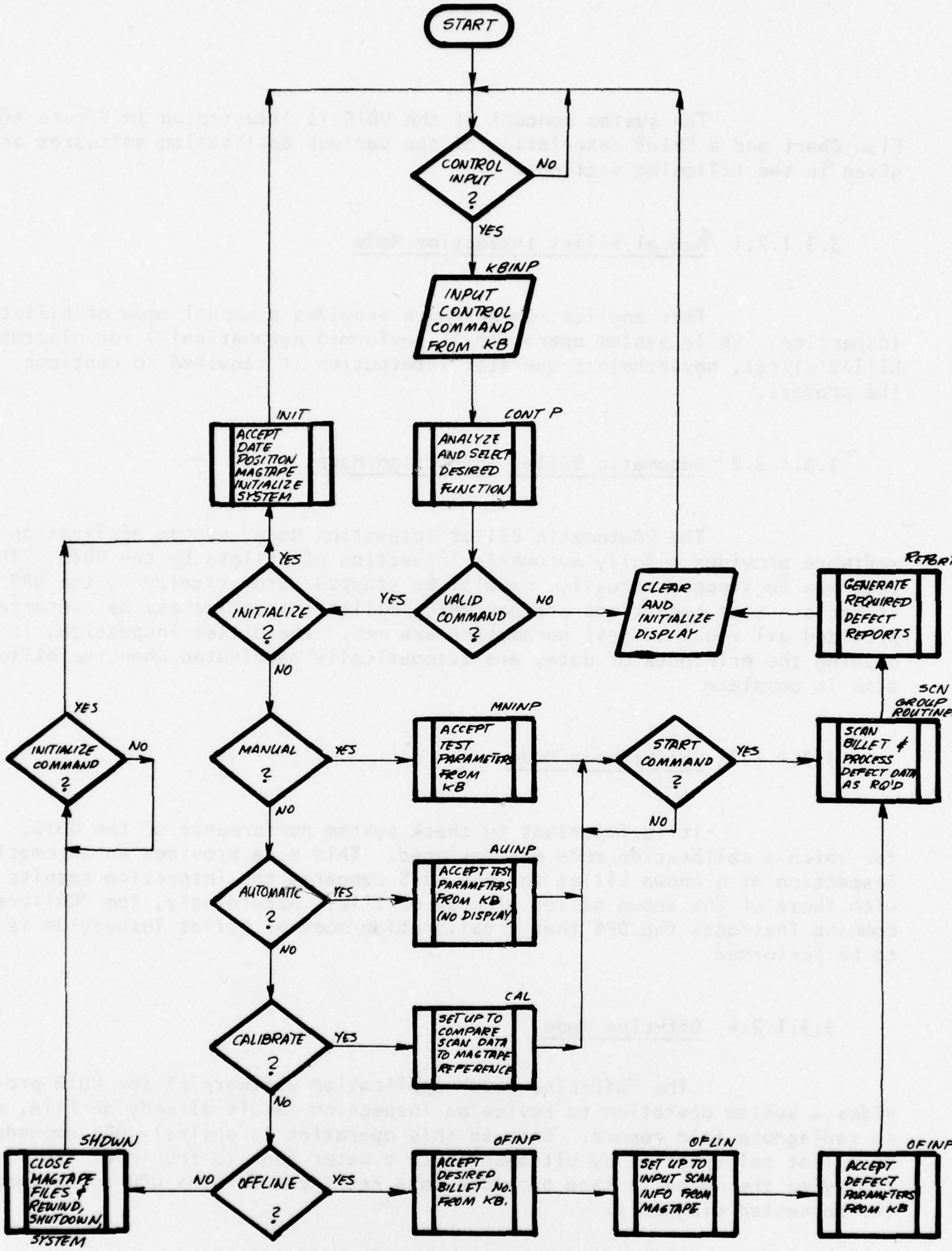


**Figure 68. Software Concept Flow Chart of the UDIS.**

3.3.1.2.5 Initialization Mode

Each day of use the UDIS must be initialized to provide the current date to be used in all report headings. The initialization mode must also be used after each case of off-line operation. After the current date is entered into the system, all necessary system initialization functions are automatically performed.

3.3.1.2.6 Stop Command

This command stops the activity in which the UDIS is currently engaged. Other softwares then may be initiated.

3.3.1.2.7 Zero Command

The "Zero Command" UDIS application software must be used in order to initialize a new magnetic tape reel or to erase previously stored test files.

3.3.1.2.8 Power Restart Mode

The power restart subroutine is called for when the electric power is restored after a power line failure and will determine whether an interrupted billet inspection may be restarted or must be started all over again from the beginning.

3.3.2 System Hardware

The DPS of the UDIS is shown in an extended block diagram form in Figure 69. All hardware components are the product of DEC, except the special Front End, I/O graphic terminal and the high speed line printer, which are the products of SDI, Tektronix and Centronics Corporations, respectively.

3.3.2.1 Minicomputer and Peripherals

Because the minicomputer and its peripherals adapted for the UDIS are off-the-shelf commercial equipment there is no discussion on these items within this report. Detailed descriptions of the PDP-11/20 processor and peripherals can be found in DEC publications 112-010701-1854 "Peripherals and Interfacing Handbook" and 112-010701-1855" "Processor Handbook". Similarly, the I/O alphanumeric-graphic terminal and the high speed line printer are described in detail in their own manuals provided by the manufacturers.

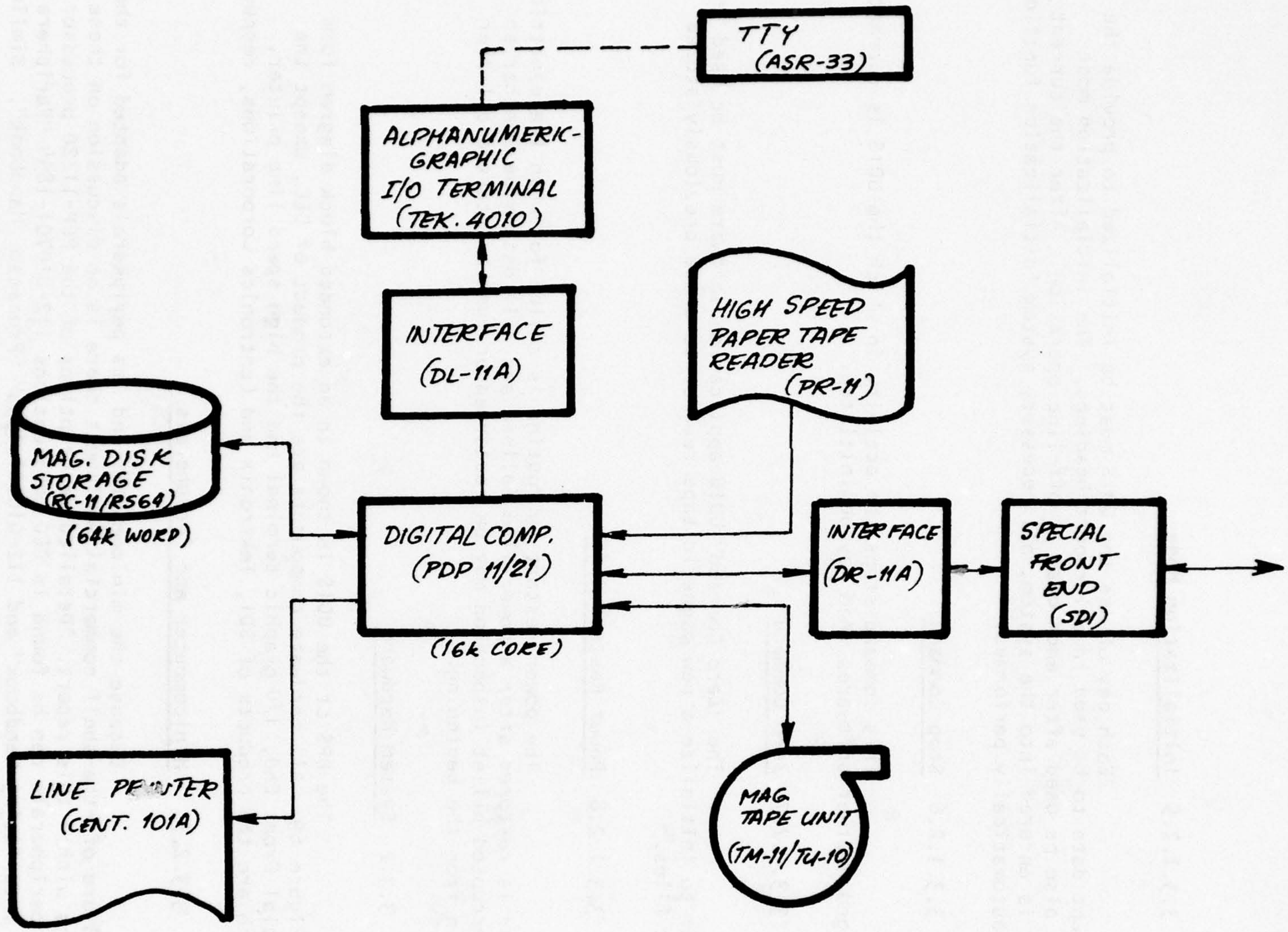


Figure 69. Extended Block Diagram of the Data Processing Subsystem of the UDIS.

### 3.3.2.2 Special Front End

The SFE instrumentation serves the purpose of automating the ultrasonic instrumentation, defect significance and location determinations and interfacing of the billet angular and axial monitoring devices with the DPS. Accordingly, this device consists of a programmable pulse repetition generator (PRF Gen), a programmable defect correlation circuit, a billet diameter counter and a modified sin-cos sweep generator. The following sections provide brief descriptions of these devices.

#### 3.3.2.2.1 Programmable PRF Generator

The purpose of the PRF generator is to supply a series of TTL-compatible pulses upon command from the CPU to the clock module of the ultrasonic instrumentation in order to initiate and maintain sonic pulses. The repetition rate of these pulses is digitally set by the CPU program control based upon operator's initial entry. Once the PRF generator is commanded to "start", the PRF generator pulses will be continuously generated at the previously selected rate until the CPU issues a "stop" command. The PRF generator also supplies initializing pulses to the programmable defect correlation circuit.

Figure 70 is a block diagram of the programmable PRF generator. The frequency is precisely controlled from 500 to 1500 Hz in 50 Hz increments by a phase-locked loop, PLL, with programmable divider and crystal-derived 50 Hz reference.

#### 3.3.2.2.2 Programmable Defect Correlation Circuit

The purpose of this circuit is to properly correlate the pulses provided by the Defect Gate module of the ultrasonic instrumentation into programmable time slots in order to form a 40-bit digital defect word representing the defects found along a radius of the titanium billet.

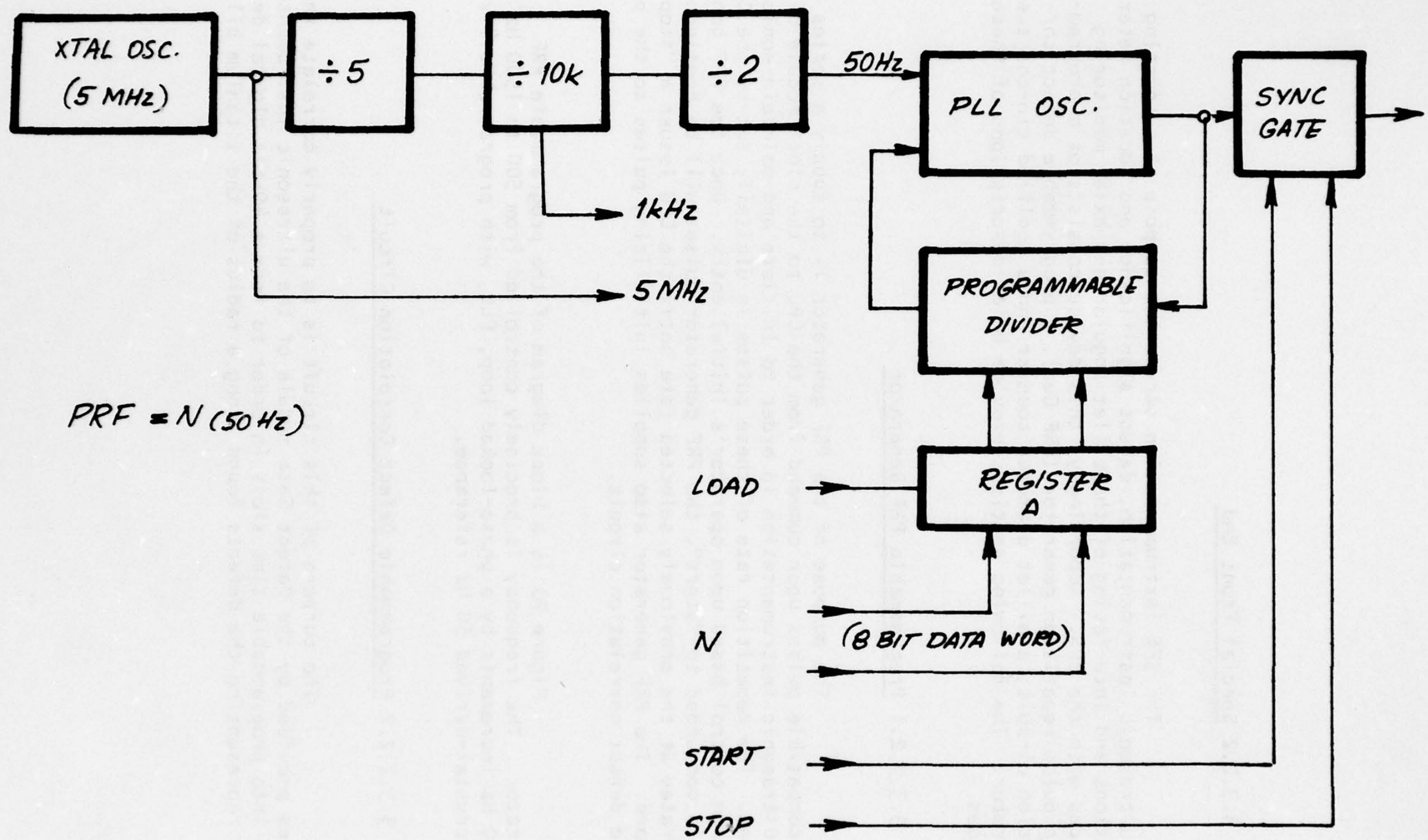


Figure 70. Block Diagram of the PRF Generator

Each bit of the word corresponds to a particular segment along billet radius R, and each segment is R/40 long for a 16" billet. The slot time is nominally 1.6 μs and may be changed under CPU program control over a range of ± 10% in 12 equal increments. The first time slot may be slightly shorter than all others, (200 ns shorter). The defect correlation circuit also provides signals to trigger and control the sin-cos sweep generator as well as inform the CPU that data are ready. Figure 71 is the block diagram of the programmable defect correlation circuit.

3.3.2.2.3 Billet Diameter Counter

The purpose of the billet diameter counter is to provide the CPU with a binary count representing the time between the billet front interface pulses and the ADAC pulses. The circuit consists of a 12 stage binary counter and control gate. The counter is reset to zero when a PRF pulse is generated. The CPU compares the output time of this device to the time slot previously selected for the defect correlation circuit and corrects as necessary. Figure 72 is a block diagram of the billet diameter counter.

3.3.2.2.4 Sin-cos Generator

The modified sin-cos generator is required to provide deflection signals for the compound B or modified PPI type scan display. The 32μs and 64μs typical sweep times of 8 and 16-inch diameter billets holds for a 1.6μs slot time. If the slot time is modified by the CPU, the sweep time will correct accordingly. The block diagram of the sin-cos generator is shown in Figure 73. The outputs of this device are fed into the X and Y channels of the Compound B-scan display oscilloscope. In addition, a composite video defect signal is also provided for Z-axis control. This Z-axis control TTL compatible signal is true only when the defect register is being loaded and a logic "1" has been detected for the current 1.6μs sample interval. The signal will remain at a true level if a defect spans more than one sample time interval.

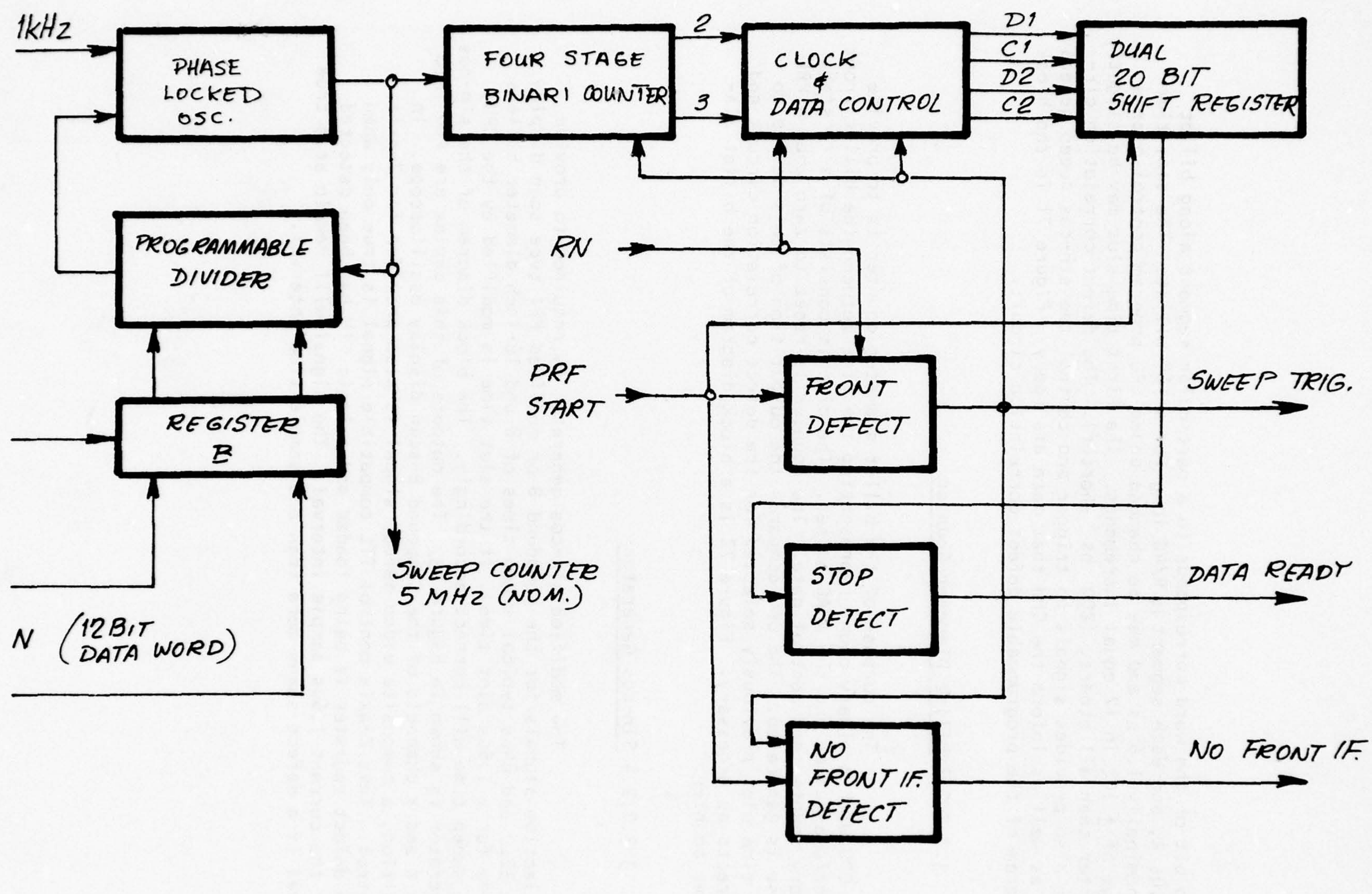


Figure 71. Block Diagram of the Programmable Defect Correlation Circuit

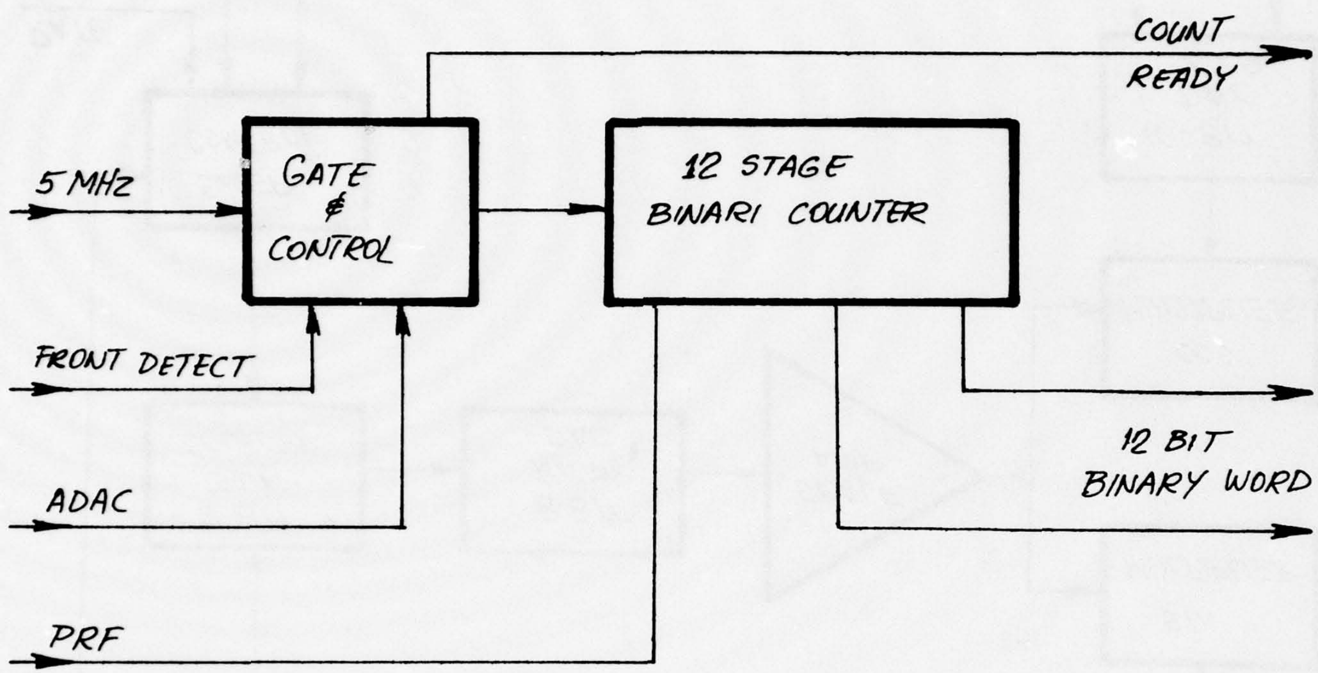


Figure 72. Block Diagram of the Billet Diameter Counter



6196 c

6198 c

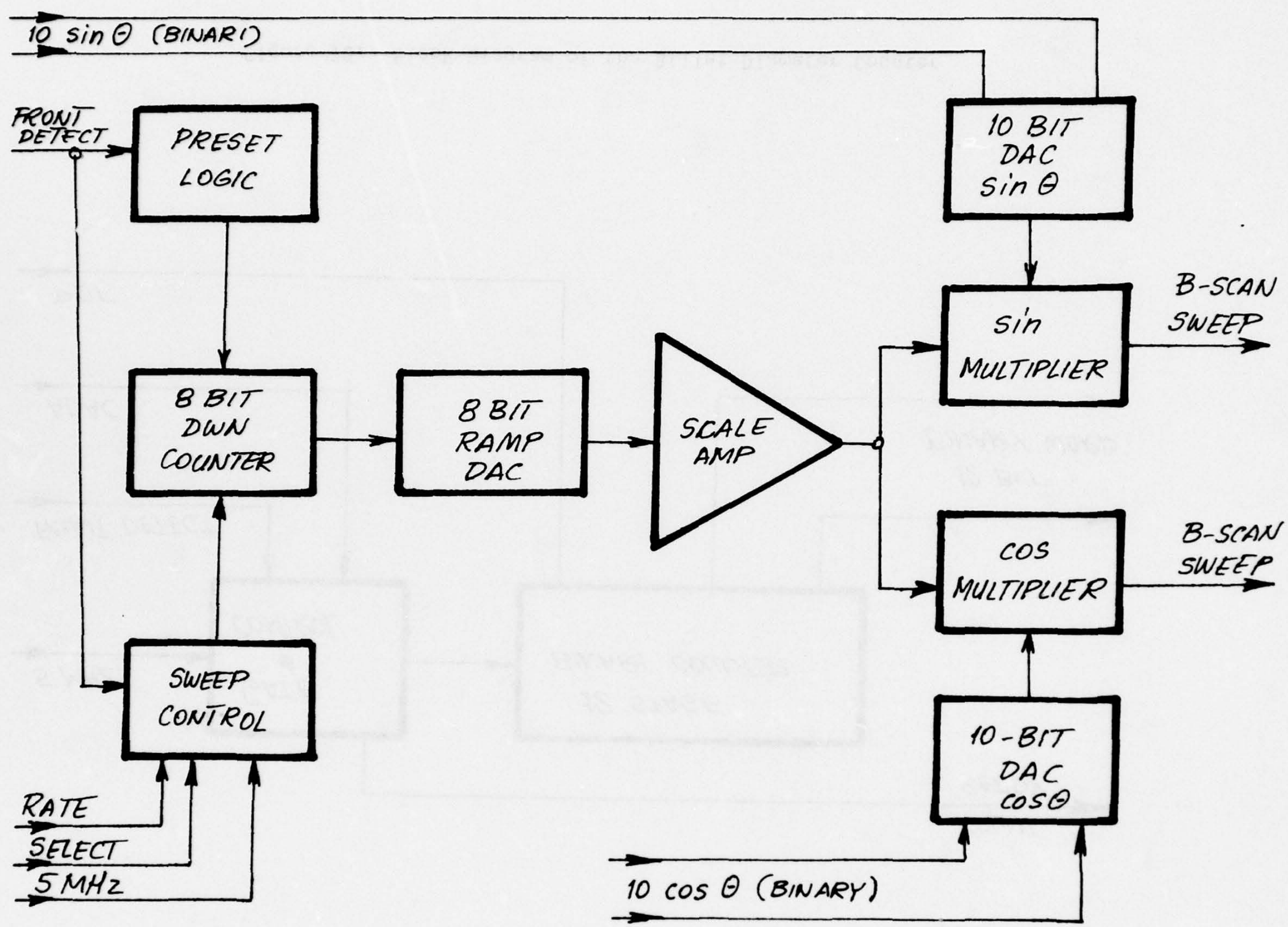


Figure 73. Block Diagram of the Sin-cos Generator

## 4. SYSTEM EVALUATION

Evaluations of the UDIS have been carried out in TRW laboratory experiments as well as in an actual production line application at the facility of the subcontractor RMI Co. These activities are discussed in the following two sections. A brief discussion of the titanium billet evaluations is also given.

### 4.1 UDIS Evaluation

#### 4.1.1 Laboratory Evaluation

The laboratory evaluations of the UDIS were oriented to check out system performance against its design criteria. Subsystem hardware operation evaluations were carried out as each of the system modules became available. Accordingly, with the completion of the entire UDIS a total system operation trial was carried out. A TRW in-house laboratory ultrasonic tank was equipped with the billet angular and axial position monitoring devices and a short billet 16 inches diameter x 8 inches was used for system evaluation. After successful trials of the UDIS, arrangements were made with the subcontractor RMI Co. to transfer the equipment to their plant to carry out the field evaluation.

#### 4.1.2 Field Evaluation

The entire UDIS equipment consisting of three relay rack cabinets, housing the ultrasonic instrumentation and the DPS, along with the separate graphic terminal and line printer peripherals were mounted onto a utility trailer. This trailer-mounted form of the equipment provided in-plant mobility to the UDIS for its field evaluation.

The system field evaluation effort was scheduled by the billet producer subcontractor RMI Co., using their production ultrasonic inspection tank facility for the second work-shift, between 4:00 p.m. and midnight during the first week of April 1974. The one week only, monday-through-friday activities, began on April 1st by moving the equipment from TRW, Cleveland, to RMI, Niles, Ohio. The first two days were spent with the installation of the billet position-monitoring digital encoders and the ultrasonic transducers as well as with electrification of the inspection system. Figure 74 shows the system installed at RMI Co. Turn-key operation of the UDIS was established during the second day and by the end of that day the first billet inspection was carried out.

One of the objectives of the system field evaluation effort was to compare inspection results of the UDIS with those of the billet producer's standard equipment and procedures. However, the 16-inch diameter billets were not currently inspected on a regular basis by the billet producer. There were only some spot-inspections using contact transducers in air, for indications equivalent to 8/64 and 12/64-inch diameter flat bottom holes (FBH). In addition, since most billets would easily pass even at the 8/64" FBH acceptance/rejection level, a more meaningful test had to be used for the UDIS evaluation.

Accordingly, the billet inspection was performed with an arbitrary setting to inspect for indications approximating that obtainable from a 5/64" FBH. Figure 75 shows the I/O graphic terminal which illustrates the system settings for the "on-line" automatic inspection and defect data diagnosis of the RMI billet No. 799310B.

For the following quality control reject criteria, QRC;

Significant cell count, SCC = 15

Dimensional coordination of adjacent cells $R = 2$

$\theta = A = 1$

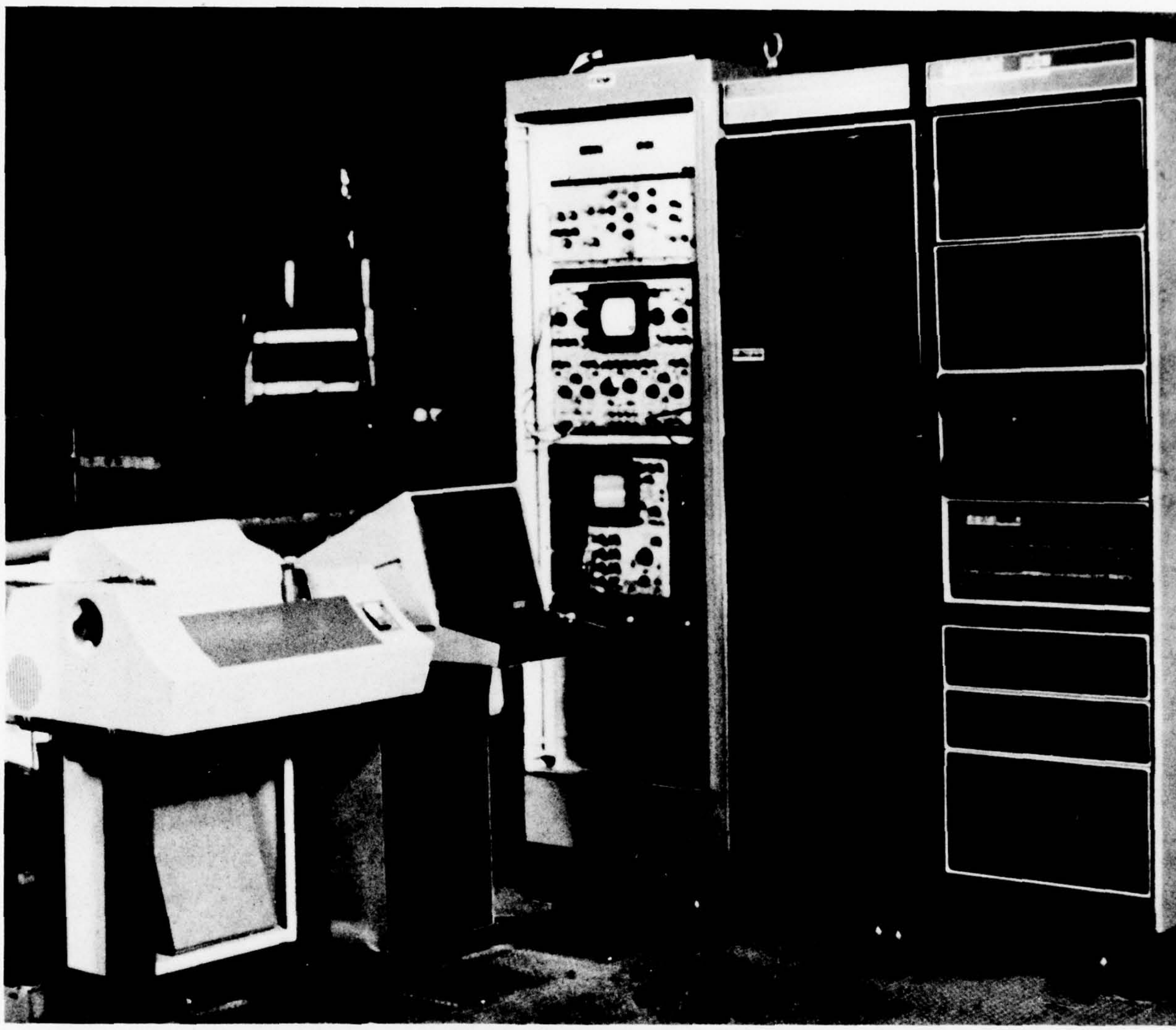

Figure 74. UDIS Installation at Subcontractor RMI Co.

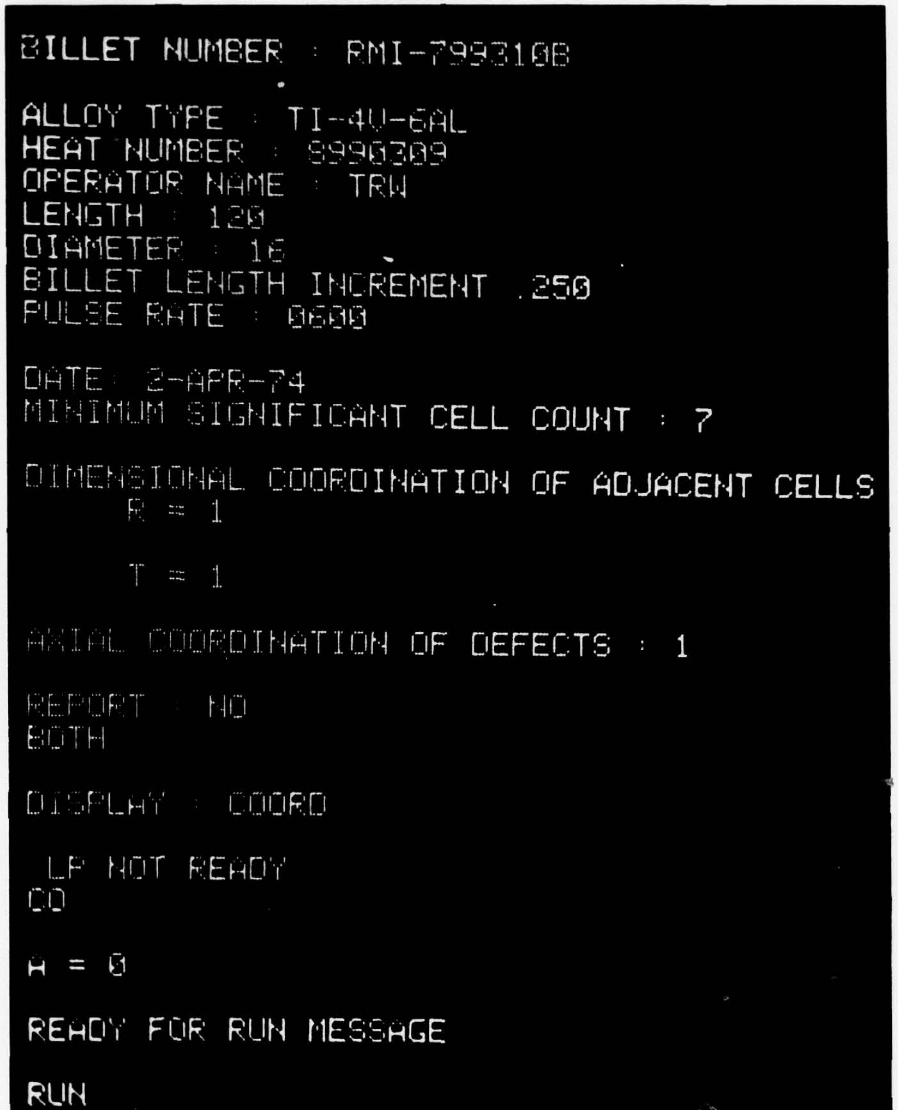


Figure 75. I/O Alphanumeric-graphic Terminal Display for the Mill Inspection of a 16-inch Diameter Titanium Billet.

the inspection revealed a single indication in the billet. The billet cross-section for the indication is displayed by the I/O graphic terminal in Figure 76. The billet Defect Coordination Report is shown in Figure 77, and the billet Reject Length Report is shown in Figure 78.

Using the diagnostic feature of the UDIS, the inspection data were retrieved and re-diagnozed for the following two successively more critical criteria. The accept/reject decision was established as shown below:

Providing a QRC for

Significant cell count, SCC = 15

Dimensional coordination
of adjacent cells $R = \theta = A = 1$

the billet cross-sections for the indications as displayed by the I/O graphic terminal are shown in Figures 79, 80 and 81 for the billet axial locations of A = 90.75, 91.00 and 91.25 inches. The billet Defect Coordination Report is shown in Figure 82 and the corresponding billet Reject Length Report is shown in Figure 83.

By providing a QRC for

Significant cell count, SCC = 7

Dimensional coordination
of adjacent cells $R = \theta = A = 1$

the billet cross-sections for the indications as displayed by the I/O graphic terminal are shown in Figures 84 through 88, for the corresponding billet axial locations of A = 90.50 through 91.50 inches. The billet Defect Coordination Report is shown in Figure 89 and the billet Reject Length Report is shown in Figure 90. It should be mentioned that this tighter criteria also caused indications of smaller sizes to show up elsewhere in the billet. Therefore, Figures 78 through 90 show data reproduced for the A = 91.25 inch defect indication and vicinity area of the interest only.

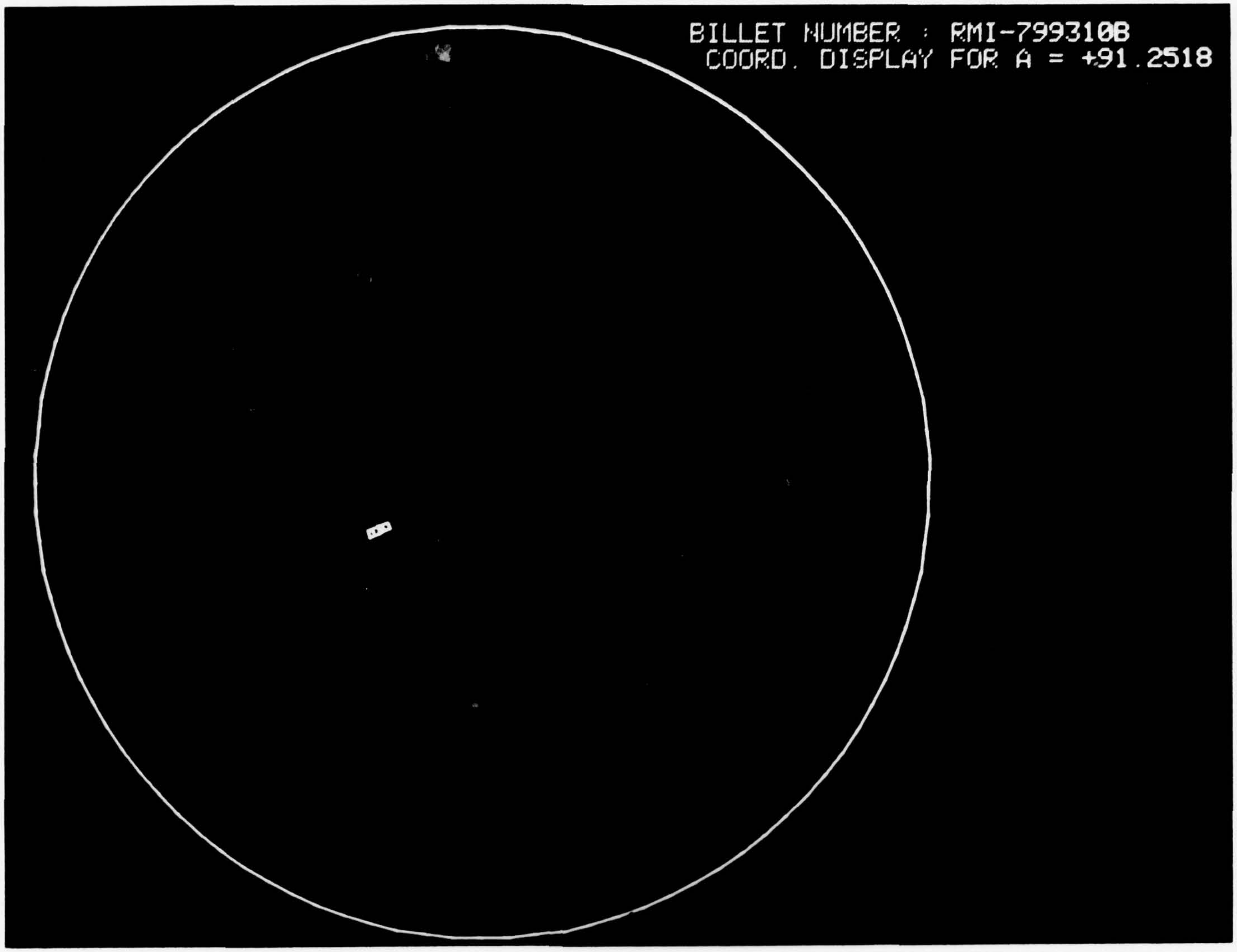


Figure 76. Defect Coordination Display (RMI-799310B, SCC = 15, R = 2, $\theta$ = A = 1, Billet Location A = 91.25-inch)

6159 C

```
ALLOY: TI-4V-6AL                    HEAT NO. 8990309       BILLET NO. RMI-799310B

DIAMETER: 16.0 INCHES   LENGTH: 120.0 INCHES   LENGTH INCREMENT: 0.250

OPERATOR: TRW                                 INSPECTION DATE: 2-APR-74

DEFECT CRITERIA:  COUNT = 15, R =  2, T =  1, A =   1  REPORT DATE: 9-MAY-74

CROSS-   DEFECT STARTS AT   DEFECT ENDS AT
SECTION   THETA   RADIUS    THETA   RADIUS
 NUMBER   (DEG)   (INCH)    (DEG)   (INCH)
==========================================

 730.     201.6    2.2      205.2    1.8

END*****OF*****BILLET
```

Figure 77. Defect Coordination Report
(RMI-799310B, SCC = 15, R = 2, θ = A = 1)

6157 C

ALLOY: TI-4V-6AL HEAT NO. 8990309 BILLET NO. RMI-799310B

DIAMETER: 16.0 INCHES LENGTH: 120.0 INCHES LENGTH INCREMENT: 0.250

OPERATOR: TRW INSPECTION DATE: 2-APR-74

DEFECT CRITERIA: COUNT = 15, R = 2, T = 1, A = 1 REPORT DATE: 9-MAY-74

| REJECTED LENGTH (INCHES) | ACCEPTED LENGTH (INCHES) |
|---|---|
| | 0.00 TO 91.25 |
| 91.25 TO 91.50 | |
| | 91.50 TO 120.00 |

END*****OF*****BILLET

TOTAL ACCEPTED LENGTH = 119.75 INCHES

TOTAL REJECTED LENGTH = 0.25 INCHES

END OF REPORT

Figure 78. Defect Reject Length Report
(RMI-799310B, SCC = 15, R = 2, $\theta$ = A = 1)

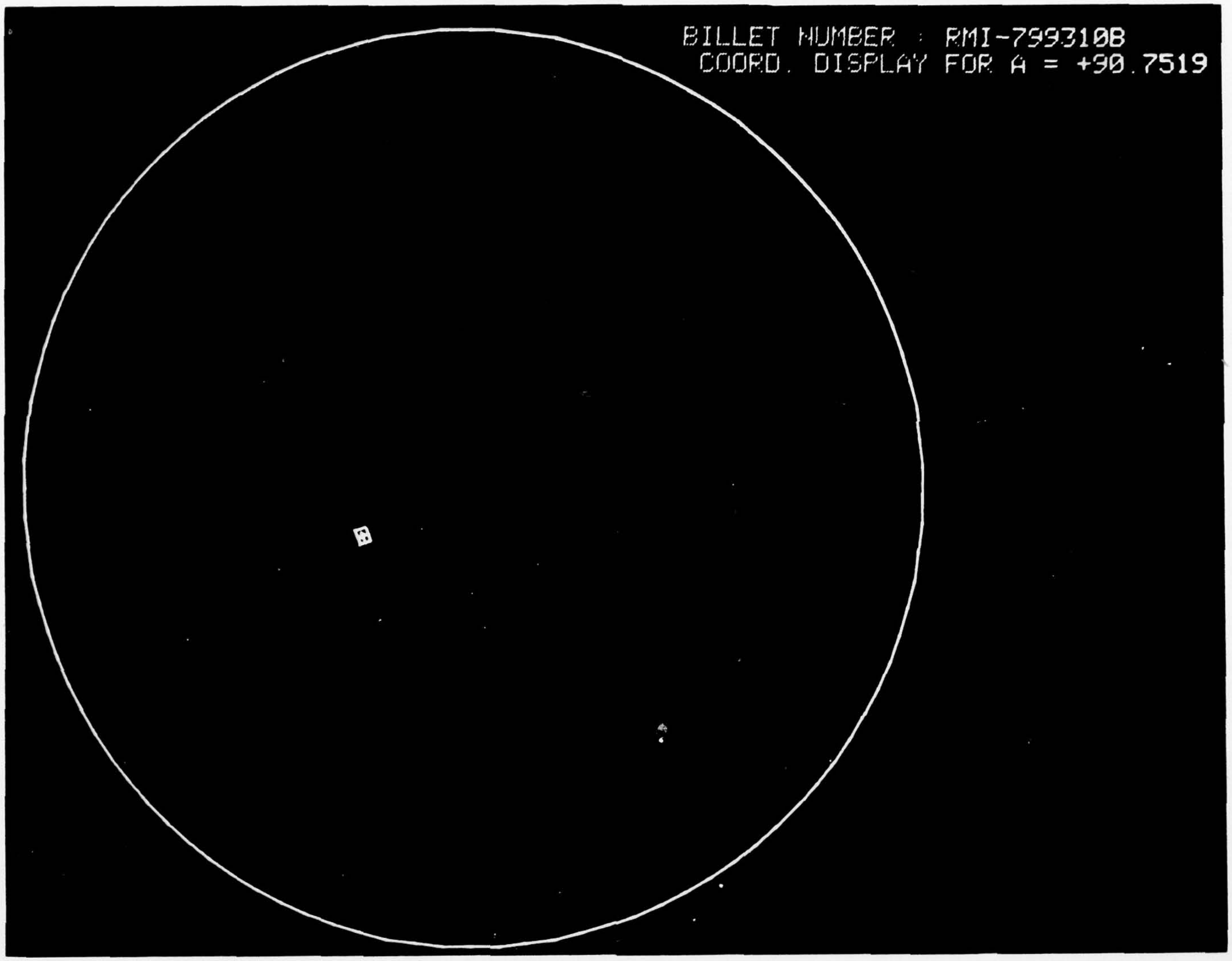


Figure 79. Defect Coordination Display
(RMI-799310B, SCC = 15, R = θ = A = 1,
Billet Location A = 90.75-inches)

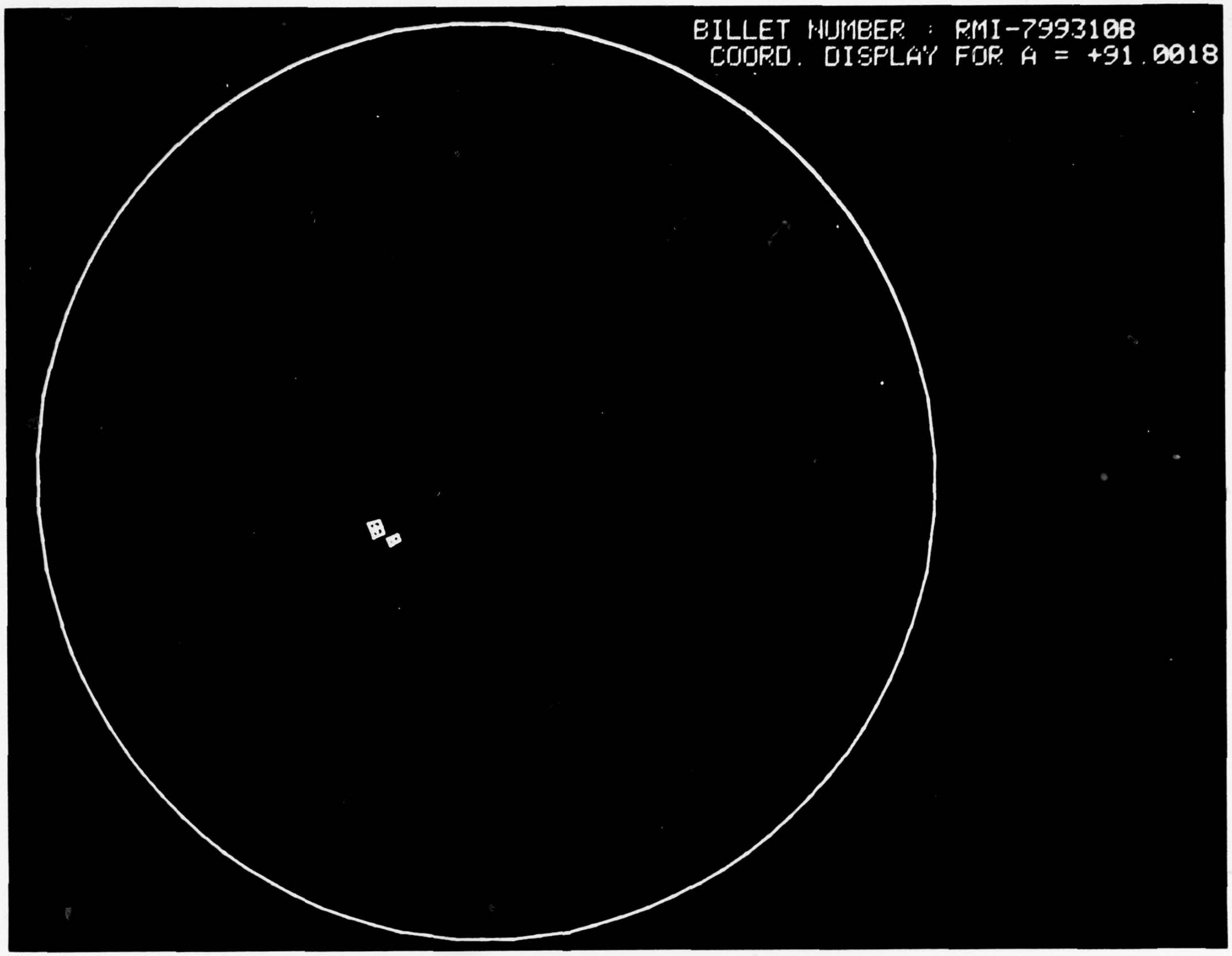


Figure 80. Defect Coordination Display
(RMI-799310B, SCC = 15, R = θ = A = 1,
Billet Location A = 91.00-inch)

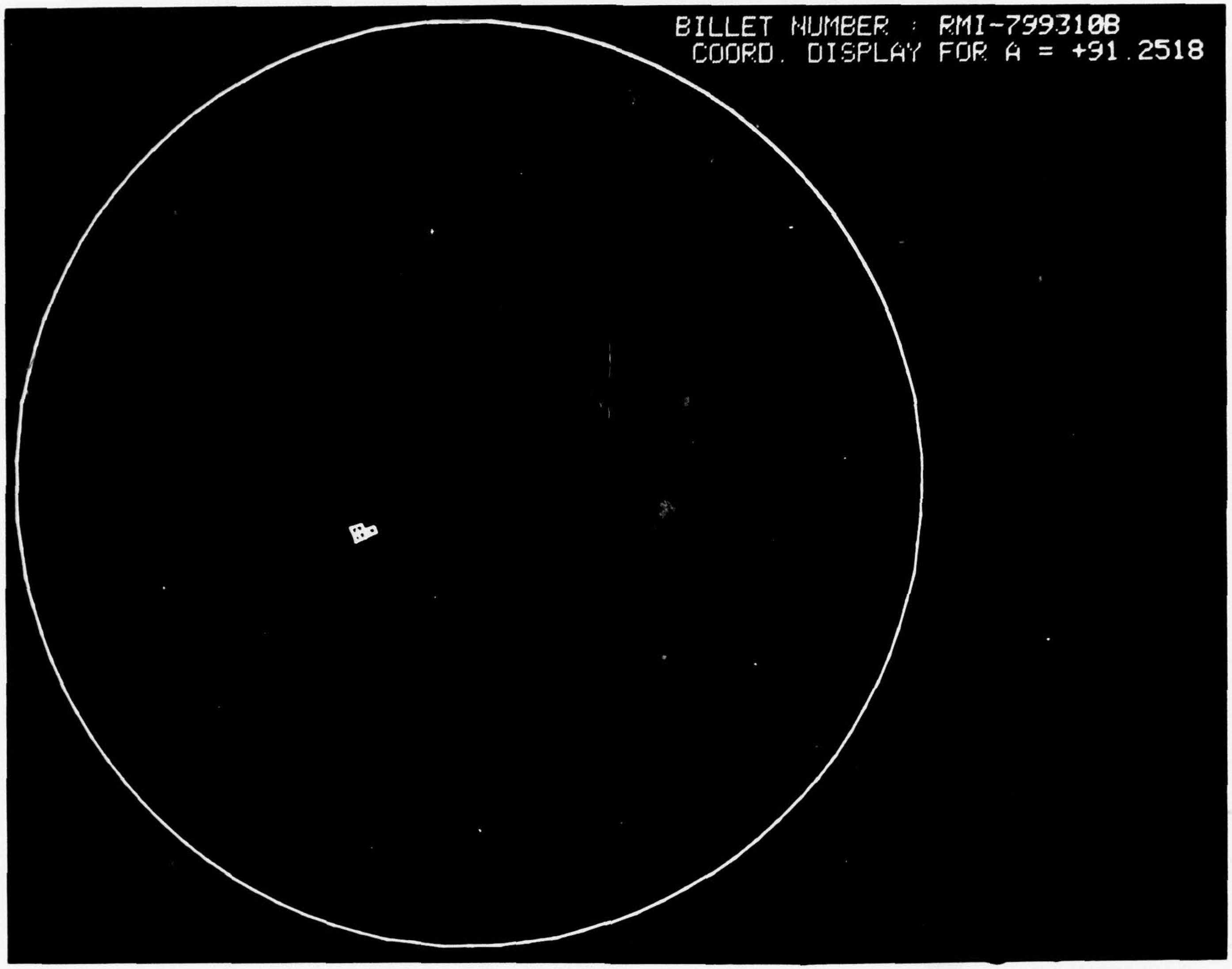


Figure 81. Defect Coordination Display
(RMI-799310B, SCC = 15, R = θ = A = 1,
Billet Axial Location, A = 91.25-inch)

6155 C

ALLOY: TI-4V-6AL HEAT NO. 8990309 BILLET NO. RMI-799310B

DIAMETER: 16.0 INCHES LENGTH: 120.0 INCHES LENGTH INCREMENT: 0.250

OPERATOR: TRW INSPECTION DATE: 2-APR-74

DEFECT CRITERIA: COUNT = 15, R = 1, T = 1, A = 1 REPORT DATE: 9-MAY-74

| CROSS-SECTION NUMBER | DEFECT STARTS AT THETA (DEG) | DEFECT STARTS AT RADIUS (INCH) | DEFECT ENDS AT THETA (DEG) | DEFECT ENDS AT RADIUS (INCH) |
|---|---|---|---|---|
| 726. | 198.0 | 2.2 | 205.2 | 2.0 |
| 728. | 198.0 | 2.2 | 205.2 | 2.0 |
| 728. | 208.8 | 2.0 | 212.4 | 1.8 |
| 730. | 198.0 | 2.2 | 205.2 | 2.0 |
| 730. | 201.6 | 2.2 | 205.2 | 1.8 |

END*****OF*****BILLET

Figure 82. Defect Coordination Report
(RMI-799310B, SCC = 15, R = θ = A = 1)

6160 C

```
ALLOY: TI-4V-6AL                    HEAT NO. 8990309       BILLET NO. RMI-799310B

DIAMETER: 16.0 INCHES   LENGTH: 120.0 INCHES   LENGTH INCREMENT: 0.250

OPERATOR: TRW                                  INSPECTION DATE: 2-APR-74

DEFECT CRITERIA:  COUNT = 15, R =  1, T =  1, A =   1  REPORT DATE: 9-MAY-74

REJECTED   ACCEPTED
 LENGTH     LENGTH
(INCHES)   (INCHES)
========   ========

              0.00
               TO
             90.75
  90.75
   TO
  91.50
             91.50
               TO
            120.00

END*****OF*****BILLET

TOTAL ACCEPTED LENGTH = 119.25 INCHES

TOTAL REJECTED LENGTH =   0.75 INCHES

END OF REPORT
```

Figure 83. Defect Reject Length Report
(RMI-799310B, SCC = 15, R = θ = A = 1)

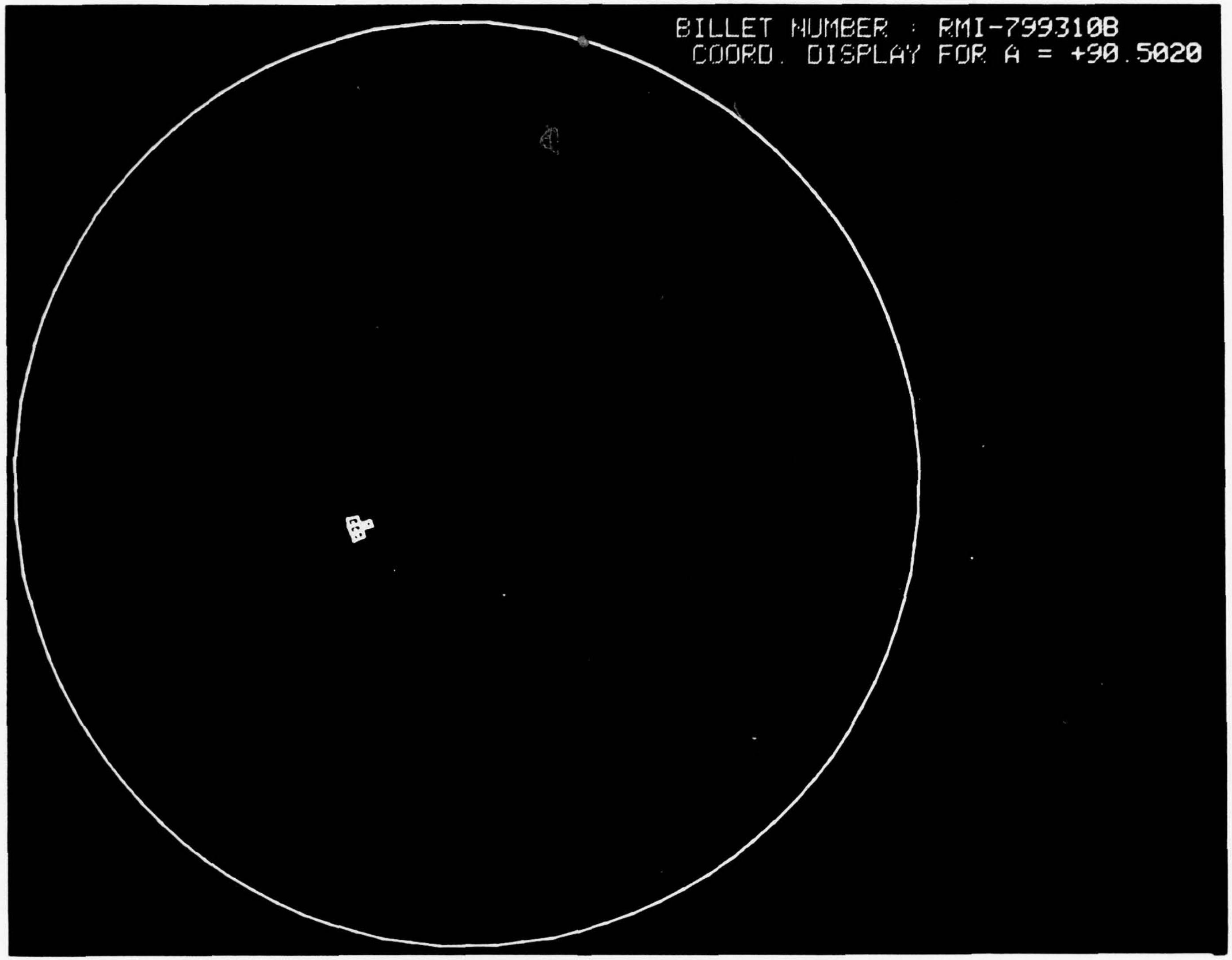


Figure 84. Defect Coordination Display
(RMI-799310B, SCC = 7, R = θ = A = 1,
Billet Axial Location A = 90.50-inch)


Figure 85. Defect Coordination Display (RMI-799310B, SCC=7, R=θ=A=1, Billet Axial Location A=90.75 inch).

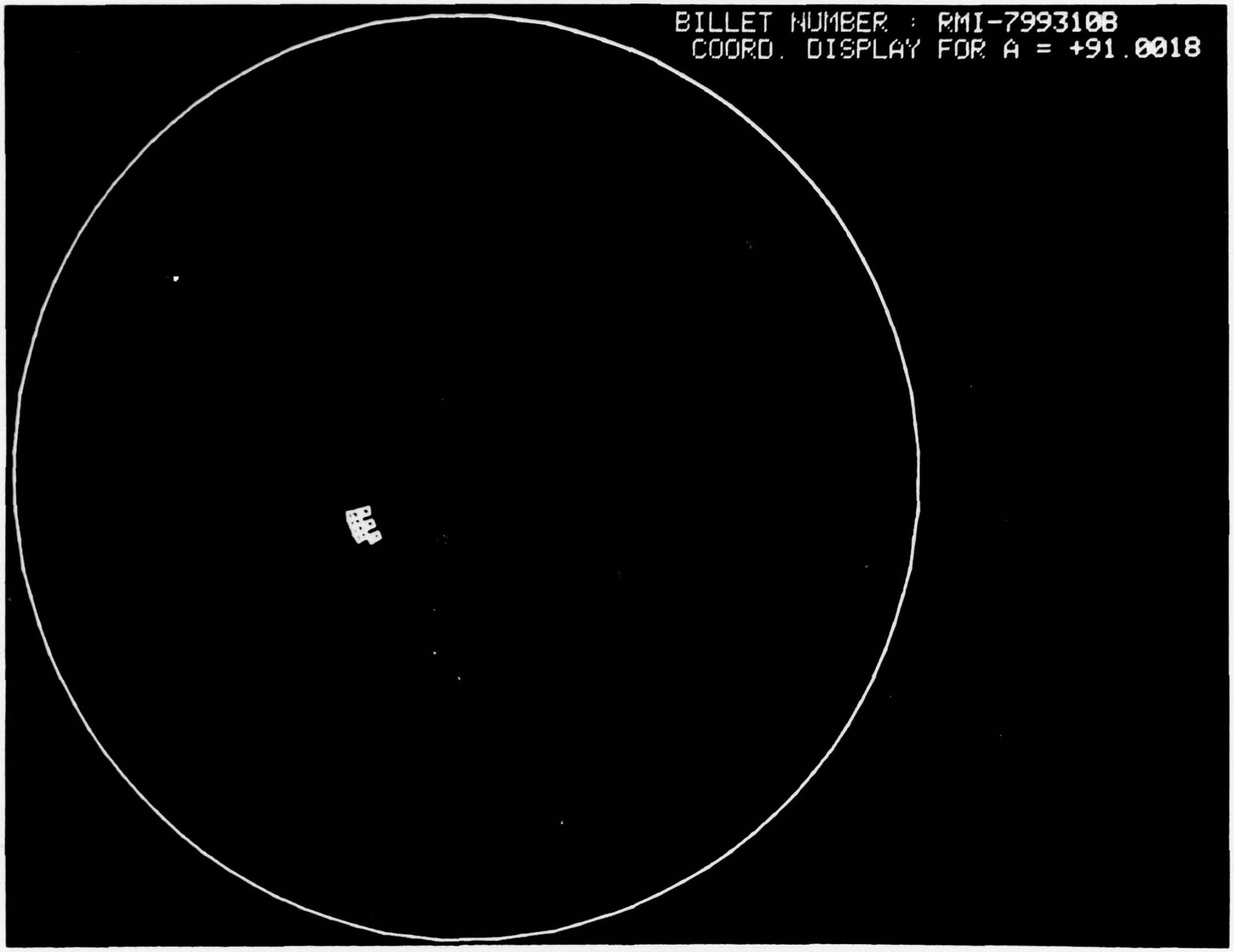


Figure 86. Defect Coordination Display (RMI-799310B, SCC=7, R=θ=A=1, Billet Axial Location A=91.00 inch).

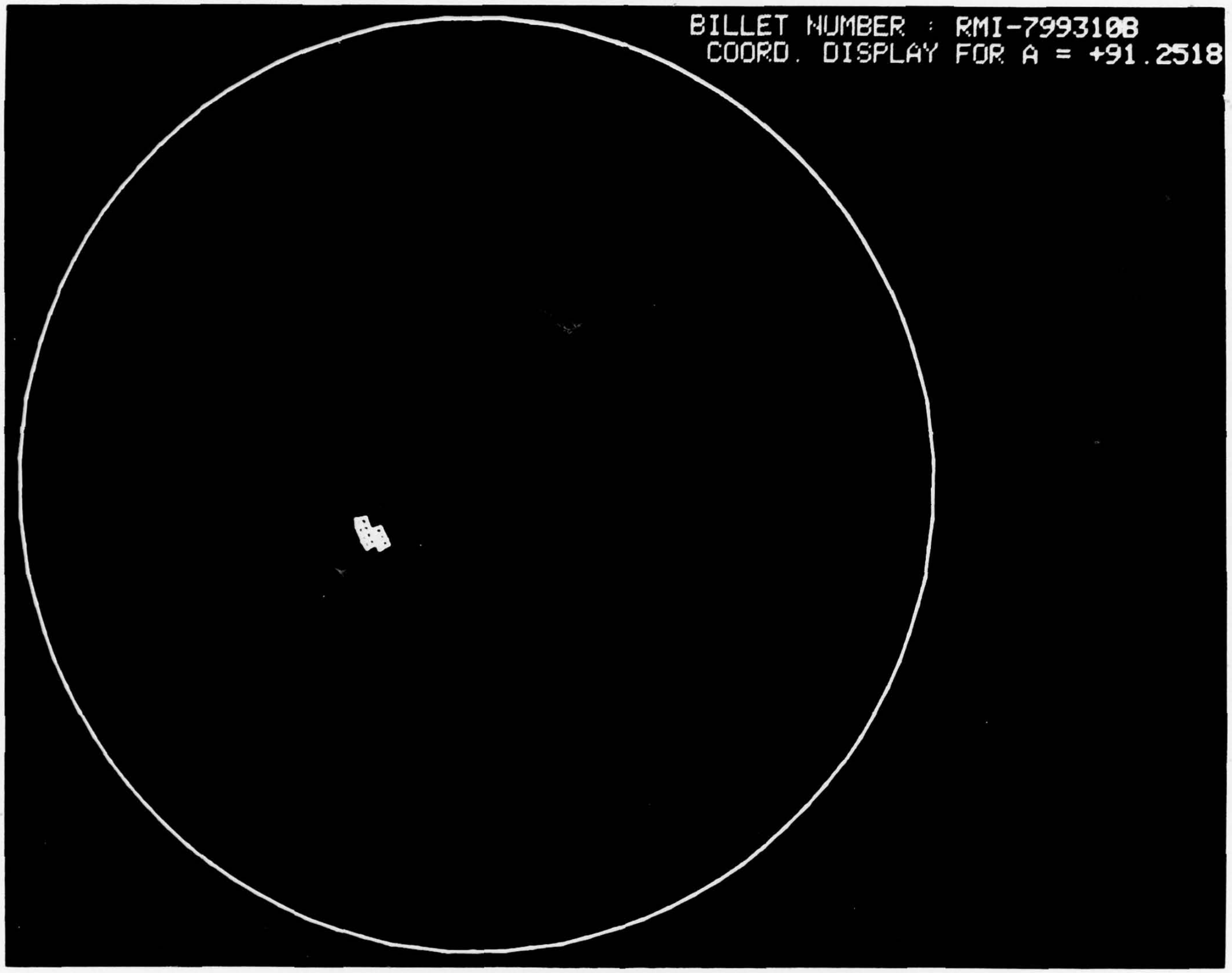


Figure 87. Defect Coordination Display (RMI-799310B, SSC=7, R=θ=A=1, Billet Axial Location A=91.25 inch).

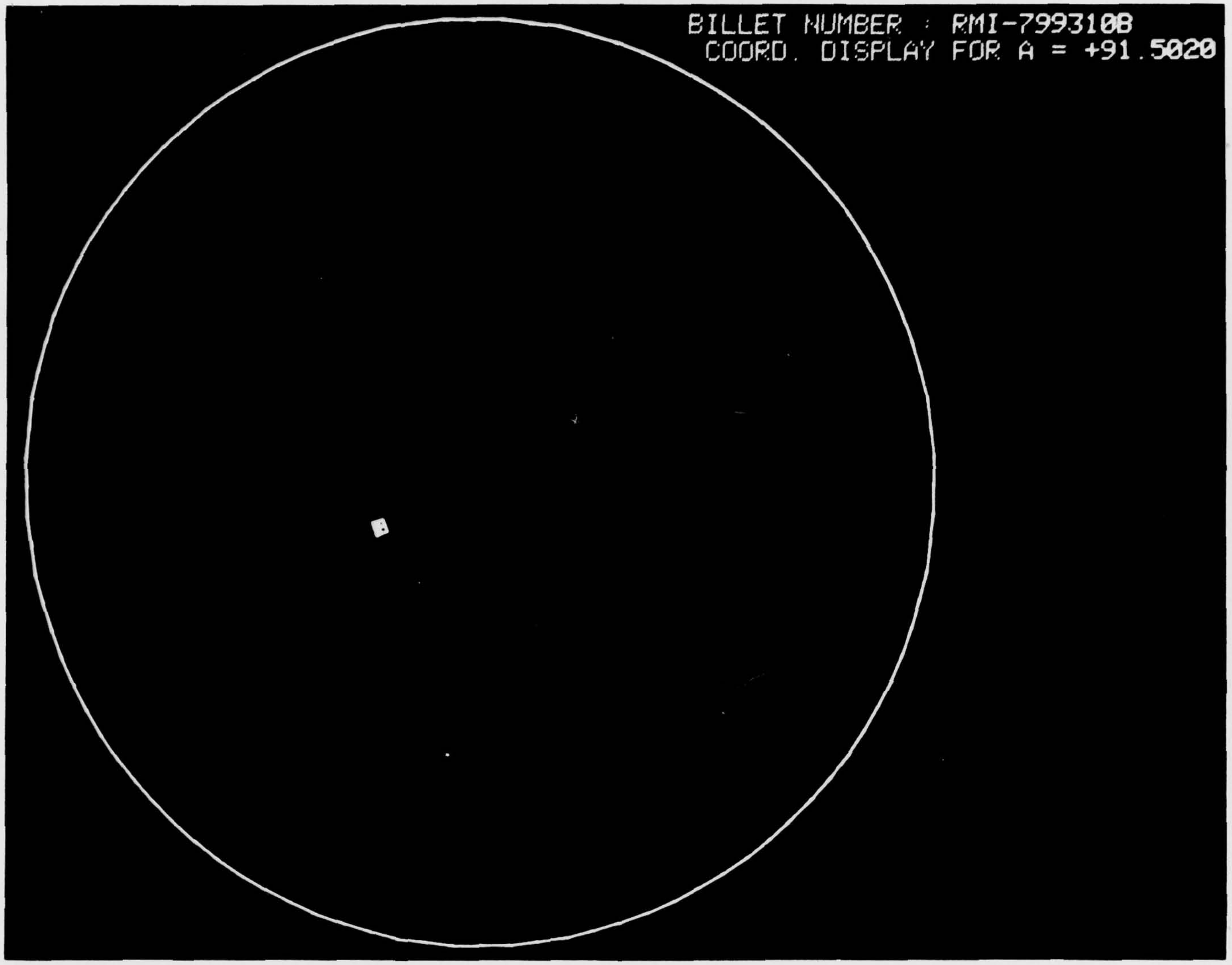


Figure 88. Defect Coordination Display (RMI-799310B, SCC = 7, R = $\theta$ = A = 1, Defect Axial Location A = 91.50-inch)

ALLOY: TI-4V-6AL HEAT NO. 8990309 BILLET NO. RMI-799310B

DIAMETER: 16.0 INCHES LENGTH: 120.0 INCHES LENGTH INCREMENT: 0.250

OPERATOR: TRW INSPECTION DATE: 2-APR-74

DEFECT CRITERIA: COUNT = 07, R = 1, T = 1, A = 1 REPORT DATE: 9-MAY-74

| CROSS-SECTION NUMBER | DEFECT STARTS AT THETA (DEG) | RADIUS (INCH) | DEFECT ENDS AT THETA (DEG) | RADIUS (INCH) |
|---|---|---|---|---|
| 726. | 198.0 | 2.2 | 201.6 | 1.8 |
| 726. | 194.4 | 2.2 | 208.8 | 2.0 |
| 728. | 194.4 | 2.2 | 198.0 | 1.8 |
| 728. | 201.6 | 2.2 | 205.2 | 1.8 |
| 728. | 194.4 | 2.2 | 208.8 | 2.0 |
| 728. | 208.8 | 2.0 | 212.4 | 1.8 |
| 730. | 194.4 | 2.2 | 208.8 | 2.0 |
| 730. | 201.6 | 2.2 | 208.8 | 1.8 |
| 730. | 201.6 | 2.0 | 212.4 | 1.8 |

END*****OF*****BILLET

Figure 89. Defect Coordination Report (Partial List) (RMI-799310B, SCC=7, R=θ=A=1).

6199 C

```
ALLOY: TI-4V-6AL                         HEAT NO. 8990309       BILLET NO. RMI-799310B

DIAMETER: 16.0 INCHES   LENGTH: 120.0 INCHES   LENGTH INCREMENT: 0.250

OPERATOR: TRW                                   INSPECTION DATE: 2-APR-74

DEFECT CRITERIA:  COUNT = 07, R =  1, T =  1, A =   1  REPORT DATE: 9-MAY-74

REJECTED   ACCEPTED
 LENGTH     LENGTH
(INCHES)   (INCHES)
========   ========
               TO
             90.50
  90.50
   TO
  91.75
END*****OF*****BILLET

TOTAL ACCEPTED LENGTH =  95.50 INCHES

TOTAL REJECTED LENGTH =  24.50 INCHES

END OF REPORT
```

Figure 90. Defect Reject Length Report (Partial List) (RMI-799310B, SCC=7, R=θ=A=1).

With the three different quality control reject criteria used, the total rejected billet length varied as 1/4, 3/4 and 1-1/4 inches, respectively. This example is an illustration of the diagnostic capability of the UDIS for the accept/reject decision making based upon the three-dimensional spatial orientation of defects.

Successive trials during the following two days of the system field evaluation consisted of five additional inspection runs of the same billet. These repeated inspection runs were made with various inspection as well as QRC settings in order to establish a realistic base-line level which would mutually be meaningful for both equipment performance evaluation as well as for billet material characterization purposes. Accordingly, the result of the last inspection run is, perhaps, the most indicative. This inspection run was carried out with an acceptance/rejection control level set to an indication equivalent to the indication which is obtainable from a 4/64" FBH. The evaluation of these data revealed excessive ultrasonic scatterings at four discrete mid-radius areas, more or less throughout the billet axial length, and the entire circumference from about 1/8 inch to 1 inch from the outer diameter measured in the billet radial direction. It is believed that the nature of this energy-material interaction is caused by excessive size grains which are originated from the square and octagon shape forging processes. A more detailed discussion of this is given in the following Material Evaluation Section 4.2.

During the fifth day of operation of the system in the mill shop environment an equipment failure occurred. The difficulty was associated with loss of vacuum in the magnetic tape recorder's transfer mechanism which could not be corrected readily. Further field inspection activities were terminated at this point upon demand of the subcontractor.

After returning the equipment to TRW, Cleveland, a careful evaluation was made for the cause of the equipment failure. While the computer had flagged at "MT FATAL ERROR" message at the field subsequent on-the-spot trials revealed a permanent loss of partial vacuum in the vacuum columns of the magnetic tape recorder's tape transfer mechanism in spite of vigorous cleaning attempts. A very extensive cleaning of the entire tape transport mechanism carried out at TRW put the magnetic tape unit back to operational conditions but the field inspection tapes were so dirty that they were unreadable by the machine. A considerable amount of cleaning of the magnetic tapes themselves eventually allowed the tapes to be used. This experience reemphasizes the need for magnetic tape operation in a clean environment. Continuous operation of the UDIS in normal mill environments would require that the unit be housed in a dust-free enclosure.

## 4.2 Material Evaluation

For the mill evaluation of both the commercial ultrasonic systems considered for application during Phase I of the program, as well as the UDIS built during Phase II of the program, actual production titanium forging billets were used. Material requirements were established with the sub-contractor RMI Co., and billets were produced in both phases of the program.

### 4.2.1 Phase I Effort

A 30-inch diameter Ti-6Al-4V alloy composition ingot was cast and successively reduced to the desired 8 and 16-inch diameters. Figure 91 shows the block diagram of the ingot conversion and the identification and location of metallographic and chemistry test specimens. With reference to Figure 91, the 30-inch diameter ingot was press-forged to 16-inch square and hot cut into two pieces. One of the pieces was press-forged to a 16-inch diameter and then finished by lathe turn. It was then designated as the 16-inch diameter T-Billet. The other ingot section was press-forged to a 11-1/2 inch octagon shape and then hot cut into three pieces. Subsequently, these octagon billets were forged automatically on a GFM machine (Geselshaft fur Fertigungstechnik and Maschinebau) to 8-inch diameter rounds and, finally, lathe turned. As indicated in Figure 91, one-inch thick test slices were cut from the end of each billet to provide macro- and microstructure records. The related information is compiled in Appendix D.

The billets were characterized by an examination of the macrostructure and by metallographic evaluation. The billets exhibited a normal grain appearance with some variation apparent especially in the 16-inch billet. The lamellar alpha plus beta microstructures of the 16-inch diameter sections show somewhat less deformation of the material at the center of the section with the prior beta grain boundaries outlined by alpha platelets. But the structure is believed to be a normal product for this size of billet. The 8-inch diameter billets exhibited a similar lamellar micro-

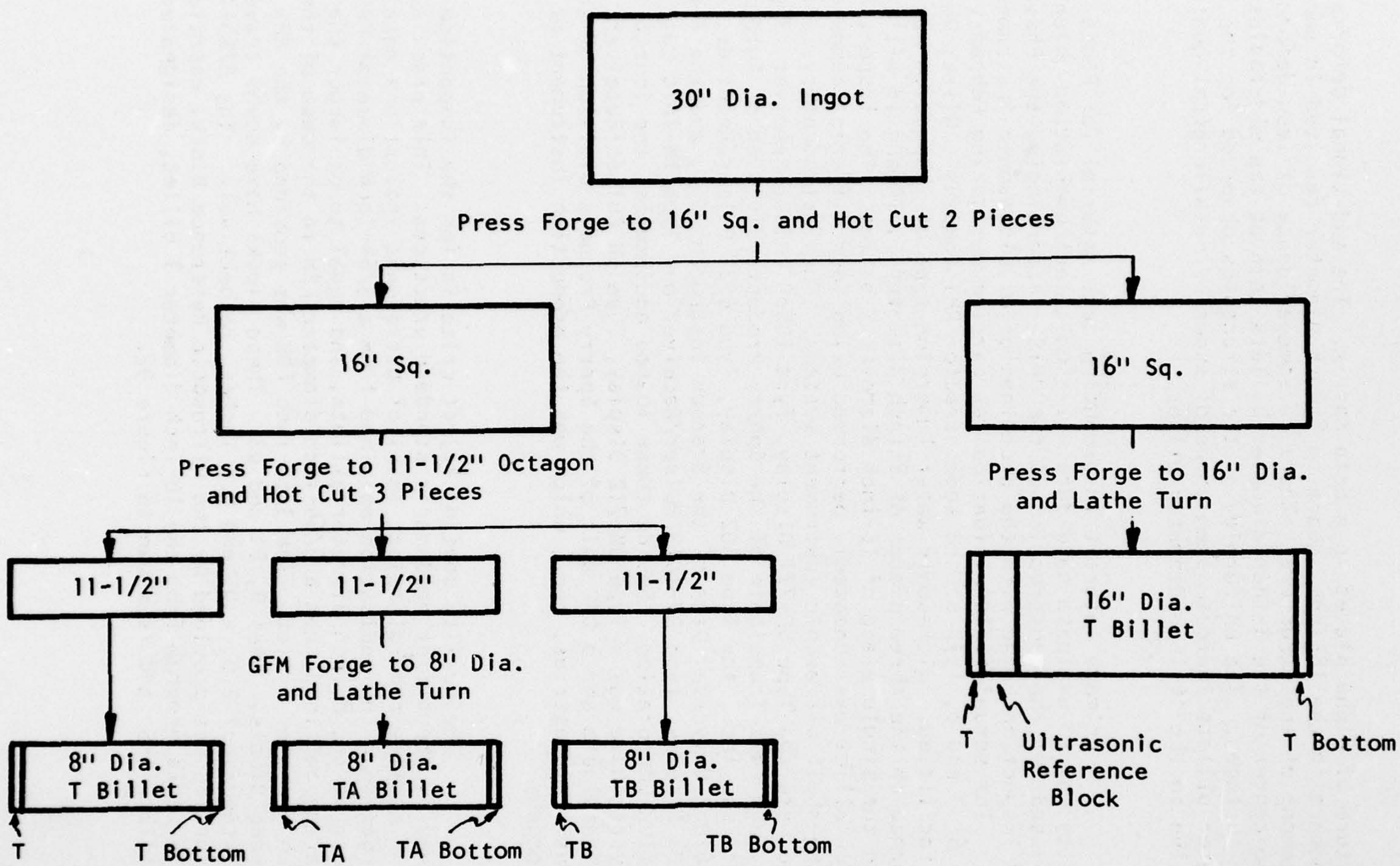


Figure 91. Block Diagram of Ingot Conversion to Final Product.

structure of alpha plates in a beta matrix. The additional deformation in converting the 16-inch square to 8-inch diameter resulted in some refinement of the structure. There is some evidence of less deformation at the center of the 8-inch diameter billets than at the mid-radius and outer surfaces. The uniformity of the structures observed for the 8-inch diameter billets indicate them to be of superior metallurgical quality relative to the 16-inch diameter billet.

Primary interest in producing test material for Phase I activity was to evaluate candidate ultrasonic instrumentation which was to be used for the construction of the UDIS. Accordingly, the Phase I field inspection began with the coordination of ultrasonic instrument loans. The actual field evaluation was carried out during February 2, 3, 4, 6, 7 and 8, 1972 at the subcontractor RMI Company's Niles, Ohio mill facilities. Ultrasonic water immersion type of inspection was performed on the three pieces of 8-inch diameter T, TA and TB billets and on the single piece of 16-inch diameter T billet. The inspection of each billet was repeatedly performed using four different commercial, off-the-shelf ultrasonic instrument systems. The instrument systems loaned were the Type UM-771 Display, Type 10SdB Pulser/Receiver, Type D Timer, and Fast Transigate of the Sperry Products Division of Automation Industries, Inc., the Type 602 Display, Type 622T Pulser/Receiver, and Type 610UI Universal Gate of the Branson Instrument Co., and the Type DS-1007 Display, Type RP-1012 Pulser/Receiver and Type TH-1010 Gate of the Magnaflux Corporation. Beside these loaned equipments, the fourth instrument system used was a Type UM-712 Display, Type 5N Pulser/Receiver, Type E550 Transigate and a DAC unit of the Sperry Products Division of the Automation Industries, Inc., which was the production instrument of the RMI Company.

The quality control reject criteria for the inspection were governed by the billet producer's standard practices. This practice provided a quality control reject level of ultrasonic indications equal to or larger than the indication obtained from a 3/64-inch diameter FBH in the case of the 8-inch diameter billets, and equal to or larger than the indication obtained from a 8/64-inch diameter FBH in the case of the 16-inch diameter billet. The 3/64-inch FBH was provided by the RMI Company's Reference Blocks, Codes D, D1 and D2. These blocks have sound travel material distances of 2.0, 4.0, and 0.5 inches, respectively. The 8/64-inch diameter FBH was provided by the Ultrasonic Reference Block, especially made for this program from the 16-inch diameter T billet, designated as TRW #111227-1-5, and is shown in Figure 92.

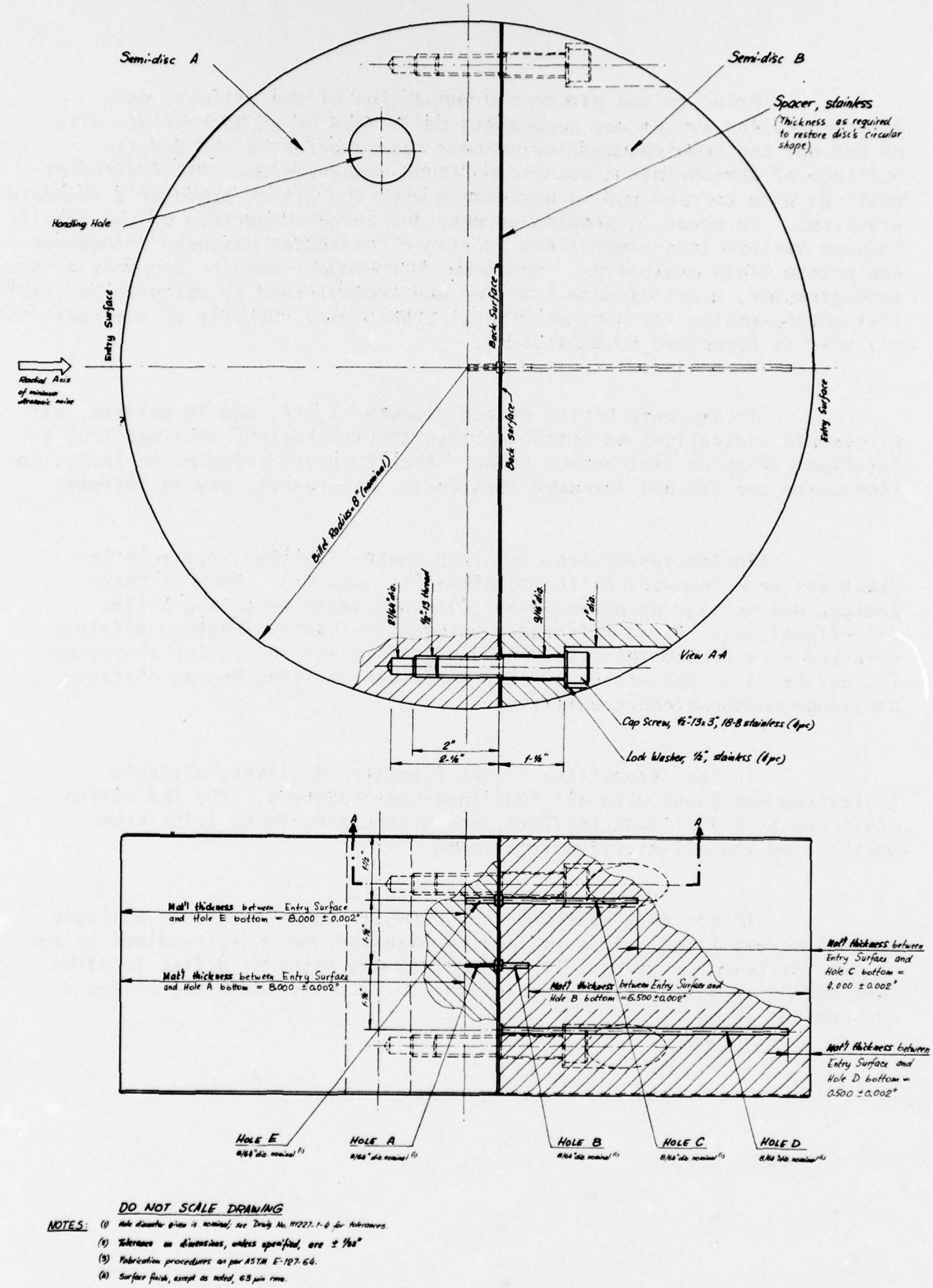


Figure 92. Ultrasonic Reference Block.

Prior to the ultrasonic inspection of the billets, each instrumentation system was separately calibrated on an appropriate size of FBH for the required quality control reject criteria and for the settings of appropriate distance-amplitude compensation. All instrument settings were carried out in accordance with the billet producer's standard practices. In order to provide an easy and quick comparison of the results between various instrumentations, a single transducer was used throughout the entire field evaluation. Since said transducer was the property of the subcontractor, a performance transfer was accomplished by using an undisturbed instrument setting for another (TRW's) transducer. Details of the performance transfer is described in Appendix E.

In the case of the 8-inch diameter T, TA, and TB billets, all ultrasonic indications were smaller than the indications obtained from the 3/64-inch diameter flat bottom holes. Metallurgical correlation investigations were carried out for such locations. The results are as follows.

In the case of the 8-inch diameter T billet, two such indications were found at billet locations T-1 and T-3. Both of these indications were at an approximate 1.25-inch depth below the billet cylindrical edge. Some difference between the instrumentation displays observed were due to their varying sensitivity and resolution characteristics, but also because one of the instrument systems had no distance-amplitude compensation capability.

In the case of the 8-inch diameter TA billet, a single indication was found with all four instrument systems. The indication was found at billet location TA-2, and at an approximate 1.75-inches depth below the billet cylindrical edge.

In the case of the 8-inch diameter TB billet, only a single indication was found. This indication, however, was only resolved by two of the instrument systems. The indication was found at billet location TB-2 and at an approximate depth of only 0.5 inches below the billet's cylindrical edge.

In the case of the 16-inch diameter T billet, the inspection could only be carried out for the 8/64-inch diameter flat bottom reference hole quality control reject level, because even at this high defect signal level the billet provided numerous indications. Three significant locations were recorded for billet locations T-1-2, T-1-3 and T-2, at billet angular positions of 270°, 0° and 225°, respectively, and at an approximate 8-inches of depth below the billet's cylindrical edge.

The areas in both the 8-inch and 16-inch billets which provided ultrasonic indications were further evaluated. Two specimens were prepared from the 8-inch diameter T billet, and one specimen was prepared from each of the 8-inch diameter TA and TB billets as well as from the 16-inch diameter T billet. The specimen preparation was carried out by the subcontractor. After sections were cut from the billets, both radiography and ultrasonics were used to trace the ultrasonic indications. Unfortunately, the radiographic evaluation was negative and the thin specimens were found also difficult to inspect by ultrasonics. Therefore, no specific defect was found. This was disappointing because the 16T-2 billet section revealed indications which were comparable to the indication obtained from the 8/64-inch FBH calibration standard. Accordingly, an effort to investigate the metallurgical and acoustical-property differences between the 8-inch diameter billets versus the single piece 16-inch diameter billet was carried out. This investigation was triggered also by the fact that a different quality control reject criteria had to be used for the 16-inch diameter billet (#8 FBH) as compared to the criteria used for the three 8-inch diameter billets (#3 FBH). Specimens used for this investigation were obtained from the final billet ends as were shown in Figure 91. Each of these billet top-end specimens was cut into a half-disc shape and then further sectioned as shown in Figure 93. The specimen sectioning was designed to provide information for various billet radius locations. Accordingly, specimen designations -E, -M and -C refer, respectively, to the billet edge, mid-radius and center locations. These samples were used to yield grain size information and their adjacent samples of -D and -F designations provided acoustic attenuation and velocity data. The grain size data were obtained by using Heyn's intercept method. Using this method, the grains were rated in terms of the average grain diameters, not magnified, as the average linear dimension of grains intercepted along a straight line. For the work reported here, Heyn's approach was taken because the linear dimension relating to grain diameters was the most relatable to the acoustic wavelength dimensions. The acoustic attenuation and velocity data were calculated using conventional through-transmission measuring techniques for a 5.0 MHz longitudinal wave. The results of measurements are shown in Table XIII.

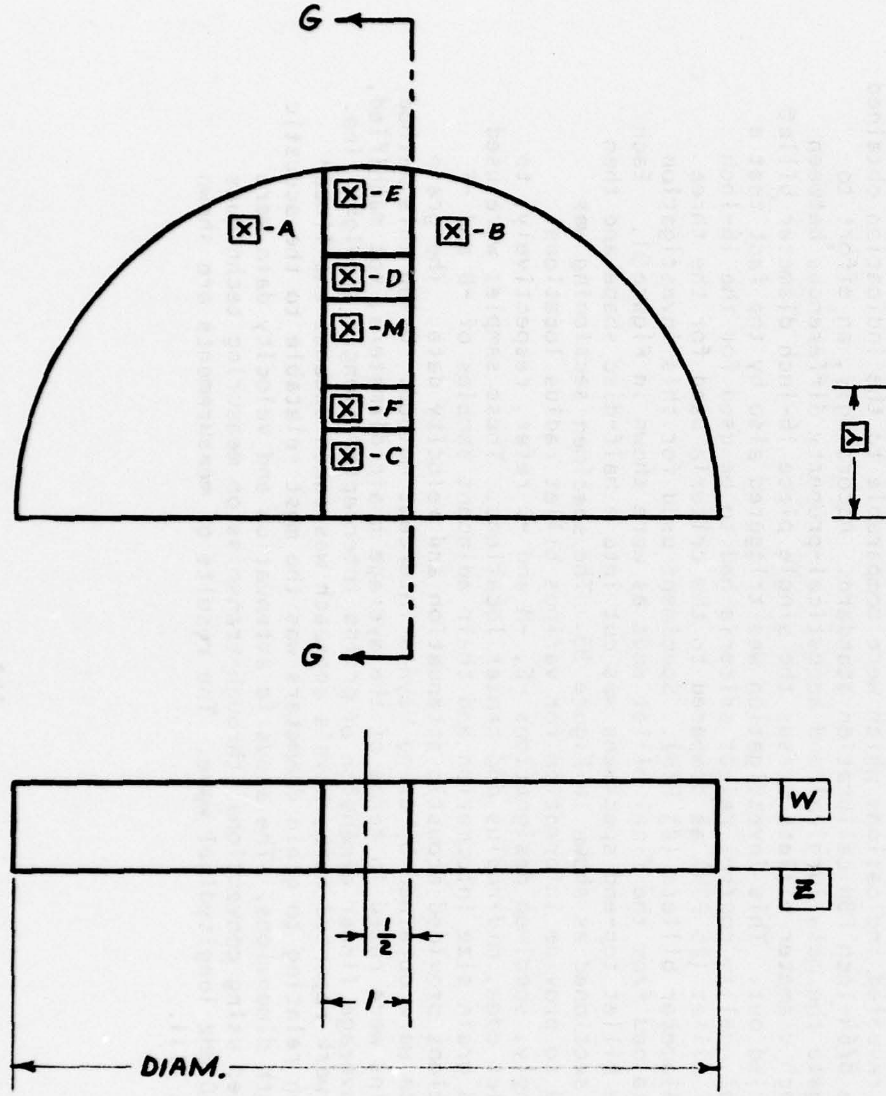


NOTES:

1) STAMP SPECIMEN DESIGNATION (E.G., 16T-A) ON EACH PIECE IN POSITION SHOWN PRIOR TO CUTTING.
2) THE Z SURFACE AND THE GG SURFACE OF SPECIMENS -E, -M AND -C SHALL BE POLISHED AND ETCHED FOR PHOTOMICROGRAPHS.
3) CARE SHALL BE EXERCISED WHILE CUTTING SPECIMENS TO AVOID OVERHEATING WHICH WOULD AFFECT GRAIN STRUCTURE.

SPECIMEN DESIGNATION PARAMETERS
(1-INCH SLICE FROM TOP END OF BILLET)
(BILLET HEAT NO. 895821)

| BILLET NO. X | NOMINAL DIAM. | NOMINAL Y DIMENSION | SURFACE W | SURFACE Z |
|---|---|---|---|---|
| 16T | 16 | $3\frac{1}{2}$ | TOP END OF BILLET | BOTTOM SIDE (HEAT NO. STAMP) |
| 8T | 8 | $1\frac{1}{2}$ | BOTTOM SIDE | TOP END (HEAT NO. STAMP) |
| 8TA | 8 | $1\frac{5}{8}$ | BOTTOM SIDE | TOP END (HEAT NO. STAMP) |
| 8TB | 8 | $1\frac{1}{2}$ | BOTTOM SIDE | TOP END (HEAT NO. STAMP) |

Figure 93. Billet Test Specimen Sectioning Diagram.

## TABLE XIII

### Grain Sizes and Acoustic Properties of Test Billets

| Billet Designation | Specimen No. | Grain Diameter (1)(2)(4) (cm) | Longitudinal Acoustic (1)(2)(3) | |
|---|---|---|---|---|
| | | | Attenuation Coeff ($cm^{-1}$) | Velocity (m/s) |
| 8-inch Dia. T Billet | 8T-E | 0.0265 | | |
| | 8T-D | | 0.0949 | 6,520.0 |
| | 8T-M | 0.0273 | | |
| | 8T-F | | 0.0249 | 6,358.1 |
| | 8T-C | 0.0472 | | |
| 8-inch Dia. TA Billet | 8TA-E | 0.0272 | | |
| | 8TA-D | | 0.0389 | 6,602.8 |
| | 8TA-M | 0.0325 | | |
| | 8TA-F | | 0.0708 | 6,373.8 |
| | 8TA-C | 0.0531 | | |
| 8-inch Dia. TB Billet | 8TB-E | 0.0318 | | |
| | 8TB-D | | 0.0200 | 6,640.7 |
| | 8TB-M | 0.0433 | | |
| | 8TB-F | | 0.0449 | 6,528.6 |
| | 8TB-C | 0.0454 | | |
| 16-inch Dia. T Billet | 16T-E | 0.0243 | | |
| | 16T-D | | 0.0794 | 6,437.3 |
| | 16T-M | 0.0675 | | |
| | 16T-F | | 0.0689 | 6,261.7 |
| | 16T-C | 0.0656 | | |

Notes: (1) Measured in billet transverse (radial) direction.
(2) Average values.
(3) Measured at 5.0 MHz frequency.
(4) Measurement taken by Heyn's intercept method.

A review of the data indicates that the 16-inch diameter billet had larger grains, higher attenuation but similar velocity as the three 8-inch diameter billets. The differences, however, were not as large as expected in view of the results of the field inspection. The random selected sample locations and the small number of the samples in use may have failed to provide a representative set of conditions. In view of Figures 94 and 95, which show segments of specimens 16T-E and 16T-C, respectively, one sees a grain size variation of less than 1:3. This, of course, is a disappointingly low grain-size ratio to provide an explanation for the ultrasonically "noisy" appearance of the 16-inch diameter billet. A quick review of the entire surfaces of the remaining quarter-disc billet specimens revealed, however, a drastic difference in grain size for some isolated locations. Figures 96 and 97 show samples 16T-E and 16T-C, respectively. Near the outer cylinder edge of the billet lies a relatively straight line of large grains, which seem to resemble the square cross section of the originally press-forged billet. A closer view of the sample 16T-B is shown in Figure 98. This picture details an enlarged area around the specimen type letter "-B" stamping and divulges a dramatic grain size variation of over 1000:1. Grain size variations like this, of course, may easily produce ultrasonic indications observed during the field inspection.

Situations like the one just mentioned can occur elsewhere in the 16-inch diameter billet, which is believed could provide an answer for the defect-like indications of ultrasonics but no apparent indications for radiography. Therefore, an effort was made to further investigate this matter by obtaining another specimen from the 16-inch diameter T billet which contained an ultrasonic indication similar to the one investigated before. The billet was reinspected by ultrasonics and the location of the ultrasonic indication was confirmed. The new specimen was then obtained by cutting it from the billet, and then was redesignated as billet section 16-T-1-2. This billet section contained two ultrasonic indications, hereinafter called "A" and "B", which were larger than the indication obtained from the 8/64-inch diameter FBH reference calibration standard. The location of these are shown in Figure 99. Sectioning diagram of the 16T-1-2 specimen is shown in Figure 100.

Figure 94. Microstructure of 16" 
(Radial Direction, Edg

Figure 95. Microstructure of 16"
(Radial Direction, Ce

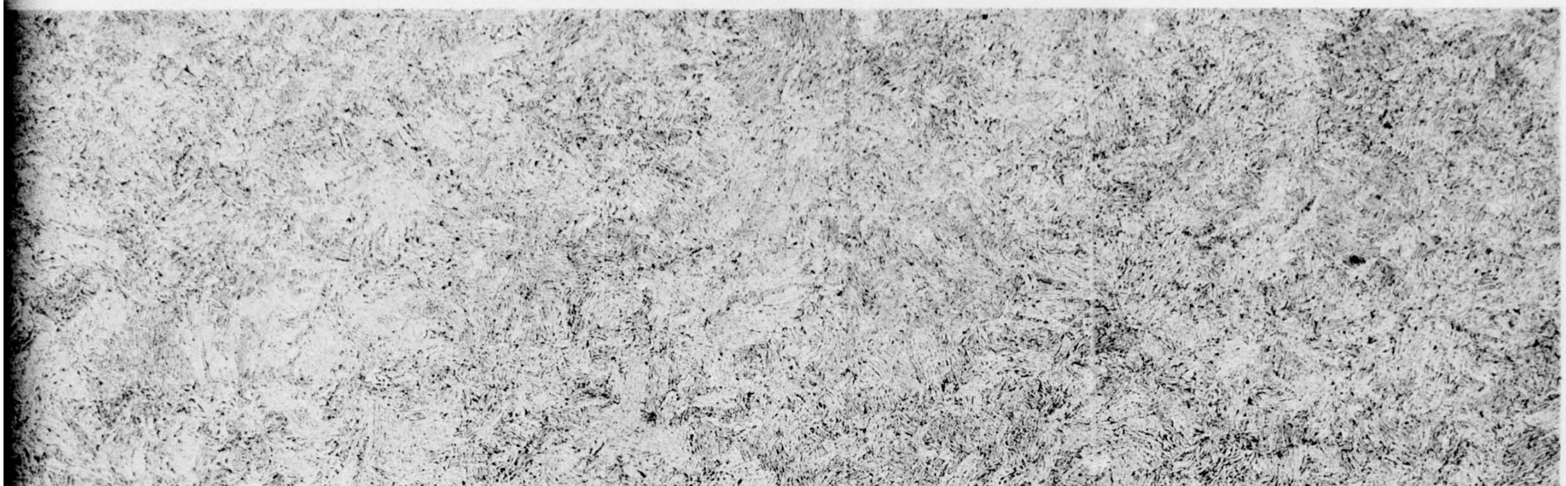

crostructure of 16" Dia. T Billet, Section 16T-E,
adial Direction, Edge Position, Approx. 40X)

icrostructure of 16" Dia. T Billet, Section 16T-C,
Radial Direction, Center Position, Approx. 40X).

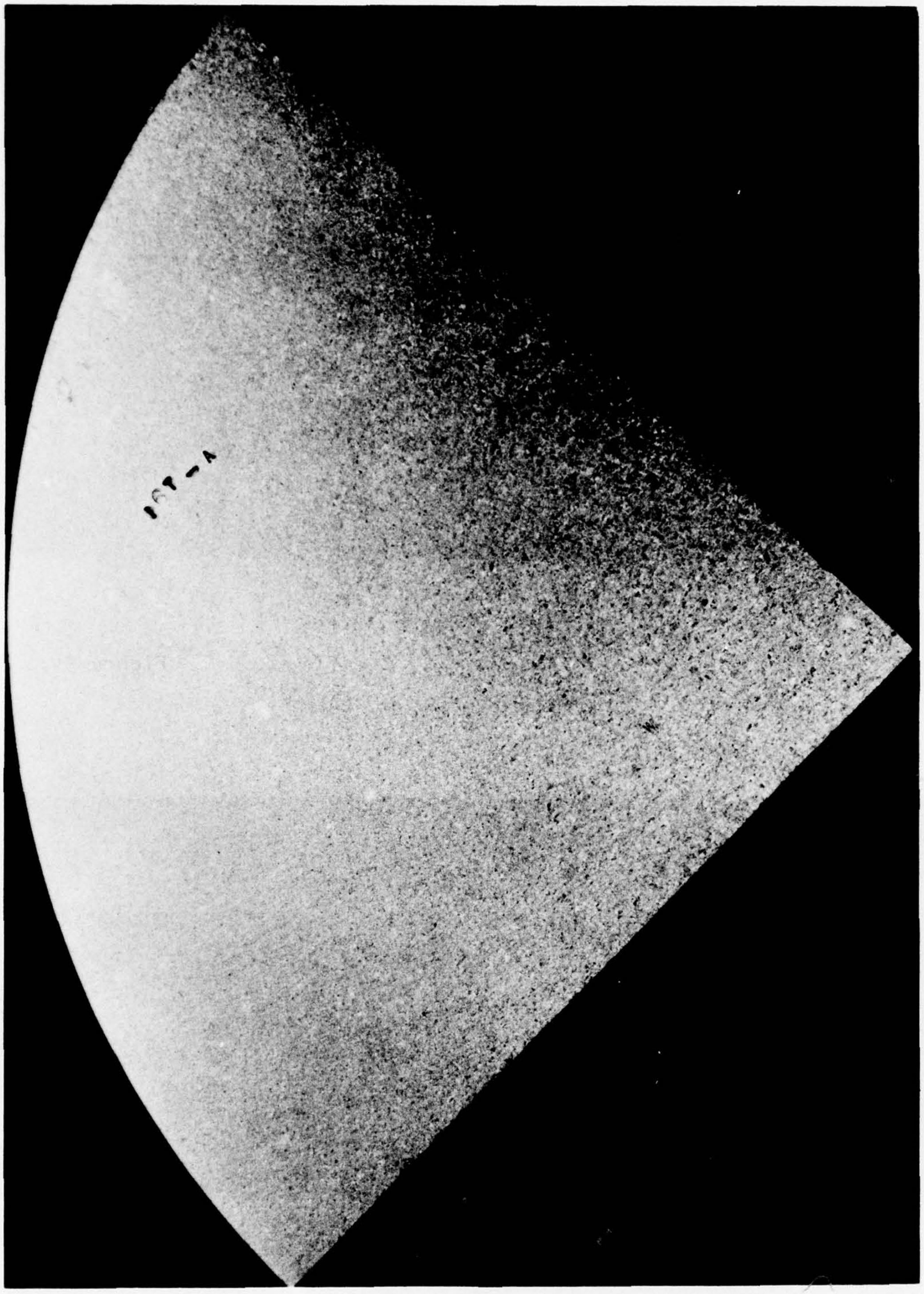


Figure 96. Macrostructure of 16T-A Specimen.
(Approx. 0.84X)

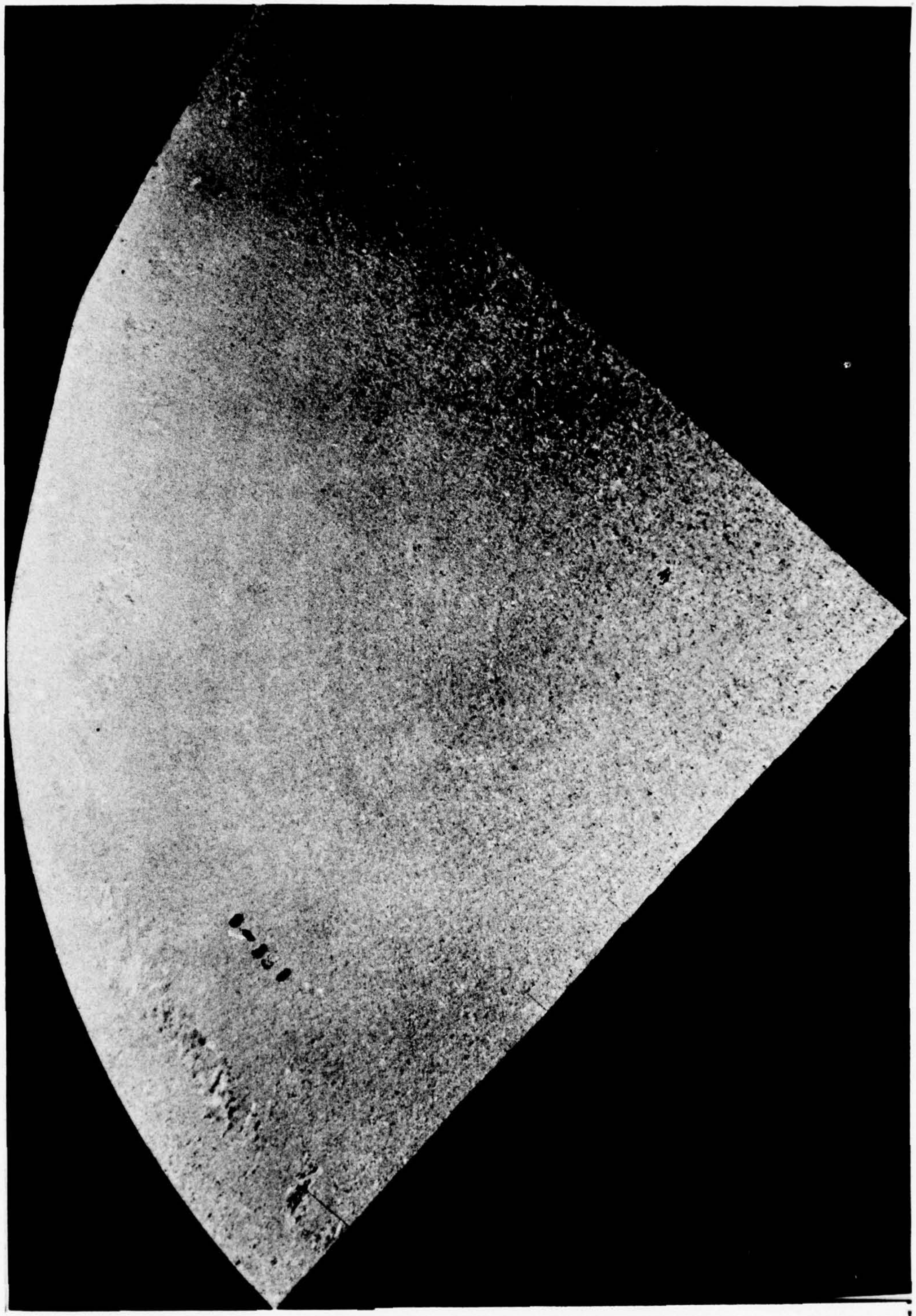

Figure 97. Macrostructure of 16T-B Specimen.
(Approx. 0.84X)

Figure 98. Grain Size Variations in 16T-B Specimen. (Approx. 4.6X)

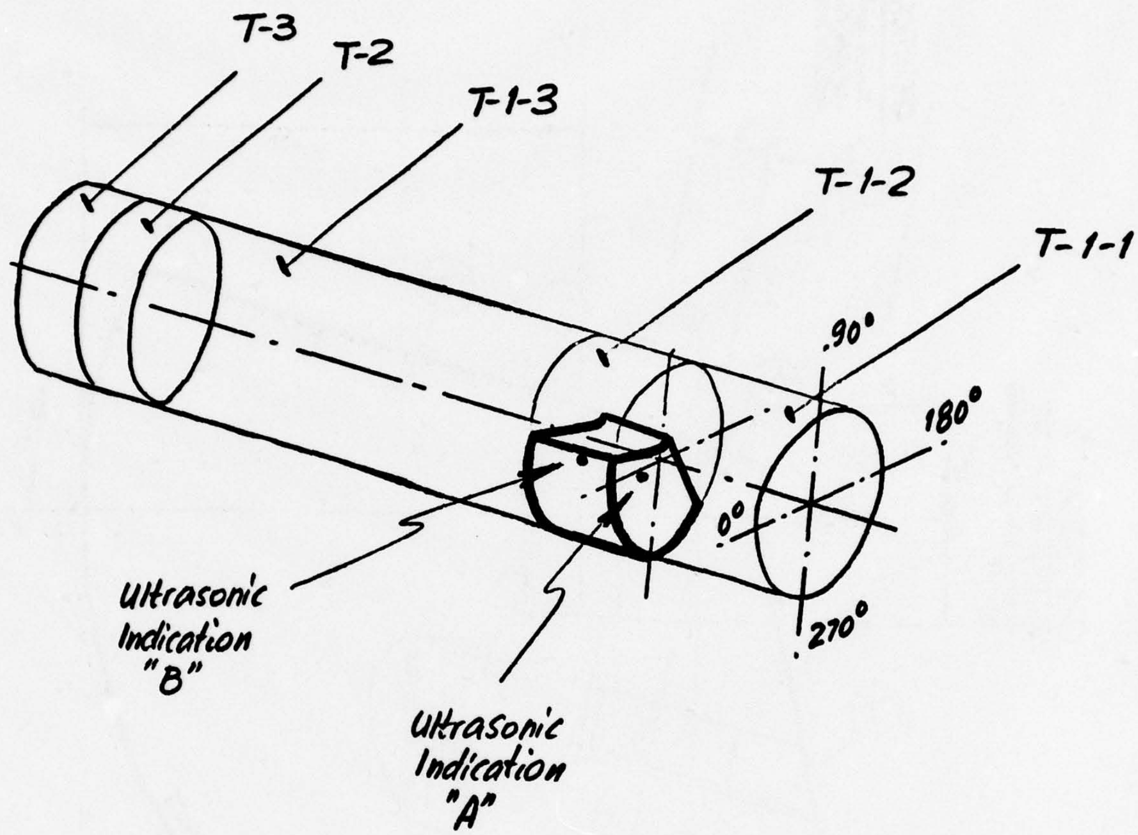


Figure 99. Sectioning Diagram of 16" Dia. T Billet.

3740 C

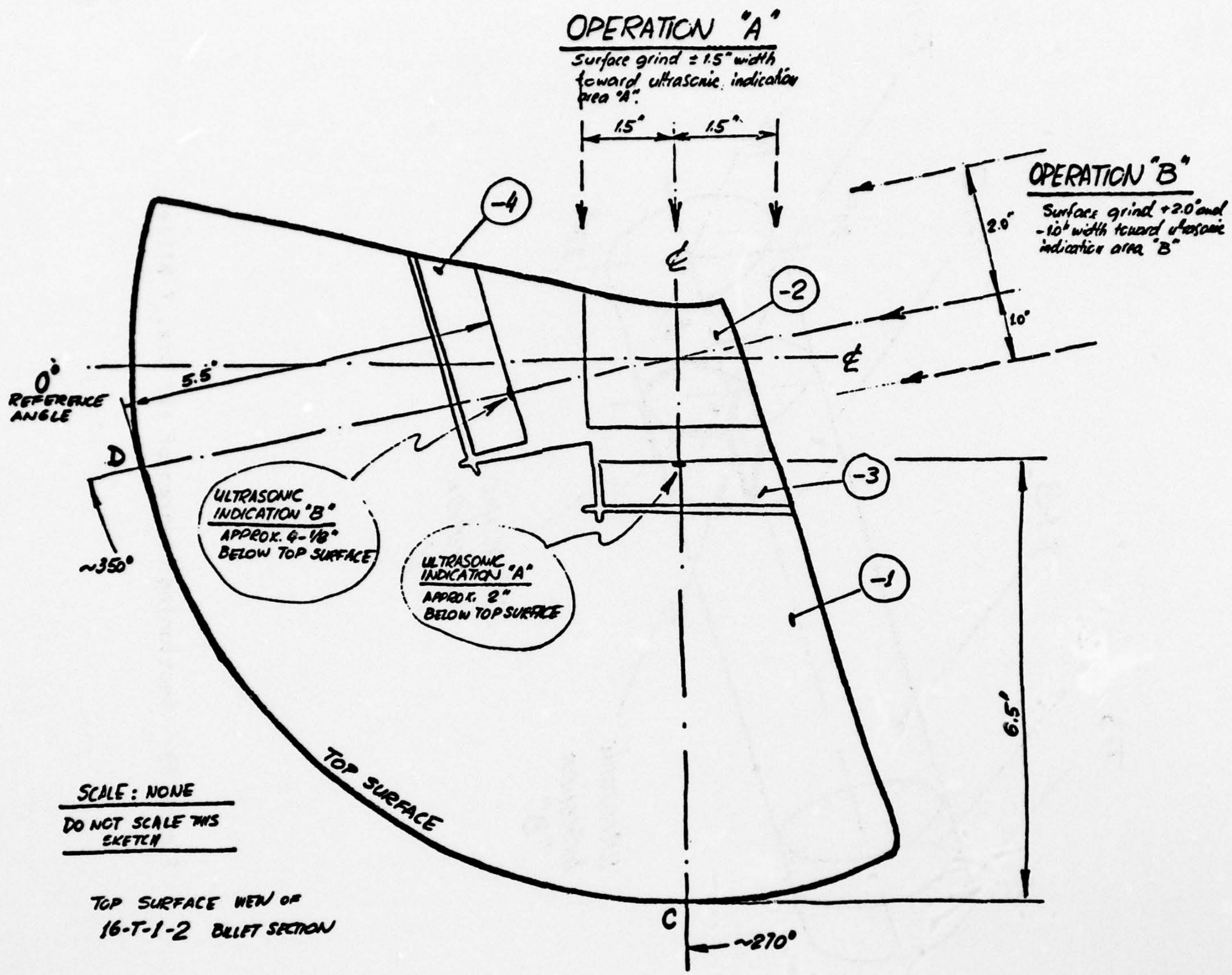


Figure 100. Sectioning Diagram of 16T-1-2 Specimen.

The 16-T-1-2 billet specimen sectioning was as follows. Ultrasonic indication locations A and B were periodically monitored by the ultrasonics from the billet outer surface points C and D, located at approximate 270° and 350° angular billet positions, while first the specimen section No. 2 was cut off, and then surface grinding operations A and B were carried out. Beside periodical ultrasonic monitoring to avoid "losing" the indications A and B, periodical surface etchings were also done to observe anything unusual. The material removal rate was kept very small in order to have a high degree of observation capability. After reaching the appropriate radial depths of 6.5 inches for the indication A, and 5.5 inches for the indication B, said indication areas were cut out and have been designated as specimens 16-T-1-2-3 and 16-T-1-2-4, respectively. The ultrasonic indications A and B, as they appeared on the ultrasonic instrument display are shown in Figures 101 and 102.

In spite of the careful machining, periodical surface etching and ultrasonic inspections, there was no true defect found for either of the A or the B ultrasonic indication areas. Significant structural differences for grain sizes were found, however, for both of the A and B areas when they were compared to the other areas of the billet. The grain size range established earlier indicated an average grain diameter of 0.0243 cm for billet edge location, 0.0675 cm for billet mid-radius location, and 0.0656 cm for billet center location. The range of the average grain variation from billet edge to center locations was thus established as less than 1:3. Grain size measurements taken for the specimens 16-T-1-2-3 and 16-T-1-2-4, however, showed an average grain diameter of 0.268 cm and 0.372 cm; a five-fold increase.

Further evaluation was carried out by sectioning the 16-T-1-2-3 specimen into smaller segments, as shown in Figure 103. Grain size measurements taken from the exact ultrasonic indication area A, redesignated now as specimen 16-T-1-2-3-5, revealed the average grain diameter to be 0.329 cm. The microstructure of this area is shown in Figure 104. Direct comparison of the dramatic grain size variations may easily be seen when one views this Figure 102 along with Figures 94 and 95 for the average billet edge and center location micrographs.

While the large grains may not affect the application performance of the material, and it may also be known to be common in large diameter billets, it does, nevertheless, hinder the ultrasonic inspection. In other words, the

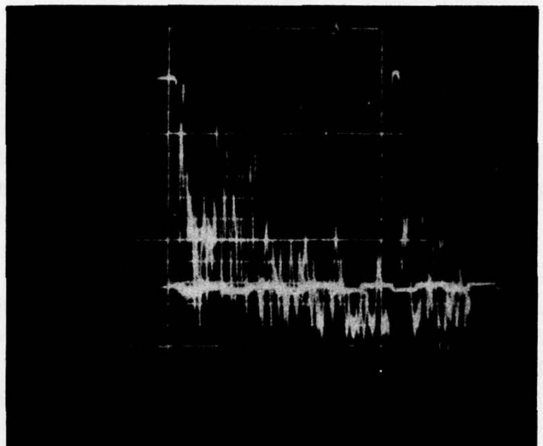

Figure 101. Ultrasonic Indication "A" in 16T-1-2 Billet.

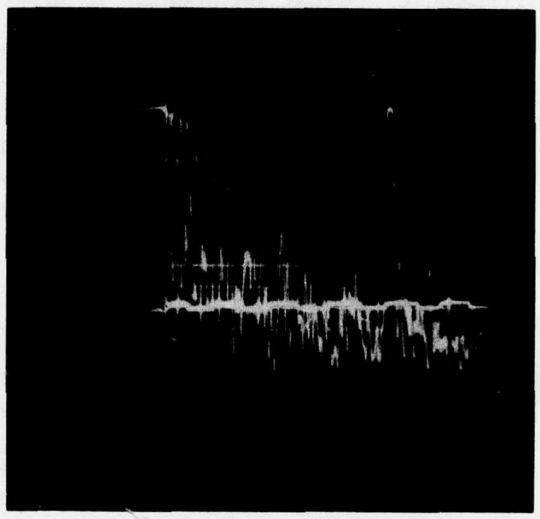

Figure 102. Ultrasonic Indication "B" in 16T-1-2 Billet.

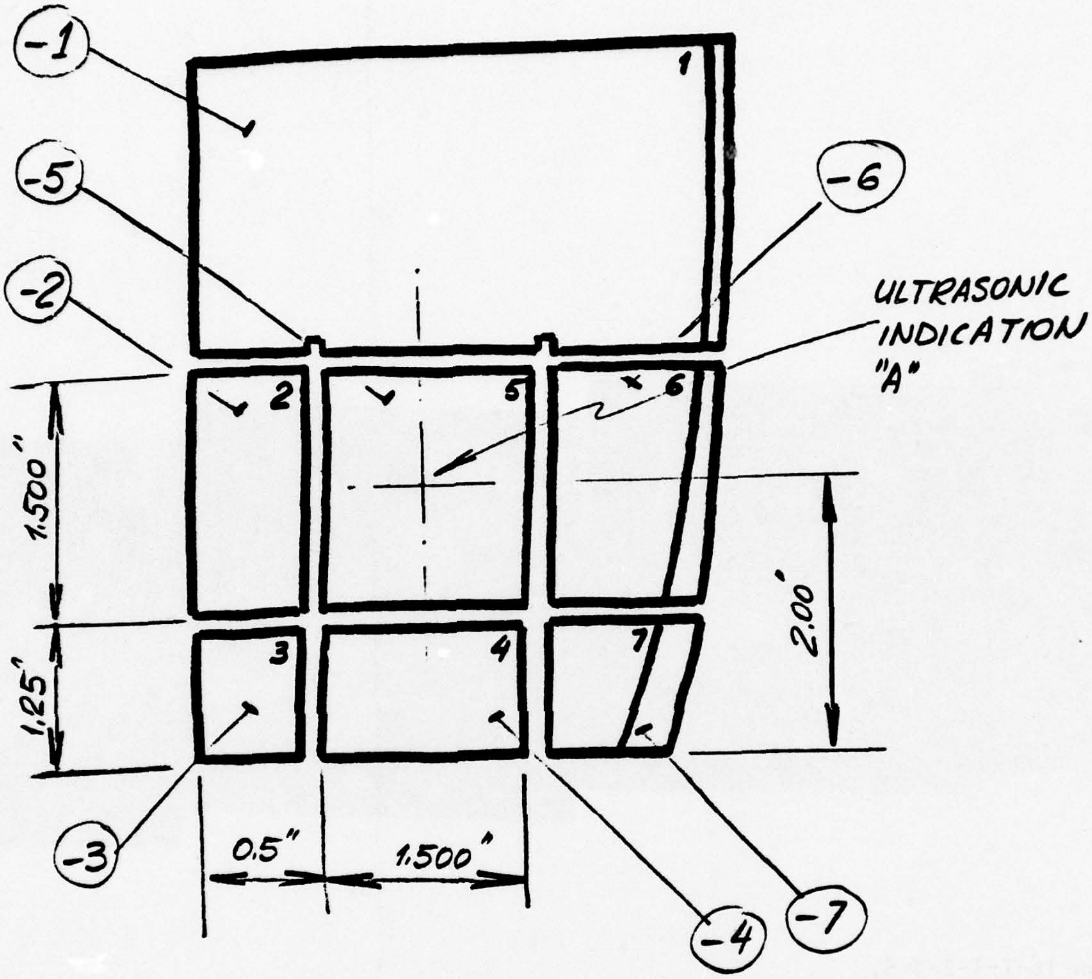


Figure 103. Sectioning Diagram of 16T-1-2-3 Specimen.

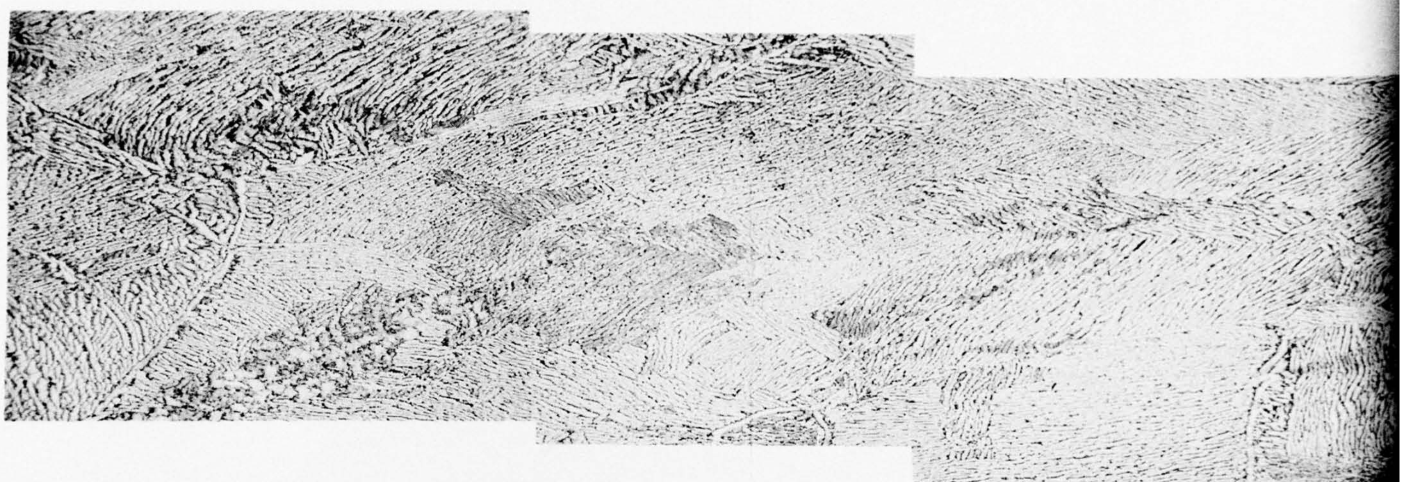

Figure 104. Microstructure of 16" Dia. T Bill
(Radial Direction, Approx. 40X).

2

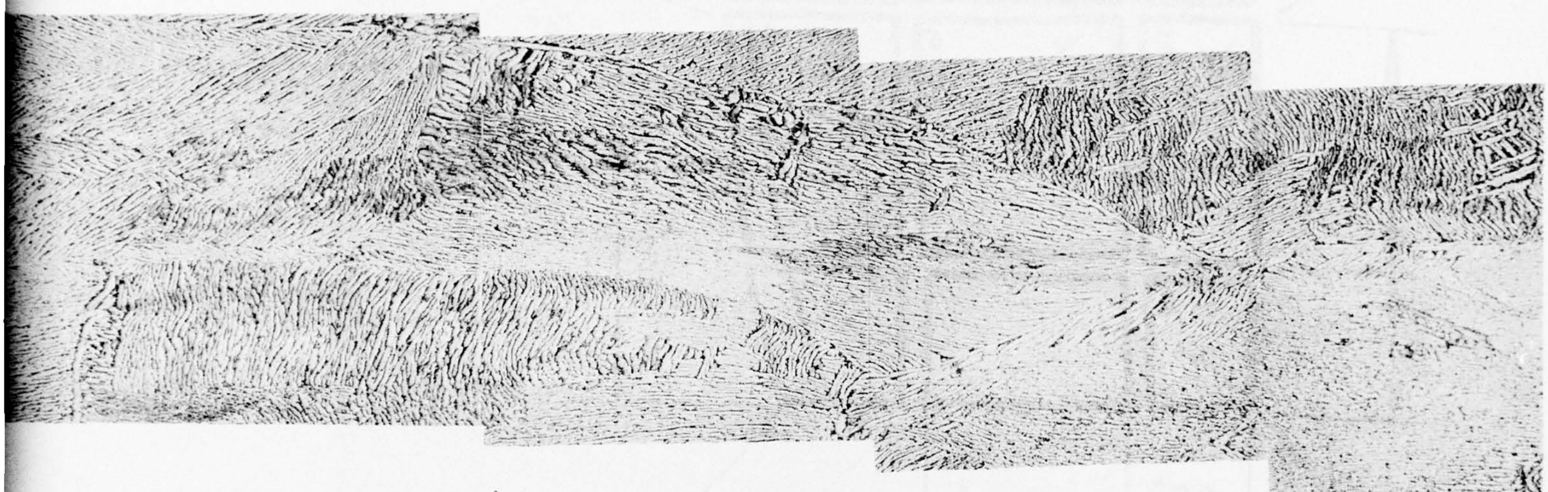

16" Dia. T Billet, Section 16-T-1-2-3-5,
(Approx. 40X).

significance of the findings is in the relation of the size of the grains to the length of the acoustic waves propagating through them. In the case of grains whose size approach the size of the wavelength, the material will appear excessively "noisy" (Ref. 10). Considering the two popular ultrasonic frequencies used for titanium alloy forging billet inspections of 5.0 and 2.25 MHz, their corresponding average wavelengths are 0.12 cm and 0.28 cm, which are both less than the average grain size of 0.329 cm measured on the specimen 16-T-1-2-3-5 specimen for the ultrasonic indication area A.

In summary, the large grains or large grained areas occurring in a smaller grain size medium may be detected as genuine defects. Although the above reasoning does explain the situation on hand, nevertheless, an additional microprobe analysis also was carried out to establish possible chemistry variations if any.

The first approach was to have a spot analysis profile carried out on the 16-T-1-2-1-5 specimen from one of its edges through its center to cover the ultrasonic indication area A and some of its surroundings. The results of this analysis are shown in Table XIV below for the X-ray counts per 100 second counting time.

Table XIV

Billet Chemistry of 16-T-2-3-5 Specimen

| Element | Location | | | | | | | | | | | |
|---|---|---|---|---|---|---|---|---|---|---|---|---|
| | A | B | C | D | E | F | G | H | I | J | K | L |
| Al | 1909 | 1863 | 1871 | 1852 | 1876 | 1873 | 1765 | 1930 | 1832 | 1823 | 1936 | 1815 |
| Ti | 27841 | 27945 | 27840 | 27770 | 27611 | 27642 | 27631 | 27636 | 27146 | 27201 | 27495 | 27437 |
| V | 14940 | 15440 | 15040 | 15210 | 15480 | 15450 | 18690 | 14210 | 19480 | 14850 | 13420 | 16640 |
| Background | 859 | 792 | 814 | 830 | 823 | 825 | 835 | 834 | 843 | 803 | 871 | 829 |

The results of this analysis revealed no significant variations for chemistry, although it may indicate that some chemical variation does exist between fine and coarse grains. Also, the higher aluminum and lower vanadium associated with fine structure and the lower aluminum and lower vanadium in coarse structure, as suggested by the analysis spots H and I, respectively, could be consistent to explain grain size variations on the basis of local variations in β transus temperatures.

A second method of microprobe analysis carried out using a beam spot size of 3 mils in diameter while the specimen was traversed so that the beam would cover an area equal to 240 square mils. This method yielded a more normalized quantity for each major element. The method was also extended to cover typical billet edge, mid-radius and center specimens of 16TE, 16TM and 16TC, respectively, which were used in the prior grain size measurement evaluations. The results are shown in Table XV below for the X-ray counts per 200-second counting time.

Table XV

Billet Chemistry of 16TC, 16TM, 16TE
and 16-T-1-2-3-5 Specimens

| Element | Specimen | | | |
|---|---|---|---|---|
| | 16T-1-2-1-5 | 16TC | 16TM | 16TE |
| Al | 2152 | 1947 | 1534 | 1731 |
| Ti | 56373 | 53351 | 56639 | 56220 |
| V | 30733 | 30470 | 36649 | 33120 |
| Background | 1699 | 1699 | 1699 | 1699 |

It should be emphasized that the method used could not yield the accuracy necessary to reveal small chemical changes because there was no comparative reference standard and the practice of normalizing the data over the background noise measurements is not a technique which could be accepted as valid. Nevertheless, billet chemistry is far more uniform than the large variations found in grain sizes.

### 4.2.2 Phase II Effort

In addition to the materials produced in Phase I of the program, two ingots of the Ti-6Al-4V composition were cast as Phase II materials. These materials were double vacuum melted and, in order to overcome the difficulties encountered with the ultrasonic inspection of the Phase I billets, the materials were made using special manufacturing techniques to produce ultrasonically "quiet billets."

One heat (#890309) provided materials for three pieces of 8-inch diameter and a single piece of 16-inch diameter billets. The second heat (#890326) provided materials for two pieces of 16-inch diameter billets. The ingot conversion to final product was, essentially, the same as used for the Phase I materials with an increased amount of thermomechanical work.

One-inch thick test slices were cut from the end of each billet to provide macro- and microstructure records. These data showed no apparent abnormalities, inclusions or segregates. The structures appeared to represent normal quality billets, showing the usual variations from top to bottom and from billet to billet. This variation is probably the result of the slightly different finishing temperatures and cooling rates. The ultrasonic inspection of the Phase II billets was discussed in Section 4.1.2 - Field Evaluation, which revealed excessive ultrasonic scatterings originating from two principal billet locations. One of these is the four discrete billet mid-radius locations and the other is the entire outer billet circumference. Both of these indications were evident, more or less, throughout the billet's longitudinal axis.

Billet metallographic studies confirmed the ultrasonic findings. Figures 105 and 106 show the macrostructures of the top and bottom ends of the 16-inch diameter T billet (Serial No. RMI-793108). Both billet top and bottom sections appear coarser in their centers than in their outer one-third. Although the billet bottom section has finer grains in its center, yet coarser ones in its circumference when it is compared with the billet top. Resultingly, the billet bottom appears to exhibit a larger grain variation from center to edge than the billet top. The coarser grained center part of the billet also appears to have a square outline, the edges of which are the probable cause of the ultrasonic scattering ("noise").

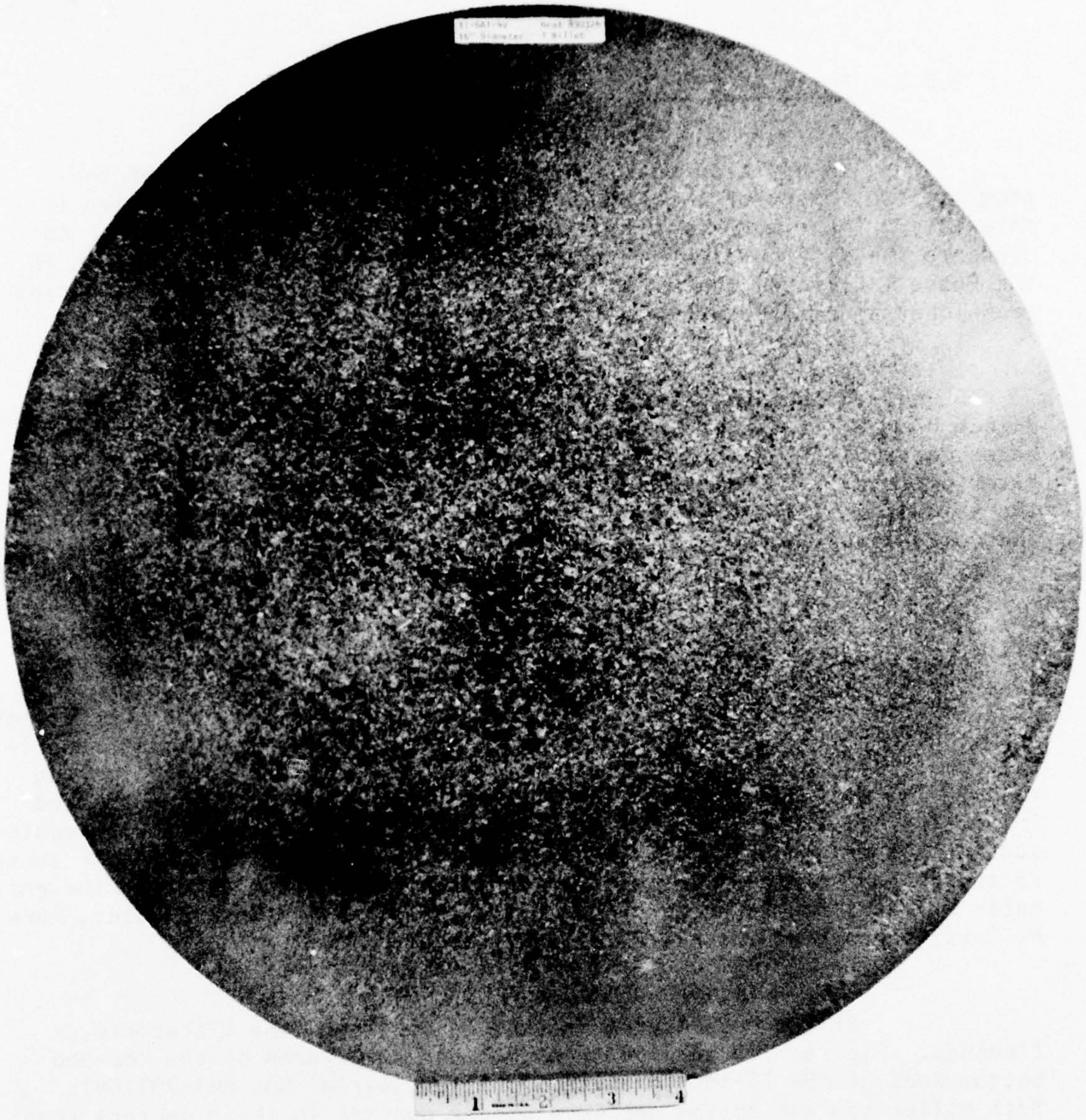

Figure 105. Macrostructure of the 16-inch Diameter T Billet (Top End)

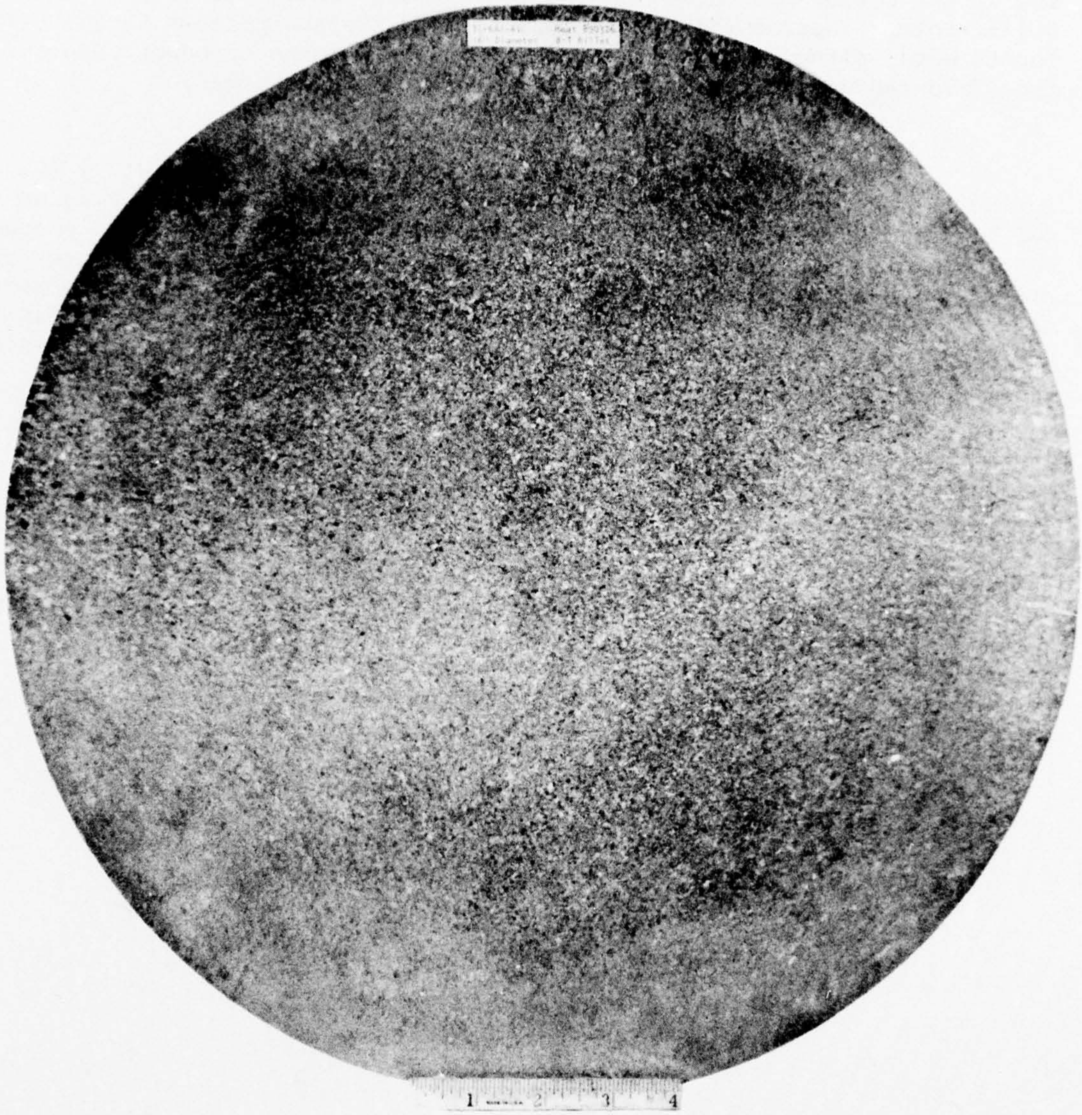

Figure 106. Macrostructure of the 16-inch Diameter T Billet (Bottom End)

Microstructure analysis of the billet top section indicated a 20-30% transformed beta in the outer billet circumference, an estimated 15-20% in the billet mid-radius and a 10% in the billet center areas. For the billet bottom section the microstructure analysis suggested a 40-50% transformed beta, although this is a more coarse transformed product than the top. Mid-radius and center parts are similar to each other.

The ultrasonic reject indication found in the billet by the UDIS during the system field evaluation was reconfirmed by RMI by turning up the DAC higher than the setting used in the original normal inspection procedure. In other words the indication was below the level necessary to trigger the alarm and call the operator's attention to the abnormality. By this procedure no record would have been made of the possible defect. A billet slice containing the reject indication area was retained for further examination.

# 5. SYSTEM SPECIFICATION AND OPERATION

System specification for the UDIS provided in this report covers both equipment specifications and inspection procedures as described in the following two sections.

## 5.1 Equipment Specification

The Ultrasonic Diagnostic Inspection System is especially designed and constructed for the ultrasonic nondestructive inspection of large-size, cylindrical-shaped, titanium-alloy forging billets. The computer automated ultrasonic method utilizes a novel combination of pulse-reflection defect detection and thru-transmission automatic distance-amplitude compensation techniques, (Ref. 2). Furthermore, the UDIS also uses a diagnostic B-scan billet inspection technique which provides the following three unique advantages: a programmable computerized ultrasonic signal-to-noise ratio enhancement; a programmable computerized defect angular direction resolution enhancement; and a billet acceptance/rejection capability for programmable computerized three-dimensional defect length size.

A comprehensive description of the system is given in Section 2.3 - Revised System Specification, and technical details of the system specification for the various subsystem components are discussed in Appendix A - Revised System Specification. Table XI of Section 2.3 is a summary tabulation of final specifications.

The UDIS was designed to carry out billet inspections utilizing the immersion method. Demonstration of the UDIS was carried out using subcontractor's immersion tank. This tank (as all commercial tanks) supports the billet by rollers. It was soon found that due to the characteristics of actual production billets, i.e., out of round, longitudinal taper, and longitudinal bent, the billets seldom stay put on the rollers. This, of course, causes angular slippages as well as axial travel or even oscillation; thus, error in defect location detection. This report does not cover an immersion tank specification, although it recommends that the billet be supported between points and rotated by a dog. This billet-supporting-and-rotating approach has an important inherent advantage which eliminates slippages of both angular and axial directions that occur for billets rotated by conventional supporting rollers. A yet more cost effective method is to use existing lathes with wheel transducers to inspect the billets right before/after billet OD turning operation(s). Obvious cost-savings is a one set-up for both machining and inspection.

Finally, because of the variety of the commercial instrumentation modules that have been utilized in the fabrication and assembly of the UDIS (such as the oscilloscope displays, the minicomputer and its peripherals) there are no separate descriptions given in this report on these off-the-shelf equipment. Rather, comprehensive reference is made in Appendix C, to their appropriate Manufacturer's Operating and Service Manuals.

## 5.2 Inspection Procedures

The UDIS consists of three main subsystems: (1) a billet handling immersion tank facility; (2) a special ultrasonic instrumentation; and (3) a data processing system. The design, construction and operation of these subsystem elements have been discussed in Section 3 - System Construction. This section of the report describes the installation and operation procedures of the UDIS.

### 5.2.1 Installation Procedures

The UDIS requires a special billet handling immersion tank equipment. The system is operational with any commercial billet handling immersion tank which is capable of providing a helical type of scan of the billet under inspection. A transducer bridge axial translation tie-in, however, shall be made to the UDIS to provide "stop-rotation" signal at appropriate times. Also, the tank must be equipped with digital shaft encoder transducers for accurate monitoring of the billet angular and axial positions during the scan. Modifications that were carried out on the water tank of subcontractor RMI Co., have been described in Section 3.2 - Billet Scan Monitoring System. These efforts were necessary to carry out the System Field Evaluation of the UDIS. The water tank modifications, however, must be custom made depending on the type of the water tank in use. Because of the difficulties that one may encounter in water tank modifications, and because of the importance of the accuracy of the billet position monitoring it is highly recommended that in future installations the billet be supported between points and rotated by a dog. This billet handling concept is the most appropriate for the accurate inspection of centerless, out-of-circle and non-straight billets.

The billet scan mechanism must also be able to accommodate two ultrasonic transducers mounted in-line but at opposite sides of the billet to provide sound transmission through the billet's center. One of the two transducers is the pulse-reflection, defect-detection transducer, which is mounted with a nominal distance of 4-1/4 inches from the billet. The second, or ADAC transducer shall be mounted at the opposite face of the billet utilizing a special fixture, such as a wheel transducer, which maintains a constant waterpath distance between transducer and billet. The two transducers must be properly aligned normal to the billet, as well as in a straight line to each other through the center of the billet.

The UDIS can be operated from either a 115, 240 or 480 volts 60 Hz single phase power source. The system can easily be converted to accept any of the listed power supply lines. A three conductor #12 AWG size standard, thermoplastic insulated hook-up cable (TRW #30-192330) is furnished. To protect operating personnel and to reduce electrical noise interferences the system must be properly grounded. The UDIS is equipped with a grounding terminal and with a single conductor of #2-1680 size stranded and rubber insulated drop cable (TRW #30-193950) which exceeds the appropriate NEMA requirements. Proper grounding of the equipment is extremely important and must be accomplished prior to electrification of the unit. It must be emphasized that the proper grounding of the water tank itself must also be accomplished.

The UDIS is constructed using high-reliability, solid-state devices. Nevertheless, proper ventilation is important. Each of the three relay-rack cabinets is equipped with a cooling fan and air filters. The system is designed to operate where the ambient temperature is between the limits of +10°C and +50°C, (50°F and 120°F), with a relative humidity from 20% to 95% (without condensation).

While the entire electronics instrumentation is not particularly sensitive to mill environmental conditions, the tape recorder computer peripheral including its magnetic tapes are very sensitive to airborne dust. For trouble-free operation, therefore, it is recommended that the entire instrumentation be housed in an environmental conditioning inspection "shack". The ultrasonic instrumentation, including its A and B scan displays, however, can be removed from the existing relay rack cabinet and mounted directly onto the bridge of the billet handling inspection tank if so desired.

AD-A049 682    TRW INC  CLEVELAND OHIO MATERIALS TECHNOLOGY    F/G 11/6
IMPROVED ULTRASONIC INSPECTION OF TITANIUM ALLOY FORGING BILLET--ETC(U)
JUL 77   I M MATAY    F33615-71-C-1712
UNCLASSIFIED    TRW-ER-7554    AFML-TR-77-111    NL

3 OF 4
AD
A049682

### 5.2.2 Operating Instructions

Operation of the UDIS should be initiated in the manual operation mode without the data processing subsystem using only the ultrasonics and transducer adjustments. This process is quite similar to existing inspection practices. Hence, this paragraph will first review the controls of the ultrasonic subsystem and then the operation of the UDIS itself.

#### 5.2.2.1 Ultrasonic Subsystem Controls

In spite of the advanced characteristics of the UDIS, its ultrasonic subsystem is still a basic pulse-reflection type of instrumentation having controls much the same as most commercial ultrasonic equipment. Accordingly, its operation is similar to existing practices. The following list describes the controls and indicators of the unit:

| Module | Control | Function |
|---|---|---|
| NIM bin | Power Switch | On-off control |
| Power Supply | Power Switch | On-off control |
| Pulser | Power Switch | On-off control |
| | Int/Ext Pulser | Selection of internal or external pulser unit |
| | Amplitude | Pulse amplitude adjustment |
| | Duration | Pulse duration adjustment |
| Clock | Auto/Man Pulse | Selection of automatic or manual clock operation |
| | PRF | Pulse Repetition Frequency course adjustment |
| | Vernier | PRF vernier adjustment |

| Module | Control | Function |
| --- | --- | --- |
| Receiver | RF/Video Display | Selection of RF or video A-scan display |
| | Man/Auto Mode | Selection of manual or automatic receiver operation |
| | Noise Reject | Amplifier bias adjustment |
| | Sensitivity | Amplifier sensitivity adjustment |
| | Vernier | Sensitivity vernier adjustment |
| | Uncal | Pilot light indicating vernier sensitivity adjustment, thus this is an uncalibrated mode of course sensitivity control |
| Defect Gate | MB/IF Sync | Selection of gate synchronization to the initial pulse (MB) or to the billet front interface pulse (IF). |
| | Start | Manual gate start time adjustment |
| | Length | Manual gate length time adjustment |
| | S & L Window | Window start and length times adjustments |
| | 8/16 Length | Selection of gate length times appropriate for 8 or 16-inch diameter billets |
| | Level | Reject level adjustment |
| | Dirt Reject | Gate bias adjustment |
| DAC/ADAC | DAC/ADAC Switch | Selection of manual or automatic DAC operation |
| | Slope DAC | Slope adjustment for DAC |
| | Slope ADAC | Slope adjustment for ADAC |
| | Delay | Time delay adjustment to start DAC/ADAC function |
| | Amplitude | Amplitude adjustment for DAC/ADAC |
| | Offset | Offset adjustment for DAC/ADAC |

#### 5.2.2.2 System Start-Up

Following installation of the equipment, the UDIS may be energized by activating each and every system component in an appropriate sequence. Therefore, in order to ensure proper operation, the following nine-step procedure should be followed:

POWER PANEL

| Sequence No. | Control Description |
|---|---|
| 1 | Main Knife Switch (Located on left-hand side of Relay Rack Cabinet) |
| 2 | SW1 Circuit Breaker (Located on right-hand side of Power Panel) |
| 3 | SW2 Circuit Breaker (Located on left-hand side of Power Panel) |

Activation of the above controls should energize their appropriate power panel pilot lights, thus indicating the availability of electric power to the particular system component.

ULTRASONIC SUBSYSTEM

| | |
|---|---|
| 4 | Power Switch (Located on right-hand side of NIM-bin) |
| 5 | Power Switch of Power Supply Module |
| 6 | Power Switch of Pulser Module |
| 7 | Power Switch of A-scan display oscilloscope |
| 8 | Power Switch of B-scan display oscilloscope |

Activation of the above switches should energize their appropriate power pilot lights, thus indicating the availability of electric power to the particular subsystem component.

9 Power Switch of the Central Processor Unit (operated by an external key)

This switch will automatically turn-on the entire data processing subsystem except the magnetic tape recorder and the line printer peripheral units. Turn-on procedure for these devices are not detailed here, instead, the reader is referred to Appendix C - Reference List of Manufacturer's Operating and Service Manuals.

After accomplishing the above-listed, nine-step system energizing procedures, the UDIS is ready for operation. The UDIS may be operated in six different modes as established by the executive software (discussed in Section 3.3.1.2 - Application Software) in response to operator commands entered through the I/O keyboard terminal of the alphanumeric-graphic display terminal. All of the commands are inserted in plain english conversational format which does not require any special skill or computer training for the UDIS operator. The conversational capability of the DPS of the UDIS is described in detail in Appendix II.

A Control C (simultaneous depression of the "Control" and "C" keys of the I/O keyboard terminal) allows the operator to enter system commands. After the Control C has been inserted by the operator, the computer will acknowledge the input by generating an *(asterisk) on the display CRT of the alphanumeric-graphic display terminal. After the asterisk displayed, the operator may request any of the following listed six different UDIS operating modes by entering at least the first two letters (capitalized) of the commands through the I/O keyboard terminals:

1. INitialize
2. CAlibrate
3. MAnual billet inspection
4. AUtomatic billet inspection
5. STop command
6. ZEro command

The DPS will look only for the first two characters of the above commands to establish the system operation mode. However, any number of alphanumeric characters up to ten may be inserted after the leading character if full word commands are desired. When the operator has completed his command input, he must insert a CR (carriage return) through the keyboard. If he has inserted a valid command prior to the CR, an appropriate message is generated on the I/O graphic terminal; if no valid command was entered, an invalid command message is generated unless the test is in progress. In this latter case, the command is ignored, and a valid command entry from the operator will be awaited by the DPS. The six system mode commands then return messages and the results are discussed below.

### 5.2.2.3 Initialization Mode

The "INitialize" command must be entered by the operator at the beginning of each day of UDIS use and after each off-line operation. The DPS will respond by requesting the current date to be inserted by the operator in alphanumeric mode through the I/O keyboard terminal. This date will then be used in all report headings until the next "INitialize" command is entered or until the completion of an off-line mode billet inspection. After the current date is entered into the system, all necessary system initialization functions will automatically be performed.

### 5.2.2.4 Calibration Mode

It is important to check system performance of the UDIS, for which a calibration mode was designed. This mode provides an automatic inspection of a known billet and the UDIS compares the inspection results with those of the known billet already on file. Accordingly, the "CAlibrate" command instructs the DPS that a calibration mode of billet inspection is to be performed. The DPS will respond by generating "BILLET NUMBER;" and then waiting for the operator to insert the billet file on the magnetic tape unit, MT0, which is to be used for calibration.

When the requested billet file is found the billet description and the first two test parameters will be displayed and the message "ACCEPTABLE COUNT DIFFERENCE =      " The operator must then enter the desired difference (0-15) and wait for "READY FOR RUN MESSAGE."

When the RUN message is inserted, an automatic mode billet test will be performed. If the test is stopped through manual input or automatic parameter monitoring, no restart can be accomplished. The test must be repeated from the beginning. Appropriate messages are generated at the conclusion of the test indicating a successful or unsuccessful calibration based upon the comparison of the data acquired from the billet test with pre-stored data describing the calibration billet.

#### 5.2.2.5 Manual Billet Inspection Mode

The "MAnual" command instructs the DPS that a manual mode of billet inspection is to be performed. The DPS will respond by generating a series of messages on the I/O graphic terminal that must be answered by the operator with data entries through the I/O keyboard terminal. These messages define all the data entries required for the test. The messages generated for this command are all of those listed for "Billet Description", "Test Parameters", and "Test Results" as shown in Appendix II, UDIS Conversational Capabilities. Each message line is terminated by a colon and space character and then the DPS will await an operator entry. All alphanumerics entered by the operator will be accepted as the input for the requested parameter until a CR is entered or input buffer length of thirty characters is exceeded. After the CR, the input data are stored in the appropriate table, and the next message is generated. The first several lines of a data entry sequence appear as follows, for example:

| | |
|---|---|
| BILLET: | A867043S-11 (CR) |
| ALLOY TYPE: | 6-AL, 4-V TITANIUM (CR) |
| HEAT NUMBER: | A8670435 (CR) |

If a non-valid operator entry is made (e.g., LENGTH 130.0) the output message is repeated until a valid entry is made. After all data parameters have been entered, the DPS will perform test initialization to effect the system configuration requested by the operator. The system then outputs "READY FOR RUN" message and waits for the next operator input through the I/O keyboard terminal. This input must be the "RUN" message followed by a CR. Immediately upon receiving the CR, the DPS will enter the On-Line test mode and the test will now proceed until either the operator enters a Control C and STop command through the I/O keyboard terminal or the test has been completed or terminated. If a test has been halted using the STop command, it can be restarted again by the operator by inserting the REstart message followed by a CR through the I/O keyboard terminal.

The message "AXIAL POSITION WRONG FOR RESTART" is generated whenever a REstart command is entered until the axial position has been corrected to be less than that existing at the STop command or that at which data recording was halted.

5.2.2.6 <u>Automatic Billet Inspection Mode</u>

The "AUtomatic" command instructs the DPS that an automatic mode of billet inspection is to be performed. The DPS will respond by generating the same series of messages for data entry as those generated for the "MAnual" command except the "DISPLAY" message of the "Test Results" parameters. After the parameters have been entered, the operator initiates the test by inserting a "RUN" message into the I/O keyboard terminal. The test can be stopped manually by entering a "STop" command through the I/O keyboard terminal or automatically by the test computer program. If either rotation or axial translation are too fast, no test restart can be accomplished and the message "NO RESTART POSSIBLE" will be generated. However, test restart can be obtained if the operator inserts "Restart" through the I/O keyboard terminal in response to a "RESTART IF DESIRED" message and the axial translation is within the limits outlined above for the Manual mode of operation. The billet inspection is automatically terminated when a billet scan is complete.

5.2.2.7 Stop Command

The "STop" command instructs the DPS that the activity it is currently engaged in must be stopped. The "STop" command, as any of the other commands, may be carried out by the operator via the Control C and "STop" command insertion through the I/O keyboard terminal.

5.2.2.8 Zero Command

The "ZEro" command must be used to initialize a new magnetic tape reel or to erase previously stored test files. This command generates two end-of-file, EOF, characters at the beginning of the tape. After this command, the system will accept only an "INitialize" command after the insertion of a Control C. The "END OF TAPE" message, EOT, is generated by the input-output terminal whenever the EOT marker is sensed and the RECORD mode is selected.

5.2.2.9 Power Restart Mode

The power restart subroutine should be used when the power is restored after a power line failure and determines whether a billet inspection may be restarted or must be started all over again from the beginning. If a momentary power failure occurs during a data record transfer from computer core memory to magnetic tape, this record will have to be recorded over. Power failure billet test restart will have to meet the same axial position criteria that operator command billet test restart must meet. No other data are lost due to power line failure.

5.2.2.10 Off-Line Mode

To review an inspection result already on file, or to re-diagnose said record the "OFF-line" command should be used to instruct the DPS. The DPS will then respond by generating a "BILLET NUMBER: " message on the I/O graphic terminal. The operator must insert then the billet number for the inspection results required. Since the files on

magnetic tape will be identified by billet number, this number must be unique for each test. The DPS will search the magnetic tape reel currently placed on the magnetic tape storage unit for the test data file for the requested billet number. If the number cannot be found, the message "NO FILE FOR THIS TEST" will be generated, and the system will await a new command or COntinue message input from the operator. If the file is found, the rest of the "Billet Description" data and "Test Parameters" data will be printed in sequence up to the end of "MINIMUM SIGNIFICANT CELL COUNT" XX when the system will await an action by the operator. This procedure is repeated for all the messages and operator inputs through the end of the "Test Results" data. After the completion of data parameter inputs, the DPS will output "A = " and the operator must insert the axial section in inches of the first billet record to be inspected. Next, the computer will display a "READY FOR RUN" message and waits for the operator's "RUN" message to be inserted through the I/O keyboard terminal. The "RUN" message must also be followed by a CR insertion. Immediately upon receiving the CR, the DPS will enter the off-line test mode and will proceed until either the operator enters a Control C and STop command or the inspection has been completed and terminated.

## 6. JOINT INDUSTRY EVALUATION OF UDIS

Laboratory evaluation demonstrated the superior features of the UDIS. The many technical advantages and the potential economic improvements that the UDIS offers for the inspection of titanium billets was partially demonstrated during a System Field Evaluation. The production plant inspection, however, was limited in both time and quantity of billet inspections performed. Visiting industry representatives also expressed interest in the system.

In order to promote acceptance of the system by industry, more extensive exposure of the UDIS was required. This was also desirable because many of the features of the system were not fully and conclusively demonstrated. Therefore, for the verification of the capabilities of the UDIS it was necessary to extend further the amount of correlation data by comparing the UDIS defect detection and diagnostic capabilities with actual billet defect characteristics. This effort was carried out by the amendment of the contract with a follow-on effort of Phase IV - Joint Evaluation of Ultrasonic Diagnostic Inspection System (UDIS) and Establishment of Improved Inspection Specifications.

The Phase IV effort included participation of the industry. In cooperation with titanium producers, processors and users, the following was undertaken.

1. Extended evaluation of the UDIS.
2. Familiarization of the industry with UDIS capabilities.
3. Identification of requirements for incorporation of UDIS into the industry.

Industry participation included two independent titanium billet user and producer evaluation teams. Accordingly, a TRW/P&WA/TIMET and a TRW/GE/WYMAN-GORDON subcontractor team carried out similar tasks concurrently and independently. The Phase IV effort was carried out in the following tasks: Task 1 - UDIS Modification, Task 2 - Billet Acquisition, Task 3 - Ultrasonic Tests, Task 4 - Metallurgical Tests and Task 5 - Conclusions/Recommendations. The Block Diagram of these efforts are shown in Figure 107. Details of the effort are discussed in the following sections.

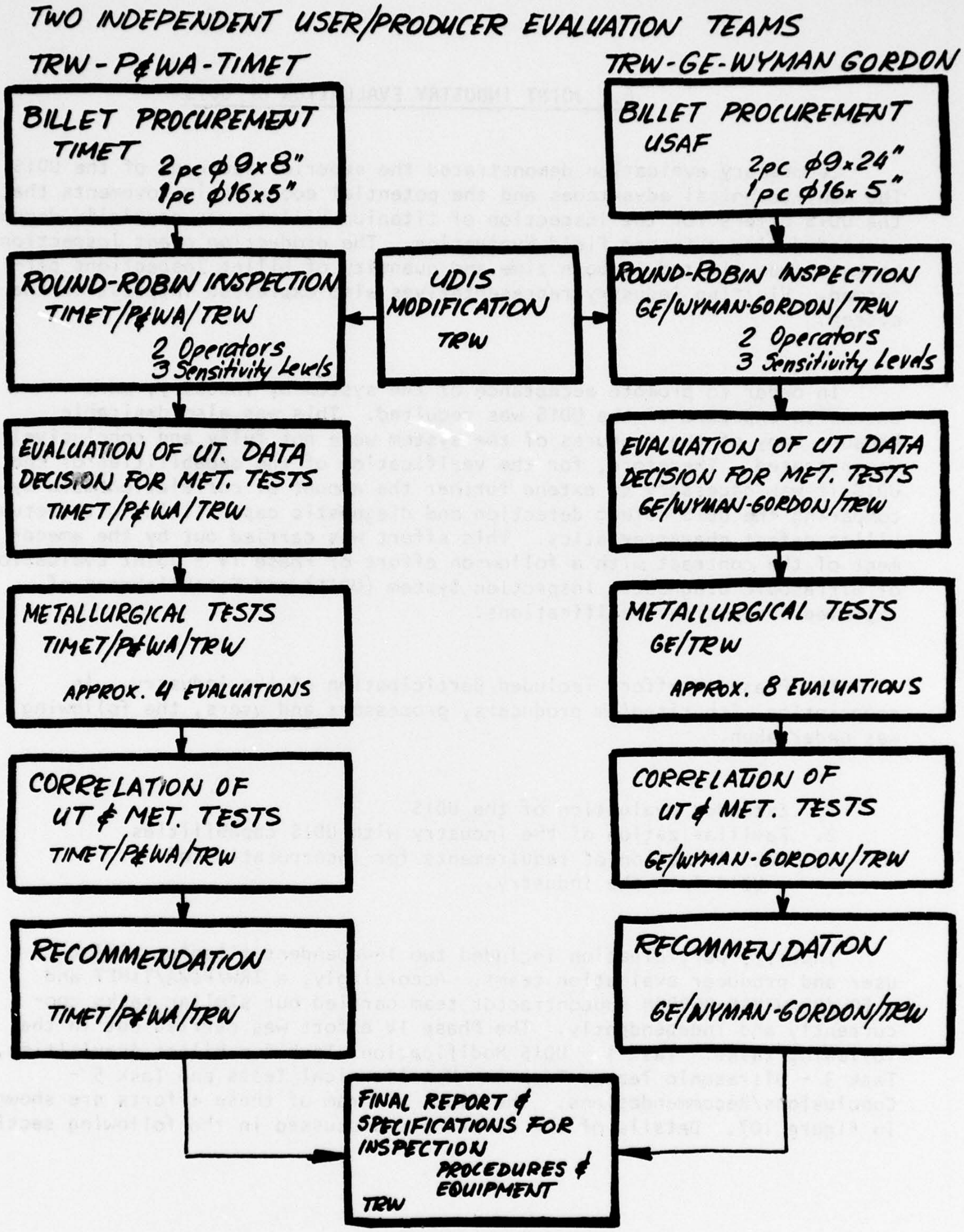


Figure 107. Block Diagram of Phase IV Effort of "Joint Evaluation of UDIS and Establishment of Improved Inspection Specifications.

## 6.1 Task 1, UDIS Modification

The original design of the UDIS instrumentation system was accomplished with special interest for only two billet sizes of 8 and 16-inches diameters; strictly for system performance demonstration in mind. Minor modifications were carried out, therefore, to both UDIS soft- and hardware configurations to expand that range.

The UDIS software modifications covered a computer program expansion to include an inspection capability range for billet rounds from two (2) to sixteen (16) inches in diameter. As a result, four ranges of 16, 8, 4, and 2 inch billet sizes are now being used for display and magnetic tape record format. In addition, billet diameters may be specified in 0.2-inch increments between the range of 2.0 to 16.0 inch billet sizes by the operator during a test initialization. All defect routines were modified to process only the data relevant to the specified billet diameter.

Existing UDIS hardware modifications covered changes to permit the unit cell width to be changed from the previous 0.2-inch width size to an improved 0.1-inch width size for billets of 8-inches in diameter or less. This hardware modification doubled the rate at which the defect data is sampled and analyzed, thereby doubling the resolution of the defect data.

Other hardware modifications included the installation of both angular and axial billet position digital shaft encoders to TRW's Laboratory ultrasonic immersion tank by a gear train, and the fabrication of an appropriate transducer support fixture of search tube for the ADAC transducer of the system.

Modifications were accomplished on the Defect Gate module of the UDIS. A defect indicator light and sound device was added to the unit in order to aid the initial calibration work and/or manual inspection of billets.

One deficiency of the UDIS system realized during the system field evaluation at RMI was the unpractical trailer installed location of the ultrasonic instrumentation. This caused difficulty during standardization of the equipment over a calibration reference block. Therefore, an

improvement was carried out by housing of the ultrasonics and its A-scan indicator oscilloscope display into a common cabinet. This instrumentation package is small enough now to be located at the job-site on the carriage bridge of the ultrasonic immersion tank, while the rest of the UDIS system may remain remotely located from the job site to be stationed in a portable trailer/van or at a permanently installed inspection enclosure.

## 6.2 Task 2, Billet Acquisition

During this phase IV of the program, actual production titanium alloy billet section of 6Al-4V compositions were used for evaluations. The GE/Wyman-Gordon/TRW team used a government owned 9-inch diameter billet that became available from the McDonnel-Douglas/GE-Air Force contract F33615-72-C-1203. The G.E. effort of billet acquisition also covered cutting the billet into two pieces of approximately 24-inch lengths and turning the outside diameter of said billets to a condition acceptable for ultrasonic inspection.

The P&WA/TIMET/TRW team originally planned to use three billets, all of which were to be furnished by TIMET; two of which originally were to be 9-inches and one was to be 14-inches in nominal diameter. TIMET acquired the two 9" size billet samples, which they considered suitable for the evaluation of natural defects. These billets, 8-inch nominal diameter were cut to 8 inches in length. In furnishing the 14-inch nominal diameter size billet, however, subcontractor TIMET was unsuccessful in locating a suitable natural defect indication in said billet size range. The failure to locate a 14-inch size billet having suitable natural defect indications, necessitated a reduction in scope of the planned evaluation. Figure 107 correctly represents this revised effort.

The billet sections acquired by both teams contain natural defects of various types and sizes, and their selection was made on the basis that they might also contain defects below detectable limits of current inspection procedures.

In addition to the billets acquired, an Air Force property 16-inch diameter billet section available from the Phase III, System Field Evaluation effort, was also used for evaluation. This billet was inspected by each member of both user/producer evaluating teams. This was the billet section containing an "indication" equivalent to an approximate 4 to 5 flat bottom hole located by the UDIS and confirmed by RMI after re-inspection.

## 6.3 Task 3, Ultrasonic Tests

Task 3 efforts includedthe ultrasonic evaluation of the billets acquired in Task 2. Each team member inspected the billets acquired within their own team and, in addition, the 16-inch diameter billet was also inspected by all team members. All billet sections were inspected at each participant's location by two of their own inspectors, both independent from the other. The 9-inch nominal size billets were inspected by each of the two inspectors, using three defect detection sensitivity levels of equivalent to numbers 3, 2 and 1.5 FBH reference defects (3/64, 2/64 and 1.5/64-inch artificial flat bottom holes).

In case of the GE/Wyman-Gordon/TRW team, G. E. obtained a set of 9-inch size ultrasonic titanium calibration blocks from TIMET. These blocks contained No. 5 FBH reference defects at material depths of 1 through 4-5/8 inches. Said reference block set was used by all members of this team in order to reduce possible deviations in measurement results. Instrument calibrations for the 16-inch billet was accomplished by all team members of both teams using a TRW furnished 16-inch diameter titanium calibration reference block (TRW No. 111227-1-5 as referenced in Figure 92, on page 141 of this report.) Team members inspected the billets using current G.E. inspection practices outlined in GEP1TF28-XS4 documents.

In the case of the P&WA/TIMET/TRW team, ultrasonic inspections were carried out using P&WA-MCL manual Section E-52 and K197. In an effort to use a single calibration reference block by all the team members of this team, and due to the fact that only the billet producer TIMET had appropriate reference blocks (which was an inconvenience for TIMET to loan out to the other team members at that time) it was recommended by TIMET that the 9-inch size billet sections containing the natural indications also contain the reference holes for calibration purposes. The recommendation was accepted by both P&WA and TRW and TIMET placed side-drilled holes of 0.020-inch diameter by 0.250-inch depth in the end of each billet. The holes were placed at a half metal (billet center) one quarter metal and one-eighth metal depths.

## 6.4 Task 4, Metallurgical Tests

After the completion of the ultrasonic tests a two-day technical meeting was held between the representatives of the Air Force, TRW and its subcontractors Pratt and Whitney Aircraft, General Electric Company, Wyman-Gordon Company and TIMET, at TRW Materials Technology's Laboratory at Cleveland, OH, during 1975 December 1 and 2. The purpose of this meeting was to compare the ultrasonic inspection results obtained by all participating parties. Tables XVI and XVII show the inspection results. In addition, decisions were reached for metallurgical evaluations to be performed in support of NDT evaluations as per Task 4 of the program.

A detailed documentation of the inspection results is beyond the frame of this report. In brief, each participating team member listed recommended ultrasonic indications as candidates for metallurgical evaluations. After comparison of inspection results, the following decisions were made. The TIMET/P&WA/TRW team was to metallurgically evaluate four (4) ultrasonic defect indications. Accordingly, TIMET evaluated two indications of A = 4.6-6.1", θ = 216-280°, R = 1.4-1.6" and A = 7.625", θ = 0-14.4°, R = 3.0-3.4", both in billet No. N7103T2; and P&WA evaluated two indications of A = 5.5-7", θ = 50-70°, R = 2" and A = 4.0", θ = 250°, R = 4-0.6", both in billet No. N6179T4. TIMET representative took the billet with him after the meeting for their cutting, machining and metallurgical evaluations. TRW shipped the other billet to Wyman-Gordon Company for cutting. The billet sections then were forwarded to P&WA for their metallurgical evaluation.

The Wyman-Gordon/GE/TRW team was to metallurgically evaluate eight (8) ultrasonic defect indications. Accordingly, GE evaluated their indication of LBE 122 (A = 17.6", θ = 304°, R = 1.5"). Wyman-Gordon's indication of CC (A = 16.5", θ = 110°, R = 2.3") and TRW's indication of 7 (A = 15.475", θ = 255-259°, R = 2.0-2.2"). In addition, the second 9-inch billet (Serial No. 1-2C-2) was reinspected by both TRW and GE with increased sensitivity to locate the fourth ultrasonic indication for GE's metallurgical evaluation.

TABLE XVI

List of Ultrasonic Indications Recommended and Those Which Were Accepted for Metallurgical Evaluations by the GE/Wyman-Gordon/TRW Team

| TEAM MEMBER | BILLET DESIGNATION | | | | | | | | | | | |
|---|---|---|---|---|---|---|---|---|---|---|---|---|
| | 1-2C-1 | | | | 1-2C-2 | | | | RMI-79310B-276 | | | |
| | DEFECT DES. | DEFECT LOCATION | | | DEFECT DES. | DEFECT LOCATION | | | DEFECT DES. | DEFECT LOCATION | | |
| | | A (IN) | θ (°) | R (IN) | | A (IN) | θ (°) | R (IN) | | A (IN) | θ (°) | R (IN) |
| GENERAL ELECTRIC | LBE109 | 14.7 | 98 | 0.3 | LBG15 | 42 | 247 | 1.3 | LY6 ▲ | 55.5 | 178 | 1.8 |
| | LBE102 | 15.4 | 27 | 1.4 | LBG22 | 42 | 220 | 0.3 | LY5 ▲ | 55.45 | 358 | 2.0 |
| | LBE121 | 16.6 | 297 | 1.3 | | | | | | | | |
| | LBE122 ⊗ | 17.6 | 304 | 1.5 | | | | | | | | |
| WYMAN GORDON | BB | 14-15 1/8 | 95 | 3.3 | P | 42.17 | 260 | 1.55 | A ▲ | 52.5 | 85 | 1.0 |
| | U | 11.5 | 170 | 2.3 | N | 43.55 | 220 | 1.3 | A1 | 54.5 | 90 | 5.5 |
| | X | 12 7/8 | 355 | 0.3 | | | | | | | | |
| | CC ⊗ | 16.5 | 110 | 2.3 | | | | | | | | |
| TRW | 7 ⊗ | | | 2.0-2.2 | 3 | 42.17 | 72-82 | 1.0-1.2 | 12 ▲ | 63.5 | 180-270 | 1.5-2.5 |
| | 9 | | | 1.6-1.8 | 11 | 41.17 | 36-39 | 1.2-1.4 | 30 | 55.75 | 4-11 | 1.6-0.2 |
| | | | | | | | | | | | | |

Notes: ⊗ Ultrasonic indications accepted for metallurgical evaluations. Work to be performed by GE.

▲ Ultrasonic indications accepted for metallurgical evaluations. Work to be performed by TRW.

TABLE XVII

List of Ultrasonic Indications Recommended and Those Which Were Accepted for Metallurgical Evaluations by the TIMET/P&WA/TRW Team

| TEAM MEMBER | BILLET DESIGNATION | | | | | | | | | | | |
|---|---|---|---|---|---|---|---|---|---|---|---|---|
| | N7103T2 | | | | N6179T4 | | | | RMI-79310B-276 | | | |
| | DEFECT DES. | DEFECT LOCATION A (IN) | θ (°) | R (IN) | DEFECT DES. | DEFECT LOCATION A (IN) | θ (°) | R (IN) | DEFECT DES. | DEFECT LOCATION A (IN) | θ (°) | R (IN) |
| TIMET | ⊕ | 4.6-6.1 | 14-37 | 1.5 | | 4 1/8 | 240 | 0.5 | No discontinuity noise spike (50% #8) 0.5"R Ave. noise 25% #8 at center of radius. | | | |
| P&WA | | 0-0.75 | 150-170 | 2.0-2.5 | ⊙ | 1.87-3.37 | 270 | 2 | | 55.5 | 90 | 3.2 |
| | | 0-1 | 210-240 | 3 | | 5.63-7.0 | 104 | 2 | | 55.5 | 95 | 0.5 |
| | | 0-1 | 250-270 | 3.2 | | 6.37-7.37 | 15-20 | 1.5 | | 52.75 | 155 | 3.0 |
| | | 0-1.5 | 290-310 | 3 | | | | | | | | |
| | | 2-3.5 | 255-300 | 3.2 | | | | | | | | |
| | | 7-8 | 290-310 | 2 | | | | | | | | |
| TRW | 61 ⊕ | 7.625 | 0-14.4 | 3.0-3.4 | 32 ⊙ | 4.0 | 260 | 0.4-0.6 | See Table I. | | | |
| | 37 | 4.6 | 216-280 | 1.4-1.6 | 22 | 2.75 | 290 | 2.6-2.8 | | | | |
| | | | | | 47 | 5.875 | 300 | 2.2-2.4 | | | | |

Notes: ⊕ Ultrasonic indications accepted for metallurgical evaluations. Work to be performed by TIMET.

⊙ Ultrasonic indications accepted for metallurgical evaluations. Work to be performed by P&WA.

The 16-inch billet was also evaluated by TRW for GE indications LY6 (A = 55.6", θ = 178°, R = 1.8") and LY5 (A = 55.45, θ = 358°, R = 2.0"), Wyman-Gordon indication A (A = 52.5", θ = 85°, R = 1.0") and TRW indication 14 (A = 53.5", θ = 180-270°, R = 1.6"). In this case, TRW performed all billet cutting, sectioning and metallurgical evaluations. TRW also cut out rectangular-shaped specimens, containing the defect indications, and forwarded them to GE for mechanical testing. TRW then received these specimens back from GE for TRW in-house metallurgical evaluations. Wyman-Gordon did not participate, in accordance with the program schedule, in the metallurgical evaluations other than as a consultant.

The results of Task 4, Metallurgical Tests, were presented by the participants in a technical meeting that was held at the Air Force Materials Laboratory, Wright-Patterson AFB, Ohio, on 1976 May 11. Each participating team member made a presentation on their efforts of metallurgical/metallographic evaluations.

Subcontractor Pratt & Whitney Aircraft reported their effort of metallurgical evaluation of two indications ultrasonically detected in the S/N N6179T4 titanium billet. The first indication, with TRW's UDIS defect designation No. 32 and the second was TRW's No. 22.

Evaluation of defect 32 determined that the ultrasonic response was due to linear porosity approximately 1/4" long and ranging from 2 to 12-mils in width. The defect was originally located in the billet in the axial direction, 0.4" from the billet's center. A cross-section that was macroetched with Knoll's Reagent (12% $HNO_3$ - 5% HF - Balance $H_2O$) chemical solution, Figure 108, shows this porosity and the surrounding large alpha grain structure. Grain structure and orientation was determined by re-etching the specimen with Margolin-Ence (29% $H_2O$ - 8% Lactic Acid - 4% $H_3PO_4$ - 4% Oxalic Acid - 4% Citric Acid - Balance Grain Alcohol) electrolytic solution. Prior to the electrolytic etch, examination of the porosity surface with a Joel JXA 50A Electron Probe Microanalyzer with a Kevex-ray energy spectro analyzer revealed that a portion of the defect is contaminated with sodium. Figure 109 is a microphotograph taken with the electron probe of the void containing the contamination. Successful detection of this defect was achieved by the diagnostic capability of the UDIS, using the quality control reject criteria of significant cell count, SCC = 12, and dimensional coordination settings of adjacent cells R = θ = A = 1.

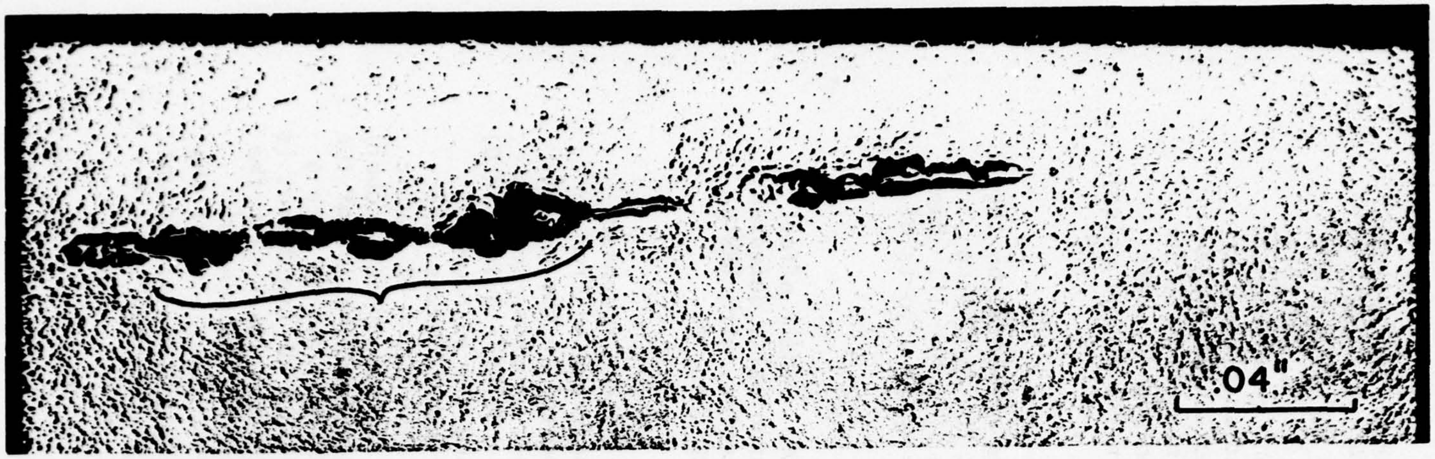


(a)

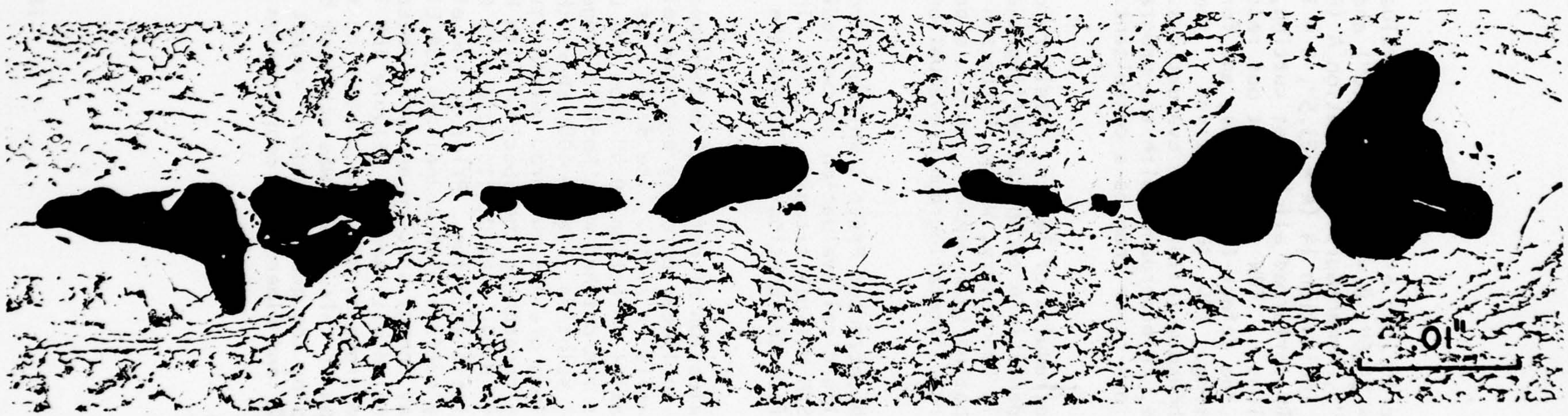


(b)

Figure 108. Discontinuity with TRW defect designation 32. Ultrasonic response was equal to 75% of the 0.020" diameter Side Drilled Hole. (a) Porosity located in the axial direction 0.4" from the center of the billet. (b) Enlargement of the bracket area in a.

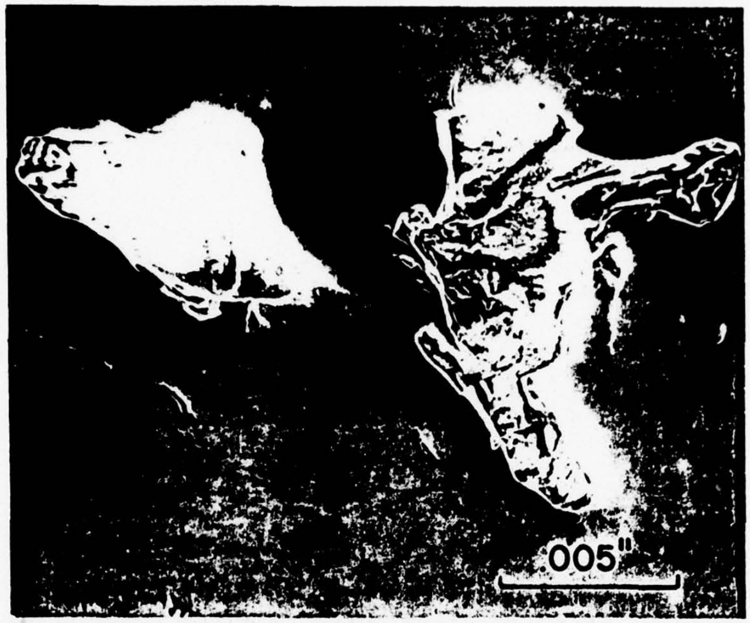


Figure 109. Photomicrograph taken with the electron probe of the right side of Figure 108b. A sodium contaminate was detected on the surface of the void to the right of the picture.

According to P&WA, this TRW defect designation No. 32 was the only indication that was not detected by the P&WA inspection team. Attached Figure 110 is a reproduction of P&WA C-Scan recording.

The P&WA evaluation of the second indication, of TRW's UDIS defect designation No. 22, determined that the ultrasonic response was due to the equiaxed Alpha phase with intergranular Beta type structure as shown in Figure 111. No other additional discontinuities could be found by P&WA by further examination.

Subcontractor TIMET also completed their effort of metallurgical tests. TIMET evaluations resulted in no success in finding "anything detrimental." TIMET indicated great care in machining to expose the discontinuity, that they were confident was in the billet, to no avail. Similarly, TIMET had no success finding anything in their effort exposing the TRW's UDIS ultrasonic indication.

Subcontractor General Electric Company reported their effort in evaluating three ultrasonic indications of GE designated No. LBE 122, Wyman-Gordon designated No. CC, and TRW designated No. 7. In addition, GE performed a low cycle fatigue test on all of the specimens which contained the referenced ultrasonic indications. The fatigue specimen having GE's No. LBE 122 ultrasonic indication failed at a 80 ksi test load at 9134 test cycles. The fatigue specimen having "Wyman-Gordon's No. CC ultrasonic indication failed at a 147 ksi test load at 10 cycles (after about 40,000 cycles at 90 to 130 ksi test loads). GE considered that this specimen had failed at the ultimate strength of the material. The fatigue specimen having TRW's No. 7 ultrasonic indication failed 100 ksi test load at 3149 test cycles and, according to GE, a probable unbond at the origin of the fatigue caused the failure.

No metallography was performed by GE on the Wyman-Gordon defect No. CC, because there were no apparent defects on the surface. Fractographic results for GE defect No. LBE122 are shown in Figures 112 and 113. The fracture surface and a void in the surface is shown in Figure 112 and a quasi-cleavage and beginnings of fatigue in Figure 113. The fracture surface for TRW defect No. 7 and probable unbond at the origin of fatigue is shown in Figure 114.

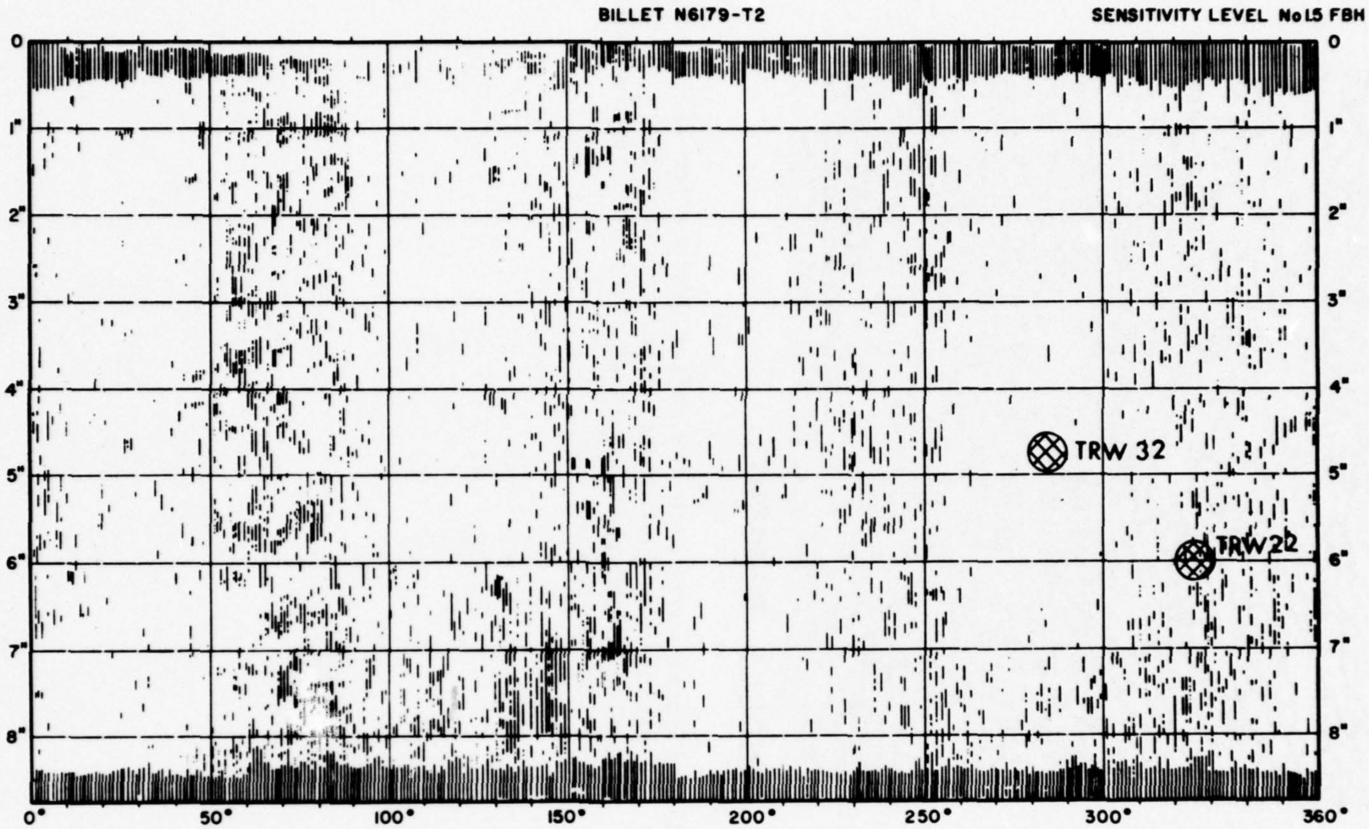


Figure 110. C-Scan of the 8" diameter billet section sonic inspected at a sensitivity level equal to the No. 2 FBH from the step block 3A minus 6 db of attenuation or No. 1.5 FBH. All indications above 'noise' are shown. Cross-hatched circles represent indications cut from the billet and metallurgically examined.

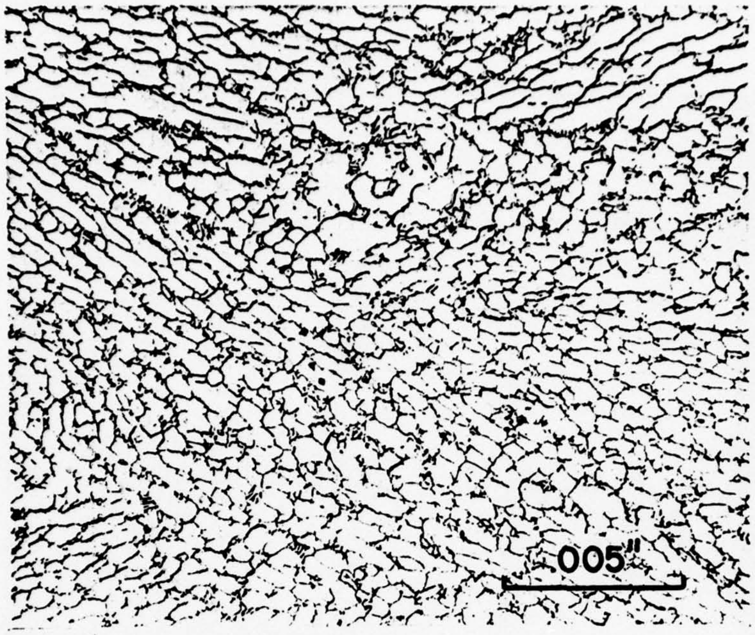


KNOLLS REAGENT

Figure 111. Discontinuity with TRW defect designation 22. Ultrasonic response was just above noise. Photograph is of the typical Alpha phase equiaxed with intergranular Beta structure found.

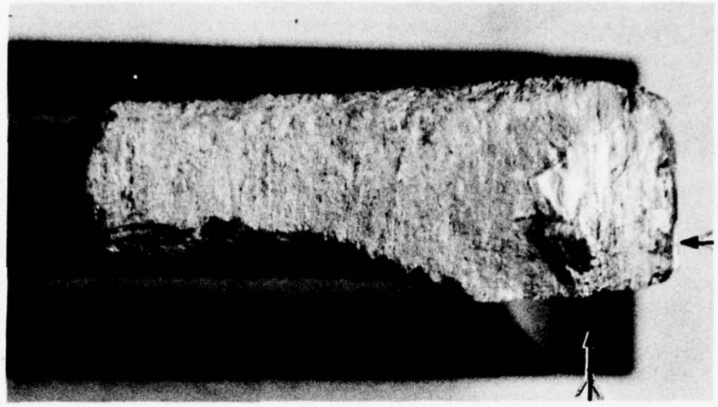

Figure 112. Fracture surface and void - Defect No. LBE122.

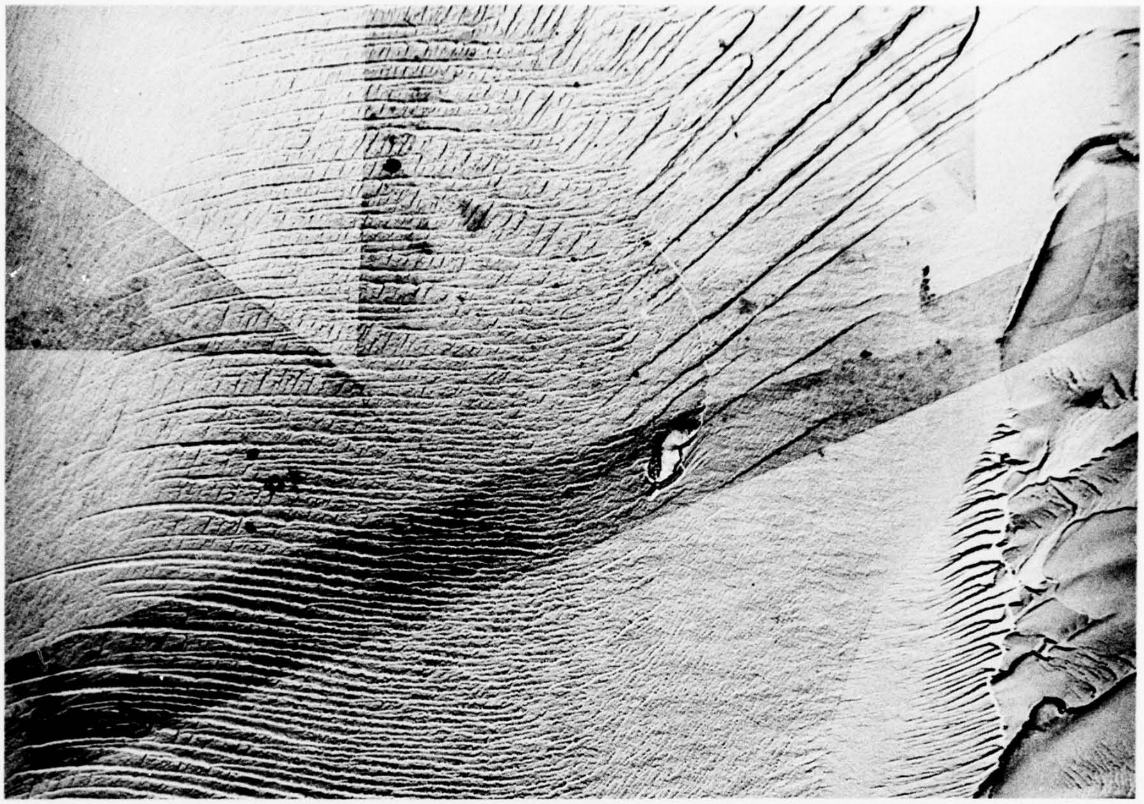

Figure 113. Quasi-cleavage within inclusion specimen.

Figure 114. Fracture surface and unbond in TRW defect No. 7.

TRW's participation covered activities of both industry teams. In the matter of the GE/Wyman-Gordon/TRW team activities, the TRW recommended defects for metallurgical evaluations are listed in Table XVI; for defects No. GE/LBE122, WG/CC, TRW/7 (for the 1-2C-1 billet) and TRW/32 (for the 1-2C-2 billet). Metallurgical evaluations of these indications were carried out by GE and have already been discussed.

For the 16-inch size billet, which was inspected by all team members, the TRW evaluated ultrasonic indications were the GE No. LY5 and LY6; the Wyman-Gordon No. A and TRW's No. 12. The test specimens were fabricated in such a way that low cycle fatigue tests were performed on all, except GE's No. LY6, by General Electric Co., while all metallographic and metallurgic efforts were carried out by TRW. The fatigue tests showed specimen failures at 118,000 and 39,000 test cycles for a test load of 80 ksi for the Wyman-Gordon ultrasonic indication No. A and TRW's No. 12, respectively, while an early failure occurred at 18,000 cycles only, at an 80 ksi test load, for GE's No. LY5 specimen. TRW's evaluations revealed no apparent defects on the fracture surfaces ofthe specimens. Since the ultrasonic indications were at the center of the gage points but the specimens failed at an offset location, TRW performed careful machining of the specimens toward their gage point centers hoping to find evidence for the ultrasonic indications. The defects that were found could not have been detrimental to material performance (the fatigue tests already showed this), nor were they large enough in size to be detected by ultrasonics. The fourth ultrasonic indication of GE's designation No. LY6 specimen was at such a confined billet location that no fatigue specimen could be prepared. Accordingly, only metallography was performed, again, however, with no apparent result.

Special attention must be drawn to TRW defect designation No. 12 found in the 16-inch billet, in view of the UDIS diagnosed data. Figures 115 through 117 show billet cross-sections for both "defect count" and "defect coordinate" displays. These data are for billet slice axial locations of A = 1.5, 1.75 and 2.0-inches, respectively. Corresponding "defect coordination" line printer report is also shown in Figure 118. This operator programmable decision-making capability of the UDIS for pattern recognition clearly identified an unmistakable crack-like cluster of "defective" unit cells. The fatigue test of the specimen containing this #12 defect, however, failed to indicate any abnormality and, as stated earlier, no apparent defect was found on the fractured surfaces either, yielding an inconclusive situation.

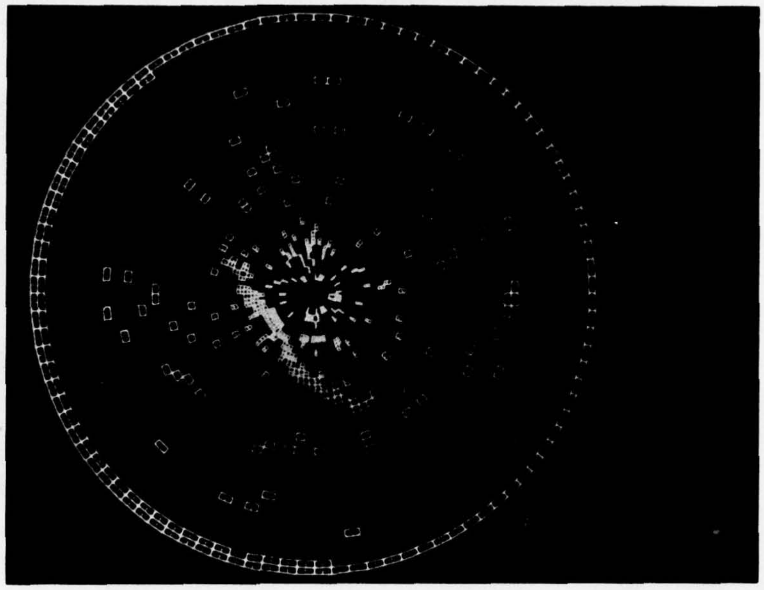

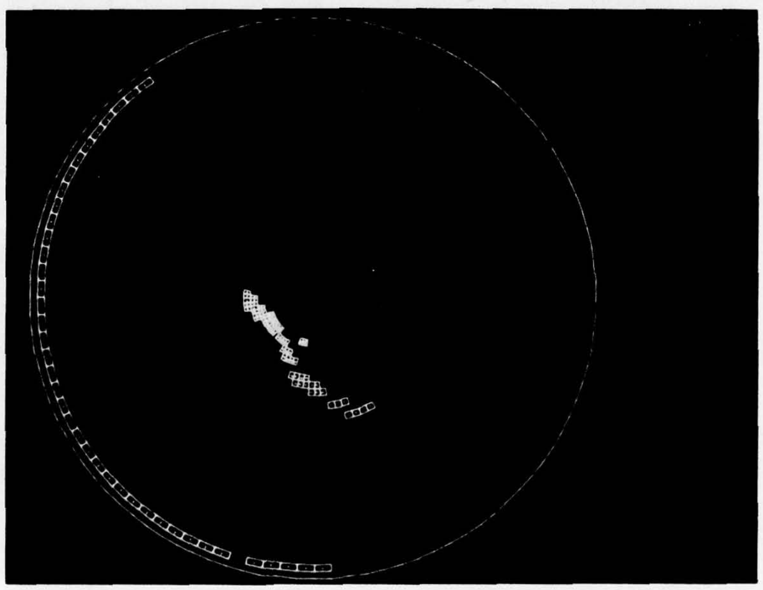

Figure 115. Defect Count (A) and Defect Coordinate (B) Displays for the 16-inch RMI Billet No. 79310B at an A = 1.5-inch Cross-section location. (The UDIS decision-making diagnostic criteria was: SCC = 1, A = R - 1, θ = 3).

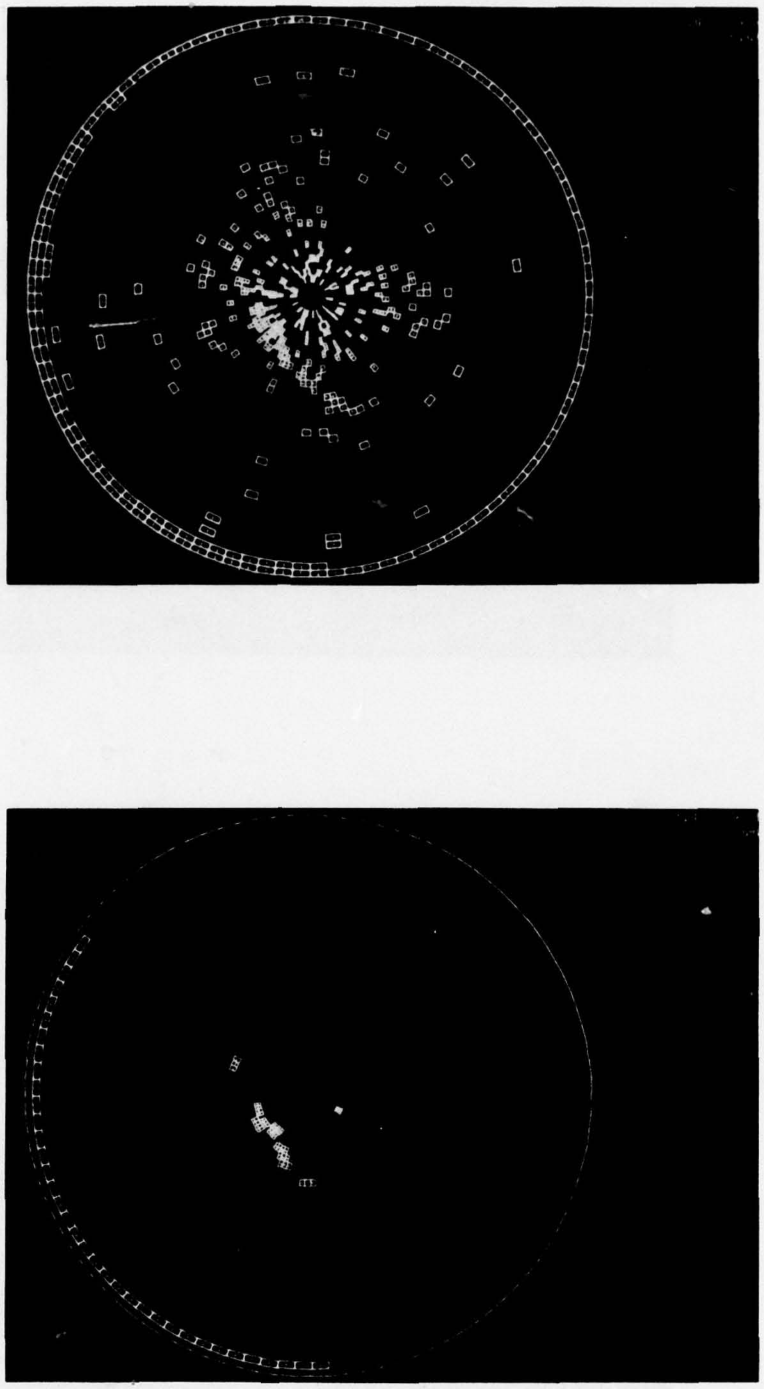

Figure 116. Defect Count (A) and Defect Coordinate (B) displays for the 16-inch RMI Billet No. 79310B, at an A = 1.75-inch cross-section location. (The UDIS decision-making diagnostic criteria was: SCC = 1, A = R = 1, θ = 2).

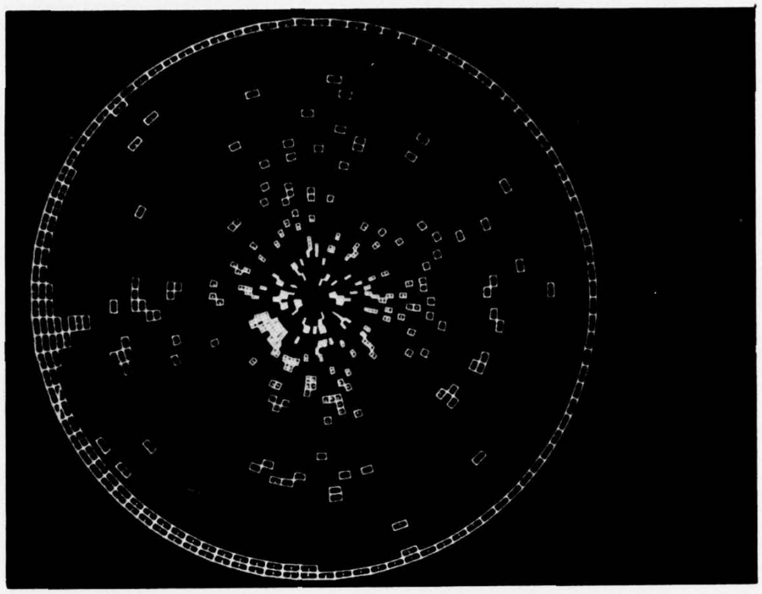

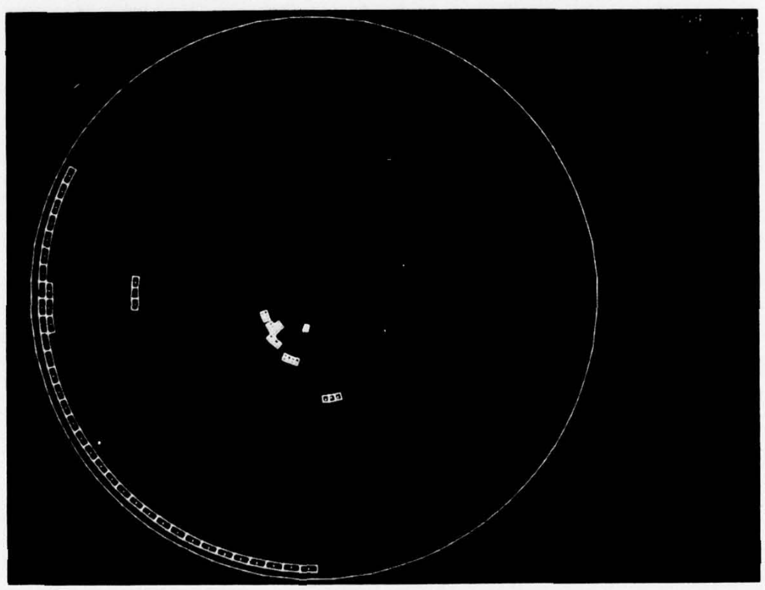

Figure 117. Defect Count (A) and Defect Coordinate (B) displays for the 16-inch RMI Billet No. 79310B, at an A = 2.0-inch cross-section location. (The UDIS decision-making diagnostic criteria was: SCC = 1, A = R = 1, θ = 3).

ALLOY 6AL-4V HEAT NO. 890309 BILLET NO. RMI-79310B-276-N

DIAMETER: 16.0 INCHES LENGTH: 004.0 INCHES LENGTH INCREMENT: 0.125 CELL SIZE: 0.2

OPERATOR J.T. INSPECTION DATE: 26-NOV-75

DEFECT CRITERIA. COUNT = 01, R = 1, T = 3, A = 1 REPORT DATE: 25-NOV-75

| CROSS- | DEFECT STARTS AT | | DEFECT ENDS AT | |
|---|---|---|---|---|
| SECTION | THETA | RADIUS | THETA | RADIUS |
| (INCH/8) | (DEG) | (INCH) | (DEG) | (INCH) |
| 12. | 172.8 | 2.0 | 190.8 | 1.8 |
| 12. | 176.4 | 2.0 | 190.8 | 1.6 |
| 12. | 176.4 | 1.8 | 201.6 | 1.6 |
| 12 | 187.2 | 1.8 | 201.6 | 1.4 |
| 12. | 187.2 | 1.6 | 223.2 | 1.4 |
| 12. | 198.0 | 1.6 | 223.2 | 1.2 |
| 12. | 198.0 | 1.4 | 226.8 | 1.2 |
| 12. | 226.8 | 1.6 | 241.2 | 1.4 |
| 12. | 237.6 | 1.8 | 248.4 | 1.6 |
| 12. | 126.0 | 7.8 | 252.0 | 7.6 |

Figure 118. Defect Coordination Report for the 16-inch RMI Billet No. 79310B revealing defect No. 12.

In the case of P&WA/TIMET/TRW team activities, the TRW recommended defects for metallurgical evaluations are listed in Table XVII. While there was no apparent success by TIMET to locate the two defect indications selected in Table XVII, P&WA successfully discovered TRW defect No. 32 (discussed earlier). The defect No. 32 was identified by the UDIS as shown in the defect coordinate display in Figure 119 and in the corresponding defect coordination line printer report in Figure 120.

## 6.5 Task 5, Conclusions/Recommendations

The participants of the TRW subcontractor teams concluded that the limited number of both mechanical testing as well as metallographic/metallurgic evaluations did not provide a conclusive support of evidence to verify the ultrasonic indications observed. The discrete success of P&WA's effort in disclosing a very small sodium contaminated linear porosity for TRW ultrasonic defect indication No. 32 (which defect was only detected by the UDIS) may not be considered strong evidence to support the sensitivity, the automatic distance-amplitude compensation (ADAC) and the diagnostic pattern recognition features of the program developed UDIS. A much larger effort of inspection and billet sectioning would be required to provide a statistically valid conclusion. Many other features of the UDIS system, specifically, its computer aided inspection concept, however, were readily recognized. The UDIS was appraised as the first computer compatible ultrasonics, pioneered by the Air Force and TRW, which is to be followed for many applications other than billet application. Further refinements in pattern recognition concepts may be required to dependably discriminate between very small defects and microstructural anomalies such as encountered in this program.

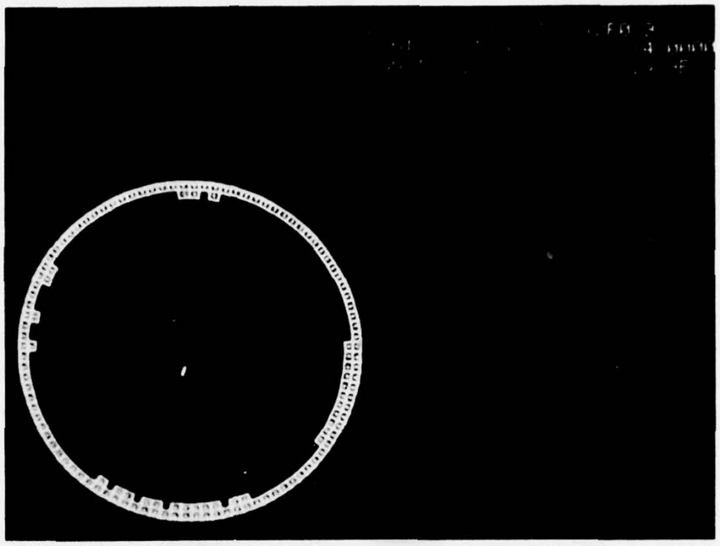

Figure 119. Defect Coordinate Display for the TIMET Billet No. N6179T4, Revealing Defect No. 32.

ALLOY: 6Al -4V HEAT NO. N6179T4 BILLET NO. TIMET2FO. 9

DIAMETER: 08. 4 INCHES LENGTH: 009. 0 INCHES LENGTH INCREMENT: 0. 125 CELL SIZE: 0. 2

OPERATOR: CWF INSPECTION DATE: 24-NOV-75

DEFECT CRITERIA: COUNT = 12, R = 1, T = 1, A = 1 REPORT DATE: 24-NOV-75

| CROSS- | DEFECT STARTS AT | | DEFECT ENDS AT | |
|---|---|---|---|---|
| SECTION | THETA | RADIUS | THETA | RADIUS |
| (INCH/8) | (DEG) | (INCH) | (DEG) | (INCH) |
| 32. | 248. 4 | 0. 6 | 252. 0 | 0. 4 |

Figure 120. Defect Coordination Report for TIMET Billet No. N6179T4, Revealing Defect No. 32.

## 7. CONCLUSION

Current practice used for ultrasonic inspection of titanium alloy forging billets for internal defects in the producer's shop uses standard, general-purpose instruments following procedure specifications which are a compromise of customer quality requirements, material, instrument and operator limitations, and cost. Today's procurement practices, therefore, are a result of negotiating mutually tolerable terms within the boundaries posed by the billet producer and user. Trends in the aerospace industry toward use of large-diameter billets as well as for increased requirements to guarantee serviceability and reliability in the delivered product have strained the capability for reliable and routine detection of small billet defects. For this reason, the Air Force Materials Laboratory funded this program conducted by TRW to reduce the scatter and uncertainty of ultrasonic inspection results due to equipment and operator variabilities; to achieve a higher sensitivity of defect detection and to establish a preliminary inspection equipment and procedures specifications.

During the course of the development program, an automatic, computer-controlled Ultrasonic Diagnostic Inspection System (UDIS) was designed and constructed incorporating the features described in the program objectives. The performance characteristics of the system were defined by laboratory operations and the feasibility of its application to mill inspection of 10-foot length billets was demonstrated by limited in-plant trials. While considerably more billet inspections are recommended to establish final specifications for a commercial version of the system, the equipment in its present form has demonstrated the following potential:

1. Fully automatic ultrasonic inspection of titanium alloy forging billets to be operated on the billet producer's production line floor.

2. Reduced human operator variability.

3. Reduced equipment variability.

4. Reduced material properties variability.

5. Increased inspection sensitivity.

6. Increased defect detection resolution.

7. Automatic defect diagnosis in real-time and/or retrieved modes.

8. Automatic decision making for accept/reject in real-time and/or retrieved modes.

9. Permanent data storate. (Offset possible product liability.)

10. Data retrieval for review, diagnosis and decision making.

11. Standardized hardware utilizing AEC/NBS standards.

12. Reduced inspection cost.

The above-listed performance features were achieved during the course of the program by discarding the available but inadequate commercial instruments and using an original design for the ultrasonic circuitry, interfacing of this ultrasonics with a minicomputer, and the development of a data display system which shows the billet in multiple cross-section slices together with all the detected indications and/or only those which meet or exceed a selected quality control reject criteria.

High-voltage, short-duration, fast-rise time pulses are provided to permit improved resolution of defects and their near-surface detection. A special pie-cut shaped acoustic illumination and echo detection method was developed and implemented. This scheme further improves inspection sensitivity, lateral resolution, and the signal-to-noise ratio. While significant advances were made for the utilization of optimum transducer performance (via specifying required characteristics), procurement of such a device had to be based on the "best effort" of the transducer industry. High sensitivity of signal detection was designed into the receiver together with broad bandwidth capabilities for a very low distortion, high fidelity signal processing. Receiver gain may be controlled manually or by an automatic distance-amplitude compensator, ADAC, to correct the attenuation characteristics of the actual billet cross-section under inspection. A statistical signal-to-noise ratio enhancement was achieved by requiring a number of pulse-echo signal returns from a single defect to be recognized by the computer system before a reject decision is made. As a result of integrating these various elements into an inspection system, a significant advance in the inspection capability of large diameter titanium billets has been achieved.

In spite of the limited number of billets inspected, some material-related conclusions may also be made. First, it appears that existing billet chemistry is far more uniform than to cause any effect on ultrasonic inspectability of the billets (in the form of acoustic scatter or "noise"). Second, the enormous grain size variations (1000:1) observed in the larger size billets is the main cause of inspectability problems, especially those grains which are much larger than the wavelength of the interrogating acoustic beam. Third, the special manufacturing technique applied to produce Phase II "quiet" billets of this program did not seem to be effective.

Many industry representatives, in addition to those participating members of this program, have visited TRW and seen the UDIS demonstrated. Representatives of one billet producer recognized the record keeping capability as the most significant feature of the UDIS. They visualized this UDIS capability as a real asset to the billet producing industry to offset otherwise possible product liability.

During the joint industry (billet producer/user) evaluation effort TRW aggressively pursued all of the subcontractor participants to provide information for a "Joint Recommendation" (a Work Statement obligation) on the appropriate course of action for the incorporation of the improved technology into the quality control system for the titanium alloy billets produced for engine makers. In summary of TRW's survey, the following conclusions may be reached.

Billet producers failed to recognize the advantages of the UDIS, or even the concept of a computer-aided inspection. It is their belief that existing conventional methods and practices are adequate and fulfill the needs. Implementation of an advanced system is not expected for the forseeable future.

Billet forger sees a minimal impact by the UDIS on the billet producers of the titanium industry. The relative low cost of sonic inspection of billets versus other billet costs prevents the justification of the necessary capital expenditures for the UDIS. It was recognized, however, that the system has the capability to speed up actual testing time of any programmable shape that would be consistent. On this basis, the UDIS is a good possibility and could impact billet forgers. Implementation of the UDIS in a forging house was seen as a possibility in the next two years. The billet forger also appreciated the capability of the UDIS for defect count display permanent records. This record was seen as an invaluable evidence of inspection if and when required.

Billet users expressed, for years, concern for an improved billet inspection. It is recognized by them that current systems miss occasional flaws which cause rejection later in the processing cycle and financial losses are significantly higher in cost. It was a general opinion that the UDIS offers the potential for improved reliability in titanium billet inspections due to the automation. It was not clearly seen, however, that the initial expense of a UDIS installation would provide billet inspection cost savings. Furthermore, it is believed that this program would have the greatest impact on billet manufacturers producing material for the airframe manufacturer. It was felt that the complicated shapes of airframe makes inspection of the finished product costly and difficult if not impossible in some cases. Therefore, any improvement in billet inspection can result in improved product reliability.

Accordingly, no immediate changes are expected in billet inspection specification requirements. Any benefits of UDIS implementation is greatly dependent on possible cost reductions in the finished product, since the present reject rate on production disk forgings is small.

A great impact of this program to the engine makers was felt by them for the application of computerized ultrasonic inspection systems for forgings which are forged near the final shape. One billet user also "recognized the results of this program as one of the major contributions to the technology. The ultrasonic instrument and the integration of the instrument with computerization and automatic billet drive are pioneers in the industry. The detailed published reports will be reference documents for those in the field for many years."

## 8. RECOMMENDATIONS

Laboratory evaluation demonstrated the potential advantages of the UDIS. The many technical improvements and the potential savings that the UDIS offers for the inspection of titanium billets was demonstrated during the System Field Evaluation. The joint industry evaluation effort provided further evidence of the value of the computer-aided ultrasonic evaluation. This program established a basis for the current efforts toward computerized ultrasonic inspection of billets forged to near-net shapes. It is evident that the automated ultrasonic inspection of simple geometric shapes, such as billets, will depend on economic success yet to be demonstrated to the billet producers. This effort, TRW believes, is to be the first step. Other recommendations are as follows:

In view of the high inspection speed capability of the UDIS, existing industry facilities for billet handling are inadequate. Centerless, out-of-round, as well as longitudinally bent billets cannot be rotated by the usual supporting rollers either accurately or safely. Existing methods can only rely on operators' "crayon" mark of defects on billets. This is a human variability dependent inspection process and has no permanent record of inspection. It is recommended, therefore, that in case of future production installations of the UDIS, the inspection should be carried out in such a way that the cylindrical shape billet is to be supported between points and be rotated by a driver ("dog"). This approach provides positive maintenance of billet reference axial and angular locations, thus, accurate defect location determination using the billet coordinates can be carried out even at high inspection scan rate. Transducer performance is also identified as a generally weak link in a high performance UNDE system, requiring further developments.

Field inspection trials of the UDIS showed sensitivity of the magnetic recording tape and the tape control vacuum mechanism of the UDIS for airborne dust. Therefore, it is also recommended that future permanent installations of the UDIS should utilize an environmentally controlled inspection booth for the entire UDIS instrumentation. The only exception should be the ultrasonic subsystem, which is to be in a self-contained sealed cabinet, mounted onto the carriage of the billet handling water tank. This installation scheme will provide easy setup of ultrasonics and transducers as well as environmental protection for the sensitive mechanism of the tape recorder peripheral and other computer assemblies.

The real benefit of the UDIS, however, is visualized beyond the simple geometry shape of billets, for more complex shapes, such as both aircraft structural and engine components. The contractors recommendation, therefore, is to implement the program's developed soft-and-hardwares, along the concept of the emerging computer-aided design and manufacturing (CAD/CAM) to a computer aided evaluation, CAE, of complex shape aircraft components.

An advanced UDIS system installed in a suitably self-contained highway portable van could be used for in-plant demonstrations for more rapid implementation. It could be used as a first of its kind comparative standard or "referee" for existing permanent inspection systems.

## REFERENCES


1. I. M. Matay and F. J. Sattler, "Advanced Nondestructive Testing Techniques for Titanium Billets and Ingots," AFML-TR-70-118, August 1970.

2. ADAC, an acronym, meaning Automatic Distance-Amplitude Compensation. U. S. Patent No. 3,690,153, dated 12 September 1972.

3. IEEE Standards No. E145/E194/42A65-0.

4. Recall the classic definition of a "kludge." "An ill-assorted collection of poorly matching parts, forming a distressing whole," Jackson W. Granholm, Datamation, February 1962, p. 30.

5. Standard Nuclear Instrument Modules, TID-20893 (Rev. 3), United States Atomic Energy Commission, Washington, D.C. prepared by Louis Costrell, United States National Bureau of Standards. For sale by the Superintendent of Documents, U. S. Government Printing Office, Washington, D.C. 20402, 1970, 0-373-142.

6. CAMAC, A Modular Instrumentation System for Data Handling, TID-25875, USAEC, Washington, D.C. 20545.

7. CAMAC, Organization of Multi-Crate System, TID-25875, USAEC, Washington, D.C. 20545.

8. Supplementary Information on CAMAC Instrumentation System, TID-25877, USAEC, Washington, D. C. 20545.

## REFERENCES (Cont'd)

9. CAMAC, Serial System Organization, TID-26488, USAEC, Washington, D.C. 20545.

10. "Theory of Sound," Lord Rayleigh, London, England, 1894.

# APPENDIX A

## REVISED SYSTEM SPECIFICATION

The following parameters, as illustrated in Figure 121, have been selected or calculated to establish the revised system specifications, using the metric system of measurements. The following values are the final selections which were drawn up as modifications to the preliminary system specifications dated October 1971.

1. Titanium Billet Dimensions

1.1 Billet Diameter Range

$Ti_{D_{min}} = 20.32 \times 10^{-2}$ m (8 inch)

$Ti_{D_{max}} = 40.64 \times 10^{-2}$ m (16 inch)

1.2 Billet Length Range

$Ti_{L_{min}} = 2.54 \times 10^{-2}$ m (1 inch)

$Ti_{L_{max}} = 3.048$ m (10 feet)

2. Acoustic Velocity Range in Titanium Billet

Calculations were not made due to lack of elastic property data; thus, measurement data of Reference 1 was utilized:

$V_{L_{min}} = 6{,}087.45$ m/s

$V_{L_{avg}} = 6{,}226.26$ m/s

$V_{L_{max}} = 6{,}325.36$ m/s

6121 C

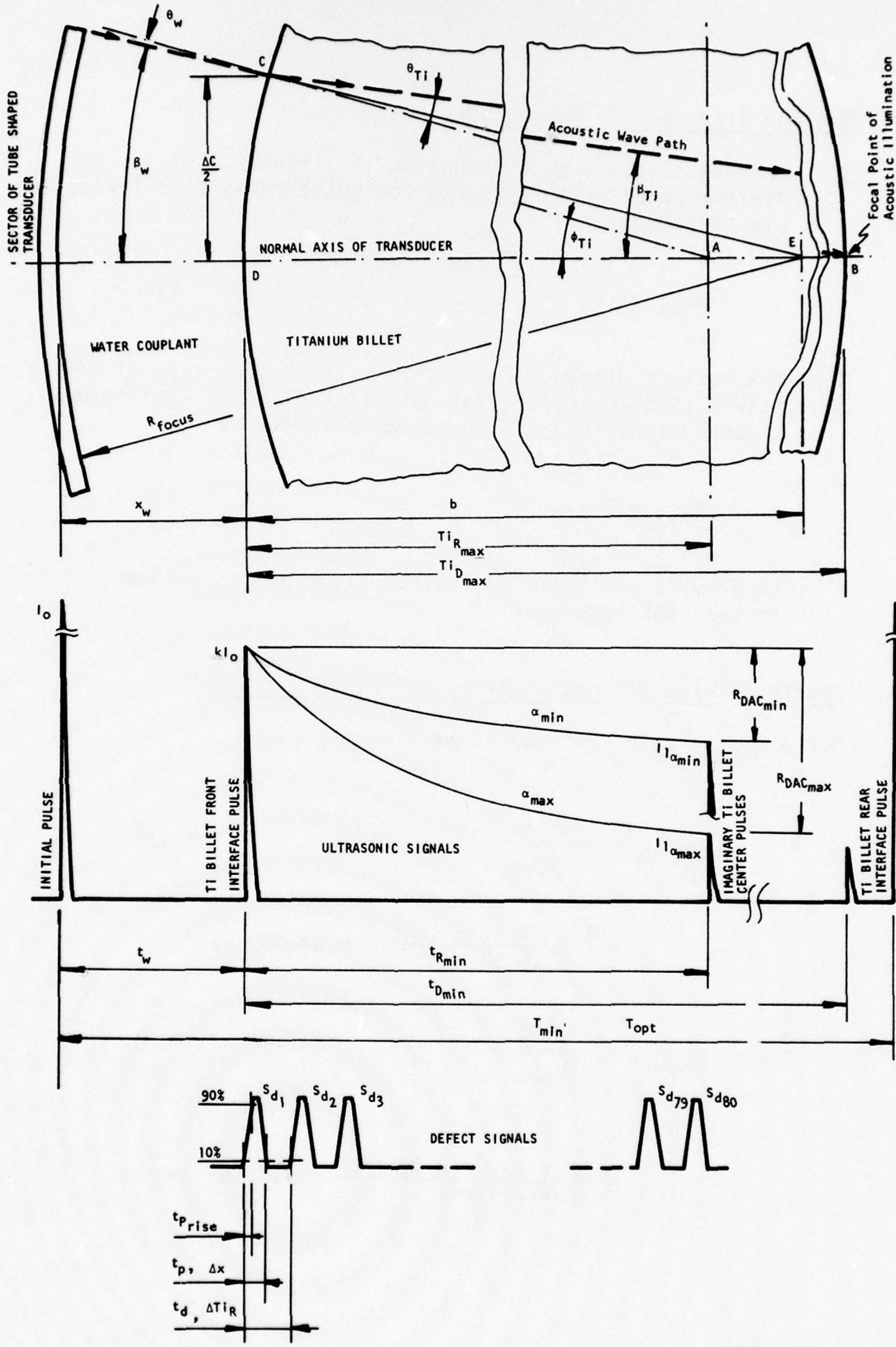


SCALE: NONE

Figure 121. Model of Ti Billet Acoustic Illumination With Related Ultrasonic and Defect Signal/Distance Time Relationship.

3. Maximum Distance for Inspection

3.1 Because of the high attenuation in titanium billets, the maximum penetration distance for pulse-reflection inspection was selected as:

$$x_{max} = Ti_R \tag{1}$$

3.2 The maximum distance for a thru-transmission type of billet attenuation monitoring for automatic distance-amplitude compensation, ADAC, purposes was selected as

$$X_{max} = Ti_D \tag{2}$$

to provide minimal signal attenuation and to ensure faster ADAC response.

4. Shortest Pulse-Reflection Time at Maximum Distance

For a $2x_{max}$ back-and-forth sound travel

$$t_{R_{min}} = \frac{2\ Ti_R}{V_{L_{max}}} \tag{3}$$

$$= \frac{2 \times 20.32 \times 10^{-2}\ \mathrm{m}}{6325.36\ \mathrm{m/s}} = 64.249\ \mu s$$

$$t_{D_{min}} = \frac{2\ Ti_D}{V_{L_{max}}} \tag{4}$$

$$= \frac{2 \times 40.64 \times 10^{-2}\ \mathrm{m}}{6325.36\ \mathrm{m/s}} = 128.499\ \mu s$$

6122 C

5. Desirable Resolving Capability Between Defects

The desirable resolving capability between defects was chosen to be

$$\Delta x = 1.190\ 625 \times 10^{-3}\ \mathrm{m}\ (3/64\ \mathrm{inch})$$

for a cylindrical defect having equal diameter and length as the minimum detectable defect size from Reference 1.

6. Maximum Allowable Modulating Pulse Width

For accurate defect location, the ultrasonic pulse should have a wide spectral bandwidth; thus, a short modulating width, or pulse width must be achieved compared to the desired resolution. The maximum allowable modulating pulse width was calculated as

$$t_{p_{max}} < \frac{2\ \Delta x}{V_{L_{max}}} \tag{5}$$

$$= \frac{2 \times 1.190\ 625 \times 10^{-3}\ \mathrm{m}}{6325.36\ \mathrm{m/s}} = 376.46\ \mathrm{ns}$$

7. Minimum Allowable Elapsed Time Between Successive Pulses

In order to avoid masking:

$$T_{min} \geq \frac{2\ X_{max}}{V_{L_{min}}} \tag{6}$$

$$\geq \frac{2 \times 40.64 \times 10^{-2}}{6087.45\ \mathrm{m/s}} = 133.521\ \mu\mathrm{s}$$

8. Maximum Allowable Pulse Repetition Frequency

From Equation 6, the

$$f_{prf_{max}} = \frac{1}{T_{min}} \tag{7}$$

$$= \frac{1}{133.521 \times 10^{-6}} = 7.489\ \mathrm{kHz}$$

6123 C

9. Radial Distance Unit Cell

For data processing purposes, the defect location shall be defined in terms of resolution measured by unit cell distances in the billet radial direction. The original value has been revised for this property based on a maximum computer input data rate of one bit per each 1.6 μs. (Or $f = 1/T = 1/1.60624 \mu s = 0.625$ MHz, or 0.625 bit/μs data rate).

$$\Delta Ti_R = 5.08 \times 10^{-3} \text{ m} (0.2 \text{ inch}) \tag{8}$$

10. Radial Distance Unit Cell Population

This property was calculated as a titanium billet radial distance segment:

$$N_R = \frac{Ti_R}{\Delta Ti_R} \tag{9}$$

10.1 In case of a 16-inch diameter billet

$$N_R = \frac{8.0 \text{ in}}{0.2 \text{ in}} = 40$$

10.2 In case of an 8-inch diameter billet

$$N_R = \frac{4.0 \text{ in}}{0.2 \text{ in}} = 20$$

11. Minimum Time Interval Between Successive Defect Signals

The random located defects defined in terms of resolution measured by unit cell distances in the billet radial direction may also be defined in terms of resolution measured by unit cell sound travel time; thus, the minimum time interval between two successive defect signals is:

$$t_d = \frac{2\Delta Ti_R}{V_{L_{max}}} \tag{10}$$

$$= \frac{2 \times 5.08 \times 10^{-3} \text{ m}}{6325.36 \text{ m/s}} = 1.6 \ \mu s$$

6124 C

## 12. Acoustic Test Wavelength

This property shall be related to the given desirable defect depth resolution as:

$$\lambda \leq \Delta x \tag{11}$$

$$= 1.2 \times 10^{-3} \text{ m}$$

## 13. Acoustic Test Frequency

From Equation 11:

$$f = \frac{V_{L_{avg}}}{\lambda} \tag{12}$$

$$= \frac{6.226 \times 10^3 \text{ m/s}}{1.2 \times 10^{-3} \text{ m}} \approx 5.0 \text{ MHz}$$

## 14. Acoustic Attenuation Coefficient Range in Titanium Billet

The acoustic attenuation coefficient range in Ti billet for a 5 MHz test frequency is quoted from Reference 1 as:

$$\alpha_{min} = 0.0276 \text{ cm}^{-1}$$

$$\alpha_{avg} = 0.123 \text{ cm}^{-1}$$

$$\alpha_{max} = 0.277 \text{ cm}^{-1}$$

## 15. Acoustic Impedance of a Water Couplant

$$Z_W = \rho_W V_{L_W} \tag{13}$$

$$= 1 \text{g/cm}^3 \times 1.48 \times 10^5 \text{ cm/s}$$

$$= 1.48 \times 10^5 \text{ g/s cm}^2$$

## 16. Acoustic Impedance of a Titanium Billet

$$Z_{Ti} = \rho_{Ti} \, V_{L_{avg}} \tag{14}$$

$$= 4.5 \text{ g/cm}^3 \times 6.2 \times 10^5 \text{ cm/s}$$

$$= 27.9 \times 10^5 \text{ g/s cm}^2$$

## 17. Acoustic Transmission Factor

The acoustic transmission factor for the water couplant and titanium billet interface for an x = 0 distance was calculated as:

$$k = \frac{4\left(\frac{Z_{Ti}}{Z_w}\right)}{\left(\frac{Z_{Ti}}{Z_w} + 1\right)^2} \tag{15}$$

$$= \frac{4\left(\frac{27.9 \times 10^5 \text{ g/s cm}^2}{1.48 \times 10^5 \text{ g/s cm}^2}\right)}{\left(\frac{27.9 \times 10^5 \text{ g/s cm}^2}{1.48 \times 10^5 \text{ g/s cm}^2} + 1\right)^2} = 0.1913$$

## 18. Acoustic Emergent Energy Intensity

The acoustic intensity as a function of depth can be determined by considering the acoustic wave for the billet under test as a plane wave, for which the emergent energy level along a distance x may be defined as:

$$I_1 = kI_o e^{-\alpha x} \tag{16}$$

where $I_o$ is the acoustic intensity established by the transducer in the water couplant, assumed to be 1.0 kV, and all other symbols are as referenced earlier.

Using this equation for a 5 MHz frequency introduces some errors in the calculation of the intensity of sound in the near field; this includes about 2 inches of titanium for a 4-inch water path distance. However, these errors have no effect on the ultimate use for which the equation is intended, since it is valid in the far field where the values calculated are located.

18.1 Acoustic Emergent Intensity Range for a Pulse-Reflection Through Maximum Titanium Billet Diameter

$$I_{1_{max}} = k\, I_o\, e^{-\alpha_{min}\, 2\, Ti_{D_{max}}}$$

$$= 0.191 \times 10^3 V \times e^{-0.0276\, cm^{-1} \times 81.28\, cm} = 20.27V$$

$$I_{1_{avg}} = k\, I_o\, e^{-\alpha_{avg}\, 2\, Ti_{D_{max}}}$$

$$= 0.191 \times 10^3 V \times e^{-0.123\, cm^{-1} \times 81.28\, cm} = 8.69\ mV$$

$$I_{1_{min}} = k\, I_o\, e^{-\alpha_{max}\, 2Ti_{D_{max}}}$$

$$= 0.191 \times 10^3 V \times e^{-0.277\, cm^{-1} \times 81.28\, cm} = 31.8\ nV$$

The emergent acoustic intensity variation or range, due to the attenuation variations, is:

$$R_{I_{1_{TiD}}} = \frac{20.27V}{31.8nV} = 0.637 \times 10^9$$

Now, repeating the same calculations for an

## 18.2 Acoustic Emergent Intensity Range for a Pulse-Reflection Through Maximum Titanium Billet Radius

$$I_{1_{max_{Ti_R}}} = k\, I_o\, e^{-\alpha_{min}\, 2 Ti_{R_{max}}}$$

$$= 0.191 \times 10^3 V \times e^{-0.0276\ cm^{-1} \times 40.64\ cm} = 62.2V$$

$$I_{1_{avg_{Ti_R}}} = k\, I_o\, e^{-\alpha_{avg} 2 Ti_{R_{max}}}$$

$$= 0.191 \times 10^3 V \times e^{-0.123\ cm^{-1} \times 40.64\ cm} = 1.29V$$

$$I_{1_{min_{Ti_R}}} = k\, I_o\, e^{-\alpha_{max} 2 Ti_{R_{max}}}$$

$$= 0.191 \times 10^3 V \times e^{-0.277\ cm^{-1} \times 40.64\ cm} = 2.47\ mV$$

Thus, the emergent acoustic intensity variation or range due to the attenuation variations is:

$$R_{I_{1_{Ti_R}}} = \frac{62.2V}{2.47\ mV} = 2.5 \times 10^4$$

19. <u>Receiver Sensitivity</u>

The receiver sensitivity shall be designed to accommodate the smallest emergent acoustic intensity as:

$$S_{min} = I_{1_{min_{Ti_R}}} \qquad (17)$$

or, in case of a pulse-reflection inspection through the titanium billet radius, the receiver sensitivity shall be 2.47 mV.

20. <u>Minimum Receiver Bandwidth</u>

Besides sensitivity to detect a weak defect signal, the receiver must also have adequate bandwidth to resolve the modulated defect signal. The receiver bandwidth is calculated as:

$$B_n = \frac{1}{t_{p_{max}}} > \frac{V_{L_{max}}}{2\ \Delta x} \qquad (18)\ (19)$$

$$= \frac{1}{t_{p_{max}}} = \frac{1}{0{:}376 \times 10^{-6}s} = 2.66\ \text{MHz}$$

21. <u>DAC Range</u>

Utilizing Equation 16 for the emergent acoustic intensity variation due to the billet acoustic attenuation coefficient in case of pulse-reflection inspection through the maximum billet radius, the required distance-amplitude compensation or DAC range is:

$$R_{DAC_{min}} = \frac{k\ I_o}{I_{1_{max_{Ti_R}}}} \qquad (20)$$

$$= \frac{0.19 \times 1000V}{62.2V} = 3.05$$

6133 C

$$R_{DAC_{max}} = \frac{k\ I_o}{I_{1_{min}} T_{I_R}} \tag{21}$$

$$= \frac{0.19 \times 1000V}{2.47\ mV} = 7.69 \times 10^4$$

22. DAC Linearity

The value selected for this property is 5%, which is typical of commercial electronic instrumentation.

23. ADAC Response Time

To ensure proper operation of the ADAC, the response time was selected to be one half of the time between successive pulses, as:

$$t_{ADAC} \leq \frac{T_{opt}}{2} \tag{22}$$

$$\leq \frac{769\ \mu s}{2} = 385\ \mu s$$

where $T_{opt}$ is defined by Equation 41. This time must also include the time required by the receiver to settle to the new sensitivity value.

24. Receiver Defect Gate Response Time

Considering the conventional definition of 10 and 90 percent amplitude levels, the desirable receiver defect gate response time was calculated as:

$$t_g \leq \frac{t_{P_{max}}}{3} \tag{23}$$

$$\leq \frac{376\ ns}{3} = 125\ ns$$

25. Minimum Allowable Water Couplant Sound Travel Time

In order to avoid overlapping of signals from the billet rear interface and water path multiples, the water couplant pulse-reflection travel time was calculated so as to be longer than the minimum titanium billet pulse-reflection travel time along the billet diameter as:

$$t_W \geq t_{D_{min}} \tag{24}$$

$$\geq 0.128\ 499\ \text{ms} \approx 129\ \mu\text{s}$$

26. Water Couplant Distance

For the transducer-to-titanium-billet front interface, the minimum allowable water couplant distance was calculated as:

$$x_W = V_W \left( \frac{t_W}{2} \right) \tag{25}$$

$$= \frac{1500\ \text{m/s} \times 0.144 \times 10^{-3}\ \text{s}}{2}$$

$$= 10.8 \times 10^{-2}\ \text{m (4-1/4 inch)}$$

The above calculation includes an extra 1/4-inch margin for travel time as a safety factor.

27. Acoustic Wavelength in Water Couplant

$$\lambda_W = \frac{V_W}{f} \tag{26}$$

$$= \frac{1500\ \text{m/s}}{5 \times 10^6\ \text{Hz}} = 0.3 \times 10^{-3}\ \text{m}$$

28. Acoustic Beam Focusing

For an ideal inspection of the rotated cylindrical shaped titanium billet the acoustic illumination was chosen to have a pie-cut shape of the cylindrical sector, as shown in Figure 28. The apex of this pie-shaped sector was selected to be at the titanium billet rear interface. Its curved surface retained the titanium billet's own front interface curvature. This design provides the most benefit for both a pulse-reflection mode of defect inspection and for a through transmission mode of attenuation monitoring, as shown in Figure 29. Details of the acoustic beam focusing are listed below.

29. Angle of Focus in Titanium Billet

To satisfy the desirable billet surface dimension unit cell, $\Delta C$ (as selected by calculation step 38), the angle of focus in the billet was calculated as:

$$\beta_{Ti} = \arc \sin \frac{\frac{\Delta C}{2}}{Ti_{D_{max}}} \tag{27}$$

29.1 For the case of $Ti_D$ = 8 inch

$$\beta_{Ti} = \arc \sin \frac{\frac{1.27 \times 10^{-2}\ m}{2}}{20.32 \times 10^{-2}\ m}$$

$$= 1.79°$$

29.2 For the case of $Ti_D$ = 16 inch

$$\beta_{Ti} = \arc \sin \frac{\frac{1.27 \times 10^{-2}\ m}{2}}{40.64 \times 10^{-2}\ m}$$

$$= 0.895°$$

30. Angle of Refraction in Titanium Billet

With reference to the triangle ABC, which is uniquely defined by the circular shaped titanium billet, the angle of refraction in titanium billet may be defined as:

$$\theta_{Ti} = \beta_{Ti} \tag{28}$$

The angle of refraction in the titanium billet, with reference to the titanium billet radius, therefore, has been calculated as:

30.1 For the case of $Ti_D$ = 8 inch

$$\theta_{Ti} = 1.79°$$

30.2 For the case of $Ti_D$ = 16 inch

$$\theta_{Ti} = 0.895°$$

31. Angle of Incidence for Titanium Billet

Using Snell's Law and with consideration to the acoustic velocity variations in titanium billets, the angle of incidence for titanium billet was calculated as:

$$\theta_W = \text{arc sin}\left(\frac{V_W}{V_{L_{avg}}} \sin \theta_{Ti}\right) \tag{29}$$

31.1 For the case of $Ti_D$ = 8 inch

$$\theta_W = \text{arc sin}\left(\frac{1500 \text{ m/s}}{6226.26 \text{ m/s}} \sin 1.79°\right)$$

$$= 0.431°$$

31.2 For the case of $Ti_D$ = 16 inch

$$\theta_W = \text{arc sin}\left(\frac{1500 \text{ m/s}}{6226.26 \text{ m/s}} \sin 0.895°\right)$$

$$= 0.216°$$

32. Angle of Focus in Water Couplant

The acoustic incident beam in the water couplant was defined, with reference to the normal axis of the transducer, as:

$$\beta_W = \phi_{Ti} - \theta_W \tag{30}$$

where the angle of the acoustic illumination for the angular displacement cell of the titanium billet is defined as:

$$\phi_{Ti} = \text{arc sin} \frac{\frac{\Delta C}{2}}{Ti_R} \tag{31}$$

32.1 For the case of $Ti_D$ = 8 inch

$$\beta_W = 3.58° - 0.431° = 3.149°$$

32.2 For the case of $Ti_D$ = 16 inch

$$\beta_W = 1.79° - 0.216° = 1.574°$$

33. Transducer Surface Curvature

Surface curvature calculation of the transducer having the shape of a tube sector was calculated as:

$$R_{focus} = b + x_W$$

where

$$b = \frac{\frac{\Delta C}{2}}{\tan \beta_w} \qquad (33)$$

33.1 For the case of $Ti_D$ = 8 inch

$$R_{focus} = 11.542 \times 10^{-2} \text{ m} + 10.8 \times 10^{-2} \text{ m}$$

$$= 22.342 \times 10^{-2} \text{ m} \quad (\sim 8\text{-}51/64 \text{ inch})$$

33.2 For the case of $Ti_D$ = 16 inch

$$R_{focus} = 21.109 \times 10^{-2} \text{ m} + 10.8 \times 10^{-2} \text{ m}$$

$$= 33.909 \times 10^{-2} \text{ m} \quad ( >13 \text{ -}11/32 \text{ inch})$$

34. Transducer Length

The transducer length was selected to satisfy the desirable axial billet surface dimension unit cell, $\Delta Ti_L$, as:

$$L_{trans} = \Delta Ti_L \qquad (34)$$

therefore, regardless of titanium billet diameter dimension,

$$L_{trans} = 1.27 \times 10^{-2} \text{ m or } 0.5 \text{ inch}$$

35. Receiver Signal-to-Noise Ratio

The signal to noise ratio may be expressed as shown below, for which the value was conveniently selected as 10:

$$S/N = \frac{S_{min}}{S_{noise}} \qquad (35)$$

36. Maximum Receiver Noise

From Equation 35, the maximum receiver noise shall be calculated as:

$$S_{noise} \leq 0.1\ S_{min} \tag{36}$$

$$\leq 0.1 \times 2.47\ \text{mV} = 247\ \mu\text{V}$$

37. Receiver Recovery Time

In order for the receiver to respond to weak defect signals following the strong ones, it must have sufficiently short recovery time. The receiver recovery time was calculated as:

$$t_{recov} = t_d \tag{37}$$

$$= 1.6\ \mu\text{s}$$

38. Billet Surface Dimension Unit Cell

For data processing purposes, the angular defect location resolution shall be defined as the unit cell in billet angular displacement. The value for this unit cell was chosen arbitrarily as:

$$\Delta C = 0.5\ \text{inch or } 1.27\ \text{cm}$$

where C is the billet circumference defined as

38.1 In the case of a 16-inch diameter billet:

$$C = 2\ \pi Ti_{R_{max}} = 127.67\ \text{cm} \approx 128\ \text{cm}$$

38.2 and, for the case of an 8-inch diameter billet:

$$C = 2\pi\ Ti_{R_{min}} = 63.84\ \text{cm} \approx 64\ \text{cm}$$

39. <u>Angular Displacement Unit Cell Population</u>

This property was calculated as a Ti billet circumferential distance segment:

$$N_C = \frac{C}{\Delta C} \tag{38}$$

39.1 For the case of $Ti_R = 8$ inch

$$N_C = \frac{128 \text{ cm}}{1.27 \text{ cm}} \sim 100$$

39.2 For the case of $Ti_R = 4$ inch

$$N_C = \frac{64 \text{ cm}}{1.27 \text{ cm}} \sim 50$$

40. <u>Billet Angular Displacement Unit Cell</u>

For data processing purposes, the defect location may also be defined as the angular displacement resolution, or unit cell. The value for this property was expressed as:

$$\Delta\theta = \frac{360°}{N_C} \tag{39}$$

40.1 For the case of $Ti_R = 8$ inch

$$\Delta\theta = \frac{360°}{100} = 3.6° \text{ cell}$$

40.2 For the case of $Ti_R = 4$ inch

$$\Delta\theta = \frac{360°}{50} = 7.2° \text{ cell}$$

41. Axial Distance Unit Cell

For data processing purposes, the axial defect location resolution shall be defined as the unit cell in billet axial distance. The value for this unit cell was chosen arbitrarily as:

$$\Delta Ti_L = 0.5 \text{ inch or } 1.27 \text{ cm}$$

42. Axial Distance Unit Cell Population

$$N_A = \frac{Ti_L}{\Delta Ti_L} \tag{40}$$

For the case of $Ti_L = 10$ feet

$$N_A = \frac{10 \times 12 \text{ inch}}{0.5 \text{ inch}} = 240$$

43. Optimum Pulse Repetition Frequency

Utilizing the maximum value given by Equation 7 as the basis, the optimum pulse repetition frequency was selected to be $f_{prf_{opt}} = 1.3$ kHz.

44. Optimum Time Duration Between Successive Pulses

$$T_{opt} = \frac{1}{f_{prf_{opt}}} \tag{41}$$

$$= \frac{1}{1.3 \times 10^3 \text{ Hz}} = 769 \text{ } \mu s$$

45. The Pulse Population for Angular Unit Cell

The pulse population or the number of pulses per angular unit cell was established as:

$$N_{P_{total}} = N_{P_{cal}} + N_{P_{insp}} \tag{42}$$

where the values were designed as

$N_{Pcal}$ = 3 pulses for ADAC calibration, and

$N_{P_{insp}}$ = 15 pulses for billet inspection, thus

$N_{P_{total}}$ = 18 pulses/$\Delta\theta$

46. Time Interval Between Successive Angular Unit Cell Locations

$$t_{\Delta\theta} = N_{P_{total}} \times T_{opt} \tag{43}$$

$$= 18 \times 0.769 \text{ ms} = 13.84 \text{ ms}$$

47. Time Interval for Unity Billet Revolution

$$t_{1_{rev}} = t_{\Delta\theta}\, N_c \tag{44}$$

47.1 For the case of $Ti_R$ = 8 inch

$$t_{1_{rev}} = 13.84 \times 10^{-3} \times 100 = 1.38 \text{ s}$$

47.2 For the case of $Ti_R$ = 4 inch

$$t_{1_{rev}} = 13.84 \times 10^{-3} \times 50 = 0.692 \text{ s}$$

48. Ti Billet Angular Velocity

Angular velocity for the Ti billet rotation was calculated using subcontractor inspection facilities as follows:

$$n_{Ti} = \frac{60 \text{ s/min}}{t_{1_{rev}}} \tag{45}$$

6153 c

48.1 For the case of $Ti_R = 8$ inch

$$n_{Ti} = \frac{60 \text{ s/min}}{1.38 \text{ s}} = 43.5 \text{ min}^{-1} \text{ or, RPM}$$

48.2 For the case of $Ti_R = 4$ inch

$$n_{Ti} = \frac{60 \text{ s/min}}{0.692} = 86.7 \text{ min}^{-1} \text{ or, RPM}$$

49. <u>Roller Drive Angular Velocity</u>

The angular velocity of the subcontractor's inspection drive roller mechanism for rotating the titanium billet was calculated as:

$$n_1 = \frac{Ti_D}{D_1} \times n_{Ti} \tag{46}$$

where $D_1$ is the drive roller diameter of 9 inches.

49.1 For the case of $Ti_R = 8$ inch

$$n_1 = \frac{16''}{9''} \, 43.5 = 77.3 \text{ RPM}$$

49.2 For the case of $Ti_R = 4$ inch

$$n_1 = \frac{8''}{9''} \, 86.7 = 77.1 \text{ RPM}$$

49.3 Thus, the inspection drive roller should be set, for any billet size, at a fixed angular velocity of 77.2 RPM.

## APPENDIX B

## UDIS CONVERSATIONAL CAPABILITIES

The following list describes all of the available commands which may be entered through the I/O keyboard terminal of the alphanumeric-graphic display peripheral in order to operate the UDIS. All of the commands listed are to be inserted as shown; in plain english conversational format. This is a feature of the UDIS, which does not require any special skill or computer training in part of the UDIS operator.

The operator inserted messages are denoted by italics; computer generated messages are shown in capitalized bold-face type.

## OPERATOR COMMANDS

*Control C*     * *(AUtomatic, CAlibrate, INitialize, MAnual, OFfline, STop, ZEro)*

## OPERATOR MESSAGES

*COntinue* - *in response to 'CO' request, or when attempting to recover from a non-fatal MT or LP error.*

*REstart* - *in response to 'Restart if desired' output message.*

*RUN* - *in response to 'Ready for run message'.*

## DATA ENTRY

| | | | |
|---|---|---|---|
| Daily | DATE | *(Day-Month-Year)* | |
| Billet Description | {BILLET NUMBER | *(Alphanumeric)* | up to 17 characters |
| | {ALLOY TYPE | *(Alphanumeric)* | up to 25 characters |
| | {HEAT NUMBER | *(Alphanumeric)* | up to 12 characters |
| | {OPERATOR NAME | *(Alphanumeric)* | up to 30 characters |
| | {LENGTH | *(1.0 to 120.0)* | |
| | {DIAMETER | *(8.0 or 16.0)* | |
| Test Parameters | {BILLET LENGTH INCREMENT | *(.5, .25, or .125)* | |
| | {PULSE RATE | *(500 to 1500 in increments of 50)* | |
| | {MINIMUM SIGNIFICANT CELL COUNT | *(0 to 15)* | |
| | {DIMENSIONAL COORDINATION OF ADJACENT CELLS | *(R, 1 to 39; T, 1 to 100)* | |
| | {AXIAL COORDINATION OF DEFECTS | *(1 to 960)* | |
| Test Results | {RECORD | *(Yes, No)* | |
| | {REPORT | *(Defect, length, both, none)* | |
| | {DISPLAY | *(Count, coordination, both, none)* | |

## INFORMATIONAL OUTPUT MESSAGES

AXIAL POSITION WRONG FOR RESTART
BILLET SCAN COMPLETE
ENTER 'CO' WHEN MTO READY TO ERASE PARTIAL FILE
ENTER 'CO' WHEN MTO WRITE LOCK REMOVED
EXEC INITIATED
INITIALIZE COMMAND REQUIRED
LP NOT READY
MT NOT READY
NO DEFECTS FOR A = ____
NO FILE FOR THIS TEST
NO RESTART POSSIBLE
POWER FAIL DETECTED
READY FOR RUN MESSAGE
RESTART IF DESIRED
SYSTEM CALIBRATED
SYSTEM NOT CALIBRATED

ERROR OUTPUT MESSAGES

AXIAL TRANSLATION TOO FAST
BIN WIDTH OUT OF TOLERANCE FOR THETA = _____
IMPROPER USER FILE LABEL
INVALID COMMAND
LOST FRONT INTERFACE
MTO END OF TAPE
MTO ERROR FLAGGED BY DRIVER
MTO FATAL ERROR
MTO NOT IBM STANDARD LABEL
MTO WRITE ERROR
MTO WRITE ERROR FLAGGED
ROTATION TOO FAST

TEST AND MAINTENANCE COMMANDS

Control C *

CC - 4010 Display Test

DAte- display date

LE - position MTO at logical end of tape

LP - Centronics 101A print test

LS - list the current IBM user label

OP - open MTO

RE - read one record from MTO

SC - 4010 display test

WR - write one record on MTO

SF - special front end tests

Messages used for front end tests (SF)

BI - display the defect bins for one theta sector

EN - display the present shaft encoder values

IN - test the SFE control and interrupts

PR - test the PRF times

The above tests will be executed each time a carriage return is input from the keyboard.

SW - continuous 1500 Hz PRF with SIN and COS outputs set to current theta encoder value

ST - stop tests and return control to the executive program

## APPENDIX C

## REFERENCE LIST OF MANUFACTURER'S OPERATING AND SERVICE MANUALS

### Centronics Corp.

| Code No. | Title |
|---|---|
| Model 101A | Line Printer |

### Digital Equipment Corp.

| Code No. | Title |
|---|---|
| DEC-00-Tu10M-D | Tu10 DEC Magtape |
| DEC-11-HPCC-D | PCM High-speed reader/punch and control unit |
| DEC-00-PCOA-D(1) | PC04/05 Paper-tape reader/punch unit |
| DEC-11-HDLAA-A-D | DL11 Asynchronous Line Interface |
| DEC-11-HMELA-A-D | ME11-L Core Memory System |
| DEC-11-HTMB-D | TM11 DEC Magtape System |
| DEC-11-HRGB-D | Conventions Manual |
| - | PDP-11/20 Processor Handbook |
| DEC-11-RILA-D | PDP-11 Line Printer Driver |
| - | PDP-11 to Centronics 101 Printer Controller |

### Ortec, Inc.

| Code No. | Title |
|---|---|
| 401A/402A-01 | NIM-Bin Power Supply |

### Tektronix, Inc.

| Code No. | Title |
|---|---|
| Model 556 | Oscilloscope Mainframe |
| Type 1A1 | Plug-in Unit |
| Model 564B | Oscilloscope Mainframe |
| Type 3A74 | Plug-in Unit |

### Topaz Electronics, Inc.

| Code No. | Title |
|---|---|
| 8LRA-240SL | Voltage Regulator |

# APPENDIX D

## PHASE I MATERIAL EVALUATION

One-inch thick test slices were cut from the end of each billet to provide macro and microstructure records. This information is displayed in Figures 122 through 153. The photomacrographs of Figures 122 through 129 were taken from the outboard position of each test slice. The photomicrographs of Figures 130 through 153 were prepared from samples of each billet. The ingot chemistry of this heat (RMI No. 895821) is compiled in Table XVIII.

The billets produced for this study were characterized by an examination of the macrostructure and by metallographic evaluation. The billets exhibit a normal grain appearance with no extreme variation in macrostructure apparent in either the 16-inch or 8-inch billet sizes. The macrosections, shown in Figures 122 through 129, are indicative of normal quality alpha beta processed billets.

The photomicrographs in Figures 130 through 153 serve to further characterize the billets. The lamellar alpha plus beta microstructures of the 16-inch diameter sections, shown in Figures 130 through 135, show somewhat less deformation of the material at the center of the section with the prior beta grain boundaries outlined by alpha platelets. This is a prime concern, of course, in terms of ultrasonic inspectability. Nevertheless, the structure is a normal product for this billet size. The 8-inch diameter billets exhibit a similar lamellar microstructure of alpha plates in a beta matrix (see Figures 136 through 153). The additional deformation in converting the 16-inch square to 8-inch diameter resulted in some refinement of the structure. There is some evidence of less deformation at the center of the 8-inch diameter billets than at the mid-radius and outer surfaces, for example, comparing Figure 142 with 144. The absence of inclusions, coarse structures and segregation classify the billets as normal metallurgical quality products.

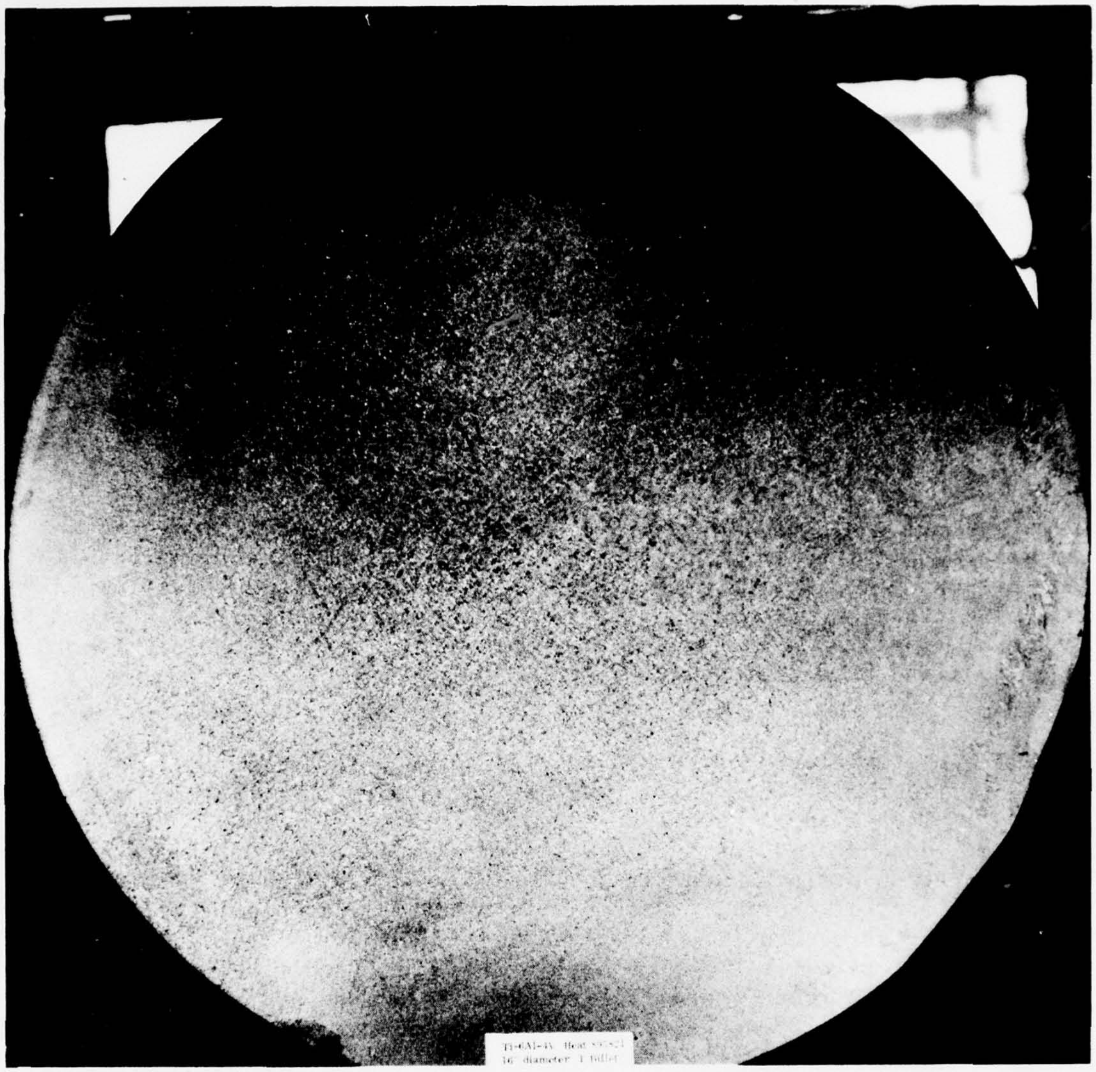

Figure 122. Macrostructure of 16" Dia. T Billet.
(Approximately 0.5X)

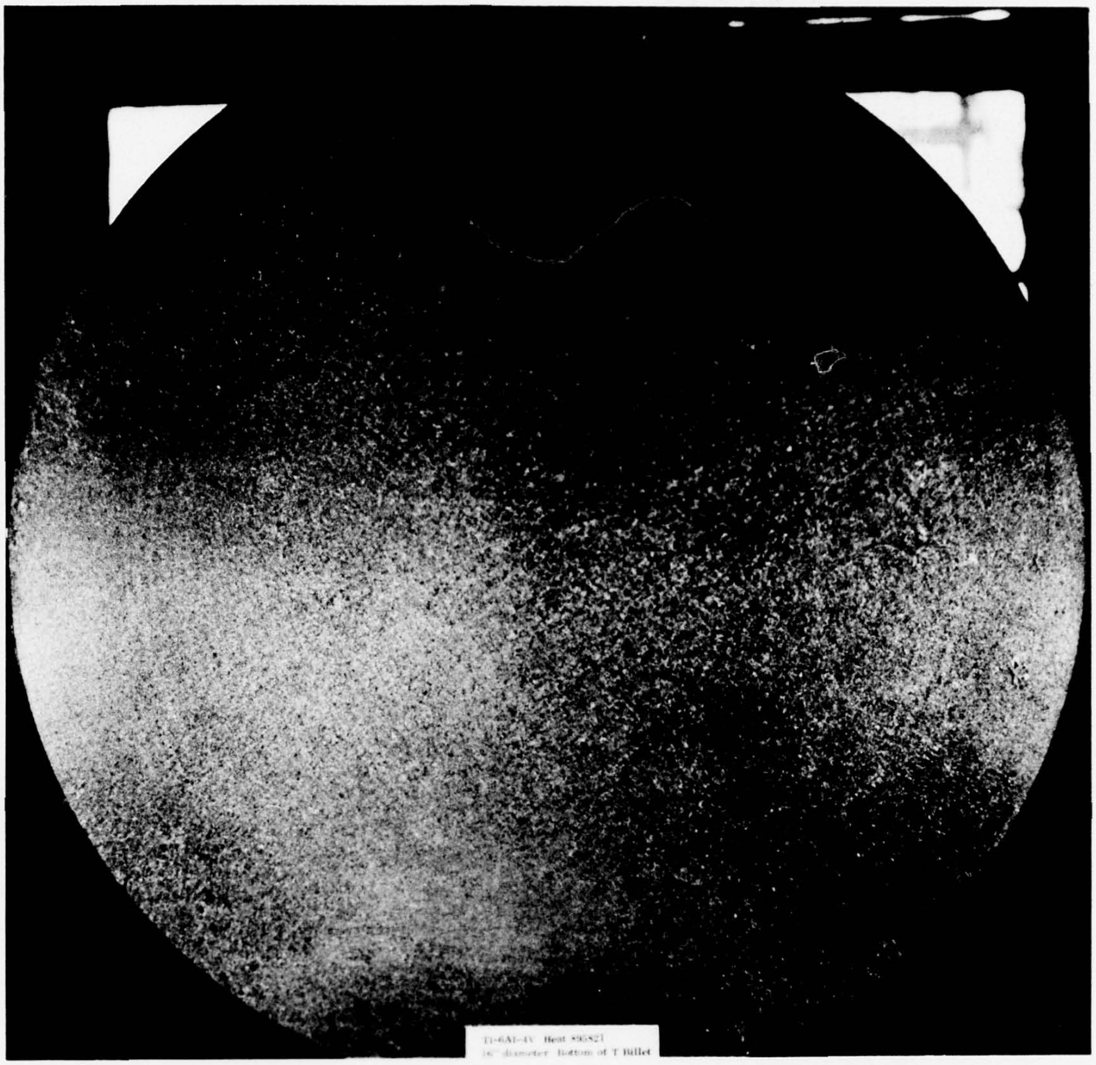


Figure 123. Macrostructure of Bottom of 16" Dia. T Billet. (Approximately 0.5X)

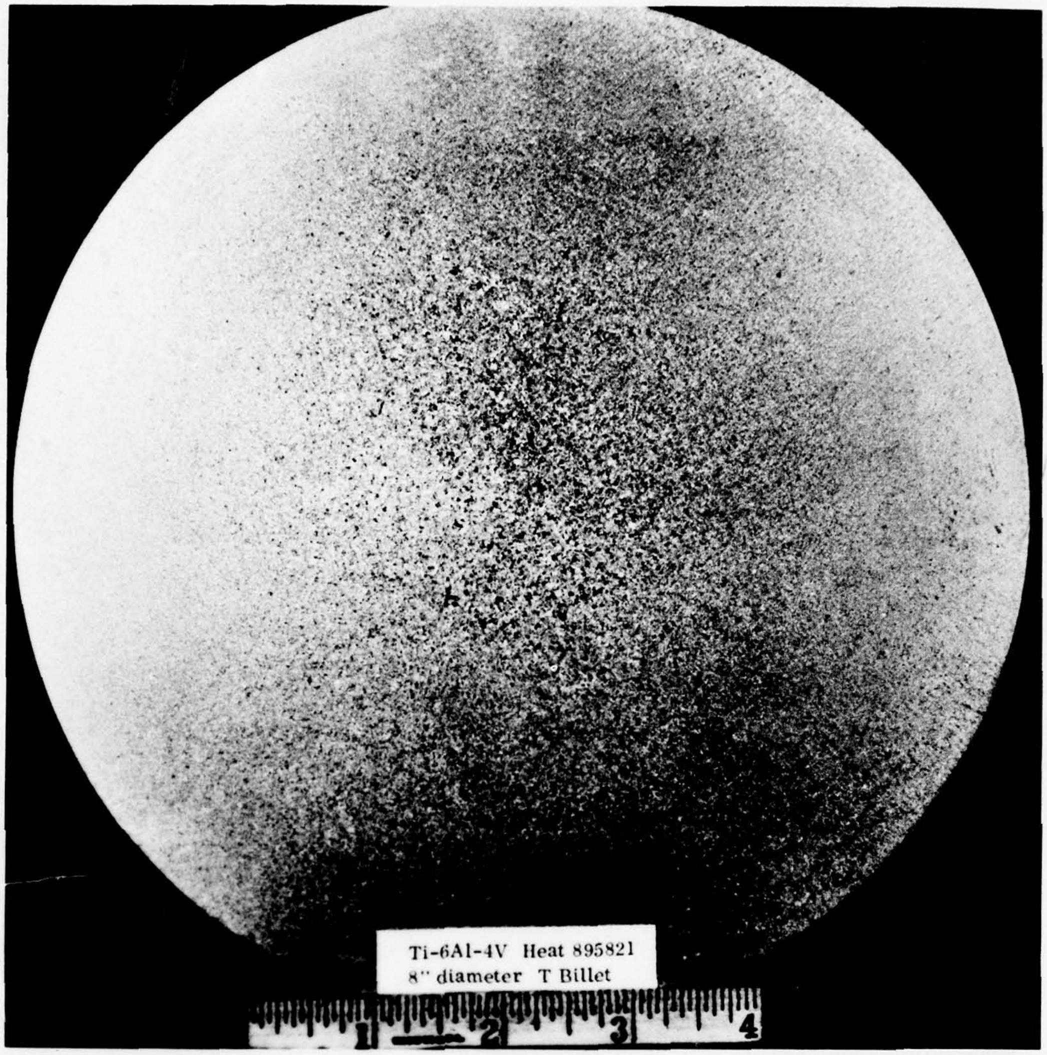


Figure 124. Macrostructure of 8" Dia. T Billet.
(Approximately 1X)

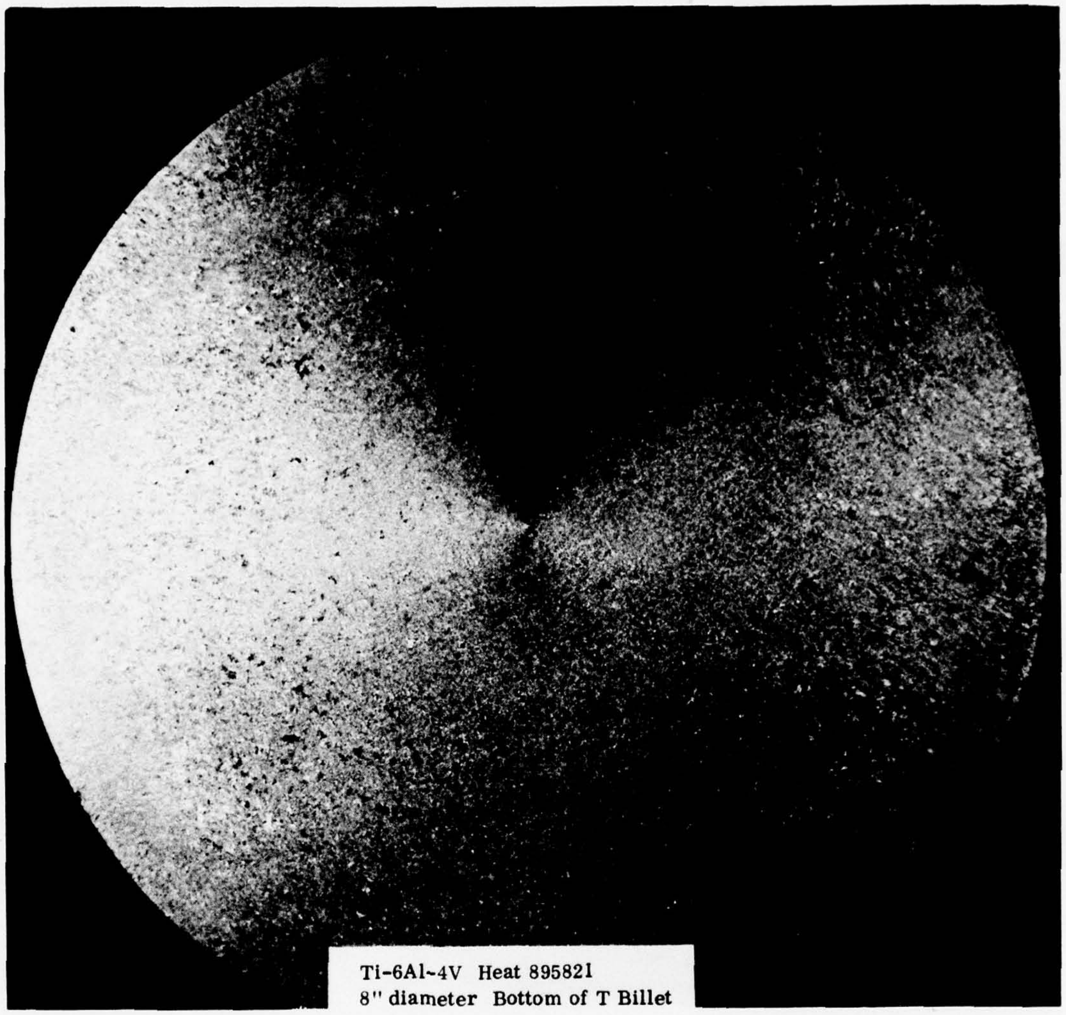


Figure 125. Macrostructure of Bottom of 8" Dia. T Billet. (Approximately 1X)

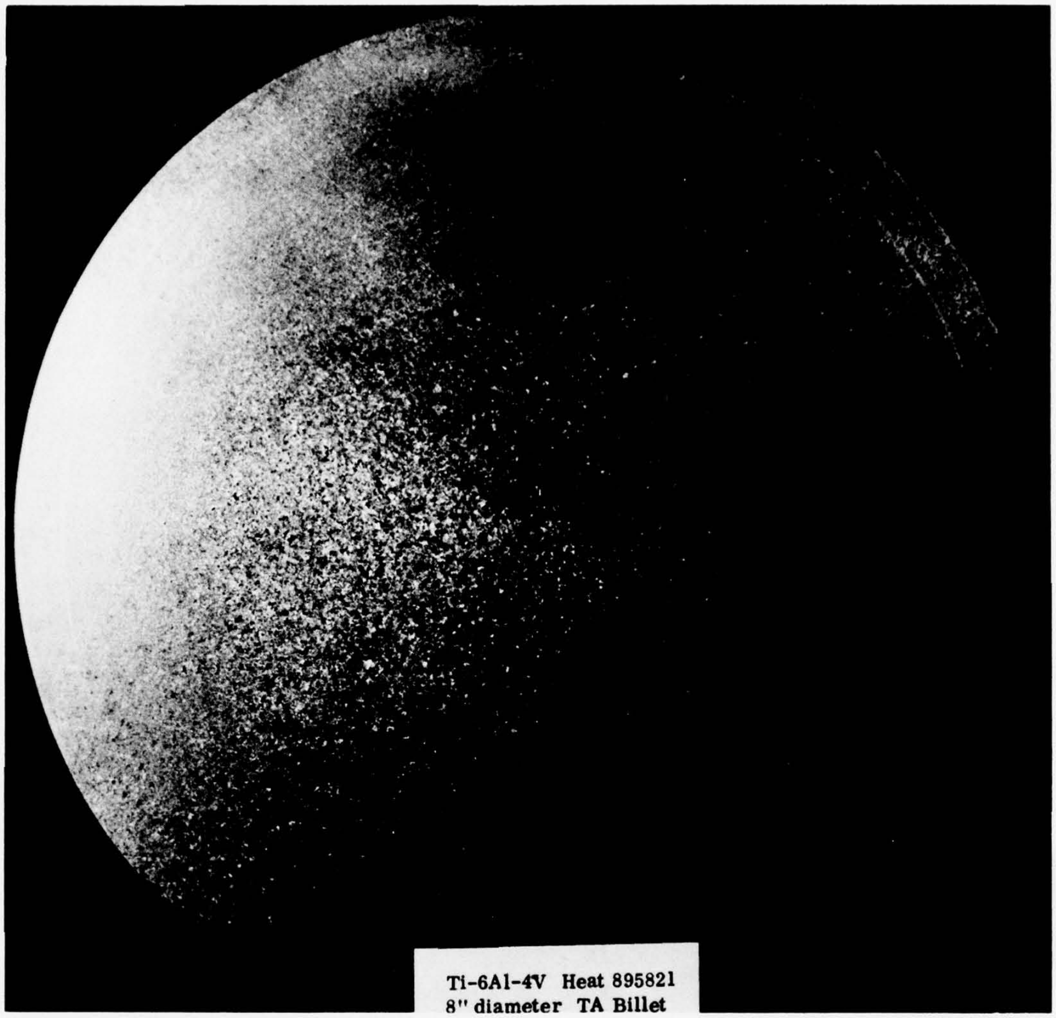


Figure 126. Macrostructure of 8" Dia. TA Billet.
(Approximately 1X)

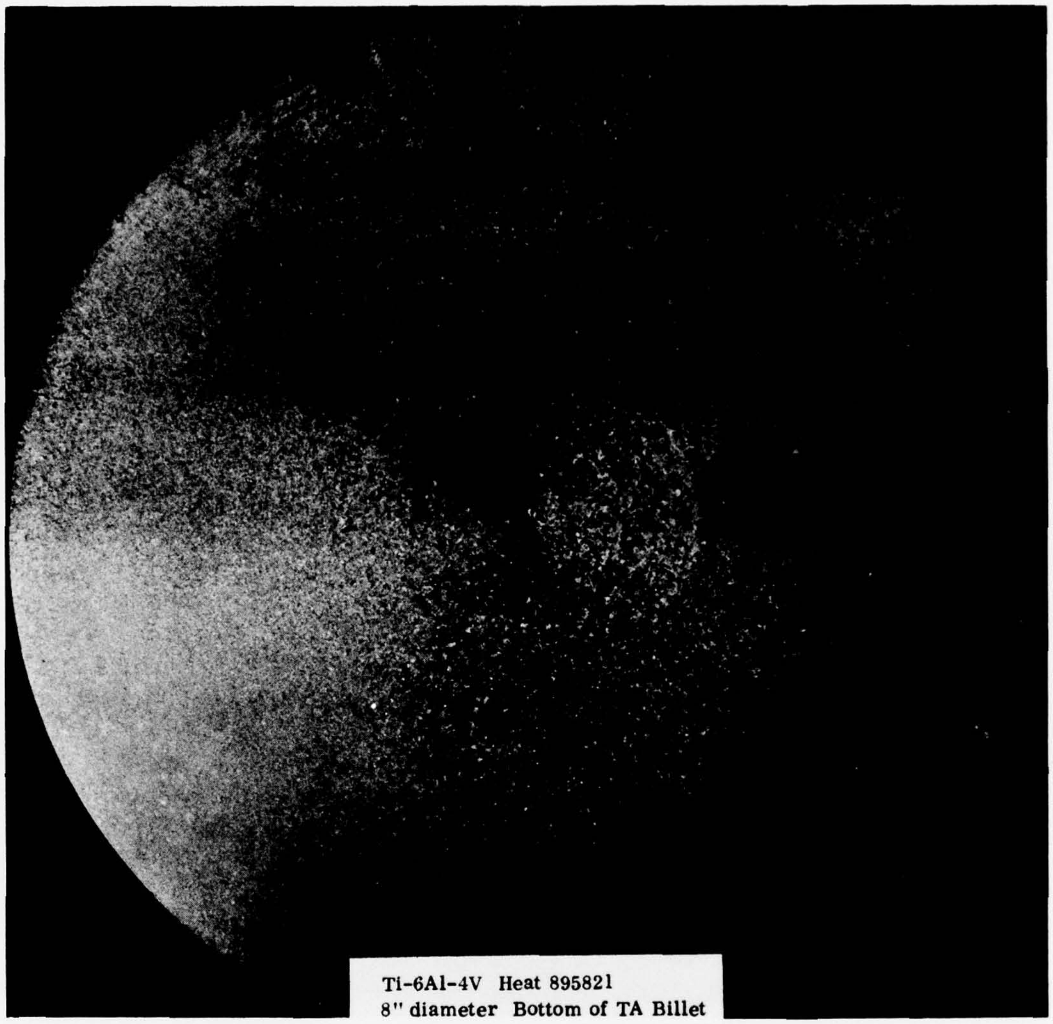


Figure 127. Macrostructure of Bottom of 8" Dia. TA Billet.
(Approximately 1X)

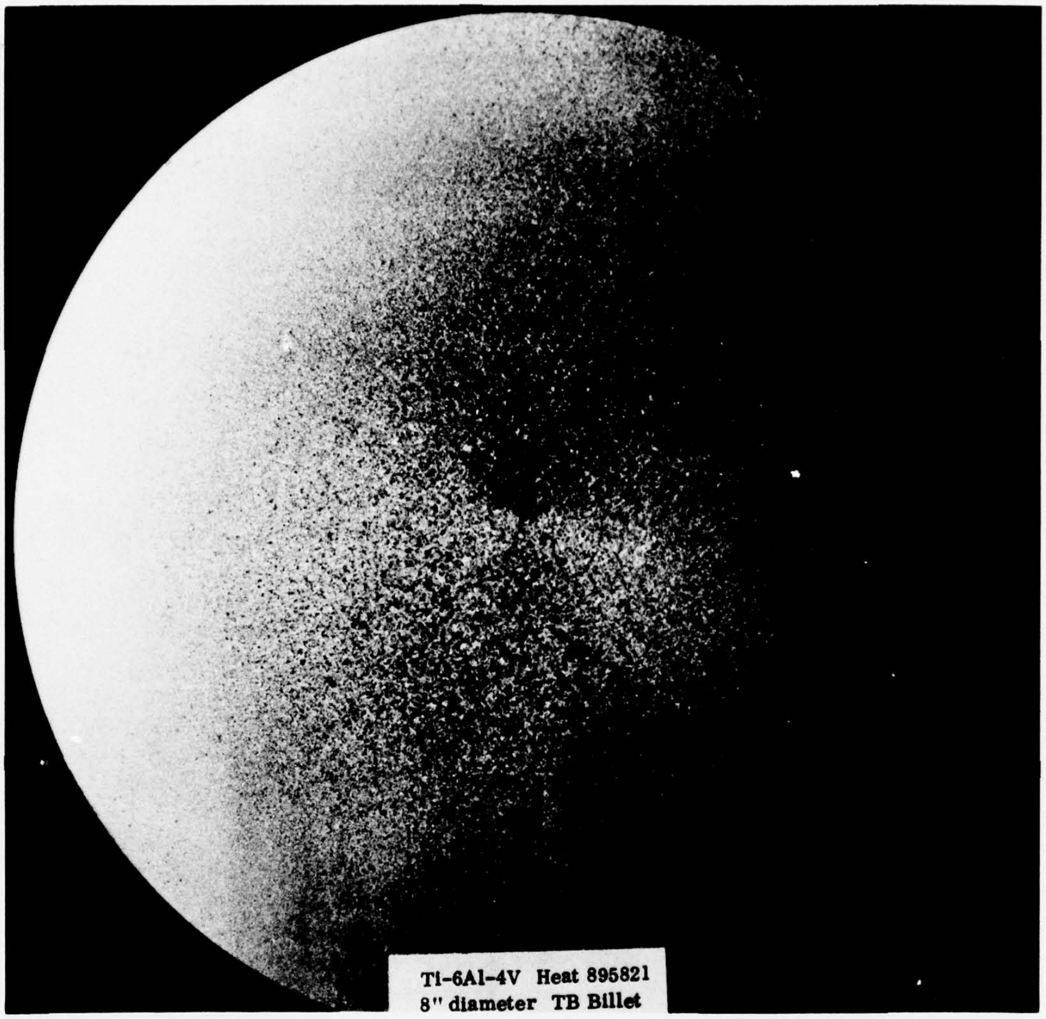


Figure 128. Macrostructure of 8" Dia. TB Billet.
(Approximately 1X)

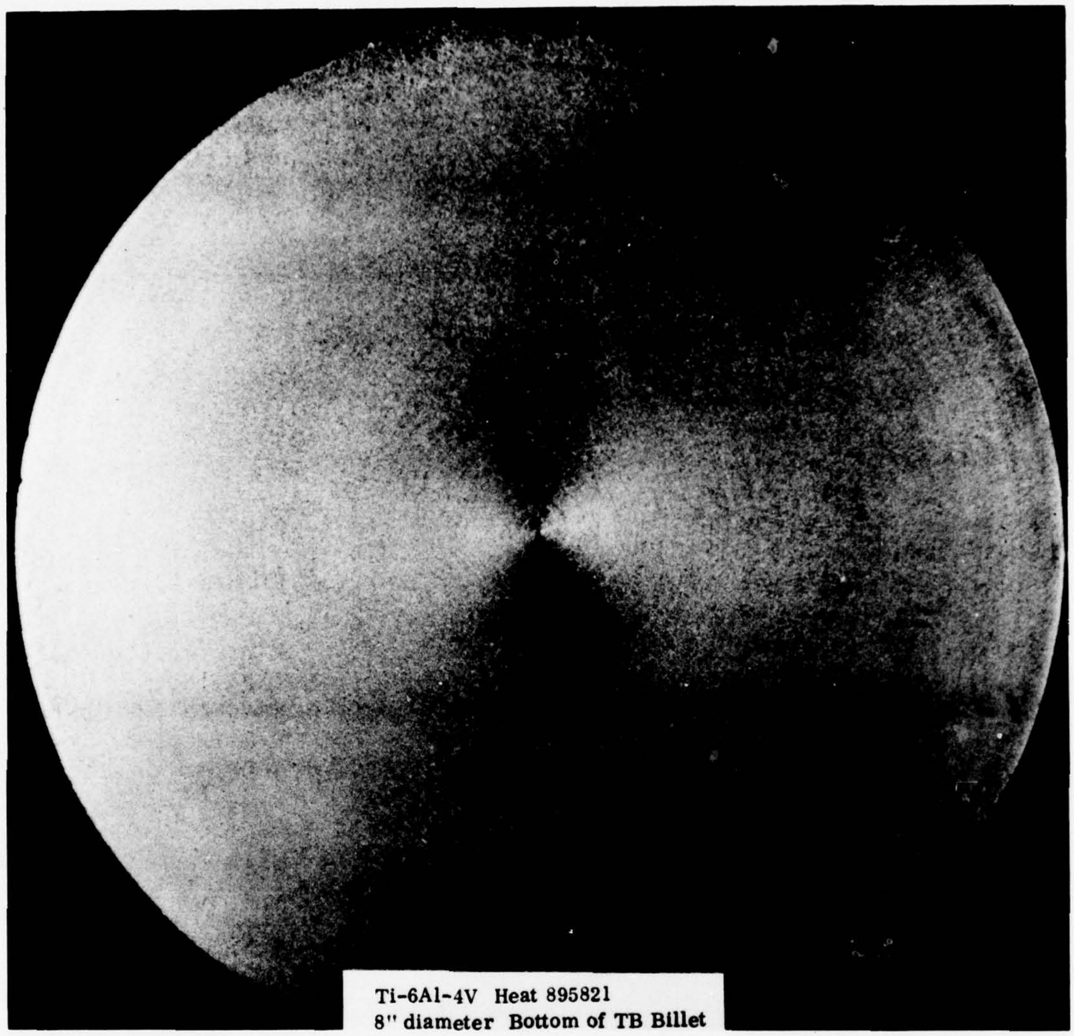


Figure 129. Macrostructure of Bottom of 8" Dia. TB Billet.
(Approximately 1X)

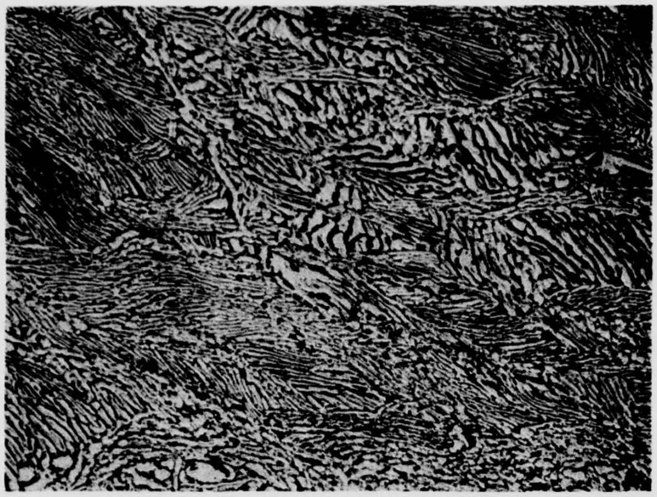

Figure 130.

Microstructure of 16" Dia.
T Billet.
(Edge Position,
L-Direction,
100X)

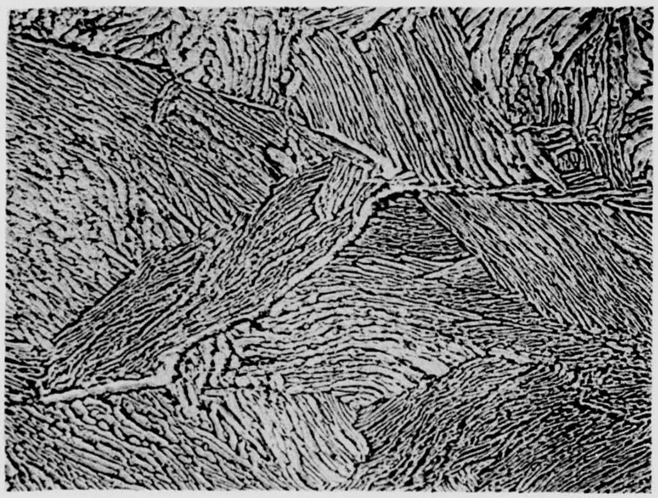

Figure 131.

Microstructure of 16" Dia.
T Billet.
(Mid-Radius Position,
L-Direction,
100X)

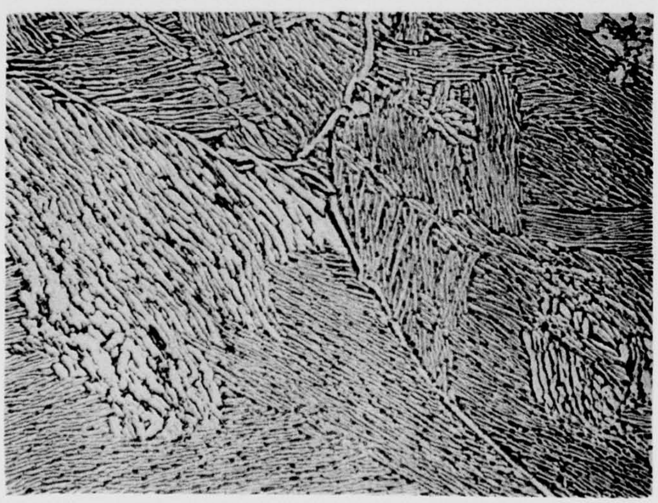

Figure 132.

Microstructure of 16" Dia.
T Billet.
(Center Position,
L-Direction,
100X)

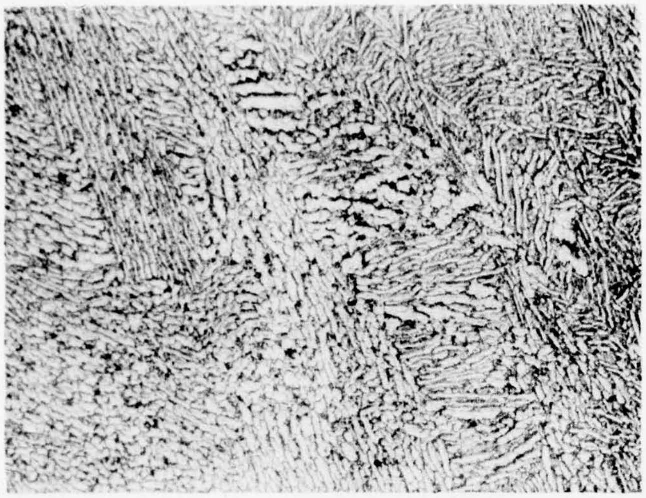

Figure 133.

Microstructure of Bottom of 16" Dia. T Billet. (Edge Position, L-Direction, 100X)

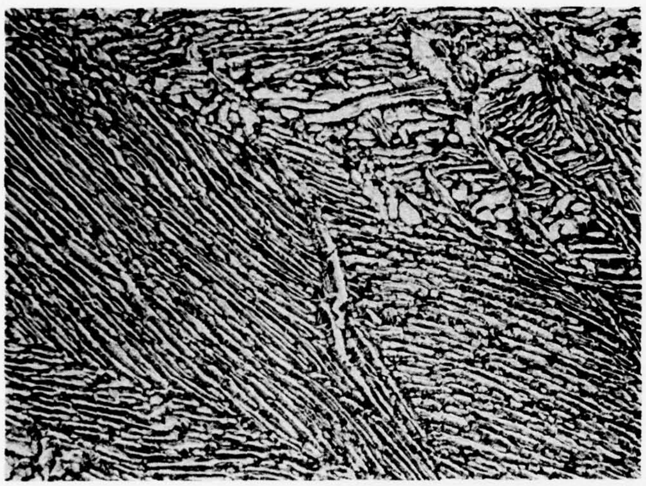

Figure 134.

Microstructure of Bottom of 16" Dia. T Billet. (Mid-Radius Position, L-Direction, 100X)

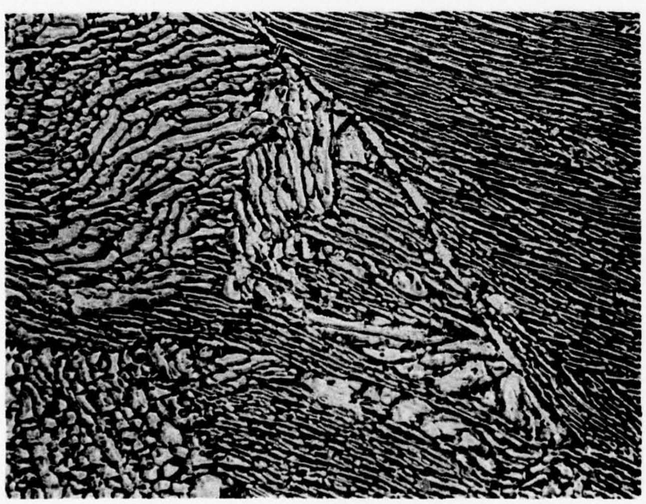

Figure 135.

Microstructure of Bottom of 16" Dia. T Billet. (Center Position, L-Direction, 100X)

2175 C

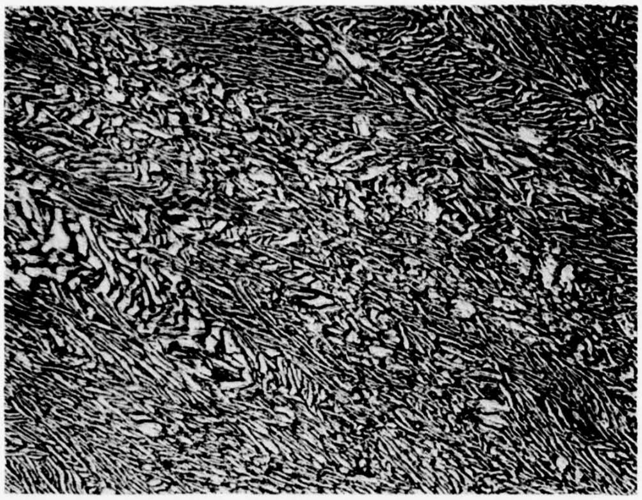

Figure 136.

Microstructure of 8" Dia. T Billet. (Edge Position, L-Direction, 100X)

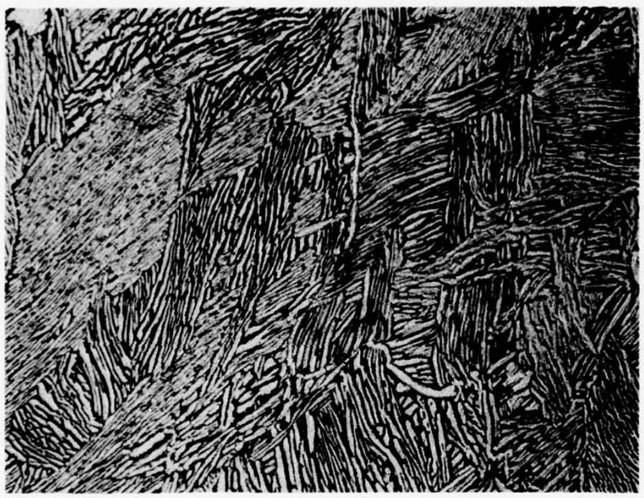

Figure 137.

Microstructure of 8" Dia. T Billet. (Mid-Radius Position, L-Direction, 100X)

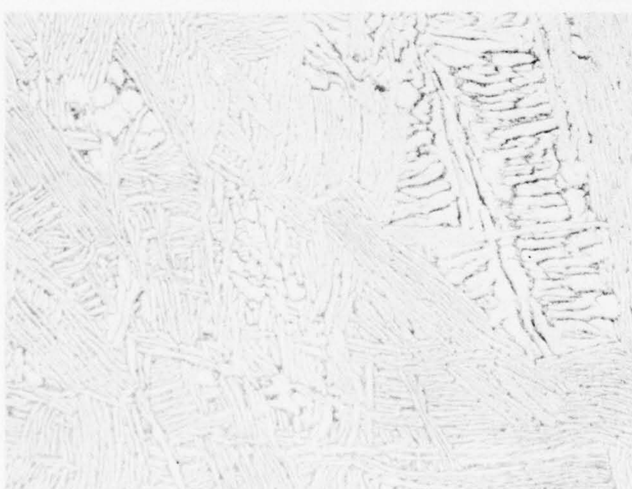

Figure 138.

Microstructure of 8" Dia. T Billet. (Center Position L-Direction, 100X)

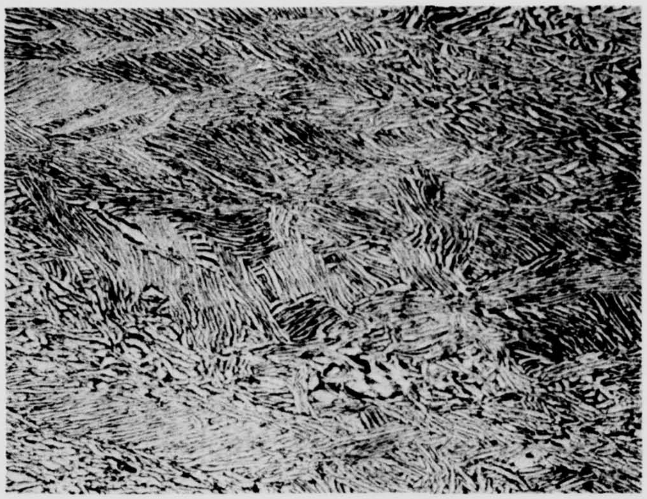

Figure 139.

Microstructure of Bottom of 8" Dia. T Billet. (Edge Position, L-Direction, 100X)

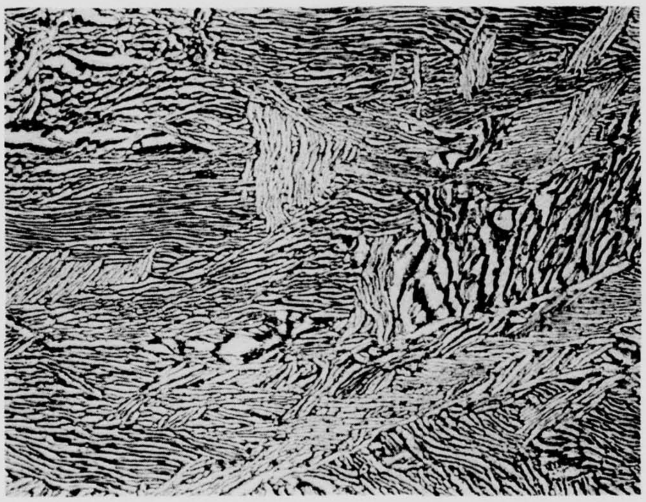

Figure 140.

Microstructure of Bottom of 8" Dia. T Billet. (Mid-Radius Position, L-Direction, 100X)

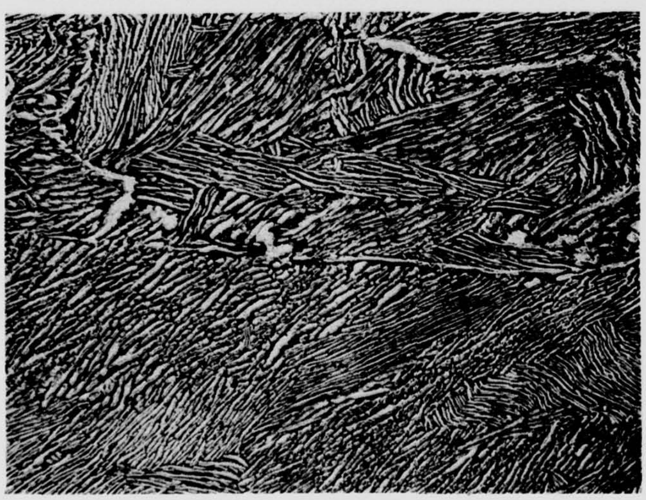

Figure 141.

Microstructure of Bottom of 8" Dia. T Billet. (Center Position, L-Direction, 100X)

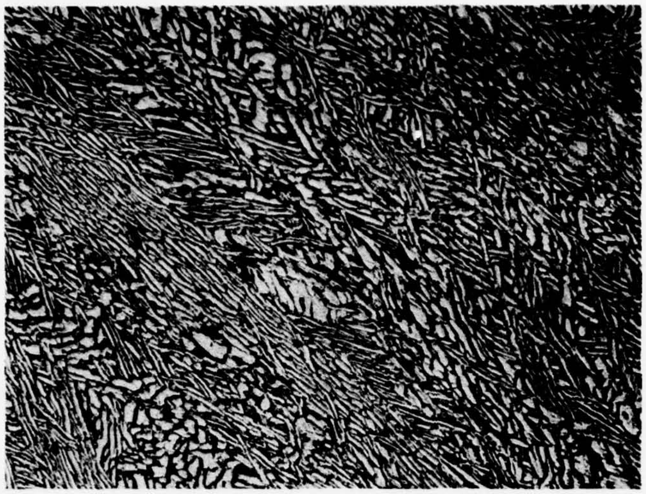

Figure 142.

Microstructure of 8'' Dia. TA Billet. (Edge Position, L-Direction, 100X)

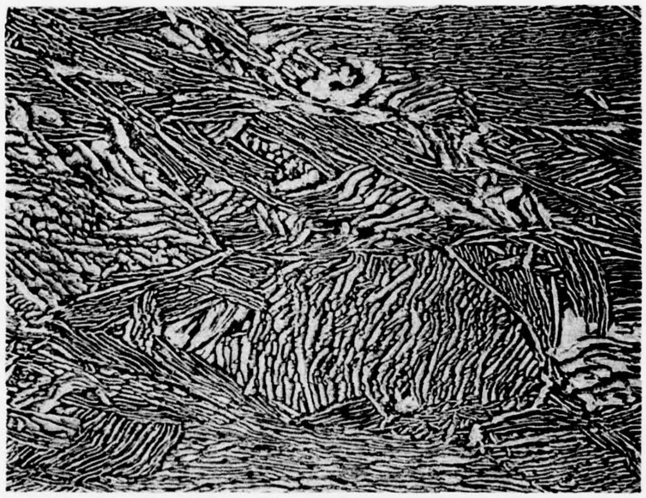

Figure 143.

Microstructure of 8'' Dia. TA Billet. (Mid-Radius Position, L-Direction, 100X)

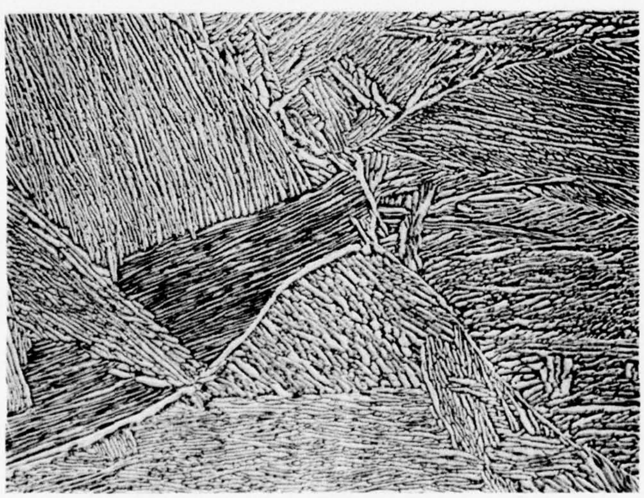

Figure 144.

Microstructure of 8'' Dia. TA Billet. (Center Position, L-Direction, 100X)

2178 C

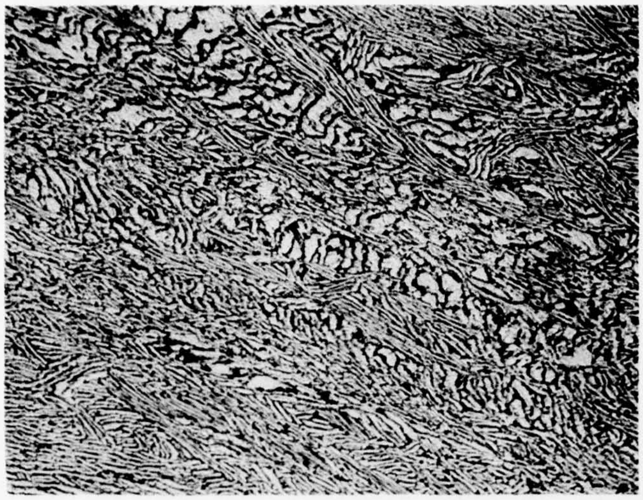

Figure 145.

Microstructure of Bottom of 8" Dia. TA Billet. (Edge Position, L-Direction, 100X)

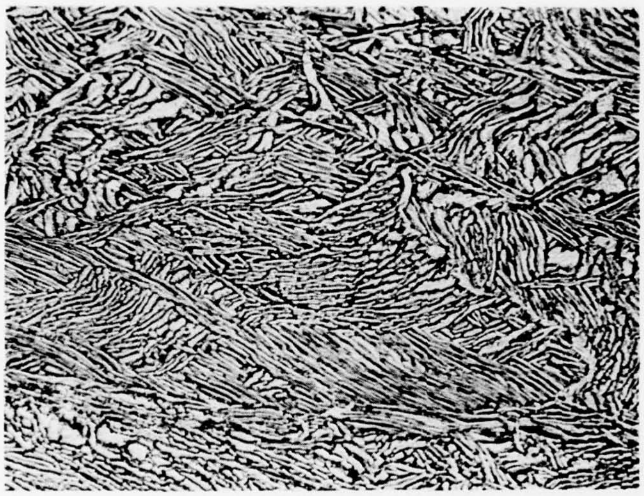

Figure 146.

Microstructure of Bottom of 8" Dia. TA Billet. (Mid-Radius Position, L-Direction, 100X)

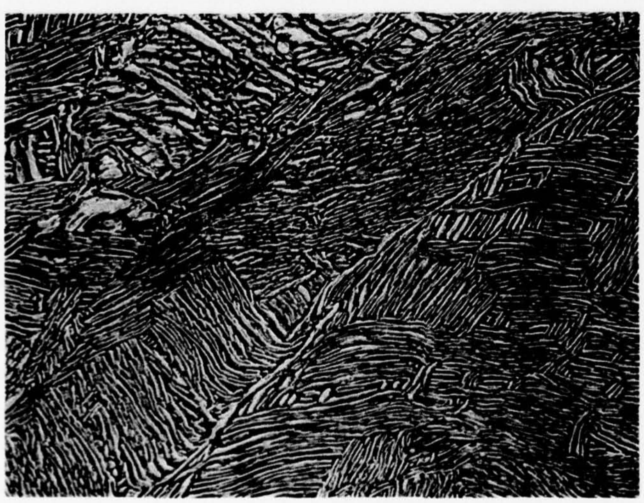

Figure 147.

Microstructure of Bottom of 8" Dia. TA Billet. (Center Position, L-Direction, 100X)

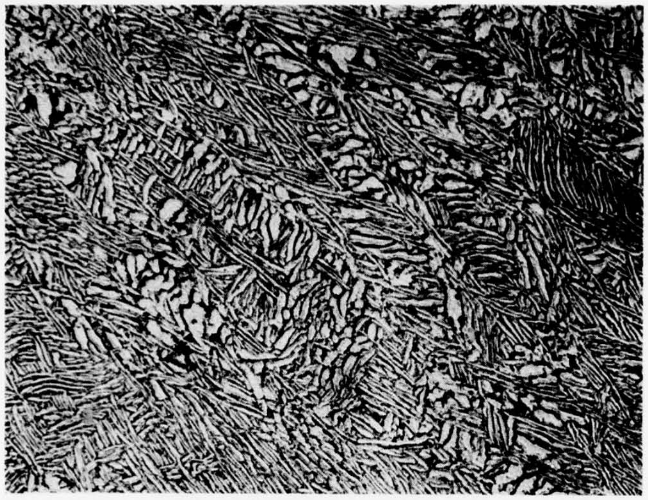

Figure 148.

Microstructure of 8" Dia.
TB Billet.
(Edge Position,
L-Direction,
100X)

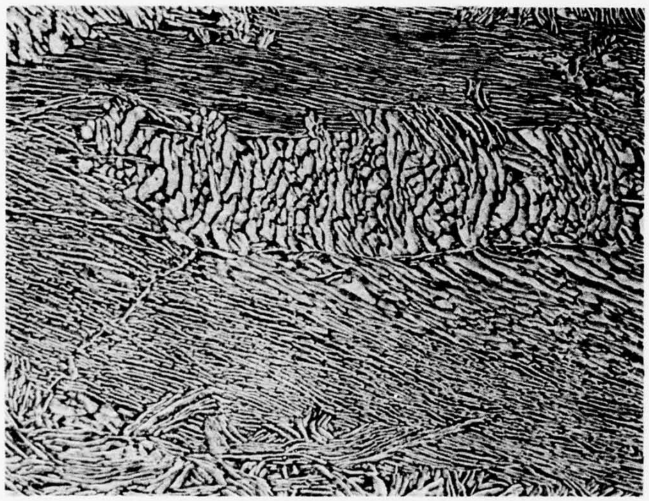

Figure 149.

Microstructure of 8" Dia.
TB Billet.
(Mid-Radius Position,
L-Direction,
100X)

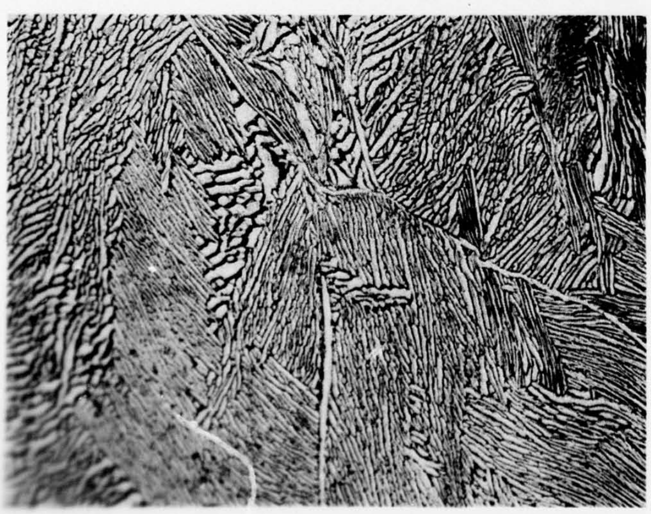

Figure 150.

Microstructure of 8" Dia.
TB Billet.
(Center Position,
L-Direction,
100X)

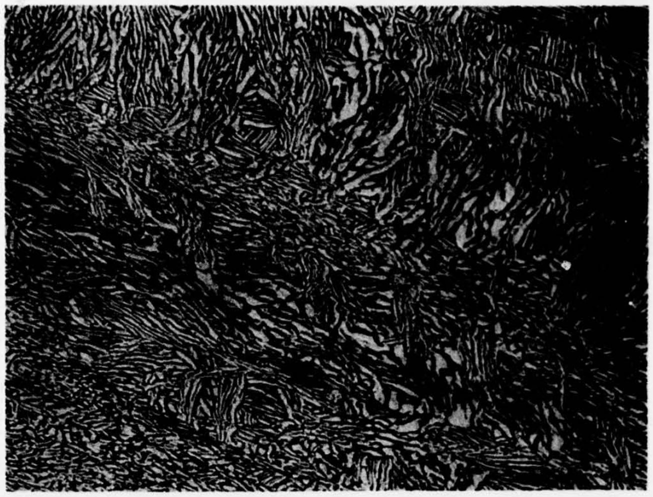

Figure 151.

Microstructure of Bottom of 8'' Dia. TB Billet. (Edge Position, L-Direction, 100X)

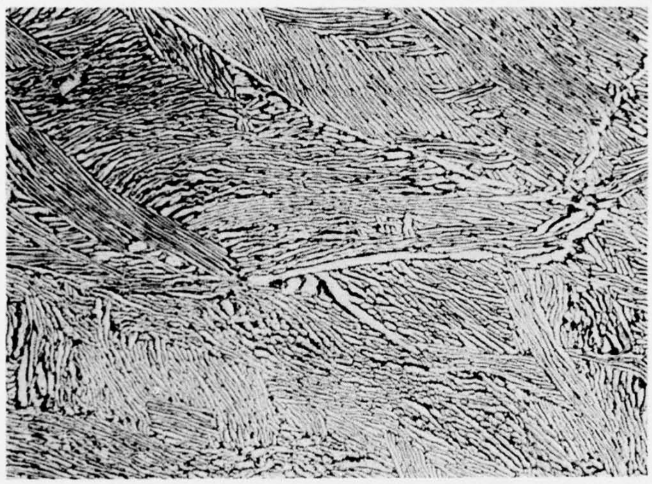

Figure 152.

Microstructure of Bottom of 8'' Dia. TB Billet. (Mid-Radius Position, L-Direction, 100X)

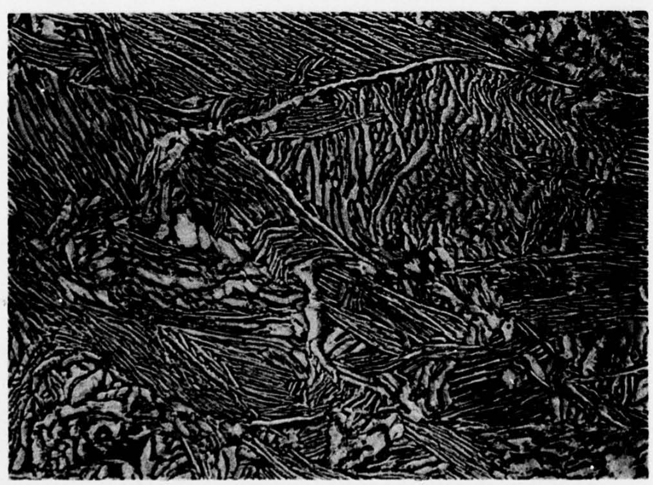

Figure 153.

Microstructure of Bottom of 8'' Dia. TB Billet. (Center Position, L-Direction, 100X)

2181 C

TABLE XVIII

CHEMISTRY OF HEAT NO. 895821 Ti-6Al-4V INGOT

| Location | C % | N % | Fe % | Al % | V % | O % | H ppm |
|---|---|---|---|---|---|---|---|
| 30" Ingot | | | | | | | |
| Top | | 0.008 | 0.18 | 6.6 | 4.0 | 0.168 | 16 |
| Center | 0.02 | 0.008 | 0.18 | 6.6 | 4.0 | 0.168 | 19 |
| Bottom | | 0.012 | 0.18 | 6.4 | 3.8 | 0.178 | 18 |
| Average | 0.02 | 0.0093 | 0.18 | 6.53 | 3.93 | 0.1753 | 17.7 |
| Final Products | | | | | | | |
| 8" Billet Top | | | | | | 0.159 | 22 |
| 8" Billet $T_B$ Bottom | | | | | | 0.168 | 48 |
| 16" Billet Top | | | | | | 0.166 | 27 |
| 16" Billet T Bottom | | | | | | 0.180 | 51 |

# APPENDIX E

## DETAILS OF PERFORMANCE TRANSFER

In order to provide an easy and quick comparison of the results between various instrumentations, a single transducer was used throughout the entire field evaluation. Since said transducer was the property of the subcontractor, a performance transfer was accomplished by using an undisturbed instrument setting for another (TRW's) transducer. Figures 154 and 155 show the performance transfer from the RMI transducer "A" to the TRW transducer "B" as accomplished on the RMI Reference Block Code D1, using a test frequency of 5.0 MHz. Since this Reference Block has a 3/64-inch flat bottom hole with a 4-inch sound travel metal distance, the performance transfer was also accomplished for the same size flat bottom hole with a 2-inch sound travel metal distance as shown in Figures 156 and 157. Similarly, for the cases of the 3/64-inch and 8/64-inch flat bottom holes having sound travel metal distances of 8 inches, performance transfers were also carried out as shown in Figures 158 through 161.

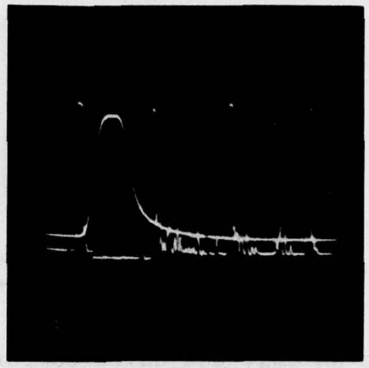

Figure 154. Transducer "A" Response on Reference Block Code D1.
(#3 Flat Bottom Hole,
4-Inch Metal Distance)

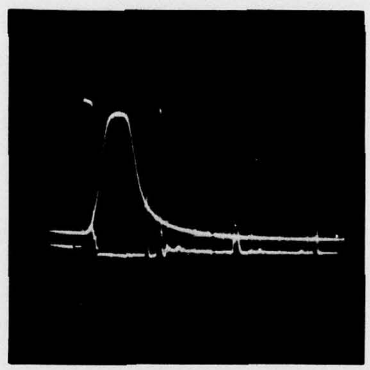

Figure 155. Transducer "B" Response on Reference Block Code D1.
(#3 Flat Bottom Hole,
4-Inch Metal Distance)

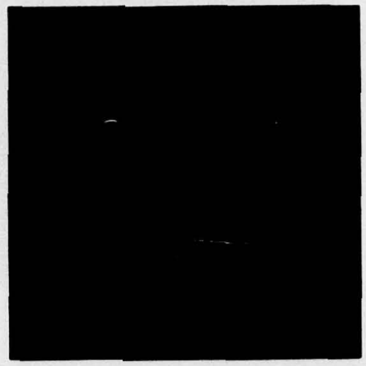

Figure 156. Transducer "A" Response on Reference Block Code D. (#3 Flat Bottom Hole, 2-inch Metal Distance)

Figure 157. Transducer "B" Response on Reference Block Code D. (#3 Flat Bottom Hole, 2-inch Metal Distance)

2517 C

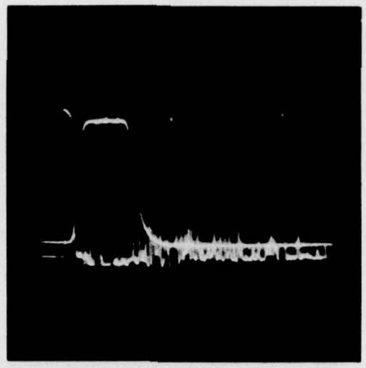

Figure 158. Transducer "A" Response on Reference Block
TRW #111227-1-5(8)
(#8 Flat Bottom Hole,
8-inch Metal Distance)

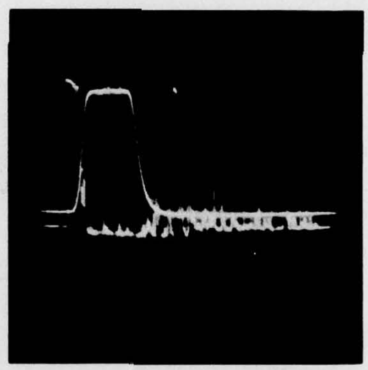

Figure 159. Transducer "B" Response on Reference Block
TRW #111227-1-5(8)
(#8 Flat Bottom Hole,
8-inch Metal Distance)

2516 C

Figure 160. Transducer "A" Response on Reference Block
TRW #111227-1-5(3)
(#3 Flat Bottom Hole,
8-inch Metal Distance)

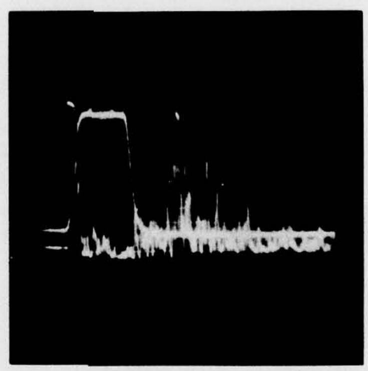

Figure 161. Transducer "B" Response on Reference Block
TRW #111227-1-5(3)
(#3 Flat Bottom Hole,
8-inch Metal Distance

## APPENDIX F

### SURVEY OF INSTRUMENT MANUFACTURERS

Survey of manufacturer's candidate commercial ultrasonic instruments resulted in the data reported in Tables I through X. The instrument types and their manufacturers' names are designated by letter codes listed below:

| Letter Designation | Manufacturer & Type No. |
|---|---|
| **Tables I - V** | |
| A | Branson Instruments, Model 600 |
| B | Sperry Division of Automation Ind., Inc.<br>Type 771 Mainframe<br>Type 10SdB Pulser/Receiver<br>Type AG-IF Timer |
| C | Magnaflux, Model PS900 |
| D | Krautkramer, Type USIP-11 |
| **Table VI** | |
| $A_1$ and $A_2$ | Branson Instruments, Type 600 with Type 610A Timer |
| $B_1$ | Sperry Division, Type UM-771 |
| $B_2$ | Sperry Division, Type UM-700 |
| C | Magnaflux, Type DS-1007 |
| D | Krautkramer, Type USE1 |
| **Table VII** | |
| $A_1$ and $A_2$ | Branson Instruments, Type 600 with Type 610A Timer |
| $B_1$ | Sperry Division, Type 771 with Timer D |
| $B_2$ | Sperry Division, Type 771 with Timer AG-IF |
| C | Magnaflux, Type DS-1007 |
| D | Krautkramer, Type USE-1 with T-6 Trigger |

| Letter Designation | Manufacturer & Type No. |
|---|---|
| **Table VIII** | |
| $A_1$ and $A_2$ | Branson Instruments, Type 600 with Type 620 Pulser/Receiver |
| $B_1$ | Sperry Division, Type 771 with Type 10SdB Pulser/Receiver |
| $B_2$ | Sperry Division, Type 700 with Type 5N Pulser/Receiver |
| C | Magnaflux, Type DS-1002 with RP1012 Pulser/Receiver |
| D | Krautkramer, Type USE-1 with Amplifier No. 12 |
| **Table IX** | |
| $A_1$ and $A_2$ | Branson Instruments, Type 600 with Type 620 Pulser/Receiver |
| $B_1$ | Sperry Division, Type UM-771 with Type 10SdB Pulser/Receiver |
| $B_2$ | Sperry Division, Type UM-700 with Type 5N Pulser/Receiver |
| C | Magnaflux, Type DS-1007 with Type RP-1012 Pulser/Receiver |
| D | Krautkramer, Type USE-1 with Amplifier No. 12 |
| **Table X** | |
| $B_1$ | Sperry Division, Type UM-771 with Fast-Transigate |
| $B_2$ | Sperry Division, Type UM-771 with AG-IF Timer |
| C | Magnaflux, Type DS-1007 with Type TM1010 |

## DISTRIBUTION LIST
Contract F33615-71-C-1712

### AIR FORCE

AFAL/TSR
Wright-Patterson AFB, OH 45433

AFAPL/TB
Wright-Patterson AFB, OH 45433

AFAPL/TBT
Wright-Patterson AFB, OH 45433

AFFDL/FB
Wright-Patterson AFB, OH 45433

AFFDL/FBA
Wright-Patterson AFB, OH 45433

AFLC/QE
Wright-Patterson AFB, OH 45433

AFML/DO (STINFO)
Wright-Patterson AFB, OH 45433

AFML/LLM
Wright-Patterson AFB, OH 45433
Attn: Mr. T. O'Hara

AFML/LLS
Wright-Patterson AFB, OH 45433

AFML/LTM
Wright-Patterson AFB, OH 45433
Attn: Mr. K. Love (5 copies)

AFML/MXA
Wright-Patterson AFB, OH 45433
Attn: Mr. P. Hendricks

AFML/MXA
Wright-Patterson AFB, OH 45433
Attn: Mr. H. W. Zoeller

AFML/MXE
Wright-Patterson AFB, OH 45433
Attn: Mr. C . L. Harmsworth

AFSC/INA
Andrews AFB, MD 20334

Air University
Library
Maxwell AFB, AL 36112

DDC/TCA (2 copies)
Cameron Station
Alexandria, VA 22314

Hq AFCMD/Pd
Kirtland AFB, NM 87117

Hq USAF/RDPI
Washington, DC 20330
Attn: Maj. Donald Mackintosh

Hq USAF/RDPS
The Pentagon
Washington, DC 20330

OCALC
OCRO/Library
Oklahoma City, OK 73145

SAMSO (SY/AFML)
P. O. Box 92960
Worldway Postal Center
Los Angeles, CA 90045

### ARMY

Army Aviation Material Command
AMSAV-PK
P. O. Box 209
St. Louis, MO 63166
Attn: Mr. L. Kiefer

Army Materials & Mechanics Research Center
Watertown, MASS 02172
Attn: Mr. S. V. Arnold

Army Mobility Equipment R&D Center
Fort Belvoir, VA 22060
Attn: Mr. E. Asher

Army Production Equipment Agency
Rock Island, IL 61201
Attn: Chief, Mfg. Tech Div (AMXPE-MT)
Director

Army Tank Automotive Command
SMOTA-RCP
Warren, MI 01608
Attn: Mr. D. M. Latson

ARMY (Cont'd)

Dept. of the Army
Attn: Mr. A. C. Williams
ANCPN-PBN-G
Munitions Production Base
Modernization & Expansion
Picatinny Arsenal
Dover, NJ 07801

Frankford Arsenal
Pittman Dunn Laboratory
Philadelphia, PA 19137
Attn: Mr. Harold Markus

U.S. Army Mat. & Mechanic Res. Center
Watertown, MA 02172
Attn: Dr. Edward S. Wright

U. S. Army Research Office
Director of Metallurgy & Mat. Sc. Div.
Box CM, Duke Station
Durham, NC 27706
Attn: Dr. H. M. Davis

Watervliet Arsenal
Watervliet, NY 12139
Attn: SARWV-RT-L
Commander

NAVY

Chief of Naval Research
Code ONR 740
Navy Department
Washington, DC 20360

Commander
Naval Weapons Laboratory
Dahlgren, VA

Commanding Officer
Naval Air Development Center
Aero Structures Department
Johnsville
Warminster, PA 18974

Naval Air Systems Command
Code AIR 52031 B
Washington, DC 20361
Attn: Mr. Irving Machlin

Naval Air Systems Command
Materials Research and Technology
Washington, DC 20360
Attn: RRMA-2/Mr. T. F. Kerns

Naval Air Systems Command
Navy Department
AIR 52031D
Washington, DC 20361
Attn: Mr. W. Ted Highberger

Naval Ship R&D Laboratories
Code A934
Annapolis, MD 21402
Attn: Mr. F. Lengenfelder

NASA

NASA
21000 Brookpark Road
Cleveland, OH 44135
Attn: Mr. Robert Hall
Library, Mail Stop 3-7

NASA
Marshall Space Flight Center
Huntsville, AL 35801
Attn: Library

NASA
Washington, DC 20036
Mr. R. H. Raring
DUZ-7026, Code RRM

OTHER GOVERNMENT AGENCIES

Oak Ridge National Laboratory
Metals and Ceramics Division
Attn: Mr. W. R. Martin
P. O. Box X
Oak Ridge, TN 37830

OTHER GOVERNMENT AGENCIES (Cont'd)

U. S. Bureau of Mines
Albany Met. Research Center
P. O. Box 70
Albany, OR 97321
Attn: Mr. F. Wood

U. S. Dept. of the Interior
Bureau of Mines
Office of Director of Met Research
Washington, DC 20240
Attn: Mr. Kenneth B. Higbie
Staff Metallurgist

INDUSTRY

Aerojet Electrosystems Company
Director, Manufacturing
Building 194/Department 7301
P. O. Box 296
Azusa, CA 91702

AIRCO
Viking Metallurgical Corp.
No. 1 Erik Circle
Verdi, NV 89439
Attn: Mr. M.V.Walberg, Pres.

AiResearch Mfg. Co. of Arizona
402 South 36th Street
P. O. Box 5217
Phoenix, AZ 85010
Attn: Supervisor, Mat. Eng. Dept.
Dept. 93-39M

Allegheny Ludlum Steel Corp.
Bar Products Division
Attn: Mr. G. F. Taylor
Watervliet, NY 12139

Allegheny Ludlum Steel Corp.
Technical Library
Brackenridge, PA 15014

Allis-Chalmers Mfg. Co.
Defense Products Division
P. O. Box 612
Milwaukee, WI 53201

Aluminum Company of America
Alcoa Research Laboratories
Attn: Asst. Director of Research
P. O. Box 772
New Kensington, PA 15068

Aluminum Company of America
1200 Ring Bldg.
Washington, DC 20036
Attn: Mr. G. B. Barthold

Aluminum Company of America
2210 Harvard Avenue
Cleveland, OH 44105
Attn: Mr. G. W. Khulman

American Welding & Mfg. Company
550 Dietz Road
Warren, OH 44482
Attn: Mr. G. W. Reeder
Technical Director

Armco Steel Corporation
Advanced Materials Division
P. O. Box 1697
3501 E. Biddle Street
Baltimore, MD 21203
Attn: Technical Librarian

Armco Steel Corporation
Research and Technology Division
Middletown, OH 45042

Automation Industries, Inc.
Sperry Division
Danbury, CT 06810

Avco Corporation
Lycoming Division
Stratford, CT 06497
Attn: Superintendent Engr.

Babcock & Wilcox Company
Attn: R&D Division
Alliance, OH 44601

INDUSTRY (Cont'd)

Battelle Memorial Institute
Physical & Process Metallurgy
Attn: Mr. T. A. Harrison
505 King Avenue
Columbus, OH 43201

Bell Aerosystems Company
Attn: Mgr. Advanced Mfg. Eng.
Internal Mail Zone C-53
P. O. Box 1
Buffalo, NY 14205

Bell Helicopter Company
P. O. Box 482
Ft. Worth, TX 76101
Attn: Mgr. Manufacturing Engr.

The Bendix Corporation
Aerospace Division
Attn: Technical Librarian
717 N. Bendix Drive
South Bend, IN 46620

Bethlehem Steel Company
Homer Research Laboratories
Mechanical Metallurgy Section
Attn: Mr. R. L. Whitely
Bethlehem, PA 18015

Boeing Aerospace Company
P. O. Box 3999
Seattle, WA 98124
Attn: Manufacturing Technology
Orgn. 2-5541, MS 1F-41

The Boeing Company
Airplane Division
Renton, WA 98055
Attn: Mat. & Process Unit Chief

The Boeing Company
Commercial Airplane Division
P. O. Box 3707
Seattle, WA 98124
Attn: Technical Library
Mail Stop 74-60

The Boeing Company
P. O. Box 3996
Seattle, WA 98124
Attn: Aerospace Group
Technical Library
Mail Stop 8K-38

The Boeing Company
Wichita Division
3801 South Oliver
Wichita, KS 67210
Attn: Organization 2700
Mail Stop K14-38

The Boeing Vertol Company
P. O. Box 16858
Philadelphia, PA 19142
Attn: Technical Library P32-01

Branson Instruments Co.
Nondestructive Testing Div.
76 Progress Drive
Stamford, CT 06904

Cabot Corporation
Stellite Division
P. O. Box 746
Kokomo, IN 46901
Attn: Technical Library

Cameron Iron Works, Inc.
Attn: Library
P. O. Box 1212
Houston, TX 77001

Canton Drop Forging & Mfg. Co.
Attn: Mr. C. Brauchler
2100 Wilet Avenue
Canton, OH 44701

Carpenter Steel Company
Metallurgical Department
Reading, PA 19603

Clevite Corporation
Attn: Library
540 E. 105th Street
Cleveland, OH 44108

AD-A049 682 TRW INC CLEVELAND OHIO MATERIALS TECHNOLOGY F/G 11/6
IMPROVED ULTRASONIC INSPECTION OF TITANIUM ALLOY FORGING BILLET--ETC(U)
JUL 77 I M MATAY F33615-71-C-1712
UNCLASSIFIED TRW-ER-7554 AFML-TR-77-111 NL

4 OF 4
AD
A049682

END
DATE
FILMED
3-78
DDC

INDUSTRY (Cont'd)

Crucible Materials Research Center
Colt Industries
P. O. Box 88
Pittsburgh, PA 15230
Attn: E. J. Dulis, President

Curtiss-Wright Corporation
Buffalo Facility
60 Grider Street
Buffalo, NY 14215
Attn: Mr. Tom Nakles

Curtiss-Wright Corporation
Wright-Aeronautical Division
Attn: Mr. R. J. Morgan, Manager
Mfg. Engineering
Wood-Ridge, NJ 07075

Douglas Aircraft Company
3855 Lakewood Boulevard
Long Beach, CA 90846
Attn: Director
Materials & Process Eng.
C1-253 (1-18)

Fansteel, Inc.
Number One Tantalum Place
N. Chicago, IL 60064
Attn: Library

Fairchild Industries, Inc.
Fairchild Republic Company
Farmingdale, NY 11735
Attn: Mr. Walter B. Trepel
Chief, Mfg. Processes

General Dynamics
Convair Division
P. O. Box 1128
San Diego, CA 92112
Attn: Mr. C. J. Kropp
Mail Zone 572-1

General Dynamics/Fort Worth
Manufacturing Technology
P. O. Box 748
Fort Worth, TX 76101
Attn: R. E. Key

General Electric Company
Attn: Mr. J. C. Stover
Materials Testing Lab.
Mail Drop 1682
100 Western Avenue
Lynn, MA 01910

General Electric Company
Aircraft Engine Group
Cincinnati, OH 45215
Attn: Technical Library

General Electric Company
Valley Forge Space Tech Center
Manufacturing Eng. R&D
Room 32100
P. O. Box 8555
Philadelphia, PA 19101

General Motors Corporation
Detroit Diesel Allison Div.
P. O. Box 784
Indianapolis, IN 46206
Attn: Mr. G. L. Vonnegut

Grumman Aerospace Corporation
Department 232, Plant 2
Bethpage, LI, NY 11714
Attn: Mr. Joseph Newman
Section Head
Mfg. Engineering

Grumman Aerospace Corporation
Materials and Processes Department
Dept. 440 - Plant 12
Bethpage, LI, NY 11714
Attn: Mr. Joseph H. Mainbardt
Deputy Department Head

Howmet Corporation
Reactive Metal Products Division
555 Benston Road
Whitehall, MI 49461
Attn: General Manager

Howmet Corporation
Titanium Ingot Division
555 Benston Road
Whitehall, MI 49461
Attn: General Manager

INDUSTRY (Cont'd)

International Harvester Company
R. A. Cellitti, Mfg. Research
7 South 600 County Line Road
Hinsdale, IL 60521

Ladish Company
Technical Library
Cudahy, WI 53110

Latrobe Steel Company
Latrobe, PA 15650
Attn: Mr. Alex Simkovich

Lockheed-California Company
P. O. Box 551
Burbank, CA 91520
Attn: Central Library
Dept 84-40
Unit 35, Plant A-1

Lockheed-Georgia Company
Department 72-34, Zone 26
Marietta, GA 30061
Attn: Manager, Sci. & Tech. Info.

Martin Marietta Aerospace
Baltimore Division
103 Chesapeake Park Plaza
Baltimore, MD 21220

Martin Marietta Aluminum
Titanium Division
19200 South Western Avenue
Torrance, CA 90509
Attn: Mr. J. J. Shaw

McDonnell Douglas Corporation
Dept H100, Bldg. HQ, Rm 788
P. O. Box 516
St. Louis, MO 63166
Attn: Mr. H. E. Soistman

McDonnell-Douglas Corporation
McDonnell-Aircraft Company
P. O. Box 516
St. Louis, MO 63166
Attn: Mr. H. C. Turner
Dept. 402, Bldg. 33

McDonnell-Douglas Corporation
Missile and Space Division
R&D Library
3000 Ocean Park Blvd.
Santa Monica, CA 90405

Northrop Corporation
Norair Division
3901 East Broadway
Hawthorne, CA 90250
Attn: Technical Information

Ontario Corporation
1200 W. Jackson St.
Muncie, IN 47305
Attn: Mr. M. G. Pasotti, Chief Eng.

Oregon Metallurgical Corporation
P. O. Box 580
Albany, OR 97321
Attn: Mr. D. Taylor

Panametrics, Inc.
Physical Acoustics Dept.
221 Crescent Street
Waltham, MA 02154

Pratt & Whitney Aircraft
Materials Eng. & Res. Lab.
Attn: Dr. James Doherty
Middletown, CT 06457

Pratt & Whitney Aircraft Group
United Technologies Corporation
Government Products Division
West Palm Beach, FL 33405
Attn: Mr. Joseph Moore

Pratt & Whitney Aircraft Group
United Technologies Corporation
Manager, Manufacturing R&D
East Hartford, CT 06108
Attn: F. J. Fennessy
Mgr, Mfg. R&D

Precision Castparts Corporation
3600 S. E. Harney Drive
Portland, OR 97206
Attn: Mr. Larry LaVoie

INDUSTRY (Cont'd)

Reactive Metals, Inc.
Niles, OH 44446
Attn: Mr. H. D. Kessler
Vice President
Corporate Tech. Director

REM Metals Corporation
320 West Queen Avenue
P. O. Box 829
Albany, OR 97321
Attn: Mr. Robert Lee, President

Republic Steel Corporation
Research Center, Library
6801 Brecksville Road
Cleveland, OH 44131

Reynolds Metals Company
Metallurgical Research Division
General Director
Richmond, VA 23261

Rockwell International Corp.
Los Angeles Division
International Airport
Los Angeles, CA 90045
Attn: Tech Library

Rockwell International Corp.
Rocketdyne Division
6633 Canoga Park
Canoga Park, CA 91304
Attn: Librarian
Dept. 586-306

Rockwell International Corp.
Rocketdyne-McGregor
McGregor, TX 76657
Attn: Technical Information Center

Ryan Aeronautical Company
Materials and Process Lab
Lindberg Field, Dept. 276
San Diego, CA 92050

Schultz Steel Company
5321 Firestone Blvd.
South Gate, CA 90280
Attn: Anthony Vinter

Sikorsky Aircraft Division
United Technologies Corporation
Stratford, CT 06497
Attn: Chief, Test Eng. Br.

Special Metals, Inc.
New Hartford, NY 13413
Attn: Library

Standard Pressed Steel Company
Attn: Materials Research Dept.
Jenkintown, PA 19046

Teledyne Allvac
P. O. Box 759
Monroe, NC 28110
Attn: C. Frank Elliott
Technology Manager

Titanium Metals Corporation
P. O. Box 2128
Henderson, NV 89015
Attn: H. R. Palmer

TiTech International, Inc.
P. O. Box 60
4000 W. Valley Blvd.
Pomona, CA 91769
Attn: E. A. Williams
Sr. Vice President

TMCA
Toronto Technical Laboratory
P. O. Box 309
Toronto, OH 43964
Attn: Manager

United States Steel Corp.
Products Development Division
525 William Penn Place
Pittsburgh, PA 15219

Universal Cyclops Steel Corporation
Refractomet Division
Bridgeville, PA 15017
Attn: General Manager

Universal Cyclops
Specialty Steel Division
Titusville, PA 16354
Attn: E. W. Altman

INDUSTRY (Cont'd)

Vought Corporation
Systems Division
Library Z50370
P. O. Box 5907
Dallas, TX 75222

Williams Research Corporation
2280 West Maple Road
Walled Lake, MI 48088
Attn: W. P. Schimmel

Wyman-Gordon Company
Attn: Mr. James A. Rossow
Research & Development
Harvey, IL 60426

Wyman-Gordon Company
Worcester, MA 01613
Attn: W. H. Couts, R&D

Wyman-Gordon Company
Attn: Mr. Robert A. Eddy
Mgr. Technical Services
105 Madison St.
Worcester, MA 01613